2022-117
6-1

*Volume 130, Nos. 1–6*

*January-February, 1960*

# PROCEEDINGS OF THE ACADEMY OF SCIENCES

## OF THE USSR

(DOKLADY AKADEMII NAUK SSSR)

## Physical Chemistry Section

*A publication of the Academy of Sciences of the USSR*

**IN ENGLISH TRANSLATION**

*Year and issue of first translation:*
*Vol. 112, Nos. 1-6 Jan.-Feb. 1957*

| | |
|---|---|
| *Annual subscription* | *$160.00* |
| *Single issue* | *35.00* |

Copyright 1960
CONSULTANTS BUREAU ENTERPRISES, INC.
227 West 17th Street, New York, N. Y.

*A complete copy of any paper in this issue may be purchased from the publisher for $5.00*

*Note: The sale of photostatic copies of any portion of this copyright translation is expressly prohibited by the copyright owners.*

*Printed in the United States of America*

# PROCEEDINGS OF THE ACADEMY OF SCIENCES OF THE USSR

## Physical Chemistry Section

Volume 130, Numbers 1-6 January-February, 1960

# CONTENTS

| | PAGE | RUSS. ISSUE | RUSS. PAGE |
|---|---|---|---|
| The Influence of Anions on the Anodic Dissolution of Indium Amalgams V. V. Losev and A. I. Molodov | 1 | 1 | 111 |
| The Adsorption of Vapors on Crystalline Adsorbents Called Molecular Sieves Ya. V. Mirskii | 7 | 1 | 115 |
| The Theory of Chemical Adsorption. V. I. Osherov | 9 | 1 | 117 |
| Deuterium-Hydrogen Exchange During the Hydrogenation of Solid Olefins By Atomic Hydrogen at -196°C. A. N. Ponomarev and V. L. Tal'roze | 13 | 1 | 120 |
| The Origin of the Preadsorption Effect and Some Other Anomalies in the Catalytic Oxidation of Carbon Monoxide on Oxide Semiconductors. S. Z. Roginskii | 17 | 1 | 122 |
| The Heat Capacity of Linear Polymers at Low Temperatures. I. V. Sochava | 21 | 1 | 126 |
| The Influence of Halide Ions on the Corrosion of 18-8 Stainless Steel in Sulfuric Acid. Hua Pao-ting, Shan Hsing-su, Z. A. Iofa, and É. I. Mikhailova | 25 | 1 | 129 |
| Concerning Some Peculiarities of the Electrochemical Solution of n-Type Silicon. E. A. Efimov and I. G. Erusalimchik | 29 | 2 | 353 |
| The Glass Transition Temperature of Cellulose. V. A. Kargin, P. V. Kozlov, and Wang Nai-ch'ang | 33 | 2 | 356 |
| The Maximum Solubility of a Component of a Gaseous Mixture in a Liquid. A. Yu. Namiot | 37 | 2 | 359 |
| Reduction Reactions at the Germanium Cathode. Yu. V. Pleskov | 39 | 2 | 362 |
| The Origin of the Compensation Effect in Chemical Kinetics S. Z. Roginskii and Yu. L. Khait | 43 | 2 | 366 |
| The Exchange of Hydrogen Isotopes on Palladium. G. N. Trusov and N. A. Aladzhalova | 47 | 2 | 370 |
| Adsorptional Changes in the Surface Conductivity of Germanium V. I. Fistul' and D. G. Andrianov | 51 | 2 | 374 |
| Phase Diagrams of Systems Containing An Ordered Phase. I. L. Aptekar' | 55 | 3 | 562 |
| The Influence of Adsorbed Oxygen on the Electronic Work Function of Germanium. R. Kh. Burshtein and L. A. Larin | 59 | 3 | 565 |
| The Heat of Wetting of Aerosil by Aliphatic Alcohols. V. F. Kiselev, K. G. Krasil'nikov and V. V. Murina | 63 | 3 | 569 |
| The Influence of Radiolysis on the Potential of a Nickel Electrode as a Function of the Gas Phase Composition. S. D. Levina and T. V. Kalish | 67 | 3 | 573 |

# CONTENTS (continued)

| | PAGE | RUSS. ISSUE | RUSS. PAGE |
|---|---|---|---|
| Investigation of Adsorption of the Unsaturated Fluorocarbons $C_2F_4$ and $C_3F_8$ in an Electron Emitter. S. Z. Roginskii and V. A. Shishkin. . . . . . . . . . . . . . . | 71 | 3 | 577 |
| Thermodynamic Study of the Reaction $UO_2(s) + \frac{1}{2}$ C (graph.) $+ Cl_2(g) = UOCl_2(s) + \frac{1}{2} CO_2(g)$ by Measuring Electromotive Forces. M. V. Smirnov, I. F. Nichkov, S. P. Raspopin, and M. V. Perfil'ev. . . . . . . . . . . . . . . . . . . . . . . . . . . . | 75 | 3 | 581 |
| The Influence of the Chromium Content on the Electrochemical and Corrosional Behavior of Iron-Chromium Alloys. G. M. Florianovich and Ya. M. Kolotyrkin | 79 | 3 | 585 |
| Adsorption of Nitrogen Gas on Modified Activated Carbon. B. P. Bering, M. M. Dubinin, E. G. Zhukovskaya and V. V. Serpinskii. . . . . . . . . . . . . . . . | 83 | 4 | 793 |
| The Reduction of Indium on the Dropping-Mercury Electrode in the Presence of Certain Organic and Inorganic Cations. Kh. Z. Brainina. . . . . . . . . . . . . . . | 87 | 4 | 797 |
| The Chemisorption of Oxygen on Germanium. R. Kh. Burshtein, L. A. Larin, and G. F. Voronina . . . . . . . . . . . . . . . . . . . . . . . . . . . . . . . . . | 91 | 4 | 801 |
| The Measurement of Detonation-Front Temperatures for Explosives. I. M. Voskoboinikov and A. Ya. Apin. . . . . . . . . . . . . . . . . . . . . . . . . | 95 | 4 | 804 |
| Alteration of the Work Function of Oxide Semiconductors by the Introduction of Additives. É. Kh. Enikeev, L. Ya. Margolis and S. Z. Roginskii. . . . . . . | 99 | 4 | 807 |
| The Interphase Surface Energy of a Metal at the Crystal-Melt Interface. S. N. Zadumkin. . . . . . . . . . . . . . . . . . . . . . . . . . . . . . . . . . | 103 | 4 | 810 |
| The Catalytic Action of Copper Ions in the Dissolution of Metals with Oxygen Depolarization. I. A. Kakovskii and N. G. Tyurin. . . . . . . . . . . . . . | 107 | 4 | 812 |
| Special Features of the Kinetics of the Hydrational Hardening of Sulfates. O. I. Luk'yanova, P. A. Rebinder, and G. M. Belousova. . . . . . . . . . . . . . . . | 111 | 4 | 816 |
| Oxidation Reactions of the Olefins. I. I. Moiseev, M. N. Vargaftik, and Ya. K. Syrkin. . . . . . . . . . . . . . . . . . . . . . . . . . . . . . . . . . . | 115 | 4 | 820 |
| A Study of the Relation Between the Diffusion Coefficient and the Coverage on Sorbent Grains of Arbitrary Form. D. P. Timofeev. . . . . . . . . . . . . . . . . | 119 | 4 | 824 |
| The Ionization of Triphenylcarbonyl in Sulfuric Acid Media Containing Isopropyl Alcohol. S. G. Éntelis, G. V. Épple, and N. M. Chirkov. . . . . . . . . | 123 | 4 | 826 |
| The Low-Velocity Detonation of Liquid Explosives. L. G. Bolkhovitinov. . . . . . . . . | 129 | 5 | 1044 |
| Kinetic Investigation Into the Electrochemical Reduction of Chromic Acid on a Rotating Disc Electrode. E. Budevskii and S. Toshev. . . . . . . . . . . . . | 133 | 5 | 1047 |
| Investigation of the Radiolytic Oxidation of Bivalent Iron at High Irradiation Doses. P. Ya. Glazunov and A. K. Pikaev. . . . . . . . . . . . . . . . . | 137 | 5 | 1051 |
| A New Chain-Initiating Reaction in Liquid-Phase Oxidation. E. T. Denisov. . . . . . | 141 | 5 | 1055 |
| Analysis of the Bond Form and the State of Water Absorbed in Dispersed Bodies, by Means of Kinetic Drying Curves. M. F. Kazanskii. . . . . . . . . . . . . . | 145 | 5 | 1059 |

# CONTENTS (continued)

| | PAGE | RUSS. ISSUE | RUSS. PAGE |
|---|---|---|---|
| An Example of a Homogeneous Extension to a Heterogeneous Catalytic Reaction O. V. Krylov. | 149 | 5 | 1068 |
| Light Absorption and Luminescence of Complex Molecules. S. I. Kubarev. | 153 | 5 | 1067 |
| Isotopic Exchange of Oxygen on Oxidation Catalysts. L. Ya. Margolis and V. A. Kiselev. | 159 | 5 | 1071 |
| Thermodynamic Properties of Indium Antimonide. A. V. Nikol'skaya, V. A. Geiderikh, and Ya. I. Gerasimov. | 163 | 5 | 1074 |
| The Effect of Alkali Metal Halides on the Amount of Hydrogen Adsorbed on Platinum Black. D. V. Sokol'skii and G. D. Zakumbaeva. | 167 | 5 | 1078 |
| Reversible Changes in the Gaseous Permeability of Polymers During $\gamma$-Irradiation. N. S. Tikhomirova, Yu. M. Malinskii and V. L. Karpov. | 171 | 5 | 1081 |
| The Limiting-Diffusion Current on Rotating Disc Electrodes During Cathodic Evolution of Hydrogen. G. P. Dezider'ev and S. I. Berezina. | 175 | 6 | 1270 |
| The Effect of the Aggregation of Quartz Particles During Grinding on Their Adsorptive Properties. V. F. Kiselev, K. G. Krasil'nikov and G. S. Khodakov. | 179 | 6 | 1273 |
| Electronic Paramagnetic Resonance Spectra of Cyanine Dyes. Yu. Sh. Moshkovskii. | 183 | 6 | 1277 |
| A Method for Determining Kinetic Constants and Flow Limits for Reactions Performed in Flow Conditions. G. M. Panchenkov and Yu. M. Khorov | 187 | 6 | 1280 |
| The Paramagnetic Resonance of Certain Inner Complexes of Copper. A. K. Piskunov, D. N. Shigorin, V. I. Smirnova and B. I. Stepanov. | 193 | 6 | 1284 |
| Intermolecular Interactions Revealed Through Fluorescence Spectra of Acetylanthracenes Dissolved in Mixed Solvents. A. S. Cherkasov. | 197 | 6 | 1288 |
| The P.M.R. Spectra and the Accumulation Kinetics of Free Radicals Produced in the Radiolysis of Certain Aromatic Compounds. I. I. Chkeidze, Yu. N. Molin, N. Ya. Buben, V. V. Voevodskii. | 201 | 6 | 1291 |
| Erratum, Vol. 128, 1959 | 205 | | |

# THE INFLUENCE OF ANIONS ON THE ANODIC DISSOLUTION OF INDIUM AMALGAMS

V. V. Losev and A. I. Molodov

The L. Ya. Karpov Physicochemical Scientific Research Institute

(Presented by Academician V. A. Kargin, June 16, 1959)

(Translation of: Doklady Akademii Nauk SSSR, Vol. 130, No.1, 1960, pp. 111-114)

Original article submitted June 12, 1959.

The velocity of processes of anodic dissolution and electrodeposition of metals depends strongly on the nature of the anions present in the solutions. Halide ions appreciably accelerate cathodic and anodic processes in amalgams of zinc, tin, bismuth, and indium [1], and also abruptly increase the exchange current between amalgams of zinc and bismuth and solutions of their salts [2]. By measuring the exchange currents of amalgams of zinc and cadmium it has been shown that, in the case of solutions containing complexes of metals with anions, the anions participate directly in a determinative stage of the electrode process [3,4]. Velocity of anodic dissolution of cadmium in sulfuric acid increases greatly in the presence of bromide ions, and even more in the presence of iodide ions [5]. The velocity of the process of anodic dissolution of platinum in sulfuric acid at constant potential is proportional to the concentration of $Cl^-$ ions in the solution [6]. The mechanism of the accelerating effect of the anions on the anodic dissolution of metals has not yet been elucidated. The solution of this problem by means of conventional stationary polarization measurements is difficult, because ordinarily, for appreciable deviation from the equilibrium potential, polarization appears at the essential concentrations, and the results of polarization measurements in the neighborhood of equilibrium cannot be used because the corresponding reverse process occurs simultaneously. Under certain conditions the last difficulty may be obviated. By combining ordinary polarization measurements with radiochemical ones, we may separate one of the conjugate electrode processes, for example the anodic one, and elucidate its mechanism in the neighborhood of the equilibrium potential, even under conditions where the reverse process predominates.

By means of this method, with certain improvements [7-10], the influence of the concentration of halides and sodium sulfate on the velocity of the true anode process, $i_a$, of the dissolution of 0.1M indium amalgam in solutions of 0.01 M $In(ClO_4)_3$ + 0.01 M $HClO_4$ at various potentials has been studied, and, in particular, at the equilibrium potential (exchange current).* The experiments were carried out at 20° at constant ionic strength (3M), which was maintained by adding the appropriate amount of $NaClO_4$. In addition, the relation between the equilibrium potential of the amalgam and the concentration of the halide and sulphate ions has been studied.

In Fig. 1 the relationship, found by radiochemical measurements, between the velocity of the anodic process, $i_a$ in amp/$cm^2$, and the potential of the indium amalgam is shown side by side with the ordinary polarization curves, plotted against the current. As can be seen, the process of ionization of the indium proceeds with a measurable velocity even in the presence of strong cathodic polarization. In Figs. 2 and 3 the curves obtained by the radiochemical method for the relationship between $i_a$ and the potential are depicted for various concentrations of $Na_2SO_4$ (0.05-0.9M), NaCl (0.05-2.7M), NaBr ($1 \cdot 10^{-3}$-2.7M) and NaI ($1 \cdot 10^{-3}$-1M). It can be seen that there is a linear relationship between $\varphi$ and log $i_a$, in which the gradient of the anodic curve, $b_a$, does not depend on the concentration of the added salt;* therefore the whole of the anode curves was sometimes not given; we measured exchange current (points on Fig. 2 and 3), and have constructed a line directly through the point giving the value of the exchange current, with the corresponding gradient.**

---

*The choice of indium was dictated by the fact that, in the absence of activating ions, the exchange current of amalgams of indium is relatively low [10]. At the same time, it is known from polarographic data [11-15] that for ions like those of indium the half-wave potentials are strongly shifted to the positive in the presence of halide ions, and the electrode process is much altered.

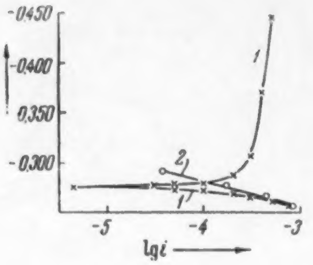

Fig. 1. Polarization curves for an amalgam of In (0.1M) in a solution containing 0.01M $In(ClO_4)_3$ + 0.1M $HClO_4$. 1) ordinary polarization curve; 2) true anodic curve obtained by the radiochemical method.

From Fig. 2 it is seen that with a rise in the concentration of the $SO_4^{2-}$ and $Cl^-$ ions, the anodic curve is shifted to the negative side, that is, the velocity of the anodic process increases. To evaluate the relationship between the velocity of the true anodic process, $i_a$, and the concentration C of these additives at a constant potential, a dotted line is shown in Fig. 2 at $\varphi = -0.330$; the points of intersection of the anodic curves on this line give the desired values of $i_a$. If we wish to express these experimental facts in the form of an equation,

$$i_a = kC^x,$$

then, at low concentrations of $Na_2SO_4$ (up to 0.2 M), the magnitude of x is about 1, while at very high $Na_2SO_4$ contents the value of x is not constant, but gradually increases with increase in C. For NaCl concentrations lower than 0.5M, the quantity x in this equation is again not constant, and increases approximately from 1.0 to 2.0 with increase in C, in the interval C = 0.5 to 2.7M, x = = 2.9. It is evident from these results that the ions $SO_4^{2-}$ and $Cl^-$ participate directly in the anode process, in the course of which the composition of the complex indium ions formed in the primary electrochemical process changes with the magnitude of the concentration of these ions. For high concentrations of NaCl in the electrode process, molecules of $InCl_3$ probably take part, while in the solution (judging from the nature of the relationship between the equilibrium potential of the amalgam and C), the ions $InCl_2^+$ predominate.

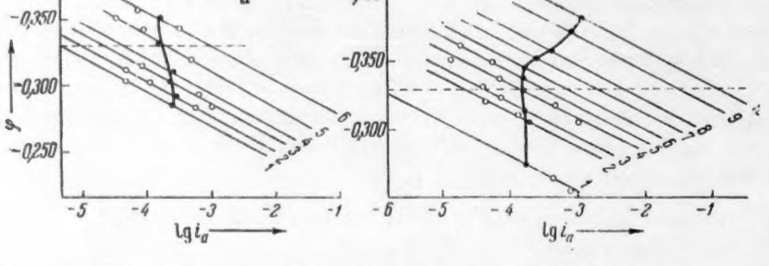

Fig. 2. Relationship between $i_a$ and the potential for solutions of 0.01M $In(ClO_4)_3$ + 0.01 M $HClO_4$, with added substances. a) $Na_2SO_4$; 1) 0.05M; 2) 0.1M; 3) 0.2M; 4) 0.3M; 5) 0.6M; 6) 0.9M; b) NaCl: 1) 0; 2) 0.05M; 3) 0.1M; 4) 0.2M; 5) 0.3M; 6) 0.5M; 7) 0.76M; 8) 1.0M; 9) 2.0M; 10) 2.7M. Black points are exchange current.

---

*b has the value of 0.026-0.027 v for solutions to which $Na_2SO_4$ is added, and 0.025 v for solutions to which NaCl or other halides is added. Hence in the presence of halide ions the transport coefficient for the anodic process, $\beta$, is equal to $2.3RT/b_a = 2.32$ (assuming that $\alpha + \beta = 3$) [9].

**For high concentrations of NaBr and NaI the exchange current is so high that the entire curve cannot be obtained because of the onset of concentration polarization, and so measurement of the exchange current must be made. In this case the quantity $b_a$ was obtained by means of measurements of the exchange current for various concentrations of indium ions in the solution (for example, the point A in Fig. 3a).

In the case of addition of NaBr and NaI (Fig. 3), increase in the halide ion concentrations is observed to cause not only the displacement of the anodic curve, but also a noticeable increase in the exchange current. For the quantitative estimation of this accelerating influence, the relationship between $i_a$ and the concentration of NaBr and NaI at a constant potential ( $\varphi = -0.276$ v) corresponding to the systems described in Fig. 3 above is presented in Fig. 4. For the addition of NaCl the relationship between log $i_a$ and log C is linear in the interval C = 0.05M to 2M, within which the slope is constant (log $i_a$, log C) and equal to 1.8; that is, our experimental facts accord with the equation,

$$i_a = kC^{1.8}.$$

It must be assumed that, under these conditions, two ions of $Br^-$ take part in the anode process, producing the ions $InBr_2^+$, which exist in equilibrium with the ions $InBr^{2+}$ the latter predominate in solutions of C = approx. 0.2M, but at C greater than 0.5M the indium is present in solution predominantly in the form $InBr_2^+$.) This conclusion agrees with the analysis of the dependence of the pure cathode process velocity, $i_k$, on the concentration of NaBr (dotted line in Fig. 4). * With high concentrations of NaBr, $i_k$ is practically independent of C, which would be expected to follow from the predominance of ions of the type of $InBr_2^+$ under these conditions in the solution.

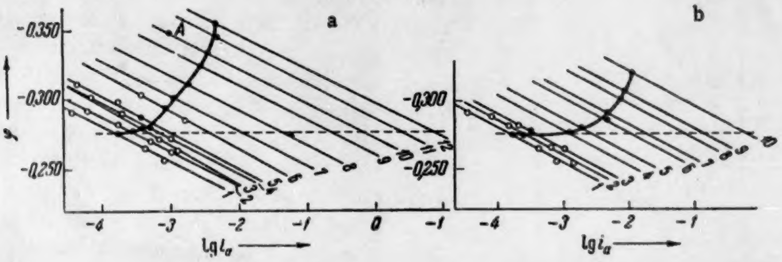

Fig. 3. Relationship between $i_a$ and the potential for the solution containing 0.01M $In(ClO_4)_3$ + 0.01M $HClO_4$ with additional salts. a) NaBr; 1) 0; 2) $1 \cdot 10^{-3}$M; 3) $2 \cdot 10^{-3}$M; 4) $5 \cdot 10^{-3}$M; 5) 0.02M; 6) 0.05M; 7) 0.1M; 8) 0.3M; 9) 0.5M; 10) 1M; black points are exchange current.

In the presence of added ions of $I^-$, the slope of the log $i_a$—log C curve in Fig. 4 is equal to 1.0 in a wide range of values of C ($2 \cdot 10^{-3}$ – 0.2M); that is, the velocity of the true anode process is directly proportional to the concentration of NaI. This relationship may be explained on the assumption that the ions $I^-$ participate directly in the anode process:

$$In + I^- \rightleftharpoons InI^{2+} + 3e.$$

Judging by the nature of the relationship between the equilibrium potential of the amalgam and the concentration of NaI, if C is less than 0.03M in the solution, the simple ions $In^{3+}$ are preponderant, existing in equilibrium with the ions $InI^{2+}$, and therefore the concentration of the latter is proportional to the concentration of the $I^-$ ions, and the velocity of the true cathode process $i_k$ is, just as in the case of $i_a$, linearly dependent on C. At very high values of C in the solution, the ions $InI^{2+}$ predominate and their concentration changes little with the value of the concentration of the ions $I^-$; therefore $i_k$ is then practically independent of C (dotted line in Fig. 4). Results obtained for the dependence of the exchange current on the temperature (in the interval 1-45°), show that the addition of NaI (0.05M) leads to a reduction in the activation energy of the electrode process from 13.4 kcal [10] to 4.5 kcal.

---

[*] To estimate $i_k$ approximately, the gradient $b_k$ of the cathode curve must be determined by means of the relationship, $b_k = 2.3RT/\alpha F$, using the value $\beta = 2.32$ found earlier, and taking into account the condition that $\alpha + \beta = 3$, thus obtaining $b_k = 0.085$ v. If we were to draw the straight lines in Fig. 3, corresponding to the pure cathode process and passing through the value of the exchange current, then the magnitude of $i_k$ at a constant potential of $\varphi = -0.276^v$ could be obtained by constructing the curve of log $i_k$ against log C.

From the relationship observed between $i_a$ and $\varphi$, and also from the observed linear dependence of $i_a$ on the concentration of the amalgam [10], we learn that our experimental facts may be expressed by the equation,

$$i_a = k(\mathrm{In})(\mathrm{I}^-)\exp(\beta\varphi F/RT),$$

where $\beta = 2.32$. An analogous equation expresses the velocity of the anode process in the presence of the ions $\mathrm{Br}^-$ and $\mathrm{Cl}^-$ (for high concentrations of NaCl), with the difference that $i_a$ will be proportional to $[\mathrm{Br}^-]^2$ and $[\mathrm{Cl}^-]^2$ respectively.

As we have already seen [16], a true parallel exists between the accelerating influence of halide ions on the electrode process in the presence of cations, and their catalytic effect on isotopic exchange processes between cations [17, 18], and on other ionic reactions between cations [19,20]. It would seem that the mechanism of the halide effect and that of some other anions is similar in both cases: the anions play the part of "bridges", or carriers of electrons, between cations, or, on the other hand, between a cation and the surface of an electrode [1,17].

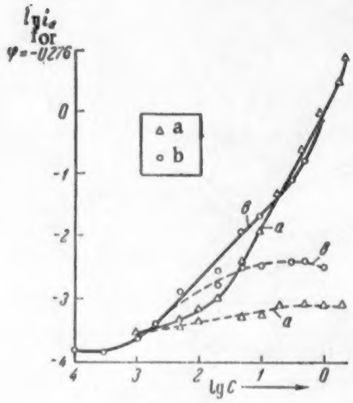

Fig. 4. Relationship between $i_a$ and the concentration of NaBr (a) and NaI (b) at a constant potential ($\varphi$ = −0.276 v). Dotted lines give the corresponding relationship for $i_k$.

The accelerating influence of $\mathrm{I}^-$ ions, and also of $\mathrm{Br}^-$ ions has not yet been mentioned, and must in general be explained by a change in the structure of the electrical double layer caused by their adsorption, and the arising of a negative $\varphi_1$ potential, which would result in the acceleration of anodic and cathodic processes [21]. In favor of this is the fact that the strongly adsorbed ions $\mathrm{I}^-$ and $\mathrm{Br}^-$ exert marked accelerating effects even at rather low concentrations, while ions such as $\mathrm{SO}_4^{2-}$ and $\mathrm{Cl}^-$, which possess a lower adsorbing capacity, accelerate anode processes only at comparatively high concentrations. In this case, however, it is difficult to explain, for example, the linear dependence of $i_a$ on the concentration of the NaI, and also the fact that the cathode process is independent of the NaI concentration in the high concentration region. * It seems to us, therefore, to be very probable that the halide ions (with the exception of $\mathrm{F}^-$), and the sulphates, take a direct part in the ionization process of indium, though for a full explanation of the observed effects, especially for low concentrations of $\mathrm{I}^-$ and $\mathrm{Br}^-$, it seems that we shall need to discover the effect of $\varphi_1$-potential measurements.

We wish to express our hearty thanks to Ia. M. Koloterkina for valuable advice during the discussion of the results of this work.

## LITERATURE CITED

[1] J. Heyrovsky, Disc. Faraday Soc. 1, 212 (1947); Z. für Elektrochem. 59, 802 (1955).

[2] J. Randles and K. Somerton, Trans. Faraday Soc. 48, 937, 951 (1952).

[3] H. Gerischer, Z. für phys. Chem. 202, 292, 302 (1953); Z. für Elektrochem. 57, 604 (1953).

[4] A. G. Stromberg, Zhur. Fiz. Khim. 31, 1704 (1957).

[5] Ya. M. Kolotyrkin and L. A. Medvedeva, Zhur. Fiz. Khim. 29, 1477 (1955).

[6] B. V. Érshler, Zhur. Fiz. Khim. 14, 357 (1940); 18, 131 (1944).

---

*In order to explain this effect, it is necessary to assume that in electrode processes only the $\mathrm{In}^{3+}$ ions take part, so that the accelerating influence of the $\varphi_1$-potential on the cathode process is exactly compensated by the retardation of the cathode process resulting from the reduction of the concentration of the $\mathrm{In}^{3+}$ ions with increase in the concentration of the NaI.

[7] V. V. Losev, Doklady Akad. Nauk SSSR, 100, 111 (1955).

[8] V. V. Losev , Trudy Inst. Fiz. Khim., Akad. Nauk SSSR, 6, 20 (1957).

[9] G. M. Budov and V. V. Losev, Doklady Akad Nauk SSSR 122, 90 (1958).*

[10] G. M. Budov and V. V. Losev, Doklady Akad Nauk SSSR 129, 6 (1959).*

[11] J. Heyrovsky, Chem. listy 19, 168 (1925); 40, 61 (1946).

[12] J. Tomеš, Coll. Czech. Chem. Comm. 9, 12 (1937).

[13] S. I. Sinyakova, Doklady Akad. Nauk 29, 375 (1940).

[14] D. Cozzi and S. Vivarelli, Z. für Elektrochem. 57, 408 (1953); 58, 907 (1954).

[15] M. Bulovova, Sborn. Chekhosl. Khim. rabot 19, 1123 (1954).

[16] A. N. Frumkin Izvest. Akad. Nauk, Otdel. Khim. Nauk, 1957, 1429.

[17] W. F. Libby, J. phys. Chem. 56, 863 (1952).

[18] K. V. Krishnamurty and A. C. Wahl, J. Am. Chem. Soc. 80, 5921 (1958).

[19] H. Taube et al., J. Am. Chem. Soc. 79, 262 (1957).

[20] H. Imai, Bull. Soc. Chem. Japan 30, 873 (1957).

[21] A. N. Frumkin et al., Kinetics of Electrode Processes (Moscow, 1952). [in Russian].

---

* Original Russian pagination. See C. B. translation.

# THE ADSORPTION OF VAPORS ON CRYSTALLINE ADSORBENTS CALLED MOLECULAR SIEVES

Ya. V. Mirskii

Grozny Scientific Oil Research Institute

(Presented by Academician M. M. Dubinin, August 2, 1959)

(Translation of: Doklady Akademii Nauk SSSR, Vol. 130, No.1, 1960, pp. 115-116)

Original article submitted August 2, 1959.

Recently there has been much interest in research on and in the use of crystalline adsorbents for which the the name molecular sieves has been coined [1-8]. These adsorbents have pores with a diameter of a few angstroms and, therefore, can only occlude a measurable quantity of substances which have molecules with a diameter less than the diameter of the pores in the adsorbent. The adsorption of various substances on natural crystalline adsorbents with pores of molecular dimensions (persorption) has formerly been studied by a series of investigators [9]. However, the natural molecular sieves, (mostly chabazite and, to a lesser extent, other zeolites), as a rule are scattered in nature and do not occur in thick deposits. The use of synthetic molecular sieves, which may be obtained in larger quantities and with better properties than the natural ones, creates new possibilities for the separation of gases and liquids. In this connection, the use of and the research on the adsorptive properties of synthetic molecular sieves is of much interest.

In this communication data on the adsorption of vapors of polar and nonpolar substances of different molecular configurations and dimensions are given for two sample molecular sieves, which are synthetic products prepared by the author in the Grozny Scientific Oil Research Institute. The synthetic molecular sieves have a crystal structure with very small interatomic distances and, therefore, they selectively adsorb a series of substances. The crystal structures of the above-mentioned molecular sieves are identical. Examining them by the powder method, using Cu radiation, we obtained the following x-ray data:

| | 1 | 2 | 3 | 4 | 5 | 6 | 7 | 8 | 9 | 10 | 11 | 12 | 13 | 14 | 15 | 16 | 17 |
|---|---|---|---|---|---|---|---|---|---|---|---|---|---|---|---|---|---|
| d,A | 9.40 | 7.22 | 5.68 | 4.31 | 3.78 | 3.38 | 3.03 | 2.68 | 2.17 | 2.08 | 1.95 | 1.76 | 1.61 | 1.52 | 1.44 | 1.37 | 1.30 |
| | m | m | ms | ms | ss | sss | ww | m | w | m | m | s | w | w | w | ms | m |

In Fig. 1,I the adsorption isotherms of water, methyl alcohol, n-hexane, isooctane (2,2,4-trimethyl pentane) and benzene vapors on the molecular sieve 102 are given, in Fig. I, II, those of the same substances on the molecular sieve 202. Both molecular sieves show a clearly pronounced selectivity in the adsorption of molecules with different configurations and dimensions. Molecular sieve 102 adsorbs 0.32 cc water and 0.26 cc methyl alcohol per gram but the adsorption of the bigger molecules of n-hexane, isooctane, and benzene is very slight. Molecular sieve 202 adsorbs 0.32 cc water, 0.28 cc methyl alcohol and 0.22 cc n-hexane per gram, but isooctane and benzene are not perceptibly adsorbed by it.

The isotherms of those substances which are adsorbed by the molecular sieves correspond to Langmuir isotherms in their shapes. Characteristic for the adsorption isotherms of the said substances on the examined molecular sieves is the occurrence of large amounts adsorbed at a low relative pressure (below 0.1). An increase of the relative pressure does not lead to a perceptible increase in adsorption, while the observed rise of the isotherm in the relative pressure range of 0.9 to 1.0 is evidently connected with the onset of capillary condensation of the interstices between the separate small crystals of the molecular sieves.

The adsorption on the molecular sieves is reversible: the desorption branches of all isotherms coincide with the adsorption branches. The specific surface of the examined molecular sieves is very large. The value, calculated from the Langmuir isotherm formula, using the data on the adsorption of methyl alcohol, lies near 1000 $m^2/g$.

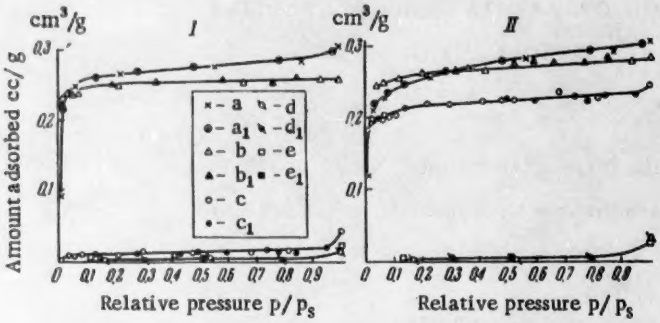

Fig. 1. Adsorption isotherms of water, methyl alcohol, n-hexane, isooctane and benzene vapors on the molecular sieve.

| | $H_2O$ | $CH_3OH$ | n-$C_6H_{14}$ | iso-$C_8H_{18}$ | $C_6H_6$ |
|---|---|---|---|---|---|
| Adsorption | a | b | c | d | e |
| Desorption | $a_1$ | $b_1$ | $c_1$ | $d_1$ | $e_1$ |

I) Molecular sieve 102, II) Molecular sieve 202.

Comparing the adsorption data on the said molecular sieves with those molecular sieves made by Linde (well known in practice abroad), it may be noticed that molecular sieve 102, in its adsorptive properties, is comparable with Linde molecular sieve 4A, and our 202 with Linde sieve 5A. However, the crystal structure of our molecular sieves differs from that of the Linde products. This follows from the comparison of the x-ray data given above with the results from [6], which were obtained by examining the crystal structure of Linde molecular sieves by means of x-ray diffraction.

The author is much indebted to M. G. Mitrofanov for his help and interest in the work.

## LITERATURE CITED

[1] R. M. Barrer, J. Chem. Soc. (1948) 127.

[2] R. M. Barrer and E. A. White, J. Chem. Soc. (1952) 1561.

[3] R. M. Barrer, J. Hinds, and E. A. White, J. Chem. Soc. (1953) 1466.

[4] R. M. Barrer and J. W. Baynhan, J. Chem. Soc., (1956) 2882, 2892.

[5] A. Guyer, W. Ineichen and P. Guyer, Helv. Chim. Acta 40, 6, 1603 (1957).

[6] D. W. Breck, W. G. Eversole, et al., J. Am. Chem. Soc. 78, 23, 5963 (1956).

[7] E. B. Brien, Petrol. Eng. 27, 3, 35 (1955).

[8] W. C. Ziegehain, Petrol. Eng. 29, 9, 6 (1957).

[9] S. Brunauer, The Adsorption of Gases and Vapors (Moscow, IL, 1948). [Russian translation].

# THE THEORY OF CHEMICAL ADSORPTION

V. I. Asherov
L. Ya. Karpov Scientific-Research Physicochemical Institute

(Presented by Academician A. N. Frumkin, July 30, 1959)

(Translation of: Doklady Akademii Nauk SSSR, Vol. 130, No.1, 1960, pp. 117-119)

Original article submitted July 6, 1959

In recent times, works on the theory of chemical adsorption have investigated the method of localized states [1-3] in molecules and crystals [4,5], which greatly simplifies the problem of finding eigenvalues. However, the method suffers from some limitations which make it necessary to use directly Bloch functions in the description of crystal adsorbents. We use this method for metals and dielectrics alike. Moreover, the possibility emerges of taking into account the effect of mutual interaction of the absorbed particles [6-11].

We consider a system of particles adsorbed on a crystal surface. The single electron Hamiltonian in an undisturbed crystal is:

$$H_1 = -\frac{\hbar^2}{2m}\nabla^2 + V_1. \tag{1}$$

in a system of adsorbed particles, no account being taken of interaction with the crystal it is

$$H_2 = -\frac{\hbar^2}{2m}\nabla^2 + V_2. \tag{2}$$

and in the system adsorbate–adsorbent it is

$$H = -\frac{\hbar^2}{2m}\nabla^2 + V_1 + V_2. \tag{3}$$

The corresponding eigenfunctions in Dirac notation are $k\rangle$, $\sum c_m m\rangle$ ($c_m$ is determined from the minimum energy condition for $H_2$), $I\rangle$; $\underline{k}$ denotes both the zone number and the wave vector within it; $\underline{m}$ is the location of the adsorbed particle; $\underline{I}$ are the new energy levels. The eigenvalues will be $\epsilon_k$, $\epsilon_0$ (neglecting the overlap of $m\rangle$), $\epsilon$.

We consider $I\rangle$ in the form of the linear combination

$$I\rangle = \mathsf{S} + \alpha_k k\rangle + \sum a_m m\rangle. \tag{4}$$

where the symbol $\mathsf{S}$ denotes summation over the zone numbers and integration with respect to momentum among them. We note that representation (4) requires us in the following to keep exact account of the nonorthogonality of $k\rangle$ and $m\rangle$.

$\alpha_k$ and $a_m$ are determined from the requirement that the energy $\epsilon$ shall be a minimum. The corresponding equations may be written in the form:

$$\begin{aligned} \alpha_k &= \mathsf{S}\,\alpha_{k'}\langle k(\varepsilon - H_1)^{-1}V_2 k'\rangle + \sum a_m \langle k(\varepsilon - H_1)^{-1}(H_2 - \varepsilon + V_1)\,m\rangle, \\ a_m &= \sum a_{m'}\langle m(\varepsilon - H_2)^{-1}V_1 m'\rangle + \mathsf{S}\,\alpha_k\langle m(\varepsilon - H_2)^{-1}(H_1 - \varepsilon + V_2)\,k\rangle. \end{aligned} \tag{5}$$

They possess the solutions:

$$\alpha_k = \mathrm{S}\, R_\alpha(k, k') \sum a_m \langle k' (\varepsilon - H_1)^{-1} (H_2 - \varepsilon + V_1)\, m\rangle. \qquad (6)$$
$$a_m = \sum R_a(m, m')\, \mathrm{S}\, \alpha_k \langle m' (\varepsilon - H_2)^{-1} (H_1 - \varepsilon + V_2)\, k\rangle.$$

The resolvents $R_\alpha(k,k')$ and $R_a(m,m')$ are easily found through the iterated kernels $K_\alpha^n(k,k')$ and $K_a^n(m,m')$ of the basic equations (5):

$$R_\alpha(k, k') = \sum_{n=0}^{\infty} K_\alpha^n(k, k'). \quad R_a(m, m') = \sum_{n=0}^{\infty} K_a^n(m, m'). \qquad (7)$$

Keeping in mind the fact that the systems k > and m> are complete we obtain:

$$R_\alpha(k, k') = \langle k\,[1 - (\varepsilon - H_1)^{-1} V_2]^{-1}\, k'\rangle, \qquad (8)$$
$$R_a(m, m') = \langle m\,[1 - (\varepsilon - H_2)^{-1} V_1]^{-1}\, m'\rangle.$$

In actuality the completeness condition may be fulfilled only approximately, which however, does not throw out the possibility of a representation of the form (4).

We now eliminate $\alpha_k$ from (6), and use (8) to obtain:

$$a_m = \sum a_{m'}\, \mathrm{S}\, \langle m V_k k\rangle \langle k V_k^{-1} m'\rangle: \qquad (9)$$

$$V_k = \frac{\varepsilon_k - \varepsilon + V_2}{\varepsilon_0 - \varepsilon + V_1}. \qquad (10)$$

In the case of the adsorption of one particle the problem resolves itself into finding the roots of the equation:

$$1 - \mathrm{S}\, \langle m V_k k\rangle \langle k V_k^{-1} m\rangle = 0. \qquad (11)$$

But in the case of adsorption of many particles, use must be made in (9) of representations of proximate neighbors of the particle of number m, which shows the effect of mutual interaction. Thus, neglecting the non-orthogonality of k> and m >, and supposing that there is substantial localization of the bond we obtain:

$$\varepsilon = \varepsilon_{k,0} + 4\pi n \frac{\langle m V_2 k\rangle \langle k V_1 m\rangle}{|\varepsilon_k - \varepsilon_0|}\, \theta. \qquad (12)$$

Here n = number of proximate neighbors; $\theta$ = degree of surface covering; and $\epsilon_{k,0}$ is independent of $\theta$.

The differential heat of adsorption, $Q(\theta)$ is found from the relation:

$$Q(\theta) = \mathrm{S}\, (\varepsilon_k - \varepsilon) + \varepsilon_0. \qquad (13)$$

where $\mathrm{S}$ is taken with respect to the occupied positions.

From (12) and (13) we obtain:

$$Q(\theta) = Q_0 - Zn \frac{\langle m V_2 V_1 m\rangle}{|\varepsilon_{k_0} - \varepsilon_0|}\, \theta: \qquad (14)$$

$Q_0$ = initial heat of adsorption; $\epsilon_{k0}$ = some mean energy in the valency band of the crystal; Z = ratio of the volumes bounded by the Fermi surface, and the surface of the nearest Brillouin zone.

In typical cases, the total decrease in heat of adsorption estimated (14) is of the order of 1 ev.

Thus, even assuming the absence of immediate interaction (i.e., interaction not dependent on the presence of adsorbent) of the adsorbed particles, a mutual interaction effect is achieved, which is conditioned on their chemical bond with the crystal; this is found to be comparable in magnitude with the energy of chemisorption.

The author would express his thanks to Prof. M. I. Temkin, Prof. Ya. Ya. Koutetskom and T. K. Rebana for their consideration of his results.

## LITERATURE CITED

[1] J. Koutecky, Trans. Farad. Soc., 54, 1038 (1958).

[2] T. B. Grimley, Proc. Phys. Soc., 72, 103 (1958).

[3] J. Koutecky, Proc. Phys. Soc., 73, 323 (1959).

[4] G. F. Koster, Phys. Rev., 89, 67 (1953).

[5] G. F. Koster, J. C. Slater, Phys. Rev., 95, 1167 (1954).

[6] M. E. Temkin, Zh. fiz. Khim., 15, 314 (1941).

[7] G. M. Schwab, Trans. Farad. Soc., 42, 669 (1946).

[8] A. Kh. Breger and A. A. Zhukhovitskii, Zh. fiz. Khim, 21, 423 (1947).

[9] D. A. Dowden, Ind. Eng. Chem., 44, 977 (1952).

[10] M. Boudart, J. Am. Chem. Soc., 74, 3556 (1952).

[11] M. E. Temkin, Sborn. Voprosy Khimicheskoi Kinetiki, Katalizi i Reaktsionnoi Sposobnosti (Collection on Chemical Kinetics, Catalysis and Reactivity), (Akad. Nauk. SSSR Press, 1955) p. 484. [In Russian].

# DEUTERIUM-HYDROGEN EXCHANGE DURING THE HYDROGENATION OF SOLID OLEFINS BY ATOMIC HYDROGEN AT -196°C

A. N. Ponomarev and V. L. Tal'roze

Institute of Chemical Physics, Academy of Sciences USSR

(Presented by Academician N. N. Semenov, August 7, 1959)

(Translation of: Doklady Akademii Nauk SSSR, Vol. 130,No.1 ,February 1960, pp. 120-121)

Original article submitted August 4, 1959.

The hydrogenation of olefins by atomic hydrogen at temperatures of -196°C has already been carried out [1,2]. It has been shown that in many cases a rapid reaction takes place, involving the addition of atomic hydrogen to the olefin, the hydrogen being produced by dissociation on a tungsten filament. Solid olefins used included propylene, butene-1, isobutene, and others.

The topic of the present investigation was the study of the deuterium-hydrogen exchange between gaseous and solid phases in the course of similar reactions, with the aim of obtaining information about the mechanism of hydrogenation. The reactor in our experiments was a spherical glass vessel, coupled with a mass spectrometer of type MX-1302 [3,4]. In the center of the vessel was placed a tungsten heating filament, upon which the atomic hydrogen would be produced. The inner surface of the reactor, which was cooled with liquid nitrogen, was coated with a layer of the olefin. Deuterium was introduced into the vessel at a pressure of about $4 \cdot 10^{-2}$mm Hg, and then the heating of the tungsten filament was switched on and simultaneous measurements were made of the total pressure, and of the partial pressures of $D_2$,HD, and $H_2$. The latter were obtained from the changes in intensity of the corresponding mass-spectrograph lines as the reaction proceeded.

Control experiments were carried out which revealed that under the conditions of the experiment diffusion in the reactor to the diaphragm of the mass spectrometer was so rapid that it had no effect on the shape of the kinetic curves.

Experiments were carried out with propylene and isobutylene. For a given temperature of the tungsten filament, and the same initial hydrogen pressure, the velocity of hydrogenation of the isobutylene was several times smaller than the velocity of hydrogen of propylene. In the experiment described below, therefore, the temperature of the tungsten filament for reactions involving propylene was maintained at a much lower value than for those using isobutylene, so as to arrange that the velocity of hydrogen absorption should be approximately the same for both reactions. It has been demonstrated that the hydrogenation is accompanied by a very rapid isotopic exchange, leading to the appearance in the gas phase of molecules of HD and $H_2$.

Curves depicting the change with time of the partial pressures of $D_2$, HD, and $H_2$, and of the over-all hydrogen pressure during the hydrogenation of propylene (a) and isobutylene (b) are shown in Fig. 1.

Figure 2 depicts the curves derived from the above, for the relative change in total pressure, $(p_{total}/p^0_{total})$, and also the relative composition with respect to deuterium in the gas phase, in the form: $(p_{D_2} + \frac{1}{2} p_{HD})/p_{total}$, in the case of propylene (a) and isobutylene (b). It can be seen that, in the case of isobutylene, the exchange velocity is close to the absorption velocity of the hydrogen while in the case of propylene the exchange velocity is appreciably less than the absorption velocity. (The small rise in the partial pressure $p_{D_2}$ during the

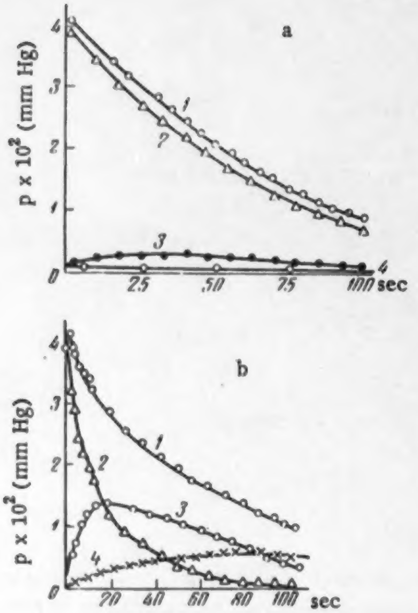

Fig. 1. Change in hydrogen pressure (1), and partial pressure of $D_2$ (2), HD (3) and $H_2$ (4), during the hydrogenation of: a) propylene; b) isobutylene.

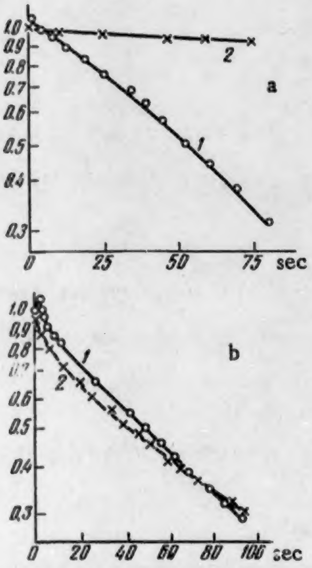

Fig. 2. Hydrogenation and isotopic exchange curves, using semilogarithmic coordinates. a) propylene; b) isobutylene. 1) relative change in total pressure; 2) relative change in the deuterium content of hydrogen in the gas phase.

first 1-2 seconds after switching on the tungsten filament is to be explained by the small general initial heating – some 4 or 5°– of the gas in the reactor).

From the data obtained, it is not yet possible to establish unequivocally the nature of the elementary processes leading up to exchange. The most probable explanation, however, which is in agreement with the views contained in the literature, is exchange between free hydrogen atoms, and the free activated radicals formed as an intermediate product during the hydration of the olefin by atomic hydrogen. Special importance in the case considered would thus be attached to the elementary process: $\dot{R} + \dot{H}$ = olefin + $H_2$ (Q = ca. 60 kcal), leading to the exchange process, and, simultaneously, to the retardation of the hydrogenation process as a whole. The opposing effects of the velocity of hydrogenation and the velocity of the exchange process, which can be seen by comparing these quantities for the cases of propylene and isobutylene, might serve as a reason for the utilization of this process. If the elementary process which has been suggested actually proceeds with a great velocity, it may have very great importance for the preparation of "frozen" alkyl radicals by the radiation method.

Actually, since in the last case atoms of hydrogen are formed side by side with alkyl radicals, the process demonstrated may be one of the causes responsible for the early "initial limitation" of the concentration of the frozen radicals, which has been observed in our laboratory on, for example, paraffins, and also in [6] in the case of polyethylene.

## LITERATURE CITED

[1] R. Klein, M. Scheer, J. Am. Chem. Soc., 80, 1007 (1958).

[2] R. Klein, M. Scheer, J. Phys. Chem., 62, 1011 (1958).

[3] Ya. A. Yukhvidin, Zav. Lab., No.1, 35 (1957).

[4] V. A. Pavlenko, A. E. Rafal'son and A. M. Shereshevskii, Apparatus and Technique of Experiment,[in Russian], No.3, 3 (1958).

[5] E. W. R. Steacie, Atomic and Free Radical Reactions, N. Y., 1954.

[6] A. T. Koritskii, Yu. N. Molin, V. N. Shamshev, N. Ya. Buben and V. V. Voevodskii, High Molecular Weight Compounds [in Russian] 1, No.8, 1182 (1959).

# THE ORIGIN OF THE PREADSORPTION EFFECT AND SOME OTHER ANOMALIES IN THE CATALYTIC OXIDATION OF CARBON MONOXIDE ON OXIDE SEMICONDUCTORS

Corresponding Member Academy of Sciences, USSR,
S. Z. Roginskii

Institute of Physical Chemistry, Academy of Sciences, USSR

(Translation of: Doklady Akademii Nauk SSSR, Vol. 130, No.1,
1960, pp. 122-125)

(Original article submitted July 13, 1959)

The oxidation of carbon monoxide on oxide semiconductors (S.C.) is one of the most studied of catalytic reactions. However, its kinetics, and the nature of the influence of various factors on the catalytic activity of these semiconductors, are quite unusual in that, in spite of the postulation of special hypotheses and models, it has not been possible to establish a comprehensive explanation free from all contradictions. As we shall show below, a part of these contradictions disappears when we apply to the oxidation of carbon monoxide the principles of electron kinetics of semiconductor catalysis.

The preadsorption effect. On $MnO_2$ [1], NiO [2], and a number of other oxides [3], the incidence of the power to catalyze the oxidation of carbon monoxide is most intimately bound up with the activated adsorption of the latter, which is often accompanied by chemical reduction of the surface of the semiconductor. These control not only the ranges of temperature of catalysis and chemisorption, but also the values of the energy of activation, $E_{cat}$ and $E_{chem}$ of both processes [1,2]. But for chemisorption carried out in the absence of oxygen on active specimens, even the initial velocity $w_0$ is appreciably less than the velocity of the catalytic reaction [1,2,4]. It has therefore not been possible to suppose that completed chemisorption is the rate determining stage of catalysis.

The adsorption of carbon monoxide reduces the work of emission, $\varphi$, of electrons from both n- and p-semiconductors, while the adsorption of oxygen increases it [5]. For mixtures of composition $CO + O_2$ an intermediate value of $\varphi$ is obtained, which shows a partial compensation of charge effects. Thus, in one of the experiments the introduction of oxygen increased $\varphi$ from NiO by 0.35 ev, the introduction of carbon monoxide diminished it by 0.20 ev, and the introduction of a mixture of the two gases increased it by 0.24 ev. On the zone model this would mean that oxygen reduces the curvature of the zones which had been brought about through the self-charging of the surface by the chemisorption of carbon monoxide, so reducing the surface Fermi level. This should reduce the free energy of the positively charged surface transitional complexes ($|\bar{k}|$), including $CO^{+}{}_{chem}$[6], by:

$$\Delta F = |e\Delta V_{\Sigma}| \cong |\gamma e \Delta\varphi|. \tag{1}$$

In equation (1), e = electronic charge; $\Delta V_{\Sigma}$ = change in the total diffusion potential of the surface; $\gamma$ = = a numerical coefficient, approximating to unity, being the estimated fraction of $\Delta\varphi$ due to the molecular dipole component and the influence of oxygen on the position of the Fermi level within the volume of the semiconductor ($\mu$).

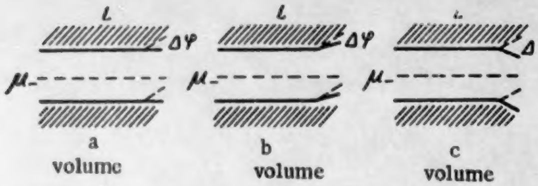

Fig. 1. Influence of the adsorption of an arbitrary quantity of acceptor molecules onto the surface zones; a) without initial curvature; b) with initial upward curvature; c) with initial curvature downward; $\Delta\varphi_b > \Delta\varphi_a > \Delta\varphi_c$.

As experiment shows, when such positive acceleration occurs, the reduction in charge caused by it causes an observed change in E given by: $\Delta E_{chem} \cong |\gamma e \Delta\varphi|$ [7]. The increase in velocity constant k and w caused by this amounts, because of kinetic compensation, only to: $\exp[(1-\alpha RT)\Delta E_{chem}/RT]$, where $0 < \alpha < 1$ the coefficient from the equation:

$$\ln k_0 = \text{const} - \alpha E. \tag{2}$$

The best catalysts for low temperature oxidation of carbon monoxide are the "hole" semiconductors, and therefore the chemisorption of oxygen increases their current carrying power, and when removal of carbon dioxide occurs (after this has been formed catalytically), in the mean period of charging the surface with oxygen:

$$\Delta\varphi_{O_2} \cong a \ln \theta/\theta_0 = a \ln \theta^*, \tag{3a}$$

$$\Delta E \cong b \ln \theta^* \tag{3b}$$

$$w \cong w_0 \theta^{*\beta}, \tag{3c}$$

where $\theta$ = the actual, and $\theta_0$ = the initial specific surface covering by oxygen; $\theta^* > 1$, the ratio of these; $\beta = -b/RT$. When irreversible adsorption of oxygen takes place, the value of $k_0$ increases, while with reversible adsorption, in view of the relationship: $\theta = f(p)$, there arises the possibility of a concentration factor $f_1(p_{O_2}) > 1$. The form of $f_1$ is defined by the isothermal relationship: $\Delta\varphi = f_2(p_{O_2})$ within the given interval $p_{O_2}$. Thus

$$\Delta\varphi \cong cRT \ln p/p_0, \tag{4a}$$

$$\Delta E \cong \delta RT \ln p^*, \tag{4b}$$

$$w \cong w_0 p^{*\delta}, \tag{4c}$$

where $p^* = p_{O_2}/p_{0O_2}$. In both the cases (3c) and 4c) the observed E for the chemisorption of carbon monoxide is not changed by the addition of oxygen. By such a mechanism a preadsorption effect is observed, characterized by a positive change in the effect of the adsorbed oxygen. The influence of the acceptor gas on the curvature of the zones is increased in the case where the initial curvature is downwards (Fig. 1), and diminished where the initial curvature is upwards [8]. Therefore it follows that the modifying effect of oxygen should be enhanced if substances are added which reduce the work of emission, and reduced by the addition of substances which increase this. It is apparently to such a cause that we may ascribe the exceptionally powerful reduction of the velocity of chemisorption of carbon monoxide on prepared ZnO which contains Li+ in its lattice [9]. If this is regarded as probable, then it would be expected that the addition of $SO_4^{=}$, and also of the oxides of tervalent metals, which increase $\varphi$ [7], ought to cause the speed of chemisorption of carbon monoxide and that of the catalytic reaction to draw closer to each other, and this is also, apparently, the case.

It should be noticed that, if such an interpretation is accepted, it should in principle be possible by using sufficiently low total pressure of the reaction mixture, and sufficiently high temperature, to cause the preadsorption effect to disappear completely. This result ought, though, to be compared with the velocities of chemisorption and catalysis obtained when equal curvature of the zones is artificially created, or with compensation of their electrical field. The values of $E_{cat}$ observed experimentally ought to coincide with the initial values of $E_{chem.obs.}$, since in the course of chemisorption the self-charge grows continuously, so displacing the distribution, and simultaneously, because of the biographical heterogeneity controlling the region of chemisorption [10], is displaced along the distribution(cf. Fig. 2), and the reduction of the surface usually takes place, even if only partially. These effects are absent during the stationary period of catalysis, occcurring in a stream of constant chemical composition with a sufficient excess of oxygen. In this situation $\Delta V_{\Sigma}$ and $\Delta\varphi$, on which not only the oxygen but also the carbon dioxide and the surface $CO_3$ complexes [11] depend, are constant; the controlling region is stationary, and reduction of the catalyst falls off.

The poisoning influence of water. For the catalytic oxidation of carbon monoxide, water vapor exerts a characteristically powerful retarding effect [12], the isobars of the vapor corresponding to a surface with a changed energy of activation [10]. An attempt has been made to explain this on the basis of adsorption-blockage formed by the surface and bulk hydroxyl groups, etc. According to the measurements of V. I. Lyashenko [13] and others, the adsorption of water has a positive effect on the surface of oxide semiconductors; that is, $\Delta V_{\Sigma}^{H_2O}$ has the same sign as $\Delta V_{\Sigma}^{CO}$ . This would be expected to produce retardation, with increase of F and E by $\gamma e\Delta V_{\Sigma}^{H_2O}$ (Fig.2), and reduction of the velocity by a factor of $\exp[-(1-\alpha' RT)\Delta E/RT]$. The large magnitude of the effect may be a simple consequence of the strong adsorbability of water. Other well-adsorbed molecules ought to show similar effects: these might be such electron donors as liquid olefins, benzene and acetone. It is usually found that the effect of carbon dioxide is slight [14], because of its small adsorbability; in addition, the carbon dioxide effect may be complicated by increase in concentration of negatively charged surface carbonate ion radicals on the semiconductor surface.

Modifying added materials. The catalytic activity of oxides may be strongly affected by small additions of oxides of metals of different valency. The principal catalysts which have been investigated for the oxidation of carbon monoxide are NiO and ZnO, with the addition of oxides of metals of the type $Me^{I}$, $Me^{III}$ and, in part, $Me^{II}$ also. Such systems are regarded as being solid solutions, although the formation of these solutions has only been demonstrated for $Li_2O$, MgO and ZnO in NiO [14]. In the simple zone model, changes in the energy of activation of the electrical conductivity show the direction and magnitude of the displacement of the volume Fermi level, which, if there is unchanged curvature of the zones, ought to be accompanied by change in the work of emission equal in magnitude but opposite in sign. If we take the chemisorption of carbon monoxide in the form of $CO^+$ as the controlling step, we may expect $E_{chem}$ and $E_{cat}$ to grow with upward shift in $\mu$ -and also both values of E to fall with downward shift in $\mu$.-For p-semiconductors this corresponds to symbatism (corresponding sign of change) and for n-semiconductors antibatism (opposite sign of change) of variation of $E_{chem}$ with $E_{\sigma}$ .

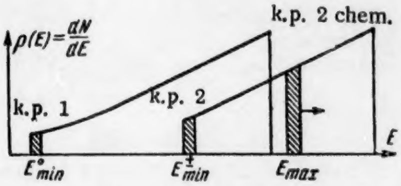

Fig. 2. Change of distribution, and displacement of controlling region with charge on mainly inhomogeneous surface of: k.p.1) controlling region of chemisorption and catalysis without charge; k.p.2) for catalysis and initiation of chemisorption with charge of $H_2O$; k.p.2 chem) with increasing chemisorption of carbon monoxide.

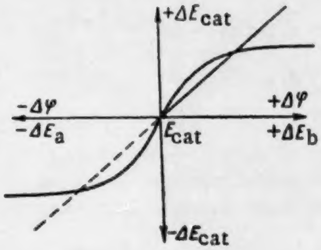

Fig. 3.Dependence of the activation energy of the catalytic reaction, $E_{cat}$, of the oxidation of carbon monoxide, on changes in the activation energy of the electrical conductivity, $E_{\sigma}$ , and change in the work of emission $\Delta\varphi$, produced by the introduction of impurities into the oxides of zinc and nickel.

The experimental relationships are quite different and very complex, as can be seen from Fig. 3. In particular, Li in NiO and ZnO produces an increase in $E_{chem}$, though in both cases it reduces the state $\mu$..

Hauffe [16], in order to explain the data of Schwab and Block [15] proposed a change in the accepted nature of the controlling stage, and suggested an additional hypothesis, involving the participation in the process of special electron "traps" on the surface. But our results cannot be fit into the framework of this theory, nor of other proposed models. These difficulties are faced directly in measurements of the work of emission [17], and it appears that changes in $\Delta\varphi$ neither in magnitude nor in sign can be correlated with those expected from measurements of $E_{\sigma}$. At the same time there is a practically exact correlation between changes in $\varphi$ and $E_{cat}$ (see Fig.3), and in both cases a fall in the value of $\varphi$ is accompanied by rise in that of E, while growth in $\varphi$ is linked with a diminution of E, as would be expected if this stage is controlled by the positive charge of the transitory complex.

Kinetics. An analysis of the kinetic anomalies appears to lie outside the scope of the present article. The most difficult of them – the stable half order in relation to initial concentration of carbon monoxide – may be explained by the appearance under certain conditions in the adsorption equilibrium on the semiconductor of a concentration proportional to the square root of the concentration of the undissociated gas being adsorbed. But on such a theory, to arrive at a single controlling stage for all systems with 1st and ½th orders, it is necessary in addition to admit the possibility of an opposite sign of the carrier in the suprasurface layer, and also the participation in the process of both chemisorbed and physically adsorbed carbon monoxide. That is, there is postulated a two-stage chemisorption: $CO \rightarrow CO_{phys} \rightarrow CO_{chem}$. The dichotomy of chemisorption and catalysis, postulated in the preadsorption mechanism , vanishes, but the division is maintained between the catalytic utilization of the carbon monoxide and its chemical reaction with the catalyst, leading up to the renewal of the surface. A different significance is also given to the lower limit of catalytic oxidation [18]. However, the facts at present available are insufficient to exclude the correlation of the controlling chemisorption of carbon monoxide with collision on the surface. In both cases the weak dependence of w on the composition of oxygen in the mixture above the "lower limit", apparently, is associated with saturation of the active part of the surface with oxygen even at low values of $P_{O_2}$.

## LITERATURE CITED

[1] S. Z. Roginskii and L. B. Zel'dovich, Acta Physicochemica USSR, 1, 545, 595 (1934).

[2] S. Z. Roginskii and T. F. Tselinskaya, Zhur. fiz. Khim., 18, 477 (1944); 21, 919 (1947); 22, 1260 (1948).

[3] M. S. Belen'kii, Doctorate Dissertation, Inst. Phys. Chem. Acad. Sci. USSR (Moscow 1946) [in Russian].

[4] S. Yu. Elovich and F. F. Kharakhorin, Problems of Kinetics and Catalysis [in Russian] 3, 222 (1937).

[5] É. Kh. Enikeev, L. Ya. Margolis and S. Z. Roginskii, Dokl. Akad. Nauk. SSSR, 124, 606 (1959).*

[6] S. Z. Roginskii, Dokl. Akad. Nauk. SSSR, 126, No.4, 817 (1959).*

[7] É. Kh. Enikeev, L. Ya. Margolis and S. Z. Roginskii, Dokl. Akad. Nauk. SSSR, 129, 372 (1959). *

[8] V. B. Sandomirskii and Sh. M. Kogan, Dokl. Akad. Nauk SSSR, 127, 377 (1959).*

[9] N. P. Keier and L. N. Kutseva, Problems of Kinetics and Catalysis [in Russian] 10, 1959.

[10] S. Z. Roginskii, Adsorption and Catalysis on Nonhomogeneous Surfaces [in Russian] (Moscow, 1948).

[11] W. E. Garner, T. J. Gray, and F. S. Stone, Proc. Roy. Soc. (A), 197, 249 (1949); W. E. Garner, Bull. Soc. Chim. Belg., 67, 417 (1958).

[12] E. V. Alekseevskii et al, An Active Manganese Dioxide [in Russian] (Leningrad 1937).

[13] V. I. Lyashenko and I. I. Stepko, Izv. Akad. Nauk, SSSR, Physics Series, 16, 274 (1952).

[14] N. P. Kreier, S. Z. Roginskii,and I. S. Sazonova, Dokl. Akad. Nauk. SSSR, 106, 859 (1956); Izv. Akad. Nauk. SSSR, Physics Series, 21, 183 (1957).

[15] G. M. Schwab, and I. Block, Zs. phys. Chem. (N.F.), 1, 42 (1954).

[16] K. Hauffe, Bull. Soc. Chim. Belg., 67, 417 (1958).

[17] É. Kh. Enikeev, L. Ya. Margolis and S. Z. Roginskii, Dokl. Akad. Nauk. SSSR, 129, No.3 (1959).*

[18] S. Z. Roginskii, F. F. Kharakhorin and S. Yu. Elovich, Acta. Physicochim. USSR, 3, 503 (1935).

---

* Original Russian pagination. See C. B. translation.

# THE HEAT CAPACITY OF LINEAR POLYMERS AT LOW TEMPERATURES

I. V. Sochava

(Presented by Academician A. F. Ioffe,1959)

(Translated from Doklady Akademii Nauk SSSR, Vol. 130, No.1, 1960, pp. 126-128)

Original article submitted July 15, 1959.

The relationship between heat capacity and temperature has been investigated for linear polymers in the neighborhood of liquid-hydrogen temperatures and above, at which, according to publications [1,2], the effect of interaction between the chains is of importance. In order to compare their behavior with theory, it is essential to investigate those linear polymers which do not possess side chains capable of rotation. The ones investigated in this work are polyethylene and polymerized trifluorethylene.

The adiabatic calorimeter described earlier [3] has been used by us in this work. The platinum resistance thermometer was after the pattern used by Strelkov [4], using spectroscopically pure platinum of IONKh-5 brand, and compared with another thermometer of the same type whose resistance had been tabulated against temperature in the range from 10.8 to 90°K. The polymer samples available to us were technically pure. The weight of polyethylene investigated was 22.6 g, and that of the polymerized trifluorethylene was 18.9 g. Measurement of the heat capacity was carried out at 0.5° intervals, and the rate of temperature equalization in the specimens was 8-10 min/deg. The heat capacity of the empty calorimeter was measured beforehand over the whole temperature range.

Our results are contained in Table 1. They are shown graphically on a logarithmic scale in Fig. 1.

Polyethylene. The heat capacity of polyethylene was measured between 17 and 100°K (measurements in a higher temperature region have been described by us in an earlier communication [5]). If we represent the relationship between heat capacity and temperature in the form: $c = AT^m$, then the figure shows that $m$ is greater than unity over the whole investigated range, varying from 2.15 to 1.1. According to publications [1,2,6], values of $m$ greater than unity are to be attributed to the effect of the forces of interaction between the chains. The results obtained in the present work and that reported in [5] show that in polyethylene the effect becomes noticeable at temperatures of the order of 90-100°K. The considerable temperature range within which the behavior of the heat capacity is not constant is bound to be given attention, but all the same the effect of interaction between the chains cannot be disregarded.

Polymerized trifluorethylene. The heat capacity of polymerized trifluorethylene was measured between 23 and 120°K. The figure shows that the value of $m$ varies from 1.3 at 23° K to unity at 30°K, and then rapidly diminishes to values less than 1. As early as about 35°K $m$ has the value of 0.65-0.70. Above 40°K the steepness of the heat capacity curve increases a little, so that at 60° $m$ has risen to 0.8. This value, $m = 0.8$, is maintained up to 120°K. The great reduction of the temperature interval in which there is any substantial effect of the interaction forces, compared with the corresponding range for polyethylene, is evidently to a considerable extent associated with the mass difference between the groups $CF_2$ and CFH on the one hand, and $CH_2$ on the other.

The temperature change of the heat capacity of polymerized trifluorethylene which we have found does not exclude the relationship described in [1,2], and it is applicable both to the region in which there is significant interaction between the chains, and to that in which this may be neglected. The change of slope noticed experimentally in the neighborhood of 60°K, may be attributed to the excitement of pendulum oscillations of the groups $CF_2$ and CFH, which will not be further treated in this paper (the so-called rocking oscillation of $CX_2$ groups which may only play a small part in the observed case involving heavy fluorine atoms) [7].

As has been observed earlier [5], the majority of linear polymers outside the very lowest temperatures show a nearly linear temperature change of the heat capacity, although there is some deviation in the direction of lower values of *m*. This fact is not difficult to correlate with the relationship discovered by Tarasov [6]. It is however, doubtful whether the experimentally observed heat capacity of such heavy polymers as polymerized trifluorethylene and teflon [8], at temperatures of the order of 80-100°K and above, is called forth only by the acoustic spectrum of their skeleton. At these temperatures it is necessary to take into consideration that portion of the heat capacity associated with the deformation oscillations of the $CF_2$ and CFH groups. This would result in still greater discrepancies between experimental results and the Tarasov formula. We do not consider at present that sufficient accuracy is available for it to be possible to distinguish from the total heat capacity of polytrifluorethylene that part which is to be attributed to the oscillations mentioned above. All the same, the values of *m* obtained in this work, 0.65-0.70 at sufficiently low temperatures, reveal the possibility of significant divergence from the relationship proposed by Tarasov.

TABLE 1

| Temp. °K | c,cal/deg • g | | Temp. °K | c,cal/deg • g | | Temp. °K | c,cal/deg • g | |
|---|---|---|---|---|---|---|---|---|
| | poly-ethylene | polytri-fluor-ethylene | | poly-ethylene | polytri-fluor-ethylene | | poly-ethylene | polytrifluor-ethylene |
| 17 | $0.012_8$ | — | 39 | $0.057_4$ | $0.043_7$ | 61 | — | $0.060_0$ |
| 18 | $0.014_0$ | — | 40 | $0.059_7$ | $0.044_4$ | 62 | — | $0.061_1$ |
| 19 | $0.015_0$ | — | 41 | $0.061_8$ | $0.045_1$ | 63 | — | $0.062_0$ |
| 20 | $0.017_3$ | — | 42 | $0.063_9$ | $0.045_8$ | 64 | — | $0.063_0$ |
| 21 | $0.019_3$ | — | 43 | $0.066_1$ | $0.046_5$ | 65 | — | $0.064_1$ |
| 22 | $0.021_4$ | — | 44 | $0.068_2$ | $0.047_2$ | 66 | — | $0.065_0$ |
| 23 | $0.023_5$ | $0.026_1$ | 45 | $0.070_3$ | $0.047_9$ | 67 | — | $0.066_0$ |
| 24 | $0.025_6$ | $0.027_6$ | 46 | $0.072_3$ | $0.048_6$ | 68 | — | $0.067_0$ |
| 25 | $0.027_8$ | $0.029_2$ | 47 | $0.074_4$ | $0.049_2$ | 69 | — | $0.068_0$ |
| 26 | $0.029_9$ | $0.030_7$ | 48 | $0.076_5$ | $0.049_9$ | 70 | — | $0.068_9$ |
| 27 | $0.032_0$ | $0.032_1$ | 49 | $0.078_5$ | $0.050_6$ | 75 | — | $0.073_4$ |
| 28 | $0.034_2$ | $0.033_4$ | 50 | $0.080_6$ | $0.051_3$ | 80 | — | $0.077_5$ |
| 29 | $0.036_3$ | $0.034_5$ | 51 | $0.082_6$ | $0.051_9$ | 85 | — | $0.081_6$ |
| 30 | $0.038_4$ | $0.035_8$ | 52 | $0.084_5$ | $0.052_5$ | 90 | — | $0.085_3$ |
| 31 | $0.040_7$ | $0.036_8$ | 53 | $0.086_5$ | $0.053_3$ | 95 | — | $0.089_1$ |
| 32 | $0.042_8$ | $0.037_9$ | 54 | $0.088_5$ | $0.054_0$ | 100 | — | $0.092_7$ |
| 33 | $0.044_8$ | $0.038_6$ | 55 | $0.090_5$ | $0.054_7$ | 105 | — | $0.096_8$ |
| 34 | $0.047_0$ | $0.039_6$ | 56 | $0.092_3$ | $0.055_5$ | 110 | — | $0.100_6$ |
| 35 | $0.049_1$ | $0.040_5$ | 57 | $0.094_1$ | $0.056_3$ | 115 | — | $0.104_4$ |
| 36 | $0.051_2$ | $0.041_3$ | 58 | $0.095_9$ | $0.057_0$ | 120 | — | $0.108_1$ |
| 37 | $0.053_3$ | $0.042_1$ | 59 | $0.097_8$ | $0.058_1$ | | | |
| 38 | $0.055_4$ | $0.043_0$ | 60 | $0.099_6$ | $0.059_1$ | | | |

In conclusion I must offer my best thanks to Corresponding Member, Academy of Sciences, USSR, A. I. Shal'nikov for his permission to carry out measurements at the temperatures of liquid hydrogen in the Department of Low Temperature Physics at Moscow State University, and for his constant interest in the work; and also to O. N. Trapeznikova for his interest in the work and his valuable advice, and A. S. Borovik-Romanov for his help in the construction of the platinum resistance thermometer.

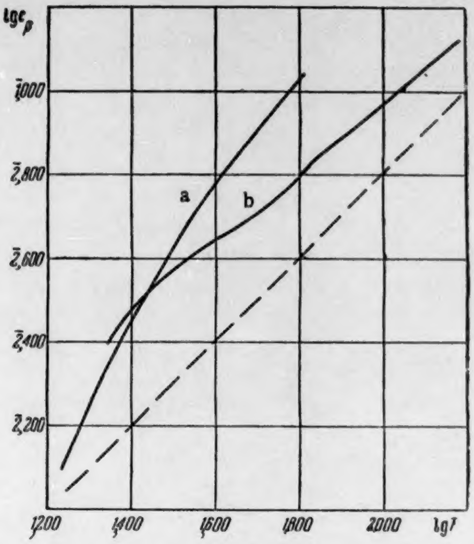

Fig. 1. Logarithmic relationship between $c_p$ and T for a) polyethylene and b) polytrifluorethylene. Dotted line denotes m = 1.

## LITERATURE CITED

[1] I. M. Lifshits, Zhur. éksp. teor. Fiz., 22, 471, 475 (1952).

[2] S. M. Genensky, G. F. Newell, J. Chem. Phys., 26, No.3 (1957).

[3] I. V. Sochava and O. N. Trapeznikova, Leningrad University Herald (Vestn. Leningr. Univ.)[in Russian] 3, 16, (1958).

[4] P. G. Strelkov, A. S. Borovik-Romanov and M. P. Orlova, Zhur. fiz. Khim., 28, v. 2 (1954).

[5] I. V. Sochava and O. N. Trapeznikova, Dokl. Akad. Nauk. SSSR, 113, No.4 (1957).*

[6] V. V. Tarasov, Zhur. fiz. Khim., 24, 111 (1950).

[7] C. J. Liang, S. Krim, and G. B. Sutherland, J. Chem. Phys., 25, 543 (1956).

[8] G. T. Furukawa, R. E. McCoskey, and G. J. King, J. Res. Nat. Bur. Stand., 49, No.4 (1952).

---

* Original Russian pagination. See C. B. translation.

# THE INFLUENCE OF HALIDE IONS ON THE CORROSION OF 18-8 STAINLESS STEEL IN SULFURIC ACID

Hua Pao-ting, Shan Hsin-su, Z. A. Iofa
and E. I. Mikhailova

Institute of Applied Chemistry Acad. Sci. ChPR, Changchun
Lomonosov State University of Moscow

(Presented by Academician A. N. Frumkin, July 30, 1959)

(Translated from: Doklady Akademii Nauk SSSR, Vol. 130, No.1, pp. 129-132, 1960)

Original article submitted July 30, 1959.

It is well known that the corrosion resistance of stainless steels is connected with their disposition to passivity. If oxides are absent, 18-8 stainless steel is dissolved in sulfuric acid at a fair rate [1]. S.M. Babitskii and Kh. L. Tseitlin [2] have found that the addition of small amounts of halides considerably decreases the dissolution rate of 18-8 stainless steel in sulfuric acid solutions.

The inhibition by halide ions of acid corrosion of pure iron was observed for the first time by Walpert [3] and has been investigated in more detail by Z. A. Iofa and co-workers [4-7]. It has been shown that halide ions from acid solutions are adsorbed on the surface of the iron and form strongly bound but ill-fitting chemisorptive layers which retard the electrochemical reaction rate on the iron, particularly the discharging of the protons. The change of the electrochemical properties of the iron surface (probably a shift of the standard potential of iron to more positive values), caused by the presence of the halide ions, facilitates the adsorption of inhibitors which are organic compounds with a basic character and, therefore, these inhibitors become effective.

When applying these conclusions to stainless steels, one meets the difficulty that halide ions, principally chlorine ions, destroy the passivating film [1,8-10] and, therefore, should increase the dissolution rate of stainless steel in sulfuric acid.

In order to elucidate the way in which the halide ions act, the dissolution rate of 18-8* stainless steel in 10 N $H_2SO_4$ was measured in the Institute of Applied Chemistry of the Academy of Science of the Chinese People's Republic and in the Electrochemistry Department of the Lomonosov State University of Moscow by determining the weight loss of the sample or the evolution rate of hydrogen as a function of the concentration of added NaCl, KBr and KI, and the polarization curves in 10 N $H_2SO_4$, pure and with addition of the said salts, in a hydrogen atmosphere at room temperature were also determined there. The curves shown in Figs. 1 and 2 were obtained in China, those of Figs. 3 and 4 in Moscow.

The curves of Figs. 1 and 2 show the dependence of the dissolution rate of steel $\rho$ (in mg / $cm^2$·hour) upon the concentration (percentage) of the added halides, and from the curves it is obvious that halide ions retard the dissolution rate of 18-8 steel in acid and that there is an optimum halide concentration at which the said retardation is largest. Table 1 gives approximate values of the optimum halide concentration and of the corresponding dissolution rates of 18-8 steel in 10 N $H_2SO_4$.

---

*In the last series of experiments a steel has been used containing (in %): Ni 9.3, Cr 16.8, C 0.14, Si 0.25, Mn 0.84, Ti < 0.05, S 0.019, P 0.013.

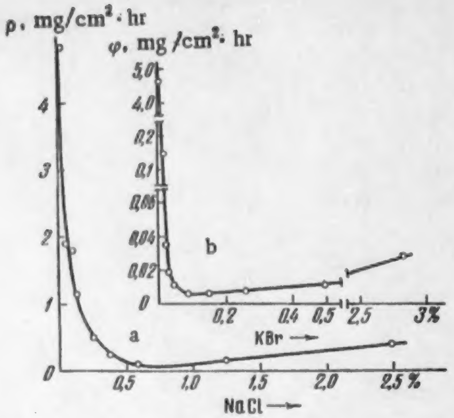

Fig. 1. The dependence of the dissolution rate of steel 18-8 in 10 N $H_2SO_4$ on the concentration of added salts: a) NaCl, b) KBr.

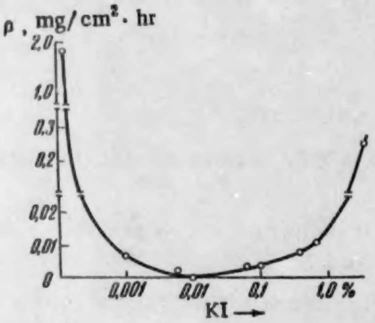

Fig. 2. The dependence of the dissolution rate of 18-8 steel in 10 N $H_2SO_4$ upon the logarithm of the concentration of added KI.

TABLE 1

| Added salt | Optimum concen-tration, M/liter | Corrosion rate, g/cm²·hr | Corrosion retardation coeff. |
|---|---|---|---|
| Without addition | — | $3\cdot10^{-3}$ | 1 |
| NaCl | 0,1 | $5\cdot10^{-5}$ | 60 |
| KBr | 0,008 | $5\cdot10^{-6}$ | 600 |
| KI | 0,0006 | $7\cdot10^{-7}$ | 4000 |

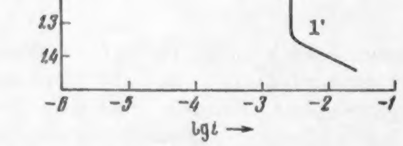

Fig. 3. Polarization curves for an 18-8 stainless steel electrode: 1,1') in 10 N $H_2SO_4$; 2,2') in 10 N $H_2SO_4$ + 0.1 N NaCl.

At a halide concentration below the optimum one the corrosion rate increases with time, but at a concentration above the optimum one it decreases. From Table 1 it is obvious that the halide concentration at which the largest suppression of corrosion is observed decreases, and the inhibitory effect increases, in the sequence Cl-Br-I.

From the polarization curves shown in Fig. 3 it follows that at the stationary potential 18-8 steel is active in 10 N $H_2SO_4$, but that the passivity starts at more positive potentials and at anodic current densities surpassing the current density of self-attack. The chlorine ions added to the acid destroy the passivity of the steel; it cannot be passivated at all values of $i_a$ shown in Fig. 3. Moreover, chlorine ions accelerate the anodic process in the range of potentials at which the steel is active in the absence of chlorine ions. Comparing the cathodic curves it is obvious that chlorine ions increase the hydrogen overvoltage and shift the stationary potential to more negative values. The corrosion retardation at the stationary potential is entirely caused by the increase of the hydrogen overvoltage. Owing to this, the destruction of passivity by chlorine ions does not lead to an increasing self-attack of the steel.

In Fig. 4 are shown the polarization curves in pure 10 N $H_2SO_4$ (curves 1,1') and after addition of KBr and KI in concentrations nearly equal to the optimum ones (curves 2,2' and 3,3'). In these cases the steel is active at the stationary potential, however, in contrast to chlorine ions, bromine and iodine ions in the said small concentrations retard the anodic ionization of the metal and, in the case of iodine ions, this causes a shift of the stationary potential to more positive values. In the presence of these ions the passivation starts at lower values of $i_a$ than in pure $H_2SO_4$, though at more positive potentials. The retardation of the anodic process and the increase of the hydrogen overvoltage cause a fair retardation of the corrosion rate. Thus, the chemisorbed layer of halide ions, which increases the hydrogen overvoltage and obviously does not disappear at more positive potentials, causes the passivation of steel at anodic polarization in the case of bromine and iodine ions and prevents the onset of passivity in the case of chlorine ions.

The fact that in the presence of chlorine ions, contrasted with bromine and iodine ions, passivity does not originate with anodic polarization shows that the adsorptive interchange occurs more easily between the passivator – chemisorbed oxygen [10] – and chlorine ions than with bromine and iodine ions. When the concentration is considerably increased above the optimum value, bromine and iodine ions, like chlorine ions, facilitate the ionization and prevent the passivation of 18-8 steel with anodic polarization. Upon increasing the concentration of KI one also observes a decrease in the hydrogen overvoltage (Fig. 4: 4, 4') and in the inhibitory effect on the corrosion (Fig. 2).

A similar increase of the dissolution rate upon addition of high concentrations of KI to an acid solution is also observed in the case of pure iron. For instance, the dissolution rate of Armco iron in 4 N $H_2SO_4$ changes with a change of the KI concentration in the following way:

| | | | | |
|---|---|---|---|---|
| KI concentration | 0,001$N$ | 0,02$N$ | 0,1$N$ | 1,0$N$ |
| $\rho$, g / cm$^2$ · hour | $4{,}2\cdot10^{-5}$ | $2{,}2\cdot10^{-7}$ | $2{,}0\cdot10^{-7}$ | $5{,}2\cdot10^{-7}$ |

One may suppose that the reversal of the effect upon addition of high KI concentrations is connected with the forming of an iodine anion layer by the side of the chemisorbed layer, which anion layer is still weakly bound to the metal and has a reverse influence upon the hydrogen overvoltage, just as is the case for the adsorption of these anions on mercury [11]. In the anodic process a participation of adsorbed anions in the elementary step of the metal ionization, initiated by the formation of complex anions, is also possible.

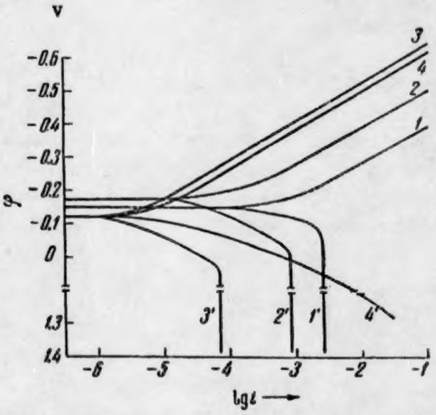

Fig. 4. Polarization curves for an 18-8 stainless steel electrode; 1,1') in 10 N $H_2SO_4$; 2,2') + 0.01 N KBr 3,3') + 0.001 N KI; 4,4') + 0.2 N KI.

TABLE 2

The Dissolution Rate of 18-8 Steel in 10 N $H_2SO_4$

| Addition | $\rho$, g/cm$^2$ · hr | Corrosion retardation coefficient |
|---|---|---|
| without addition | $1.5\cdot10^{-3}$ | 1 |
| 0,0005 $N$ KI | $8\cdot10^{-7}$ | 1800 |
| 0,001 $M$ $[N(C_4H_9)_4]_2SO_4$ | $9.4\cdot10^{-4}$ | 1,60 |
| 0,001 $M$ $[N(C_4H_9)_4]_2SO_4$ + + 0,0005 $N$ KI | $1.2\cdot10^{-7}$ | 12000 |
| 0,003 $N$ $Na_2S$ | $7.2\ 10^{-4}$ | 2.1 |
| 0,003 $N$ $Na_2S$ + 0,001 $M$ $[N(C_4H_9)_4]_2SO_4$ | $5.6\cdot10^{-6}$ | 270 |

The resemblance in behavior of 18-8 steel and of iron is also observed in other processes, for instance, in the fact that the presence of halide ions [6] or sulfides [12] increases the inhibitory effect of organic cations in an acid solution. In Table 2 the dissolution rate of steel in 10 N $H_2SO_4$ is given.

The data obtained in this investigation, particularly the promotion of the passivation by bromine and iodine ions, are, in our opinion, of interest to the general theory of passivation, because they are incompatible with the assumption that the adsorbed layers form a distinct phase, and because they affirm the importance of adsorption phenomena.

## LITERATURE CITED

[1] G. V. Akimov, Elementary Textbook of Metallic Corrosion and Protection [In Russian] (Moscow, 1946).

[2] S. M. Babitskii and Kh. L. Tseitlin, Research on Stainless Steels [In Russian] (Acad. Sci. USSR Press, 1956), p. 69.

[3] G. Walpert, Zs. phys. Chem., A. 151, 219 (1931).

[4] Z. A. Iofa, E. I. Lyakhovetskaya and K. Sharifov, Doklady Akad. Nauk SSSR 84, 543 (1952).

[5] Z. A. Iofa and G. B. Rozhdestvenskaya, Doklady Akad. Nauk SSSR 91, 1159 (1953).

[6] Z. A. Iofa, Vestnik Moskov. Univ., 2,139 (1956).

[7] E. O. Ayazyan, Doklady Akad. Nauk SSSR, 100, 473 (1955).

[8] U. R. Evans, Metallic Corrosion, Passivity and Protection (Moscow, 1941) [Russian translation].

[9] G. V. Ershler, Transactions of the Second Conference on Metallic Corrosion [In Russian] 2, 58 (1943).

[10] L. Vanyukova and B. Kabanov, Doklady Akad. Nauk SSSR 59, 917 (1948).

[11] Z. Iofa, B. Kabanov and others, Zhur. Fiz. Khim. USSR 26, 1326 (1939).

[12] Z. A. Iofa, Theses, Proceedings and Communications of the All-Union Scientific-Technical Conference on Metallic Corrosion and Protection, 3, 11 (1958) [In Russian].

# CONCERNING SOME PECULIARITIES OF THE ELECTROCHEMICAL SOLUTION OF n-TYPE SILICON

E. A. Efimov and I. G. Erusalimchik

(Presented by Academician A. N. Frumkin, September 8, 1959)

(Translation of: Doklady Akademii Nauk SSSR, Vol. 130, No.2,
1960, pp. 353-355)

Original article submitted September 8, 1959.

The question of the character of the holes in the case of anodic semiconductor solution is of great interest in the study of the effect of the electrochemical reaction mechanism upon germanium and silicon electrodes.

Direct evidence has recently been obtained [1-3] that during the anodic solution of germanium the holes, which are indispensable for the electrochemical reaction, are supplied mainly from the volume of the semiconductor. This cannot be said of silicon. By studying the anodic solution of n-type silicon in 5% HF solution, Flynn [4] discovered that the hole saturation current is of the order of magnitude of $10^{-5}$ amp/cm$^2$. This experimental value of the saturation current in conjunction with a series of theoretical calculations made by the author gave him the idea that in the process of silicon solution (as opposed to germanium solution) mainly those holes were expended which had been formed at the electrolyte interface as the result of generation in the space-charge region of the semiconductor, and only a neglible amount of the expended holes had been created within the semiconductor volume.

Flynn's hypothesis can be verified experimentally, and an unambiguous answer can be given by employing as the electrode under study a thin wafer of n-type silicon with a p-n junction.

In the present work the method described in [3] was used. The experiments were carried out using a wafer of n-type silicon with a specific resistivity of 3 ohm · cm for which the lifetime of the minority current carriers was about 100 μ sec. By means of aluminum melting a p-n junction was formed on one side of the plate with an over-all surface of 0.03 cm$^2$. A circular ohmic contact (the base) was alloyed to this side of the electrode. The entire plate together with the leads was insulated first with silicone varnish and then with paraffin, except for a region lying opposite the p-n junction and somewhat smaller in area. The width of the n-type silicon stratum located between the boundary of the p-type region and the electrolyte was about 20-25μ.

All experiments were carried out in 2.5 N HF at 20°. The electrolyzer and all the cell elements were made of teflon. The potential was measured against a saturated calomel semielement with subsequent recalculation on the hydrogen scale. The electrical arrangement made possible the measurement of the electrode potential during the application of reverse bias to the p-n junction, as well as during the interval when the inner junction circuit was opened. Before each experiment the surface of the electrode was treated with a mixture of nitric and hydrofluoric acids (4:1) and then with concentrated hydrofluoric acid.

In Fig. 1 the polarization curves for the anodic solution of silicon are shown for current densities of from $10^{-6}$ to $5 \cdot 10^{-4}$ amp/cm$^2$. Curve 1 was obtained for the case where the inner circuit of the p-n junction was open and the positive pole of the current source was connected to the ohmic contact. Curve 2 was obtained when a reverse bias of 100 v was applied to the p-n junction. It coincides fully with curve 1. In other words the anodic solution potential of silicon was not affected by the application of reverse bias to the p-n junction. For comparative purposes we show curves drawn for ordinary silicon electrodes of 3 ohm · cm (Curve 3) and 10 ohm · cm (Curve 4) specific resistivity. It can easily be seen from Fig. 1 that the process of anodic silicon solution (Curves 1,3) was not affected by a sharp change in the width of the electrode for the same specific resistivity, contrary to the observations for the germanium electrode [3].

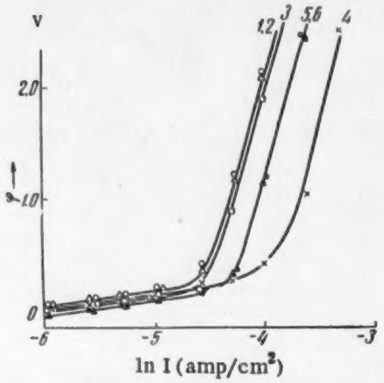

Fig. 1. Anodic polarization during the solution of n-type silicon. (Explained in text).

These experimental data obviously show that the holes used up in the electrochemical reaction were formed principally within the surface layers of the electrode and not within its volume. If this assumption were not correct,then the decrease in the electrode width and especially the increase in width of the zone, impoverished as far as current carriers are concerned due to the application of a large reverse bias to the p-n junction, would have sharply decreased the volume of the semiconductor in which are generated the holes that are used in the reaction. This phenomenon, in turn, would have resulted in a noticeable decrease in the saturation current ;this is what takes place in the case of germanium [3]. A noticeable increase in the hole saturation current due to an increase in the specific resistivity of silicon from 3 ohm · cm (Fig. 1,3) to 10 ohm · cm (Fig. 1,4) is obviously connected with the increase in the width of the space-charge region at the electrolyte boundary in which the holes used during the anodic reaction are generated [5].

If we assume that all the holes used in the anodic solution of silicon are formed only as the result of surface generation, then it is doubtful whether the value of the saturation current would be so strongly dependent upon the specific resistivity of silicon. Besides – as Flynn has pointed out – such an assumption would lead to inadmissibly high values of surface recombination for silicon. The fact that the holes used up during the anodic solution of silicon are formed mainly in the space-charge region of the semiconductor at the electrolyte boundary must exert a special influence upon the character of the action of the additional reducers and oxidizers. It was shown in [6] that the presence of the $C_2O_4^{2-}$ leads to an increase in the hole saturation current in n-type germanium. The authors connected this effect with the appearance at the surface of an additional number of holes which must have come from the depths of the semiconductor depth as a result of the action of a strong electric field. It is obvious that such an effort should not be observed at a silicon electrode since the holes generated within the volume of the semiconductor take practically no part in the anodic process. The experimental data fully confirm this assumption. The anodic curves taken for silicon with specific resistivities $\rho$ = 10 ohm · cm and $\rho$ = 3 ohm · cm in 2.5 N HF + 1.0 N $K_2C_2O_4$, coincide with curves 3 and 4, Fig. 1, which were obtained without the addition of potassium oxalate.

Therefore the increase of the hole saturation current during the introduction of an oxidizer of the type $K_3Fe(CN)_6$, as discovered by Gerisher and Beck [7], must also occur for the case of a silicon electrode, since in this case an additional number of holes immediately appears on the semiconductor surface. This is confirmed by curves 5 and 6, Fig. 1 obtained for the solution 2.5 N HF + 0.05 N $K_3Fe(CN)_6$. Both curves, the one obtained when a reverse bias was applied to the p-n junction and the one obtained with an open inner circuit, coincide.

Thus the experiments which we have conducted provide direct proof of the fact that the holes used during the anodic solution of silicon are generated principally in the space-charge region at the electrolyte boundary and not within the volume of the semiconductor.

## LITERATURE CITED

[1] D. Turner, J. Electr. Soc., 103, 252 (1956).

[2] E. A. Efimov and I. G. Erusalimchik, Zh. F. Kh., 32, 413, 1103 (1958).

[3] E. A. Efimov and I. G. Erusalimchik, Dokl. Akad. Nauk 122, 632 (1958).*

---

*Original Russian pagination. See C. B. translation.

[4] J. Flynn, J. Electrical Soc., 105, 715 (1958).

[5] W. Shockley, Bell System Technical Journal, 28, 435 (1949).

[6] E. A. Efimov and I. G. Erusalimchik, Dokl. Akad. Nauk, 128, 1 (1959).[*]

[7] H. Gerisher and F. Beck, Z. Phys. Chem., Neue Folge, 13, 389 (1957).

---

[*] Original Russian pagination. See C. B. translation.

# THE GLASS TRANSITION TEMPERATURE OF CELLULOSE

Academicians V. A. Kargin, P. V. Kozlov,
and Wang Nai- ch'ang

M. V. Lomonosov Moscow State University

(Translation of: Doklady Akademii Nauk SSSR, Vol. 130, No. 2, 1960, pp. 356-358)

Original article submitted October 9, 1959.

It is well known that cellulose, a very rigid polymer, does not show temperature transitions from one physical form into another. We assume that this is connected with the fact that such temperature points lie above the thermal decomposition temperature of cellulose. At the same time it would be of considerable theoretical interest to establish by some indirect method whether there are two transition temperatures, i.e., a glass transition temperature $T_g$ (the transition point from the vitreous to the highly elastic state) and a flow temperature $T_f$.

It is also well known that for a given polymer $T_g$ may be lowered by introducing plasticizers into the polymer. This has been shown for nitrocellulose [1] and for a synthetic polymer such as polyurea, in which the molecular chains have a very rigid configuration [2]. By introducing into a polymer different concentrations of plasticizer, and plotting the dependence of the change of $T_g$ upon the plasticizer concentration, it seemed reasonable to extrapolate the experimental curve to the zero concentration of plasticizer and thus to determine $T_g$ for the given polymer. We chose this method for determining the glass transition temperature of cellulose.

The cellulose used for this purpose was ordinary sulfite pulp, such as is used in viscose manufacture, having an average molecular weight of 210426. It was first extracted with dichloroethane in a Soxhlet apparatus for 24 hours to remove resins and fats, dried, and dissolved in a 36.5% aqueous solution of triethylphenylammonium hydroxide to convert it into a powdered form. The cellulose was precipitated from this solution with a 10% solution of hydrochloric acid, filtered off, carefully washed first with water, then with ethyl alcohol and diethyl ether, treated with acetone, and dried. The molecular weight of the regenerated cellulose was not determined because it is known that the specific viscosity of different types of cellulose in aqueous solutions of triethylphenylammonium hydroxide changes only slightly on standing for two days [3].

To a weighed sample of cellulose powder was added a measured quantity of an aqueous solution of triethylphenylammonium hydroxide as a plasticizer. Acetone was added in the proportion of 10 ml to 1 g of cellulose powder, and samples were air-dried at 75°. The mixture of powder and plasticizer was pressed at a pressure of 100 $\text{atmos}/\text{cm}^2$ and 160° into tablets, which were used for determining the thermomechanical properties of the products on a tensile-testing machine [4]. The temperature was raised at the rate of 1° per min.

The results of the thermomechanical tests are depicted in Fig. 1.

From the inflections of the thermomechanical curves the glass transition temperatures of cellulose plasticized with different concentrations of triethylphenylammonium hydroxide were determined. These points were plotted on a curve relating the glass transition temperature to the plasticizer concentration (see Fig. 2, curve 2). Extrapolation of this curve to the zero concentration of plasticizer gave the glass transition temperature of cellulose, which corresponds to about 370° for this particular sample. However, the definition of $T_g$ as the temperature of the inflection of the thermomechanical curve gives us temperature values which indicate the appearance of highly elastic deformation at a given loading rate. In practice, this means the appearance of highly elastic, rubberlike properties in a polymer, and it may therefore be stated that rubberlike properties would become evident in cellulose only at temperatures above 370°.

On the other hand, we are also justified in evaluating the temperature at which the chains have a minimum mobility, which characterizes the first indications of highly elastic deformation. At this temperature the velocity of the relaxation processes is such that any structural changes connected with the mobility of the chains may take place. This value of $T_g$ is defined by the deflection of the thermomechanical curve, which corresponds to the classical determination of $T_g$ for substances of low molecular weight. By way of illustration, in Fig. 1 (curve 3, thermomechanical) both temperature points ($T_1$ , $T_2$).

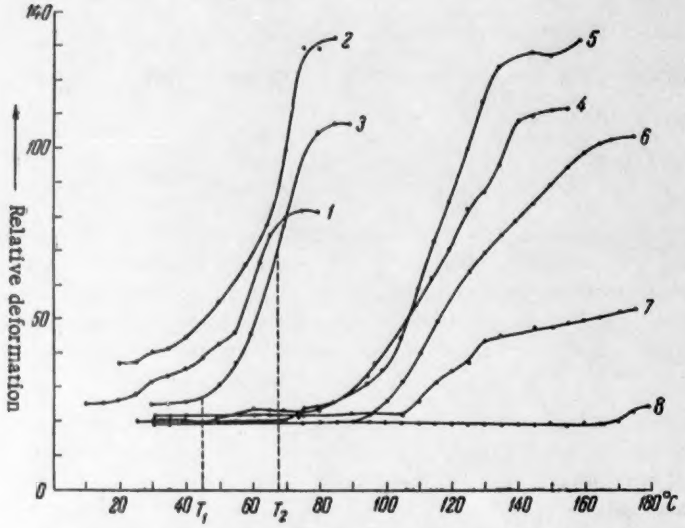

Fig. 1. Thermomechanical curves of samples of cellulose plasticized with triethylphenylammonium hydroxide. Concentration of plasticizer by weight of mixture: 1) 37%; 2) 35%; 3) 32%; 4) 30%; 5) 28%; 6) 25%; 7) 20%; 8) 10%.

In Fig. 2 are given values of $T_g$ as determined from the beginning of the deflection of the thermomechanical curves ($T_1$), as well as the temperature corresponding to the beginning of rubberlike elasticity ($T_2$).

From these data it follows that rubberlike properties may develop in cellulose at temperatures above 370°, and that the glass transition temperature, below which the appearance of highly elastic properties or spontaneous structural changes is impossible, corresponds to 220°.

For mainly historical reasons, cellulose has always occupied a special place among high molecular weight compounds. At the same time cellulose is a polymer with linear and regularly formed chains, and it appeared to us quite essential to establish its proper place among other polymers since we would now like to treat it as a synthetic polymeric product. In this case the transition temperature of one physical form into another is a fundamental characteristic of the properties of a polymer, and therefore the determination of the glass transition temperature seemed to us very important for an understanding of the properties of cellulose.

In view of the experimental data presented above, we are convinced that the glass transition temperature of cellulose lies about 40° above its chemical decomposition temperature, since, as is well known, a fairly rapid chemical decomposition of cellulose begins at 180° [5]. Consequently, very pure cellulose always exists in the vitreous state. This fact is related to a number of properties which separate cellulose from a whole series of synthetic polymers which were intentionally synthesized in such a way that their transition temperatures were always below their chemical decomposition temperatures. In the first place, cellulose very easily forms strained structures, because the mobility of molecular chains in polymeric glasses is insignificant, and any treatment of cellulose will naturally change the mutual positions of the chains, and hence the structure of the material. The fact that the application of external forces is necessary for the formation of particular structures, especially oriented, highly ordered ones, is also associated with the vitreous state.

Finally, the reason for the amorphous nature of cellulose becomes quite clear because, in general, a substance cannot be crystallized if it exists in the vitreous state. Introduction of low molecular weight substances, capable of lowering the glass transition temperature of a polymer, destroys the geometrical order in the positions of the molecular chains, which is present in pure linear polymers, and which is necessary for crystallizing a polymeric substance.

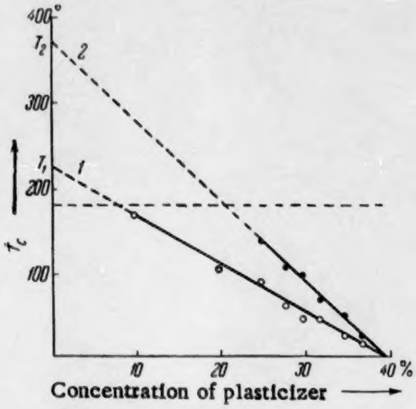

Fig. 2. Dependence of the glass transition temperature of cellulose $T_g$ upon the plasticizer concentration (triethylphenylammonium hydroxide), determined from the thermomechanical curves: 1) from the point of deflection; 2) from the point of inflection.

## LITERATURE CITED

[1] P. V. Kozlov and E. F. Russkova, Doklady Akad. Nauk SSSR 99, 105 (1954).

[2] P. V. Kozlov, A. Endrykhovskaya and V. A. Kargin, Doklady Akad. Nauk SSSR 129, 4 (1959).

[3] N. S. Nikolaeva, E. M. Mogilevskii, and Z. K. Lin'kova, Tekstil'. Prom. 4, 9 (1958).

[4] V. A. Kargin and T. I. Sogolova, Zhur. Fiz. Khim. 23, 530 (1949).

[5] Z. A. Rogovin, V. A. Kargin, and T. A. Finkel'shtein, Tekstil'. Prom. 8, 9 (1950).

# THE MAXIMUM SOLUBILITY OF A COMPONENT OF A GASEOUS MIXTURE IN A LIQUID

A. Yu. Namiot

The All-Union Scientific Research Institute for Petroleum Gas

(Presented by Academician S. I. Vol'fkovich, August 12, 1959)

(Translation of: Doklady Akademii Nauk SSSR, Vol. 130, No. 2, 1960
pp. 359-361)

Original article submitted July 22, 1959.

The solubility—pressure relations for the dissolving of certain pure gases in liquids are known to show maxima [1]. The thermodynamic analysis of I. R. Krichevskii [1] has given the following conditions for the appearance of a solubility maximum in a binary system:

$$N''_1(\bar{v}'_1 - \bar{v}''_1) + N'_2(\bar{v}'_2 - \bar{v}''_2) = 0. \tag{1}$$

here $N_1$ and $N_2$ are, respectively, the mole fractions of the solvent, component 1, and the dissolving gas, component 2; $\bar{v}_1$ and $\bar{v}_2$ are the partial molar volumes of the respective components; and the indices (stroke) and " (double stroke) designate the liquid phase and the gaseous phase,respectively.

This condition for the existence of a maximum will take the more simple form of

$$\bar{v}'_2 = v_2^{0''} \tag{2}$$

when the solvent vapors in the gas phase can be neglected, i.e., the partial molar volume of the dissolved gas at maximum solubility is then equal to the molar volume of the pure gas ($v_2^{0''}$) under the same pressure and temperature.

The known cases of a solubility maximum for the dissolving of pure gases in liquids are met at high pressures ranging from one thousand to several thousand atmospheres. A solubility maximum for the dissolving of a component of a gas mixture in a liquid is observed in certain cases at comparatively low pressures. Thus our calculations on the dissolving of propane – methane mixtures containing a fixed small amount of propane in water at 40° have shown the dissolved propane to increase up to a pressure of approximately 90 atmospheres. A further increase in the pressure of the mixtures diminishes the amount of propane in the gas-saturated aqueous solution.

An analysis of the solubility maximum for the dissolving of a component of a ternary mixture can be based on the differential equation for two-phase equilibrium. The ternary system in question here will consist of one liquid component 1, the solvent, and two gaseous components 2 and 3. The solvent vapors in the gaseous phase will be neglected. Equating the differential of the chemical potential of component 3 in the gaseous phase, $d\mu''_3$, and the differential of the potential of this same component in the liquid phase, $d\mu'_3$, and imposing the condition of phase equilibrium at constant temperature with a gaseous phase of fixed composition, gives

$$\left(\frac{\partial N'_3}{\partial P}\right)_{\text{equ. } T, N''_2, N''_3} = \frac{\bar{v}'_3 - \bar{v}''_3 - (\partial\mu'_3 / \partial N'_2)_{P, T, N'_3} (\partial N'_2 / \partial P)_{\text{equ. } T, N''_2, N''_3}}{(\partial\mu'_3 / \partial N'_3)_{P, T, N'_2}} . \tag{3}$$

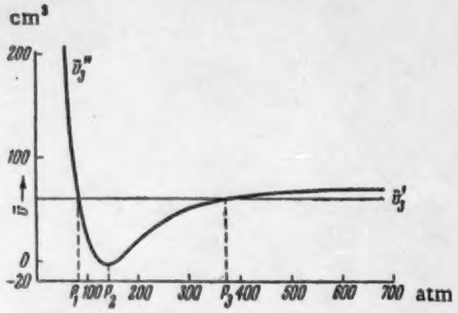

Fig.1.

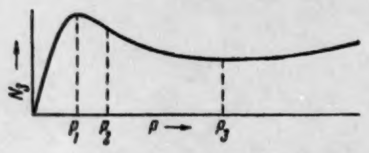

Fig.2.

The condition for maximum solubility is that the derivative $(\partial N_3'/\partial P)$ equ. $T, N_2'', N_3''$, i.e., the numerator of the fraction of Eq. (3) should be zero.

Values of the terms entering into the numerator of Eq. (3) are known for the water (1) – methane (2) –propane (3) system. Partial molar volumes of propane, $\bar{v}_3''$, in binary mixtures with methane have been determined by Sage and Lacey [2]. Partial molar volumes of propane dissolved in water were measured in [3]. Experimental studies on the solubility of propane –methane mixtures in water which we have carried out with M. M. Bondareva [4] have shown the product $(\partial \mu_3'/\partial N_2')_{P,T,N_3'} \times (\partial N_2'/\partial P)$ equ. $T, N_2'', N_3''$ to be small in comparison with $\bar{v}_3'$. If this quantity is neglected, the condition for a solubility maximum in the dissolving of propane from a methane mixture reduces to the requirement that the partial molar volume of the propane in the gaseous phase be equal to the partial molar volume of the propane in the liquid phase.

Fig. 1 shows the partial molar volume of propane in the gaseous phase, $\bar{v}_3''$, as a function of pressure, at 37.8° and with $N_3' = 0.1$ [2]. A line representing the partial molar volume of propane dissolved in water at 29.1° and one atm [3] has been drawn through this figure. The low accuracy of the determinations makes it permissible to neglect difference between the temperatures under which $\bar{v}_3''$ and $\bar{v}_3'$ have been determined, as well as the pressure dependence of the molar volume of the propane dissolved in water.

The derivative $(\partial N_3'/\partial P)$ equ. $T, N_2'', N_3''$ must be equal to zero at the two points $P_1$ and $P_3$ of Fig. 1 where the $\bar{v}_3''$ curve crosses the $\bar{v}_3'$ line; extrema in the solubility – pressure relation are to be expected there. The extremum at $P_1 = 90$ atm corresponds to a solubility maximum, while that at pressure $P_3$ corresponds to a minimum. The pressure $P_2$ corresponds to a flex point on the solubility curve, the general form of which is shown in Fig. 2.

The peculiarities of the dissolving of propane in liquids from gaseous methane mixtures are due to the fact that the partial volume of the propane in such mixtures at relatively low pressures is less than the volume of either pure liquid propane or dissolved propane. It is even true that the partial molar volumes of propane in gas-phase mixtures with methane are negative [2] over the range of temperatures, pressures, and compositions which are in question here.

Mixtures of butane, or still heavier members of the paraffin series, with methane behave similarly [2]. Solubility maxima for the dissolving of these components of methane mixtures into water and other liquids must appear at relatively low pressures.

## LITERATURE CTIED

[1] I. R. Krichevskii, Gaseous Equilibria in Solutions at High Pressures [in Russian] (1952).

[2] B. H. Sage and W. N. Lacey, Thermodynamic Properties of the Lighter Paraffin Hydrocarbons and Nitrogen (New York, 1950).

[3] W. L. Masterton, J. Chem. Phys. 22, 1830 (1954).

[4] A. Yu. Namiot and M. M. Bondareva, Vsesoyuz. Neftegazovyi N-I., Nauchno-Tekhn. Sborn., II, 1959, p. 60.

# REDUCTION REACTIONS AT THE GERMANIUM CATHODE

Yu. V. Pleskov

Institute of Electrochemistry, Academy of Sciences, USSR

(Presented by Academician A. N. Frumkin September 17, 1959)

(Translated from Doklady Akademii Nauk SSSR Vol. 130, No.2, 1960, pp. 362-365)

Original article submitted September 10, 1959.

Free electrons and holes can participate in the electrochemical processes at semiconducting electrodes. It was believed earlier [1] that free electrons are involved in reduction reactions at the germanium electrode. Another suggestion [2] was to the effect that the reduction of $K_3Fe(CN)_6$ at the germanium electrode involved a transfer of electrons from the valence band of germanium to the $Fe(CN)_6^{3-}$ ions, with the production of holes in the metal. A previous paper of the author [3] has given direct proof of the injection of holes in n-germanium during reduction of $Fe(CN)_6^{3-}$ and $MnO_4^-$ ions. Thus the germanium – electrolyte interface can function as a emitter in certain reduction processes.

It has been the aim of the present work to study the kinetics of certain reduction reactions at the germanium electrode and to measure the coefficient of injection, i.e., the proportion of valence electrons in the total reduction current.

## EXPERIMENTAL METHOD

The electrodes which were used in measuring the coefficient of injection were in the form of discs, 6 mm in diameter and approximately 0.12 mm in thickness; these were prepared from monocrystalline n-germanium and had a specific resistance $\rho$ of 2.5 ohm • cm, a hole-diffusion path L of 0.5-0.7 mm and a (111) crystallographic orientation. A circular ohmic nickel contact soldered with tin was placed around the periphery of each disc. Indium was imbedded in the center of one side of the germanium plate to form a p-n junction approximately 3 mm in diameter. The quality of these two contacts was tested by obtaining their volt-ampere characteristics with direct current, and with alternating current and a cathodic oscillograph. The entire surface of the electrode, with the exception of a circle 1-2 mm in diameter on the side opposite the p-n junction was covered with a silicone lacquer and paraffin. The free surface was immersed in the electrolyte along with an auxiliary electrode for polarization and a reference electrode. The germanium–electrolyte interface functioned as an emitter when a cathodic current was passed through it, the p-n junction serving as the collector. A PÉ-312 electronic polarograph was used to record the alteration of the reverse current of the collector $I_{col}$ (with a bias $V_{col} = 3$ v) as a function of the reduction current, $I_{red}$; these data were employed in evaluating the coefficient of current amplification, $\alpha = \frac{\Delta I_{col}}{I_{red}}\Big|_{V_{col}}$ of this particular triode, all measurements being carried out with direct current.

The distance between the p-n junction and the electrolyte was no greater than 70-80$\mu$ so that practically all of the holes injected into the electrode by the electrochemical reaction reached the collector (the transfer coefficient in plane triodes of similar construction is 0.96-0.99). Thus the measured value of $\alpha$ is practically equal to the coefficient of injection $\gamma$, provided the rate of recombination at the germanium – electrolyte interface is low. The data of [4,5] and the low values obtained for $\Delta I_{col}$ when dry electrodes were put into the test electrolyte (with $I_{red} = 0$) all show clearly that this assumption is justified for electrodes free of adsorbed hydrogen.

Polarization curves for rotating disc electrodes of platinum, and monocrystalline germanium of types n ($\rho = 1.8$ ohm · cm, L = 0.3 mm) and p ($\rho = 2.8$ ohm · cm, L = 0.3 mm) were obtained with the aid of the PÉ-312 polarograph.

The germanium electrodes were etched in SR-4 before making measurements. The reactants were of high purity. All measurements were carried out in the dark in an atmosphere of purified nitrogen. The cited values of the electrode potentials are with reference to the normal hydrogen electrode.

## RESULTS

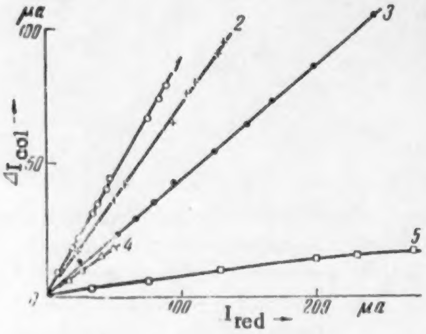

Fig 1. The relation between the reverse current of the collector and the reduction current; 1) $KMnO_4$; 2) $K_3Fe(CN)_6$; 3) $KI_3$; 4) quinone; 5) $K_2Cr_2O_7$.

Measurements of the injection coefficient. Curves showing the $\Delta I_{col}$—$I_{red}$ relations for five different oxidizing agents are given in Fig. 1. The value of $\alpha$ lies between 0 and 1 in each case, and is independent of $I_{red}$ in every case except that of $Cr_2O_7^{2-}$ (Table 1).

The reduction of $H_2O_2$ does not alter $I_{col}$ and is therefore not accompanied by hole injection in the germanium. The concentration of the oxidizing agent has a certain effect on $\alpha$ in $K_3Fe(CN)_6$ and $KMnO_4$, but not in $KI_3$.

The measured values of $\alpha$ are very sensitive to changes in the surface state of the electrode. The value of $\alpha$ begins to diminish as the germanium electrode is made more negative and approaches the potential for hydrogen evolution (Fig. 1, 5). The hydrogen which is evolved at the germanium cathode is either adsorbed on the semiconductor or penetrates into its crystal lattice, increasing the rate of surface recombination [6] and bringing about changes in the electrochemical properties of the metal [3,5]. It is clear that hydrogen adsorption begins at potentials which are less negative than that corresponding to visible evolution on the electrode, thus decreasing the electrode's transfer coefficient $\omega$ and the value of $\alpha$. The low value of $\alpha$ for the $K_2Cr_2O_7$ reduction and the absence of injection in the $H_2O_2$ reduction can possibly be explained by the fact that these reactions proceed at high negative potentials which are in the neighborhood of the value for the evolution of hydrogen, and the electrode is therefore hydrogenized.

The polarization curves for each of the investigated substances (solution compositions are indicated in Table 1) on platinum and n-germanium electrodes have clearly expressed wave form (there are two waves in the curve for the reduction of $KMnO_4$ on germanium), the saturation current density $i_{sat}$ being the same on each of the two metals. The saturation current density is proportional to the square root of the angular velocity of rotation, $\sqrt{\omega}$, of the electrode (Fig. 2, 4); the maximum reaction rate for reduction on a Pt or an n-Ge electrode is thus fixed by the speed at which the reducing particles diffuse through solution to the electrode surface [7] and is independent of the material of which the electrode is constructed. Illumination of the electrode has no effect on the wave height and is almost without influence on the form of the n-germanium polarization curve.

The curves for the reduction of $K_3Fe(CN)_6$, $K_2Cr_2O_7$, quinone, and $H_2O_2$ also contain a single wave (the $KMnO_4$ curve shows two waves), the value of $i_{sat}$ being the same as on Pt and n-Ge electrodes up to densities of 20 ma/cm$^2$, or 100 ma/cm$^2$, in the case of $K_3Fe(CN)_6$. The limit current approaches $\sqrt{\omega}$. These curves depart from the curves on n-Ge at 0.2 - 0.3 v, moving toward negative potential values; they approach similar curves developed on electron germanium when the electrode is illuminated.

The height of the reduction wave for $KI_3$ on p-Ge (Fig. 3, 1) is less than that for reduction on n-Ge and only slightly dependent on the agitation of the solution (Fig. 2, 1). Not only does this curve move toward positive potentials when the electrode is illuminated, but the saturation current then increases and reaches the value

TABLE 1

| Substance reduced | Concentration of substance reduced, moles/liter | Indifferent electrolyte | Germanium potential, v | Coefficient of injection, $\gamma$ | Maximum value of $I_{red}$, ma/cm² |
|---|---|---|---|---|---|
| $KMnO_4$ | 0,12 | 1 $N$ $H_2SO_4$ | 0.2 | 0.78—0.88 | 13.5 |
| $K_3Fe(CN)_6$ | 0.28—0.56 | 1—2 $N$ KOH | —0.2 | 0.66—0.80 | 8.6 |
| KI | 0.1—0.33 | 1 $N$ KI | 0.2 | 0.42 | 22 |
| Quinone | 0.4 | 1 $N$ $H_2SO_4$ | —0.4 | 0.38 | 3.3 |
| $K_2Cr_2O_7$ | 0.04—0.12 | 1 $N$ $H_2SO_4$ | —0.4 | 0.03—0.08 | 83 |
| $H_2O_2$ | 0.4 | 0,3 $N$ $K_2SO_4$ | —0.7 | 0 | 20 |

characteristic of Pt and n-Ge electrodes (Fig. 3,2). A 1-2 min preliminary hydrogenizing of the electrode at a current density of 10 ma/cm² has a similar effect on the reduction wave of $KI_3$. The saturation current of p-germanium under strong illumination or hydrogenization proves to be proportional to $\sqrt{\omega}$ over almost the entire range of experimental current densities (Fig. 2, 3). Moderate illumination of the electrode gives rise to a direct proportionality between $i_{sat}$ and $\sqrt{\omega}$ over a wide interval of $i_{sat}$ values (Fig. 2, 2).

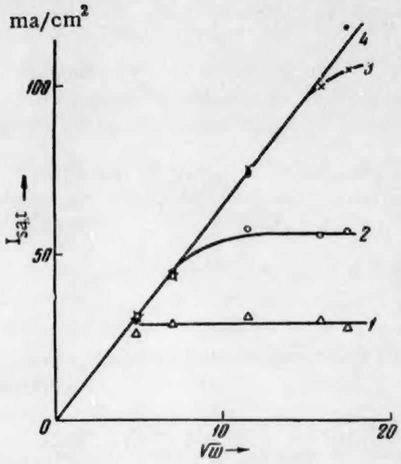

Fig. 2. The relation between the saturation current for the reduction of $KI_3$ (0.096 N) at a rotating disc germanium electrode and $\sqrt{\omega}$. 1) p-Germanium; 2) the same, with moderate illumination of the electrode; 3) the same, with electrode hydrogenized; 4) n-germanium.

## DISCUSSION OF RESULTS

The values of the injection coefficient which have been adduced above indicate that both free electrons and valence electrons are involved in all of the considered instances of reduction at the germanium electrode, with the exception of that of $H_2O_2$. The fact that the value of $\gamma$ is fractional and not entirely constant makes it clearly impossible to relate the proportions of free electrons and valence electrons through a molecular reaction scheme. It is likely that reaction proceeds simultaneously along two paths, and that the proportions in any one case will be fixed by the position of the energy level of the reducing ions or molecules with respect to the energy bands of the semiconductor.

The opinion has been expressed repeatedly [1,5] that the rate of reduction on hole-type germanium electrodes is lower than the rate on electronic germanium because of a lower concentration of free electrons to participate in the cathodic processes in the hole material. The lack of retardation in the reduction of $KMnO_4$ and $K_3Fe(CN)_6$ on p-germanium is related to the fact that these reactions proceed largely through valence electrons. Saturation currents for the reduction of quinone, $K_2Cr_2O_7$, and $H_2O_2$ are established on hydrogenized electrodes where the rate of surface recombination is high and they are for this reason independent of the type of Ge conduction. The fact that the overvoltage on p-Ge is higher than on n-Ge can possibly be explained by a potential drop in the free-carrier-impoverished surface layer which is formed by cathodic polarization of the hole semiconductor with respect to the solution [8]. Illumination of the electrode eliminates this effect since it is accompanied by a generation of free carriers.

There is a high proportion of free electrons (about 60%) in the $KI_3$ reduction current. The saturation current for this reaction on p-germanium in the dark (Fig. 2, 1) is almost independent of the agitation in the solution,

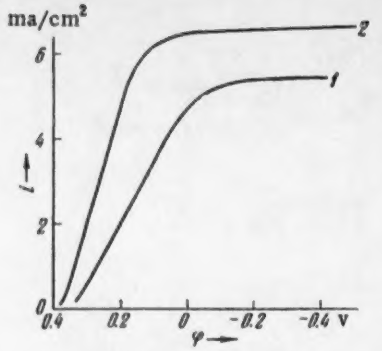

Fig. 3. Polarogram for the reduction of $KI_3$ ($2.07 \cdot 10^{-2}$ N) at a p-germanium rotating disc electrode: 1) In the dark; 2) under illumination. Electrode rotating at 440 rpm.

being fixed by the rate at which the free electrons diffuse from the body of the semiconductor to the electrode surface to participate in the reaction. Illumination or preliminary hydrogenization of the electrode will result in the generation of an excess of free electrons, either by the action of the light or in the layer with high rate of recombination, and the rate of the electrode reactionis then determined by the slowest step, which is the diffusion of the $I_3$ ions through the solution to the electrode surface.

Certain conclusion concerning the chemical etching of germanium can be based on the data which have been obtained here. The common etching mixtures contain $HNO_3$, $H_2O_2$, $I_2$, $Br_2$, $K_2Cr_2O_7$, etc., as oxidizing agents [9]. It is possible that valence electrons are involved in the reduction of many of these oxidants on germanium and that holes are thereby formed which can then participate in the dissolving of the n-germanium. Such a mechanism does not seem very probable in the case of $H_2O_2$, however.

I wish to express my deep thanks to Professor B. N. Kabanov for his help in discussing these results and to I. G. Erusalimchik for having supplied the electrodes.

## LITERATURE CITED

[1] W. H. Brattain and C. G. B. Garrett, Bell System Techn. J. 34, 129 (1955).

[2] H. Gerishcher and F. Beck, Zs. phys. Chem., N. F. 13, 389 (1957).

[3] Yu. V. Pleskov, Doklady Akad. Nauk SSSR 126, 111 (1959).*

[4] W. W. Harvey and H. C. Gatos, J. Appl. Phys. 29, 1267 (1958).

[5] J. B. Flynn, J. Electrochem. Soc. 105, 715 (1958).

[6] M. Green, in: Modern Aspects of Electrochemistry, J. O. Bockris, ed. (London, 1959) p. 396.

[7] V. G. Levich, Physicochemical Hydrodynamics [in Russian] (Moscow, 1959).

[8] E. A. Efimov and I. G. Erusalimchik, Doklady Akad. Nauk SSSR 124, 609 (1959).*

[9] P. Wang, Sylvania Technologist 11, 50 (1958).

---

* Original Russian pagination. See C. B. translation.

# THE ORIGIN OF THE COMPENSATION EFFECT IN CHEMICAL KINETICS

S. Z. Roginskii, Corresponding Member, Acad. Sci.,
USSR and Yu. L. Khait

(Translation of: Doklady Akademii Nauk SSSR Vol. 130, No.2,
1960, pp. 366-369.

Original article submitted September 6, 1959.

The fact that the kinetic coefficients $k_0$ and E of the Arrhenius Equation, $k = k_0 \exp(-E/kT)$, are exponentially related by $\ln k_0 = \text{const} + \beta E$ was first brought out in the late twenties through the work of various authors in comparing the activities of certain catalysts with respect to a single reaction [1-3]. The existence of a similar relation between the kinetic constants of monomolecular homogeneous reactions was brought out simultaneously and independently by L. V. Rozenkevich and one of the present authors through a comparison of the literature data [4]. Hinshelwood contested these findings at one time, but his own investigations later convinced him of the reality and generality of the compensation effect [5], forcing him to recognize it as one of the principal, but unexplained, laws of chemical kinetics [6]. A compensation effect has been observed even in such purely physical phenomena as diffusion in crystals, and electronic and hole conduction in semiconductors [7]. The kinetics of the most varied types of processes and systems show a compensation effect. However, the presence of a condensed phase is either essential to the appearance of this effect, or at least favorable to it, since there are but few authentic instances of a compensation effect in homogeneous gas reactions where a comparison of analogous simple reactions usually shows $\underline{k}$ to be either constant, or only weakly dependent on E. The compensation effect is of particular importance in catalytic reactions where its existence is brought out by comparing the activities of: a) catalysts which have been prepared by different methods and subjected to different thermal treatment [8], b) catalysts containing different amounts of modifiers, or c) various catalysts of a single type [9], with respect to a single reaction. The data on the compensation effect in related reactions on a single catalyst are less systematic [10]. The exact form of the $k_0$ (E) relation cannot be considered as finally established since there is no possibility of an experimental check in which the value of E would range over several orders. G. M. Zhabrova has shown [11] that the greater part of the experimental data can be satisfactorily described by an equation of the form

$$\ln k_0 = \text{const} + \beta E^n, \qquad (1)$$

in which $\underline{n}$ ranges from 1 to 3. It is possible to set $n \approx 1/2$ in many cases [4]. The existence of a compensation effect has the result that the activity series at $T_{\text{inv.}}$ will be upset at a certain temperature. Such an effect is lacking in the schematic equations of the theory of absolute reaction rates of simple reactions. The introduction of a kinetic multiplying factor, $\exp(\beta E^n)$, into a theory of absolute reaction rates based on statistical thermodynamics is equivalent to the introduction of a kinetic multiplying factor into the theory of the equilibrium state; this is not consistent with statistical thermodynamics. The possibilities for a compensation effect are greater in complex reactions, although introduction of the factor $\exp(\beta E^n)$ into the theory of absolute reaction rates would still entail the appearance of this same factor in the theory of the equilibrium state.

A number of hypotheses have been advanced to explain the compensation effect: it has been postulated that such an effect in a heterogeneous reaction reflects the existence of nonuniformity and an exponential distribution of active centers with respect to the energy of activation [2], an explanation which is not applicable to homogeneous reactions. Additional equilibria with Brönsted relations between E and the heats of reaction have also been postulated.

Resort to such quantum mechanical effects as tunnel transfer [4,10] would only be justified for certain electronic mechanisms or for hydrogen reactions at low temperatures [12,13]. No general explanation of the compensation effect could be obtained in this way. The old statistical theory of monomolecular reactions of Kassel, Rice, et al [14, 16] involves a multiplying factor $k_0 \sim E^n$ which is scarcely different from exp ( $\beta$ E) when $\underline{n}$ is large. This theory is no longer acceptable in the light of the work of L.D. Landau [15]. Thus it must be acknowledged that the efforts of more than thirty years have not produced a satisfactory explanation of the compensation effect. The fact that such an effect is observed in systems and processes which are radically different from one another gives reason to believe that it arises from some of the general principles of statistical kinetics.

The specific characteristics of a system or process can lead to an intensification or weakening of that part of a compensation effect which is common to a wide class of systems and processes. The attempt has been made below to explain the compensation effect without having recourse to detailed mechanical models by working with the statistical method of calculating rates of activated process in condensed bodies which has been developed by one of the authors. This method is based on the supposition that an activated process consists of a finite number of elementary acts. Each of these elementary acts results from the fact that a certain energy E', equal to, or exceeding, the critical value $E \gg kT$, will occasionally concentrate in the individual bonds of a region, $d^3$, which is of the order of the volume of a single particle, this concentration being at the expense of a reduction in the energy of other degrees of freedom in a surrounding volume, $l^3$. The volume $l^3$ proves to be microscopically small since the rate of transfer of energy in the system is finite and not very large (electromagnetic energy transfer is not supposed to take place in the system) and the elementary act is of brief duration. The average dimensions of the volume $l^3$ from which the energy $E' \gg E \gg kT$ is taken up are limited more exactly by the conditions

$$l^2 < \frac{Ed^3}{a\hbar l_0}\tau_0; \qquad \frac{l^3}{ad^3} > \frac{E_0}{kTa}, \tag{2}$$

$l_0$ and $\tau_0$ being, respectively, the mean free path and the mean time of free travel of the particle or quasiparticle (an ion, for example) which transfers the energy when $E \gg kT$. The parameter $\underline{a}$ of the inequalities of (2) is of the order of several units. The elementary act of the activated process was considered as being accompanied by a considerable discontinuous, but temporary, alteration in the state of the region $l^3$ in [17] (a random explosive process [18]).

A combination of the methods of statistical thermodynamics with the Principle of Detailed Balancing has shown the probability, W, of an elementary act in an activated process of given type in volume $l^3$ in unit time to be given by the integral of the expression

$$\frac{kT\,(U_c - E)}{\hbar}\exp\left(-\frac{F_c - F_0}{kT}\right)\exp\left(\frac{S\,(U_c - E) - S\,(U_c)}{k}\right) \tag{3}$$

evaluated over all permissible values of the energy, $U_c$, of this volume [17]. Here $F_c$, $S(U_c)$, $S(U_c - E)$, and $T(U_c - E)$ represent, respectively, the free energy, entropy, and temperature of the volume $l^3$ corresponding to the energies $U_c$ and $U_c - E$.

The fact that (3) has a maximum was used in [17] to avoid integration over $U_c$. The result was an approximation equation

$$W \approx W_0\, q \exp\left(-\frac{E}{kT}\right), \tag{4}$$

in which no account was taken of the dependence of $W_0$ on E ($\underline{q}$ is the relative concentration of the substances which are responsible for the process, $\rho$, which is under consideration). Here, the number of elementary acts of the activated process of given type in the volume V per unit time was determined from the equation $N_1 = \frac{V}{l^3} W$, V being the system volume. We will now consider the problem of the relation between $W_0$ and E, making use of the expression

$$W \approx q \frac{k}{\hbar\sqrt{2\pi}} \int T(U_c - E) \exp\left(-\frac{(\Delta U)^2}{2\alpha^2}\right) \exp\left(\frac{S(U_c - E) - S(U_c)}{k}\right) \frac{dU_c}{\alpha}, \qquad (5)$$

in which $\Delta U = U_c - \bar{U}$, $\bar{U}$ is the mean energy of the volume $l^3$; $\alpha \approx kcT^2$ is the mean-square fluctuation of the energy in this volume, and $\underline{c}$ is its heat capacity. Equation (5) was obtained by integration of (3) after replacing $\exp[-(F_c - F_0)/kT]$ by a normal Gaussian distribution, this being necessary if the Boltzmann Principle is to be applicable [19]. We will limit ourselves to the case in which $\partial^n c/\partial T^n \approx 0$ $(n = 1, 2, \ldots)$, a condition which is satisfied under ordinary circumstances. Expanding $S(U_c - E)$ as a function of $E < U_c$ and making use of the fact that $\partial^n c/\partial T^n = 0$, leads to $S(U_c - E) - S(U_c) \approx k \ln\left[1 - \frac{E}{cT(U_c)}\right]^{c/k}$. If it is considered that $c/k \gg 1$ and that $\lim (1 - x/n)^n = e^{-x}$, we will find that $S(U_c - E) - S(U_c) = -\frac{E}{T(U_c)}$; this together with (5) gives

$$W \approx \frac{kq}{\hbar\sqrt{2\pi}} \int T(U_c - E) \exp\left(-\frac{(\Delta U)^2}{2\alpha^2}\right) \exp\left(-\frac{E}{kT(U_c)}\right) \frac{dU_c}{\alpha}. \qquad (6)$$

The possibility of representing $T(U_c)$ and $T(U_c - E)$ as $T(U_c) = T + \frac{\Delta U}{c}$, $T(U_c - E) = T + \frac{\Delta U - E}{c}$ is utilized in evaluating the integral of (6). Carrying out the change of variable $y = (\Delta U - E)/\alpha$ in (6), considering that it is usually true that $\left(\frac{\Delta U}{cT}\right)^2 \ll 1$, and integrating over the interval $(-\infty, \infty)$, leads to the final result

$$W \approx q \frac{kT}{\hbar}\left(1 + \frac{kT}{\alpha}\right) \exp\left(\frac{E^2}{2\alpha^2}\right) \exp\left(-\frac{E}{kT}\right) \qquad (7)$$

or

$$W_0 \approx q \frac{kT}{\hbar}\left(1 + \frac{kT}{\alpha}\right) \exp\left(\frac{E^2}{2\alpha^2}\right). \qquad (8)$$

The condition

$$E^2/2\alpha^2 > 1, \qquad (9)$$

must be satisfied if the term $\exp(E^2/2\alpha^2)$ is to play any marked role, while the inequality of (9) shows that $E^2/2\alpha^2$ must be of the order of several units or even more. It follows from (2) that $l^2 < \frac{Ed^3}{a\hbar l_0} \tau_0$, and $\alpha^2 \approx kT^2 c_0 \rho l^3$ ($c_0$ is the specific heat capacity and $\rho$ is the density), so that (9) is fulfilled under the condition that

$$\frac{E^2}{\alpha^2} > \sqrt{\frac{E}{kT}} \left(\frac{k}{c_0 \rho d^3}\right)\left(\frac{\hbar v a}{dkT}\right)^{3/2}. \qquad (10)$$

Thus the inequality of (10) and condition (9) will both be satisfied if the value of E is not too small. It follows from (10) that the appearance of a compensation effect is favored by increasing the rate of energy transfer, $\underline{v}$, or the density $\rho \sim 1/d^3$. Thus condensed media, and solid bodies in particular, are favorable to the appearance of such an effect. The equations which have been obtained show that $\exp(E^2/2\alpha^2)$ is, in general, dependent on T. It will be seen in the sequel, however, that such dependence is of little significance in comparison with that of the term $\exp(-E/kT)$. Experimental data are usually presented in the form of graphs showing the dependence of $Z = \ln W$ on $x = 1/kT$. By taking logarithms of (7) and setting $\alpha^2 = kT^2 c$, we find that

$$Z = A - xE\left(1 - \frac{Exk}{2c}\right), \qquad (11)$$

where $A = \ln \frac{kT}{\hbar}\left(1 + \frac{kT}{\alpha}\right)$. The conditions are usually such that $cT = \frac{c}{kx} > E$ (since $cT \approx 10$-50 ev and $E \approx 1$ - 4 ev. Thus the second member in the parenthesis of (11) gives rise to only minor deviations from a straight line of slope -E over the relatively narrow temperature interval within which measurements are commonly carried out, and this despite the strong dependence of this member on T. This conclusion is in agreement with experimental results. On the other hand, $E^2/2\alpha^2$ is a product of two factors, $E/2cT < 1$ and $E/kT >> 1$. Thus (9) will be satistified for certain values of E, and the term $\exp(E^2/2\alpha^2)$ can alter the reaction rate by several orders.

It is therefore possible that the compensation effect can be explained by the fact that the probability of concentrating an excess energy $E' \geq E \gg kT$ proportional to $\exp[-E/T(U_c)k]$ in that region $l^3$ in which the elementary act takes place is dependent on the temporary local temperature $T(U_c)$. But the value of $T(U_c)$ corresponding to the maximum of (3)[ or to the maximum in the integral expressions in (5) and (6) ]is equal to $T_m \approx T + E/c$ and is therefore dependent on E. This leads to a more involved relation between the reaction rate and E, and results in the appearance of a compensation effect. It is to be noted that definite limits are imposed on this explanation of the compensation effect by the introduction of the condition $\partial^n c/\partial T^n \approx 0$, the neglect of a correlation between the $l^3$ volumes, and the application of a Gaussian distribution.

It is desirable to: a) carry out a quantitative evaluation of the proportionality coefficients which enter into the basic equations, thus obtaining the possibility of a more exact determination of $\exp(E^2/2\alpha^2)$ in individual cases, b) verify the use of various values of n in (1), and (c) test and review in detail the temperature dependence of $\exp(E^2/2\alpha^2)$, and also to elucidate other problems connected with the application of the results which have been obtained here and the prospects for their further development.

## LITERATURE CITED

[1] H. Constable, Proc. Roy Soc. A 108 , 355 (1926).

[2] G. M. Schwab and E. Cremer, Zs. phys. Chem. A. 144, 243 (1929).

[3] A. Balandin, Zs. phys. Chem., B 19, 451 (1932); Zhur. Fiz. Khim. 4, 257 (1933).

[4] S. Z. Roginskii and L. V. Rozenkevich, Zhur. Fiz. Khim. 1, 293 (1930), S. Roginskii and L. Rozenkevich Zs. phys. Chem. B 10, 293 (1930).

[5] C. Hinshelwood et al.,J. Chem. Soc. 538, 858, 862, 1575 (1937).

[6] C. Hinshelwood, J. Chem. Soc. 694 (1947).

[7] F. F. Vol'kenshtein, The Electrical Conductivity of Semiconductors [in Russian] (1947).

[8] A. B. Shekhter, Dokaldy Akad. Nauk SSSR 89, 619 (1953).

[9] S. Z. Roginskii, Adsorption and Catalysis on Nonuniform Surfaces [in Russian] (Izd. AN SSSR, 1947).

[10] E . Cremer Adv. in Catl. 7, 75 (1955).

[11] G. M. Zhabrova, Usp. Khim. 24, 598 (1955).

[12] R.P.Bell et al., Trans.Farad. Soc. 54 (1958); Reports, Eighth Mendeleev Conference on General and Applied Chemistry, Collection of Abstracts of Reports and Communications of Foreign Scientists [in Russian] (1959)p.40.

[13] V. I. Gol'danskii, Doklady Akad. Nauk SSSR 124, 6, (1959).*

[14] L. S. Kassel, The Kinetics of Homogeneous Gas Reactions [Russian translation] (Leningrad, 1937).

[15] L. D. Laudau, Sov. Phys. 10, 67 (1936).

[16] V. N. Kondrat'ev, The Kinetics of Chemical Reactions [in Russian] (1958).

[17] Yu. L. Khait, Abstracts of Reports, Second All-Union Conference on the Physics of Dielectrics [in Russian] (Izd. AN SSSR, 1958).

[18] B. V. Gnedenko, Course in the Theory of Probability [in Russian] (1954).

[19] M. A. Leontovich, Statistical Physics [in Russian] (1944).

---

* Original Russian pagination. See C. B. translation.

# THE EXCHANGE OF HYDROGEN ISOTOPES ON PALLADIUM

G. N. Trusov and N. A. Aladzhalova

L. Ya. Karpov Scientific,Research Institute for Physical Chemistry

(Presented by Academician A. N. Frumkin August 18, 1959)

(Translated from Doklady Akad. Nauk SSSR, Vol. 130, No.2, 1960, pp. 370-373)

Original article submitted June 25, 1959.

Deuterium and tritium have been used to measure the rate of hydrogen exchange between an electrolyte and a layer of hydrogen adsorbed on a palladium cathode. Exchange proceeded through the reactions:

Variant I experiments; $\mathrm{Pd}(\mathrm{H})_n + \mathrm{D}_2^*\mathrm{O} \rightarrow \mathrm{Pd}(\mathrm{H})_{n-1}\mathrm{D}^* + \mathrm{HDO}.$

Variant II experiments; $\mathrm{Pd}(\mathrm{H})_{n-1}\mathrm{T}^* + \mathrm{H}_2\mathrm{O} \rightarrow \mathrm{Pd}(\mathrm{H})_n + \mathrm{T}^*\mathrm{HO}.$ (1)

The hydrogen exchange is more complex than the exchange of metallic ions on amalgams which was studied in [1,2]. Theoretical treatment of this problem by the authors of [3-5] has led to the conclusion that the true rate of exchange between an electrolyte and an adsorbed surface layer does not necessarily coincide with the rate calculated from extrapolated overvoltage curves ($i_{ext}$).

The experiments which we have carried out were aimed at obtaining experimental data which would permit a comparison of the true rate of hydrogen exchange on palladium with the rate of exchange found by extrapolating overvoltage and ionization curves to the equilibrium overvoltage. The values of the exchange rate obtained by extrapolation in [6] can be considered as equilibrium rates of ionization and discharge since the linear portions of the $\eta$, log i curves for moderate polarization of palladium in alkaline solutions are fixed by the rates of these same steps in the evolution and ionization of hydrogen.

A purely electrochemical mechanism for Reaction (1) would call for diminished isotopic exchange when the rate of the reverse ionic reaction is reduced by applying a cathodic or anodic overvoltage to the exchanging surface.

The isotopic method can be applied to give a test of the validity of this view of the nature of Reaction (1).

The polyethylene apparatus in which these measurements were carried out consisted of three sections; the working palladium membrane was clamped between the sections marked *b* and *c* in Fig. 1, and auxiliary membrane between sections *a* and *b*. Sections *a* and *b* contained solutions prepared from water of natural isotopic composition. Section *c* contained a solution of KOD, or $D_2SO_4$ (90%D), in Variant I experiments, and an alkaline solution enriched in tritium (0.2 C/cm$^3$) in Variant II experiments. One of the faces of the working membrane cathode also served as the exchange surface. Cathodic polarization (0.05 amp/cm$^2$) of the other face of this membrane held the exchanging surface in a steady state of hydrogen saturation and ensured constancy in the amount of hydrogen on it. Maintenance of the saturation current during an experiment also ensured a continuous and uniform evolution of gas over both faces of the membrane. Supersaturation by the external polarizing current displaced the stationary potential of the exchanging surface in the cathodic direction by 0.02-0.04 v. The structure of the apparatus was such as to allow the overvoltage of the exchanging surface to be carried to ± 0.250 v by anodic or cathodic polarization. This result was achieved with current densities which did not exceed 1-5% of saturation value. The individual measurement showed that the composition of the adsorbed layer on the exchanging surface was not affected by such small counter polarizations.

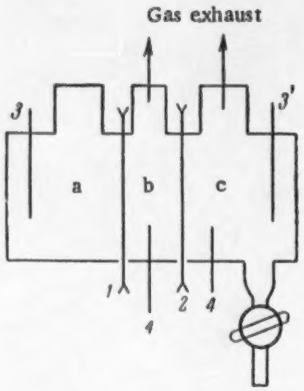

Fig. 1. Diagram of polyethylene apparatus for measuring exchange currents. 1, 2) Palladium membranes; 3) platinum anodes; 4) reference electrodes.

The Variant I experiments involved exchange between the heavy electrolyte of section c and an adsorbed layer of light hydrogen which was formed on the right face of the test membrane by saturating it from section b. The resulting exchange enriched the body of the membrane, and the gases evolved on both of its faces with deuterium. Measurements of the rate of evolution and isotopic composition of the gases made it possible to calculate the exchange rate with an accuracy of 25%.*

In Variant II experiments the adsorbed layer of hydrogen which had been formed on the exchanging left face of the test membrane by saturating it with enriched hydrogen from section c was tagged with tritium. The tritium passed into solution as exchange proceeded. The activity of the solution increased with time and was measured by an internally filled Geiger-Muller counter, the accuracy of a determination being at least 7%. These experiments were carried out so as to almost completely prevent the introduction of oxygen into the enriched electrolytes, use being made of a technique which will be described in detail elsewhere. Figure 2 represents the course of experiments on two membranes which showed different activities in the exchange reaction. An exchange rate in amp/cm² was obtained by measuring the rate of tritium enrichment of the electrolyte during anodic polarization of the exchanging surface with a current of fixed magnitude.

TABLE 1

| Membrane No. | Solution | Deviation from $\eta$ sta | Equilibrium isotopic exchange, $a/cm^2 \cdot 10^{-4}$ | Isotopic exch. under polarization $a/cm^2 \cdot 10^{-4}$ | $i_{ext}$, $a/cm^2 \cdot 10^{-4}$ |
|---|---|---|---|---|---|
| | | **Variant I** | | | |
| 1 | KOD (90% D). 1*N* | 0 | 0.6 | — | 0.25 |
| | | +0.040 | — | 0,5—0.4 | |
| | | +0.084 | — | 0.39 | |
| | | +0.130 | — | 0.25 | |
| | | +0.130 | — | 0.31 | |
| | | +0.060 | — | 0.50 | |
| | | 0 | 1.2 | — | |
| 2 | The same | 0 | 0.4 | — | |
| | | +0.170 | — | 0.16 | |
| | | **Variant II** | | | |
| 1 | KOH, 1*N* | 0 | 1.5 | — | 1.25 |
| | | —0.240 | — | 1.9 | |
| 2 | | 0 | 3.0 | — | 1.6 |
| | | —0.160 | — | 3.0 | |
| 3 | | 0 | 0.8 | — | 0.3 |
| | | —0.240 | — | 0.8 | |
| 4 | | 0 | 1.6 | — | 0.3 |
| | | —0.200 | — | 0.7 | |
| 5 | | 0 | 2.75 | — | 1.6 |
| | | —0.200 | — | 1.25 | |
| 6 | $H_2SO_4$,1*N** | 0 | 22.5 | — | — |
| | | —0.075 | — | 12 | |

*Similar results were obtained in a number of other experiments with acid solutions.

---

*The gases were analyzed with a mass spectrometer, the accuracy being 0.005%.

TABLE 2

The Effect of Surface Activation on the Exchange Rate in Variant I Experiments

| Membrane no. | Solution | External saturation current, ma/cm$^2$ | Isotopic exchange, (amp$^2$) $\cdot 10^{-4}$ | $i_{ext}$, (a/cm$^2$) $\cdot 10^{-4}$ |
|---|---|---|---|---|
| 1 | $D_2SO_4$ | 10 | 3.7 | 1.0 |
|  | (90% D), |  |  |  |
|  | 1N | 40 | 4.0 | 1.0 |
| 2* |  | 30 | 150 | 100 |
|  |  | 60 | 150 | 100 |

*Exchanging surface activated by anodic-cathodic polarization.

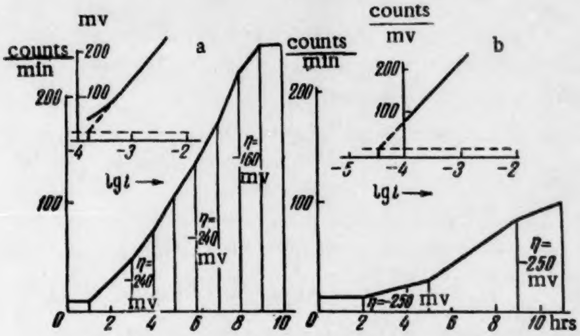

Fig. 2. Enrichment of the electrolyte with tritium during exchange with the adsorbed layer. a) Surface active to exchange; b) less-active surface. Overvoltage curves on these same electrodes are above. (a) $i_{ext} = 1.6 \cdot 10^{-4}$ a, $i_0 = 3 \cdot 10^{-4}$ a, b) $i_{ext} = 3 \cdot 10^{-5}$ a, $i_0 = 1 \cdot 10^{-4}$ a)

The experimental results are presented in Tables 1 and 2. The data of these tables show the rate of isotopic exchange on each of our electrode surfaces to be from two to three times greater than the exchange current calculated from extrapolation of the overvoltage curve. These and other rates proved to be of about the same order of magnitude.*

The value of the true rate of exchange and the extrapolated exchange current are similarly affected by changing the activity of the exchanging surface and the electrolyte composition (Tables 1 and 2). Application of an anodic overvoltage to the exchanging surface somewhat diminishes the rate of enrichment of the gas with respect to the heavy isotope. But the rate of enrichment is diminished by no more than a factor of two or three, even with a + 0.130 v overvoltage, whereas extrapolation of the overvoltage curve shows the rate of hydrogen discharge to be reduced by a factor of more than ten. From this it follows that the discharge-ionization reaction on the exchanging surface must be accompanied by another reaction which proceeds by a different mechanism; this can be designated as a catalytic exchange reaction.

---

*The overvoltage curves for the ionization of hydrogen were developed on electrodes saturated with light hydrogen in the Variant I experiments (Table 1), while the overvoltage curves for the evolution of hydrogen were developed during polarization of the electrodes in the light electrolyte in the Variant II experiments; thus the $i_{ext}$ values refer to reactions of the light isotope. Actually, the difference between the true exchange rates and the values of $i_{ext}$ are somewhat greater than is indicated in Table 1.

In most experiments, the rate of enrichment of an alkaline electrolytic solution was unaltered by the application of a cathodic overvoltage to the exchanging surface (Table 2). The cases showing a diminution (this applies especially to acidic solutions) were such that this diminution was less by a factor of five or six than the decrease in the rate of ionization of the hydrogen obtained by extrapolation of the ionization curve. Thus the "catalytic" exchange is not retarded by the cathodic polarization but rather experiences a certain acceleration.

The following mechanism for exchange on the hydrogen electrode can be proposed on the basis of the data which have been obtained here.* The water molecule (or the hydroxyl ion) will be adsorbed on a hydrogen-saturated palladium surface in such a way that one of the hydrogen atoms will rest directly on the surface of the metal. This arrangement makes it possible for the hydrogen atom to split away from the water molecule and be replaced simultaneously by an atom from the adsorption layer, thus producing a chemical exchange reaction which is not directly dependent on the metal-solution potential drop. The rate of isotopic exchange would then be determined by the ability of the surface to adsorb and deform water molecules. The adsorption and deformation of the adsorbed molecules can be markedly altered, so that polarization can give rise to cases in which isotopic exchange through the "catalytic" mechanism is so accelerated by an increase in the cathodic potential that the retardation of the ionization reaction becomes insignificant.

It is to be emphasized that the increase in the rate of isotopic exchange with increasing cathodic potential cannot be related to an increase in the activity of the hydrogen on the exchange surface, since this was held constant by saturating the outer face of the membrane.

The authors express their thanks to Professor V. I. Veselovskii for his interest in this work and for his participation in the discussion of it.

## LITERATURE CITED

[1] N. B. Miller and V. A. Pleskov, Doklady Akad. Nauk SSSR 74, 323 (1950).

[2] G. M. Budov and V. V. Losev, Doklady Akad. Nauk SSSR 122, 90 (1958).**

[3] P. D. Lukovtsev, Disssertation; L. Ya. Karpov Institute for Physical Chemistry (1940); P. D. Lukovtsev and S. D. Levina, Zhur. Fiz. Khim. 21, 599 (1947).

[4] V. I. Veselovskii, E. I. Kuchinskii, et al, Records of Electrochemical Laboratory for 1947-1952, L. Ya. Karpov Institute for Physical Chemistry.

[5] A. N. Frumkin, Doklady Akad. Nauk SSSR 119, 318 (1958).**

[6] A. N. Frumkin and N. A. Aladzhalova, Zhur. Fiz. Khim. 18, 492 (1944).

---

*In a private communication, A. N. Frumkin has expressed the opinion that these results might be explained in terms of a so-called electrochemical desorption mechanism without having to take recourse to a supposed catalytic exchange. It would then be necessary to assume that the exchange current for desorption is considerably greater than the exchange current for discharge.

**Original Russian pagination. See C. B. translation.

# ADSORPTIONAL CHANGES IN THE SURFACE CONDUCTIVITY OF GERMANIUM

V. I. Fistul' and D. G. Andrianov

(Presented by Academician A. N. Frumkin September 15, 1959)

(Translation of: Doklady Akademii Nauk SSSR Vol. 130, No.2, 1960, pp. 374-376)

Original article submitted September 9, 1959.

A p-n junction is often shorted by surface conduction when the inverse current passing through it is increased [1]. This effect can be diminished by treating the germanium crystals with etching mixtures based on hydrofluoric and nitric acids, such etchants being held to high standards of purity because of the contaminating Na, Cu, Al, Zn, Mg, Mn, Fe, Cr, Pb, etc., which chemical analysis shows to be present in the components.

The adsorption of atoms of these elements from the etchant onto the semiconductor surface can result in an increase in the surface conductivity. No direct experiments have as yet been carried out, however, to indicate how the surface conductivity would be altered by the adsorption of one or another of these impurities. The present study was set up to deal with this problem.

The test substance was a monocrystalline n-germanium with a specific resistance of approximately 40 ohms • cm. Measurements of the surface conductivity were carried out by the "wedge" method of [2]. Wedge-shaped specimens were cut from a pig of pure uncompensated germanium which had a uniform variation (to within ± 5 % of specific resistance along its length.

The etchant was composed of $HNO_3$, HF, and $CH_3COOH$ in the proportions 3 : 2 : 1. These acids had been subject to a preliminary twofold distillation so that the total amount of impurities in each was $10^{-6}\%$ or less. A definite amount of the impurity under study was specially introduced into the etchant. Treatment of the wedge-shaped specimens was carried out in the customary manner, the temperature being ~ 100° and the time of etching, 30 seconds. The etched specimens were washed with ion-exchange water and then dried in an oven for 15 minutes at 80°.

The experimental results are illustrated by the data of Fig. 1 on a specimen which had been first treated with the pure etchant, and then with etchant containing 0.5% iron impurity by weight. A similar increase in the surface conductivity was observed when 0.05-1.0% by weight of contaminating Cu, K, Cr, Ca, or Ag was introduced into the etchant.

At the same time, it was found that the surface conductivity was diminished by etching in a Zn-contaminated mixture. This "anomalous" zinc effect calls for special consideration.

It proves to be very difficult, however, to interpret this effect on the basis of the simple model of an electron redistribution in the impurity atom–base system. A diminution in the surface conductivity is observed to result from the adsorption of Cd also. It is characteristic that this effect is not common to the elements of a single group in the periodic system. Thus adsorption of Ca gives rise to this effect, while adsorption of Zn or Cd fails to do so. Composite data on the effect of each of the investigated impurities on the surface conductivity are presented in Table 1.

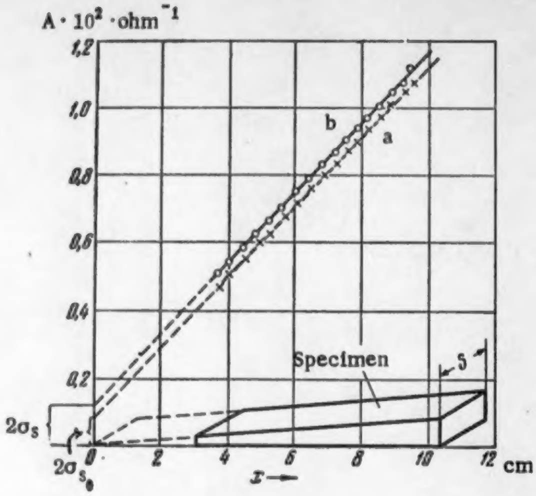

Fig. 1. Graph of $A = \frac{I}{S} \cdot \frac{dx}{dU} = f(x)$. (I is the strength of the current passing through the specimen and dU/dx is the potential gradient); a) pure etchant, b) etchant with 0.5% Fe. S is the width of the wedge-shaped specimen, $\sigma_{s0}$ is the surface conductivity after treatment with the pure etchant, and $\sigma_s$ is the surface conductivity after treatment with the contaminated etchant.

The greatest alteration in the surface conductivity was observed when Br was introduced into the etchant. Thus treatment with an etchant into which 1.0% Br had been introduced in atomic form reduced the surface conductivity so strongly that the ratio $\sigma_s/\sigma_{s0}$ was only ~0.17. On the other hand, 1.0% Br introduced into the etchant through KBr gave a considerably higher value of $\sigma_s/\sigma_{s0}$, this ratio being then equal to 0.5. It is obvious that this is to be explained as being due to counteracting effects from simultaneously adsorbed K and Br atoms.

These experiments point to the possibility of preparing germanium with a predetermined value of the surface conductivity, adsorption of various impurities from etchants resulting in a kind of surface alloying with "donors" and "acceptors."

A special case of such alloying is met when counteracting impurities are simultaneously introduced into an etchant to produce a compensate surface with a very low $\sigma_s$ value.

The practical applications of these effects seem to us to be quite promising but such applications await a study of the stability of the effect, the form in which the impurities adsorb on the cyrstal surface and the alteration in the rate of surface recombination resulting from adsorption; it is also necessary to determine whether adsorption leads to an inversion in the type of conduction in the surface layer.

The authors express their deep thanks to M. L. Ioselevich who participated in planning and executing this work.

TABLE 1

| Element | Compound through which the element was introduced into the etchant | Amount element in etchant, % by wt. | $\sigma_s/\sigma_{s0}$ |
|---|---|---|---|
| Cu | $Cu(NO_3)_2 \cdot 3H_2O$ | 1.0<br>0.5 | 1.375<br>1.00 |
| K | $KNO_3$ | 0.355<br>0.05 | 1.5<br>1.0 |
| Cr | $Cr(NO_3)_3 \cdot 9H_2O$ | 0.5<br>0.05<br>0.005 | 2.5<br>1.5<br>1.0 |
| Fe | Filings | 0.5<br>0.05 | 1.5<br>1.0 |
| Zn | $Zn(CH_3COO)_2$ | 1.0<br>0.5 | 0.25<br>0.625 |
| Ca | $Ca(NO_3)_2 \cdot 4H_2O$ | 1.0 | 1.58 |
| Cd | $Cd(NO_3)_2 \cdot 2H_2O$ | 1.0 | 0.75 |
| Ag | $Ag(NO_3)$ | 1.0 | 2.0 |

## LITERATURE CITED

[1] W. Dunlap, An Introduction to the Physics of Semiconductors [Russian translation](IL, 1959).*

[2] R. N. Rubinshtein and V. I. Fistul', Doklady Akad. Nauk SSSR 125, 3, 542 (1959).*

---

*Original Russian pagination. See C. B. translation.

# PHASE DIAGRAMS OF SYSTEMS CONTAINING AN ORDERED PHASE

**I. L. Aptekar'**

Institute of Precision Alloys at the Central Scientific-Research Institute
of Ferrous Metallurgy

(Presented by Academician G. V. Kurdyumov, September 19, 1959)

(Translation of: Doklady Akademii Nauk SSSR, Vol 130, No.3,
1960, pp. 562-564)

Original article submitted September 1, 1959.

The results obtained from theoretical phase diagrams depend to a large extent on the type of expression used for the configuration energy of alloys.

Although the energy of mixing (the nonadditive in portion of energy), which is a function of temperature, pressure, concentration, and order, is expressed in various forms in different theories, it can always be reduced to the form:

$$E_{\text{mix.}} = Uc_A c_B + V\eta^2 + W\sigma. \tag{1}$$

In this case $\eta$ is the degree of long-range order, $\sigma$ the degree of local order, $c_A$ and $c_B$ the concentrations, while U, V, and W can be described as energy parameters for the mixing, the long-range order, and the local order, respectively.

In all of the commonly used order-disorder theories, such as that of Bethe [1], Bragg and Williams [2], the quasichemical theory [3], and the Kirkwood theory generalized for arbitrary concentrations [4], the parameters U, V, and W depend on the same physical constant $v = 2v_{AB} - v_{AA} - v_{BB}$ ($v_{AA}$, $v_{BB}$, and $v_{AB}$ are the energies of individual atomic pairs). This results from the fact that in all these approximate theories the energies include only the closest-neighbor interactions with the additional assumption that $v_{AA}$, $v_{BB}$, and $v_{AB}$ are independent of temperature and concentration.

The relationship between the parameters U and V may vary from system to system, even if only direct atomic interactions are considered, but the interaction of higher coordination spheres [5] and the "elastic" energy due to the different interatomic distances at various concentrations [7] are taken into account.

However, the difference between the parameters U, V, and W does not depend exclusively on the interaction in higher spheres and the existence of "elastic" energy. The difference arises from the intrinsic nature of the alloy energy, which besides the direct central interaction of neighboring atoms ($E_1$) includes the interaction of ions with the common electrons ($E_2$) and the energy of the electrons themselves ($E_3$). The parameter W seems to be mainly connected with energy $E_1$. Parameter V may also depend on the changes produced in $E_3$ by the creation of a long-range order (new Brillouin zones) [8], while parameter U may depend on all three forms of energy [7].

Thus, in different systems depending on the nature of the components (valence, electron density, affinity, atomic dimensions, etc.) the three parameters may be interrelated in entirely different fashions. Therefore it is quite obvious that a theory in which the energy is characterized solely by parameter $\underline{v}$ should have a limited applicability.

Thus these theories lead to the following erroneous conclusion: that in any one system even by varying the temperatures and concentrations no processes can be induced which would change a predominance of unlike neighbors to a predominance of like neighbors.

Indeed, when $v < 0$ processes leading to the increase of AB combinations would be energetically favorable, while for $v > 0$ processes leading to the formation of AA and BB should predominate. These conclusions, however, are contradicted by experimental facts. In the Au–Ni system, for example, at higher temperatures pairs of the type AB (local order) tend to increase, while at lower temperatures the number of AA and BB pairs increases (decomposition) [9].

In addition to this, when the Bragg and Williams theory [2] is applied to a body-centered crystal lattice it fails to predict phase separation even at absolute zero, which contradicts the third law of thermodynamics, since solid solutions cannot have a zero entropy at $T = 0$. When the theory of Bragg and Williams is corrected for the correlation interaction [4] it does predict decomposition at lower temperatures. However, this theory is only valid for a single type of phase diagram where the critical decomposition points are located at precisely fixed concentrations ($C_A = 0.22$ at. % and $C_B = 0.22$ at.%).

It is quite interesting (even if we disregard the question why in a given system the parameters U, V, and W should be interrelated in a particular manner) to examine the various phase diagrams corresponding to different combinations of these parameters. The problem is similar to that which is solved by analyzing the shape of phase diagram as a function of the energy of mixing [10].

To simplify the problem we will disregard the correlation energy, which is equivalent to the assumption that $W = 0$. We will use the free-energy expression given in the Bragg and Williams theory [2] without subdividing the parameters U and V into their respective components and will assume that they are independent of each other:

$$F = E_A c_A + E_B c_B + U c_A c_B + V\eta^2 + RT\,[(c_A + {}^1/_2\eta)\ln(c_A + {}^1/_2\eta) + (c_A - {}^1/_2\eta)\ln(c_A - {}^1/_2\eta) + (c_B + {}^1/_2\eta)\ln(c_B + {}^1/_2\eta) + (c_B - {}^1/_2\eta)\ln(c_B - {}^1/_2\eta)]. \qquad (2)$$

Let us note that the second order dependence between the order energy and the degree of long-range order $\eta$ can be derived without invoking an approach of closest neighbors [11,12].

With the help of Equation (2) it is possible to obtain the following equation for the Kurnakov temperature as a function of concentration:

$$T_{Kr} = 8 c_A c_B \frac{V}{R}. \qquad (3)$$

If the critical decomposition point lies on the line of Kurnakov points, then according to [13]:

$$\frac{\partial^2 F}{\partial c'^2_A} = \frac{\Delta c_p}{T_{Kr}} \left(\frac{\partial T_{Kr}}{\partial c'_A}\right)^2. \qquad (4)$$

Using Equations (2) and (4) and the functions used in them, and assuming that the specific heat jump at the Kurnakov point ($T_{Kr}$) is equal to $\frac{3}{2}\,\frac{c'_A c'_B}{c'^3_A + c'^3_B}$ (see, for example, [14]), we will get:

$$c'_A c'_B = \frac{2 - U/V}{12 - 3U/V}. \qquad (5)$$

In this case $C'_A$ and $C'_B$ are the respective concentrations at the critical decomposition points.

Analyzing the free-energy curves at various temperatures (including $T = 0$), and using Equation (5), one can get the relationship between the shape of the phase diagram and the value of $\alpha = U/V$. This function is represented schematically in Fig. 1. Dotted lines are drawn through Kurnakov's points, while the solid lines encompass the two-phase regions.

If one considers the fact that in the regular Bragg and Williams theory $\alpha = +4$ (Fig. 1,a, no decomposition) it is easy to see why no phase separation was anticipated. A detailed analysis also shows that in a system where $\alpha = -4$ three phases would be in equilibrium at all temperatures below the critical decomposition point.

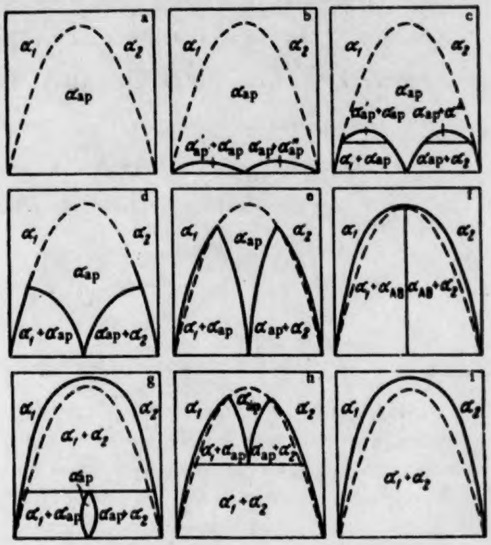
a
$\alpha_1$
$\alpha_2$
$\alpha_{ap}$
b
$\alpha_1$
$\alpha_2$
$\alpha_{ap}$
$\alpha'_{ap}+\alpha_{ap}$
$\alpha_{ap}+\alpha''_{ap}$
c
$\alpha_1$
$\alpha_2$
$\alpha_{ap}$
$\alpha'_{ap}+\alpha_{ap}$
$\alpha_{ap}+\alpha''$
$\alpha_1+\alpha_{ap}$
$\alpha_{ap}+\alpha_2$
d
$\alpha_1$
$\alpha_2$
$\alpha_{ap}$
$\alpha_1+\alpha_{ap}$
$\alpha_{ap}+\alpha_2$
e
$\alpha_1$
$\alpha_{ap}$
$\alpha_2$
$\alpha_1+\alpha_{ap}$
$\alpha_{ap}+\alpha_2$
f
$\alpha_1$
$\alpha_2$
$\alpha_1+\alpha_{AB}$
$\alpha_{AB}+\alpha_2$
g
$\alpha_1$
$\alpha_2$
$\alpha_1+\alpha_2$
$\alpha_{ap}$
$\alpha_1+\alpha_{ap}$
$\alpha_{ap}+\alpha_2$
h
$\alpha_1$
$\alpha_{ap}$
$\alpha_2$
$\alpha_1+\alpha_{ap}$
$\alpha_{ap}+\alpha_2$
$\alpha_1+\alpha_2$
i
$\alpha_1$
$\alpha_2$
$\alpha_1+\alpha_2$

Fig. 1. Schematic representations of phase diagram shapes as a function of the ratio $\alpha = U/V$. a) $\alpha \geq 4$; b) $2 \leq \alpha < 4$; c) $0 < \alpha < 2$; d) $\alpha = 0$; e) $-4 < \alpha < 0$; f) $\alpha = -4$; g) $\alpha = \alpha_0 - kT$, $\alpha_0 > -4$; h) $\alpha = \alpha_0 + kT$, $\alpha_0 < -4$; i) $\alpha < -4$.

Such a result is obviously in conflict with Gibbs phase rule and results from several approximations made by us. Thus, we have assumed (as is done in a great number of papers on the theory of solid solutions) that the parameters U and V remain constant in a given system. But even a slight temperature or concentration dependence would remove the conflict with the phase rule.

Let us assume, for example, that $\alpha = \alpha_0 + kT$, then there is only one temperature at which three phases are in equilibrium if $\alpha = -4$. When $\alpha_0 > -4$ and $k < 0$ the phase diagram has the form shown in Fig. 1, g. The diagram in Fig. 1, h corresponds to $\alpha_0 < -4, k > 0$.

Since the dependence of U and V on temperature seems to be usually slight, then if it is included in calculations the shape of phase diagrams for $\alpha$ other than $-4$ should not be measurably affected.

## LITERATURE CITED

[1] H. A. Bethe, Proc. Roy. Soc. A150, 552 (1935).

[2] W. L. Bragg and E. J. Williams, Proc. Roy. Soc. A151, 540 (1935).

[3] R. H. Fouler and A. Gugenheim, Statistical Thermodynamics (Cambridge, 1939).

[4] I. M. Lifshits, Zhur. Éksper. Teoret. Fiz. 9, 481 (1939).

[5] B. Ya. Pines, Zhur. Éksper. Teoret. Fiz. 11, 725 (1941).

[6] B. Ya. Pines, Zhur. Éksper. Teoret. Fiz. 11, 147 (1941).

[7] I. L. Aptekar' and B. N. Finkel'shtein, Zhur. Éksper. Teoret. Fiz. 21, 900 (1951).

[8] J. C. Slater, Phys. Rev. 84, 179 (1951).

[9] P. A. Flinn, B. L. Averbach and M. Cohen, Acta Metallurgica 1, 664 (1953).

[10] B. Ya. Pines, Zhur. Éksper. Teoret. Fiz. 13, No.11-12 (1943).

[11] W. S. Gorsky, Zs. Phys. 50, 64 (1928).

[12] W. L. Bragg and E. J. Williams, Proc. Roy. Soc., A 145, 699 (1934).

[13] M. A. Krivoglaz and A. A. Smirnov, The Theory of Ordered Alloys [In Russian] (Moscow, 1958) p. 97.

[14] M. A. Krivoglaz and A. A. Smirnov, The Theory of Ordered Alloys [In Russian] (Moscow, 1958) p. 148.

# THE INFLUENCE OF ADSORBED OXYGEN ON THE ELECTRONIC WORK FUNCTION OF GERMANIUM

R. Kh. Burshtein and L. A. Larin

Institute of Electrochemistry, Academy of Sciences of the USSR

(Presented by Academician A. N. Frumkin, October 7, 1959)

(Translation of: Doklady Akademii Nauk SSSSR Vol. 130, No. 3, 1960, pp. 565-568)

Original article submitted October 7, 1959.

We have devoted a series of papers to the investigation of the influence of adsorbed gases on the work function of germanium [1-4]. These have not, however, included any investigation of adsorbed oxygen on germanium, so that it has not been possible to discuss the special problem of the effect of this on the contact potential difference. We have in previous work investigated the kinetics of the adsorption of oxygen on germanium [5]. Now, to elucidate the influence of the various stages of chemisorption of oxygen on surface characteristics, we discuss its action on the work function.

To measure contact potential difference, Kelvin's vibrating condenser method has been used. The fundamental defect of this method for adsorption measurements is that adsorption of gases occurs both on the measuring and on the comparison electrode, which prevents an accurate measurement of the influence of adsorbed gases on the work function. We have removed the defect by using an apparatus developed earlier [6], in which the comparison electrode is fused into glass. Since the adsorption of a variety of gases on glass is considerably smaller than on metals, such an electrode is very stable. Interference is avoided by heating the apparatus to 400° and then keeping it sealed off. Such an apparatus, with the comparison electrode sealed into glass, makes possible investigation of the work function of germanium over a wide range of temperatures.

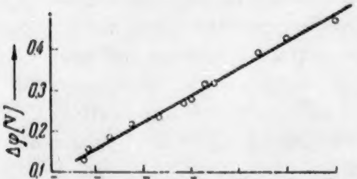

Fig. 1. Variation of contact potential difference between germanium and a comparison electrode with the logarithm of the oxygen pressure.

The method of cleaning the germanium surface is described in [5]. We have investigated a series of samples of n- and p-germanium of varying conductivity, and found that in all cases a clean germanium surface possessed a very constant contact potential difference in relation to the comparison electrode.

The work function for both n-and p-germanium was 0.73-0.75 volt less than that of the comparison electrode. The absence of any noticeable change, even when the position of the Fermi level varies considerably between n- and p-germanium, is believed to be due to the large density of the surface states [7]. Results for the variation of the contact potential difference with oxygen pressure are shown in Fig. 1. These refer to a sample of n-type germanium, $\rho = 20$ ohm · · cm. Similar results (with variation ± 0.02 volt) have been obtained for other samples of both n- and p-types and of varying conductivity.

The relation between adsorption and work function has been examined within the pressure range $10^{-3}$ to 100 mm mercury. For each pressure the constant potential difference was measured for a period of 20 minutes.

It appears from the results that the work function increases with oxygen adsorption for both n- and p-germanium. There is a straight-line relationship between contact potential difference and the logarithm of the pressure over a considerable pressure range. Comparison of the work function data with the adsorption data shows that the fast stage of adsorption of oxygen on germanium, corresponding to the formation of a monatomic layer, and complete even at $10^{-3}$ mm mercury pressure, changes the contact potential difference by 0.15 volt. Further pressure increase, accompanied by further oxygen adsorption, gives rise to the slow stage of adsorption; the contact potential difference continues to increase, and at 100 mm has reached 0.48 volt. These results do not agree with those of Dillon [2], where it is stated that the maximum increase of 0.2 volt is observed at a pressure of $10^{-6}$mm, that there is then a fall to 0.1 volt at $10^{-5}$ mm, and that there is then no further change as the pressure is increased. The work of Dillon and Farnsworth [3] gives an increase of 0.2 volt in the work function in the presence of adsorbed oxygen. In these authors' opinion the contact potential difference does not change with pressure. However their pressure variation was only from $1 \cdot 10^{-7}$ to $2 \cdot 10^{-5}$ mm. Under these conditions the slow stage of adsorption would be difficult to observe.

Our results show that several days are needed to complete the slow stage of chemisorption at 0.07 mm pressure. The rate of this stage increases with pressure according to $P^{0.52}$ [8]. This may account for the change in contact potential difference with pressure increase. The change for the entire rapid stage is smaller than that for the slow adsorption. It is concluded from the results that the formation of a second layer on the germanium surface is associated with the formation of a new compound. If the rapid stage of chemisorption is taken to correspond to the reaction:

$$2Ge + O_2 \rightarrow 2GeO, \qquad (1)$$

then the slow stage of adsorption is evidently associated with the formation of a layer of $GeO_2$ on the germanium surface, according to the equation:

$$2GeO + O_2 \rightarrow 2GeO_2. \qquad (2)$$

adsorbed irreversibly on the germanium surface. This is further confirmed by the fact that degassing at $10^{-6}$ mm after adsorption of oxygen does not cause any change in the contact potential difference. However, if the effect of adsorbed oxygen is investigated under pressures of 100 mm or more, a reversible adsorption occurs as well as the irreversible adsorption, and this has some effect on the contact potential difference. Thus, after adsorption at an oxygen pressure of 100 mm, degassing left an increase in the work function of 0.04 - 0.05 volt, which may be due to physical adsorption of oxygen on the surface of the oxide.

To investigate the behavior of chemisorbed oxygen on a germanium surface at various temperatures, a definite amount of oxygen was adsorbed at room temperature. The contact potential difference was measured, and then the germanium with its chemisorbed oxygen was heated to various temperatures in the absence of gaseous oxygen. After 1 hour heating the apparatus containing the germanium was cooled to room temperature and the contact potential difference again measured. The results are shown in Fig. 2. From the results it seems that after heating to temperatures from 100 to 400° the electronic work function of germanium containing chemisorbed oxygen diminishes (Fig. 2,1) which may be due to the penetration of oxygen into the germanium, and to the evaporation of the germanium oxide from the surface, or to the decomposition of the surface oxide. Heating to 200° gives a work function 0.2 volt less than before heating. Heating to 400° gives a work function 0.08 smaller than on a pure germanium surface.

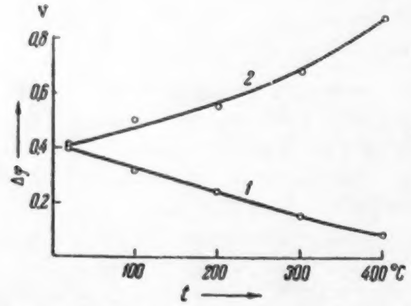

Fig. 2. Change in contact potential difference at a germanium surface on which oxygen is chemisorbed with temperature of heating. 1) in a vacuum of $10^{-6}$mm; 2) in oxygen at 5-6 mm.

These results agree with those of Schlier and Farnsworth [9] who, using the electron diffraction method, showed that germanium containing chemisorbed oxygen, after heating to 500° in a vacuum, behaves like a clean germanium surface. But according to our results desorption of oxygen does not occur with pressure variation at 400°. Neither does removal of GeO from the surface occur, according to the data of Wolsky. Our adsorption measurements have shown that germanium on which both the rapid and the slow stages have been completed will again undergo the slow stage of adsorption at room temperature [5]. Since there is no desorption of oxygen, it must be supposed that on heating this reaction occurs:

$$GeO_2 + Ge \rightarrow 2GeO. \qquad (3)$$

The GeO formed is again converted to $GeO_2$ on contact with oxygen at room temperature.

Thus, when germanium is heated to 400° in a vacuum, oxidation of the surface by chemisorbed oxygen does not occur, but a change in the character of the germanium–oxygen bond takes place. Thus the change in contact potential difference on heating may be explained by reaction [3].

A number of results have been obtained for the heating of germanium in the presence of a certain quantity of oxygen (5 mm) in the gas phase. These are shown in curve 2, Fig. 2. From these it is seen that the work function of germanium increases with the heating temperature, up to a value of 0.9 volt at 400°, which is evidently due to increasing thickness of the $GeO_2$ oxide layer.

It follows from our experiments that the work function of germanium continues to change even when there are several oxidized layers on the surface. These results are in agreement with our earlier ones on the absorption of oxygen on iron, and may be explained by Mott's theories [11] of the diffusion of atoms in a metal – in this case of a semiconductor on an oxide surface.

We wish to express our thanks to Academician A. N . Frumkin for his help in discussing these results.

## LITERATURE CITED

[1] W. Brattain, and I. Bardeen, Bell Syst. Tech. J. 32, 1 (1953).

[2] J. A. Dillon, Bull. Am. Phys. Soc. 1, 53 (1958).

[3] J. A. Dillon and H. E. Farnsworth, J. Appl. Phys. 28, 174 (1957).

[4] V. I. Lyashenko and V. G. Litovchenko, Zhur. Tekh. Fiz., 28, 447, 454 (1958).

[5] R. Kh. Burshtein , L. A. Larin and G. F. Voronina, Doklady Akad. Nauk. SSSR 130 , 4 (1960).

[6] R. Kh. Burshtein and L. A. Larin, Zhur. Fiz. Khim. 32, 194 (1958).

[7] I. Bardeen, J. Phys. Rev. 71, 717 (1947).

[8] M. Green, J. A. Kafalas and P. H. Robinson, Semiconductor Surface Physics, 1956, p. 349.

[9] R. E. Schlier and H. E. Farnsworth, Semiconductor Surface Physics, 1956, p.3.

[10] S. P. Wolsky, J. Appl. Phys. 29, 1132 (1958).

[11] N. F. Mott, Trans. Far. Soc. 43, 422 (1947).

# THE HEAT OF WETTING OF AEROSIL BY ALIPHATIC ALCOHOLS

V. F. Kiselev, K. G. Krasil'nikov and V. V. Murina
M. V. Lomonosov Moscow State University

(Presented by Academician M. M. Dubinin, September 29, 1959)
(Translation of: Doklady Akademii Nauk SSSR, Vol. 130, No.3,
1960, pp. 569-572)
Original article submitted September 25, 1959.

The systematic investigation of the heats of adsorption of a homologous series of substances is of interest in elucidating the connection between the structure of adsorbed molecules and their energy of adsorption. Measurement of differential heat of adsorption of the vapors of higher alcohols, which have relatively low vapor pressures, is difficult in practice, and it is simpler to measure integral heats of adsorption in such cases, and especially the heat of wetting. Measurement of the heat of wetting of ionic crystals and of oxidized carbon black by aliphatic alcohols has already been carried out in our laboratory [1-4], but these investigations did not include consideration of the chemical nature of the surface of the adsorbents. The composition of the surface must exert a considerable influence on the adsorptive and energetic properties of unit surface of the adsorbent, and so it is of interest to carry out similar investigations on silica specimens, the nature of whose surface has already been studied [5-7].

The material used in these investigations was a nonporous silica known as "Aerosil", a finely divided silica prepared in our laboratory by the ignition of ethyl orthosilicate [8]. Separate portions of the starting material were ignited in air for 24 hours at each of the temperatures shown so as to obtain different surface conditions. The specific surface of each sample was calculated from the adsorption isotherm of nitrogen gas at its boiling point, using the B.E.T. method. The percentage of structural water was obtained from the weight loss on ignition. The facts are set out in Table 1.

TABLE 1

Adsorption Characteristics of Aerosil Sample BC-2.

| Ignition temp. °C | Specific surface, m$^2$/g | Structural water content, μ M/m$^2$ |
|---|---|---|
| 300 | 156 | 6.3 |
| 500 | 143 | 3.1 |
| 700 | 120 | 1.8 |
| 900 | 112 | 1.5 |

The method used to prepare samples for calorimetric measurements and for determining the bound water have been described in [5-7]. Alcohols used in this work were carefully freed from water and distilled through a column. Measurement of the heat of wetting was performed in a constant heat-exchange calorimeter, through

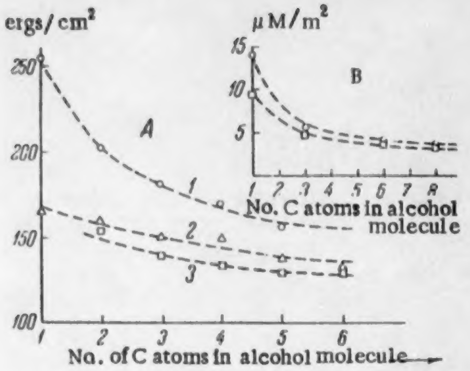

Fig. 1. Relationship between the magnitude of the heat of wetting (A), and the adsorption limit (B) [10], for a homologous series of n-alcohols on samples BC-2, T = 300° (1); BC-2, T = 500° (2); BC-2, T = 700° (3).

which dry air was blown for many hours before measurements were made. The heat of wetting by organic liquids is affected by even minute quantities of moisture, and therefore the calculation was performed only when the heat change obtained by breaking successive ampoules of each calorimetric liquid had reached constancy.

It can be seen from Fig. 1A that the heat of wetting diminishes steadily as the length of the hydrocarbon chain of the alcohol increases, but from amyl alcohol on, the figures are practically constant. The specific heat of wetting is proportional to the energy of binding of the molecules with the adsorbing centers on the surface, and to the surface concentration of the molecules. The latter is measured by the magnitude of the adsorption limit, $a_m$, when the alcohol is adsorbed from a nonpolar solvent, since in such a case the adsorption of the solvent, as we have shown [9,10], is vanishingly small. The reduction in the heat of wetting for these alcohols depends essentially, we must suppose, on the reduction in the surface concentration of the adsorbed molecules (Fig. 1B). For the higher alcohols the decrease in the magnitude $a_m$ with increase in hydrocarbon radical length becomes smaller (Fig.1B), since, apparently, the adsorbed molecules are inclined to the surface [9,10]. On the other hand, the interaction energies due to alcohol molecules will increase with length of hydrocarbon radical, both because of increase in dispersion interaction with the surface, and because of the lateral attraction between hydrocarbon radicals of neighboring molecules. The constancy of the heat of wetting for the higher alcohols is apparently due to the mutual compensation of the factors named.

It has already been shown [5-7], that the heat of wetting of silica gels with water and methanol shows a linear relationship with the degree of hydration of the surface. It is shown in Fig. 2 that the heat of wetting of nonporous silica BC-2 by water and methanol fits satisfactorily the straight line obtained formerly for silica gels [5]. This shows again that pores exert no noticeable effect on the heat of wetting of silica gels with methanol [5].When we come to n-propyl alcohol, a straight line is again found for the heats of wetting of silica gels with effective pore diameters of 65 and 60 A, lying close to the line for nonporous silica. The slight difference in the gradient of the lines is associated with some increase in the strength of the adsorption interaction of the hydrocarbon radicals in the fine pores. The straight line for a specimen with finer pores (d = 44A) is displaced in the direction of lower heats of wetting because of the increasing pore influence.

The silica surface is not homogeneous, since it consists of silanol and siloxane portions. During thermal dehydration there is a change both in the ratio between these portions and in their properties. At low processing temperature the surface of the specimens must contain both structural water and physically adsorbed water, and it is still a matter of discussion whether the surface also contains coordinately linked water, whose existence is inferred by Weyl [11] from the screening of surface silicon atoms. Existing methods of determining structural water give only the total water in the sample, and do not enable us to distinguish from each other the various methods of binding. The problem of establishing the exact temperature conditions under which water bound in the various ways can be removed from the sample is still unsolved [6, 14, 17]. With sufficiently high surface concentration of hydroxyl groups these may form hydrogen bonds among themselves, with consequent reduction of energy properties of the silica surface [6,7], as has been inferred from the infrared spectra of the silica surface layer [12,13]. Increase in the ignition temperature causes surface dehydration, which involves a transformation of some of the silicon-oxygen tetrahedra [10]. The first effect, evidently, involves the tetrahedra linked with the bulk material by one bond, subsequently those linked by two bonds, and finally those linked by three. Thus, dehydration causes not only a change in the surface concentration of the hydroxyl groups, but also in the surface configuration. For samples treated at high temperatures it is believed that the silanol portion of the surface will consist essentially of isolated hydroxyl groups [14].

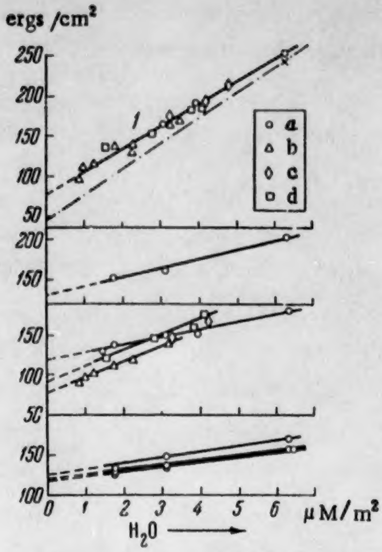

Fig. 2. Heat of wetting of aerosil samples (a), silica gel K-2 (b) KOK-1 (c) and KCK-2 (d) by alcohols, for variation in the degree of hydration of the surface. Numbers on the lines denote the number of carbon atoms in the alcohol molecule. The dotted line in the top figure gives the heat of wetting by water of silica gels [7] and aerosil (x).

The siloxane part of the surface is apparently also nonhomogeneous. We have shown that the rehydration of a silica surface dehydrated at high temperatures is irreversible [6], showing that such a surface contains at least two types of packing for the $SiO_4$ tetrahedra: those binding into the surface at all four apexes [6], and those having edges containing strained oxygen bridges which are capable of being hydrated. Thus the extent of ignition of the silica determines not only the degree of hydration of the surface, but also the properties of the surface, and may have a surprising effect on the adsorption of different molecules.

In the case of water molecules, which are capable of forming from four to one bonds with the hydroxyls of the surface, the degree of bonding may be changed both in the process of saturating the surface and in that of dehydration [6, 14], which will result in a change in the configuration of the adsorption centers on the surface.

Alcohol molecules are linked to the surface by one hydrogen bond [10,14]. The linear dependence of the heat of wetting on the degree of hydration (Fig. 2) shows that within the studied limits of the degree of hydration of the samples, the heat of wetting is mainly determined by the ratio between the silanol and siloxane parts of the surface, while variation in the properties of these parts has in this case no significant effect. Reduction in the degree of hydration of the surface has the greatest effect in the case of methanol. Increase in the hydrocarbon radical length and in the area occupied per molecule (Fig.1B), probably results in the molecules of the higher alcohols screening part of the surface hydroxyl groups. As a result of this, change in the degree of hydration is less significant in determining the size of the adsorption limit [10]; that is, the concentration of adsorbed molecules changes only slightly with the degree of hydration of the surface. Account must also be taken of the fact that the alcohol molecules may interact with the siloxane portion of the surface. The gradient of the heat of wetting changes as we move toward the higher alcohols: increase in hydrocarbon radical length gives rise to increased influence in the adsorption interaction, and the heat of wetting of the alcohols approaches that of hydrocarbons, the adsorption and energy of which is but little affected by change in the silica surface composition [5,16].

The authors express their thanks to B. V. Il'in for his interest in the work and his support.

## LITERATURE CITED

[1] B. V. Il'in, A. V. Kiselev, et al., Doklady Akad. Nauk. SSSR 75, 827 (1950).

[2] B. V. Il'in and V. F. Kiselev, Doklady Akad. Nauk. SSSR 82, 91 (1952).

[3] V. F. Kiselev, Doklady Akad. Nauk. SSSR 89, 113 (1953).

[4] B. V. Il'in, V. F. Kiselev, and G. I. Aleksandrova, Doklady Akad. Nauk. SSSR 102, 1155 (1955).

[5] G. I. Aleksandrova, K. G. Krasil'nikov, et al., Doklady Akad. Nauk. SSSR 108, 283 (1956).*

[6] B. V. Il'in, V. F. Kiselev, and K. G. Krasil'nikov, Vestn. Moskovsk. univ. 6, 35 (1957).

[7] B. V. Il'in, V. F. Kiselev, and K. G. Krasil'nikov, Vestn. Moskovsk. univ. 2, 223 (1958).

[8] A. K. Bonetskaya, E. A. Leont'ev, and E. A. Kharlamov, Zhur. Prikl. Khim. 30, 1237 (1957).*

---

* Original Russian pagination. See C. B. translation.

[9] A. K. Bonetskaya and K. G. Krasil'nikov, Doklady Akad. Nauk. SSSR 114 (No.6), 1257 (1957).*

[10] L. G. Ganichenko, V. F. Kiselev, and K. G. Krasil'nikov, Doklady Akad. Nauk SSSR 125, 1277 (1959).*

[11] E. A. Hauser and W. A. Weyl, Kolloid-Z. 124, 72 (1951).

[12] M. Folman and D. J. C. Yates, Trans. Faraday Soc. 54 (11), 1684 (1958).

[13] M. C. Donnald, J. Phys. Chem. 62 (10), 1168 (1958).

[14] S. P. Zhdanov, Zhur. Fiz. Khim. 32, 699 (1958).

[15] T. S. Egorova, V. F. Kiselev, and K. G. Krasil'nikov, Doklady Akad. Nauk. SSSR 123, 1060 (1958).*

[16] A. A. Isirikyan and A. V. Kiselev, Doklady Akad. Nauk. SSSR 115, 343 (1957).*

[17] W. Stöber, Kolloid-Z. 145, 17 (1956).

---

* Original Russian pagination. See C. B. translation.

# THE INFLUENCE OF RADIOLYSIS ON THE POTENTIAL OF A NICKEL ELECTRODE AS A FUNCTION OF THE GAS PHASE COMPOSITION

S. D. Levina and T. V. Kalish

Electrochemical Institute, Academy of Sciences USSR

(Presented by Academician A. N. Frumkin, October 7, 1959)

(Translation of: Doklady Akademii Nauk SSSR, Vol. 130, No.3 1960, pp. 573-576)

Original article submitted September 28, 1959.

As is well known, a nickel electrode in an alkaline solution in a hydrogen atmosphere attains the potential of a reversible hydrogen electrode. It was shown [1] by the authors of this communication that the interaction of atomic hydrogen with nickel in an alkaline solution gives a potential which is 45-70 mv* more negative than a reversible hydrogen electrode. In connection with these experiments it seemed interesting to elucidate the behavior of a nickel electrode under conditions where oxygen atoms or OH-radicals, as well as hydrogen atoms, are supplied to the electrode.

We used the radiolysis of aqueous solutions to effect such conditions. According to numerous literature data [2], the primary products of the radiolysis of water are hydrogen atoms and free OH radicals, but hydrogen molecules and hydrogen peroxide are also formed by the reaction

$$H_2O \rightsquigarrow H_2,\ H_2O_2,\ H,\ OH,\ HO_2$$

with a yield (g) per 100 ev

$$g_H = 2{,}8,\ g_{OH} = 2{,}2,\ g_{H_2O_2} = 0{,}8,\ g_{H_2} = 0{,}42.$$

As was shown by Zalkind and Veselovskii [3,4], the potential (+800 mv) of a Pt-electrode in sulfuric acid is shifted by $\gamma$-ray bombardment to lower values and after 10-15 minutes it attains the potential of a reversible hydrogen electrode, which it retains during the irradiation. These authors explain this effect by the disposition of platinum to adsorb hydrogen selectively and they assume that the observed shift of the potential is evoked and maintained by the free hydrogen atoms formed by the radiolysis.

In this investigation the change of the nickel potential in an alkaline solution caused by irradiation with x-rays was studied at various hydrogen pressures, and also in the absence of gases and in an inert gas atmosphere (neon).

The nickel electrode — a sheet with dimensions 1.5 × 1.5 cm (A) — was reduced in a hydrogen atmosphere at 400° and was kept in hydrogen. Before the experiment the electrode was rapidly transferred to the apparatus shown in Fig. 1. The electrode was placed as near as possible and parallel to the horizontal bottom (B) of the apparatus. A mercurous oxide-mercury electrode (C) was used as reference electrode and was separated from the rest of the apparatus by the glass filter (D). The vessel (E) contained a previously degassed alkaline solution. The radiolysis of the solution was effected by irradiation from an x-ray tube working at a voltage of 80 kv and an anodic current of 200 ma. Under these conditions the energy absorbed by 1 cc solution was equal to $6.8 \cdot 10^{16}$ ev/sec. The irradiation was effected through the bottom (B) of the apparatus which was as near as possible to the radiation source.

---

*Against a reversible hydrogen electrode at atmospheric pressure.

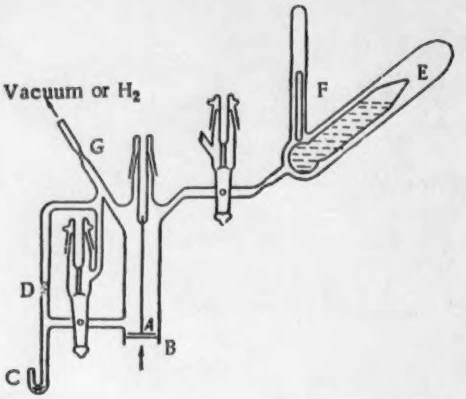

Fig. 1. The apparatus for the investigation of the course of the electrode potential in an electrolyte solution under the influence of irradiation.

Before the start of an experiment the apparatus was evacuated ($10^{-6}$mm Hg), then gas was introduced until the desired pressure was attained, and the apparatus was sealed off at (G) from the rest of the system. With the aid of an electromagnetic hammer (F) the bottom of the vessel was crushed and the solution (0.68 N NaOH) filled the apparatus, after which the measuring of the electrode potential was started.

Figure 2 shows the change of the nickel electrode potential with time under the influence of radiolysis in the absence of gases. As is obvious from Fig. 2, the initial nickel electrode potential is about 250 mv more positive than a reversible hydrogen electrode, because it is covered with an oxide film as a result of the transfer through air. As was shown in the investigation by Shurmovskaya and Burshtein [5], a limited oxide film, corresponding to $1.3 \cdot 10^{15}$ oxygen atoms per $cm^2$ original surface, is formed on the nickel surface upon contact with air. By the action of the irradiation the potential is shifted to less-positive values and after 10-12 minutes this shift amounts to about 200 mv, i.e., for 50 mv the potential does not attain the value of a reversible hydrogen electrode at atmospheric pressure. Upon continuing the irradiation this potential is retained for some minutes after which it is gradually shifted to more positive values. If the irradiation is interrupted, the potential is shifted again in the negative direction and attains its lowest value. The said shift of the potential in the positive direction upon continuing the irradiation and in the negative direction upon switching off may be observed many times in succession on one and the same electrode. The effect comes to a stop when the electrode under the influence of prolonged irradiation is oxidized to a value about 500 mv more positive than a reversible hydrogen electrode, i.e., when a stable oxide film has just been formed on the nickel. From the curve in Fig. 2 it is obvious that hydrogen is adsorbed on the nickel during the first stage of the irradiation. This causes the shift of the potential in the negative direction. However, as oxidizing agents accumulate in the solution, the nickel potential is shifted in the positive direction. From the course of the curve one may draw the following conclusion. Judging from the relatively slow shift in the positive direction under the influence of irradiation, the gradual accumulation of $H_2O_2$ in the solution must play some role in this process. On the other hand, the very rapid return of the potential to a less-positive value upon interruption of the irradiation is obviously connected with the disappearance of the oxidizing, short-lived radicals from the solution. At the same time $H_2O_2$ must also decompose because it is unstable in an alkaline solution, but this process does not proceed as rapidly. Thus, the mechanism of the said phenomenon is not wholly clear as yet, and will afterward be studied in more detail. The curves obtained in neon (at a pressure of 6-10 mm) show the same course as the curves obtained in the absence of gases.

According to the investigations by Scheuble [6], the adsorption of hydrogen from the gas phase proceeds more rapidly if it is adsorbed not on a clean nickel surface but on a nickel surface which has previously adsorbed oxygen. In our experiments the hydrogen to be adsorbed is liberated on a nickel surface which has already been covered with oxygen. Using the analogy of the data mentioned on the adsorption from the gas phase of hydrogen on nickel, one may explain why, in the absence of gases or in a neon atmosphere, the shift of the potential caused by the irradiation, in the first instance, goes in the negative direction.

In Fig. 3 is shown the change of the nickel potential in the same solution at hydrogen pressures equal to 80 mm (I), 6 mm (II), and also in a mixture of hydrogen and neon with about 1 mm hydrogen and 6 mm neon (III). When the radiation is switched on, the nickel potential is shifted in the negative direction and after 4-5 minutes the shift attains its maximum value. In contrast with the experiments in the absence of gases or in neon, the potential in these cases changes only a little—when the radiation is switched on or off. The initial nickel potential is nearly equal to the potential of a reversible hydrogen electrode at the corresponding pressure. For curves I and II it differs by 5 mv and 15 mv, respectively, and for curve III it practically coincides with the latter potential.

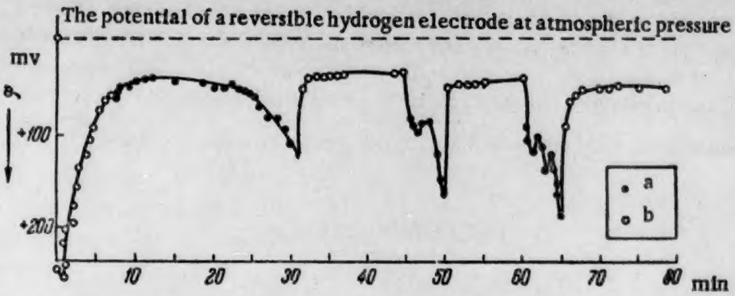

Fig. 2. The change of the nickel electrode potential with time under the influence of irradiation in the absence of gases: a) radiation switched on; b) radiation switched off.

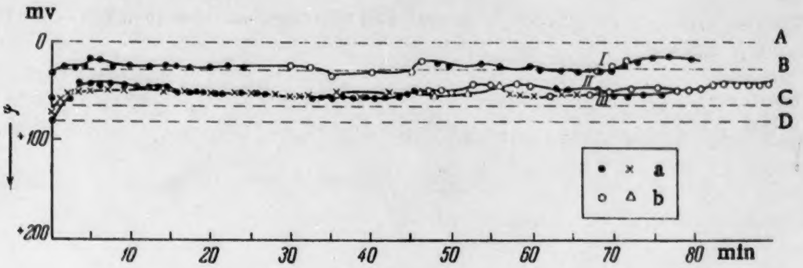

Fig. 3. The change of the nickel electrode potential with time under the influence of irradiation at various hydrogen pressures. The dashed lines show the potentials of a reversible hydrogen electrode: A) at atmospheric pressure, B) at 80 mm hydrogen, C) at 6 mm, D) at 1 mm hydrogen + 6 mm Ne. a) Radiation switched on, b) radiation switched off.

Under the influence of the irradiation at a hydrogen pressure of 80 mm the potential is shifted not more than 5-10 mv in the negative direction. An interruption of the irradiation causes a return of the potential to the initial value. At a pressure of 1 mm hydrogen + 6 mm neon the shift of the potential averages 30-35 mv in the negative direction. The concentration of molecular hydrogen in the solution at an absorption of $6.8 \cdot 10^{16}$ ev/sec per cc may attain a value of the order of $10^{-4}$ mole/liter* in 4 minutes (the time needed for the adjustment of the potential). From this it is obvious why the hydrogen liberated by radiolysis has an imperceptible influence on the potential at 80 mm hydrogen pressure, for at this pressure the solubility of hydrogen is equal to $0.75 \cdot 10^{-4}$ mole/liter. On the other hand, since at a pressure of 1 mm the solubility of hydrogen is of the order of $10^{-6}$mole//liter, the hydrogen liberated by radiolysis must cause a perceptible shift in the negative direction. An exact calculation is difficult, because the hydrogen is shared between the solution and the gas phase. Moreover, part of the formed hydrogen reacts with the oxygen on the nickel surface. At all events, a shift of 30-35 mv in the negative direction under the influence of the irradiation at 1 mm hydrogen pressure may be explained by the increase in molecular hydrogen in the solution. Thus, under our experimental conditions, the assumption that atomic hydrogen has an effect is not needed in order to explain the shift of the nickel potential to values which are more negative than the potential of a reversible hydrogen electrode.

For the results obtained both at 1 mm hydrogen and at higher pressures, contrasted with the experiments in the absence of gases, it is characteristic that the electrode potential changes only a little during the irradiation.

---

* The amount of molecular hydrogen liberated in 4 minutes at a radiation dose of $6.8 \cdot 10^{16}$ ev/sec·cc and a yield of 0.42 per 100 ev will be equal to: $\frac{6.8 \cdot 10^{16} \cdot 0.42 \cdot 240 \cdot 1000}{100 \cdot 6.03 \cdot 10^{23}} = 1.12 \cdot 10^{-4}$ mole/liter.

The observed small scattering of the potential may be ascribed either to temperature effects or to the counteracting influence of reducing and oxidizing substances. Within the first couple of minutes after the switching on of the irradiation, a strong shift in the negative direction takes place and the most negative potential value attained is kept for some time. As is obvious from the curves of Fig. 3, some shifting of the potential is often observed also after switching off the irradiation, but the cause of this shift is not wholly clear as yet.

We thank Academician A. N. Frumkin and P. I. Dolin for the discussion of the results.

## LITERATURE CITED

[1] S. D. Levina and T. V. Kalish, Proc. Acad. Sci. USSR, 109, 971 (1956).*

[2] A. O. Allen and H. A. Schwarz, Proceedings of the Second International Conference on the Peaceful Use of Atomic Energy (Geneva, 1958). Aqueous Solutions, p. 1 [Russian translation].**

[3] Ts. I. Zalkind and V. I. Veselovskii, Collected Papers on Radiation Chemistry, 1955, p. 66 [in Russian].

[4] Ts. I. Zalkind and V. I. Veselovskii, The Action of Ionizing Radiation upon Inorganic and Organic Systems, 1958, p. 66 [In Russian].

[5] N. A. Shurmovskaya and R. Kh. Burshtein, J. Phys. Chem. USSR, 31, 1151 (1957).

[6] W. Scheuble, Zs. Physik 135, 125 (1953).

---

* Original Russian pagination. See C. B. translation.

** Paper No. 1403 in the English edition.

# INVESTIGATION OF ADSORPTION OF THE UNSATURATED FLUOROCARBONS $C_2F_4$ AND $C_3F_6$ IN AN ELECTRON EMITTER

Corresponding Member of the USSR Academy of Sciences
S. Z. Roginskii and V. A. Shishkin

Institute of Physical Chemistry, Academii of Sciences USSR

(Translation of: Doklady Akademii Nauk SSSR, Vol. 130, No.3, 1960, pp. 577-580)

Original article submitted July 9, 1959.

Lately, much research has been devoted [1-4] to the origin of the discrete bright spots which appear on the screen of an electron emitter at pressures of $10^{-6}$- $10^{-5}$mm Hg. At the moment it is possible to consider established only the immediate connection of the spots with adsorption of individual molecules. From the relationship between the number of moving spots and the pressure, Müller considers that a "molecular picture" results from absorption. Becker [2] on the contrary, considers their emergence as migration of molecules directly bound to the substrate in a weakly adsorbed condition. Both authors consider that one necessary condition is contact of the tip with the gas at $p \geq 10^{-6}$mm Hg. However, for vapors of heavy substances this condition does not seem obligatory since Gomer [5] observed the four-leaf picture of phthalocyanine at $p < 10^{-9}$mm Hg and $\theta < 1$.

I. I. Tret'yakov [3] adds to the necessary conditions exposure in a field in the presence of a gas, which is necessary in the author's opinion for the formation of "microtips", which increase the resolution. The results of comparison of the shape of the spots arising from adsorption of large organic molecules of different geometrical structure and different dimensions [6] point to the absence of any correlation between the geometry of the "molecular picture" and the geometry of the molecules. On the other hand, experiments with small molecules indicate a definite correlation between electronic structure of the molecules and the shape of the spots [3].

From [6] in particular, it was established that "doublets" and "rings" were observed only in the presence of double bonds, but the four-leaf pictures were observed for more complex structures.

To explain this relationship, one of the authors [4] put forward the hypothesis of direct participation of the $\pi$-electrons of double bonds in emission, with the formation of spots of complex shape, whereupon the main role is ascribed to the affiliated biradicals produced on adsorption. The present paper sets as its goal the examination of this hypothesis using the chemically inert, stable molecules of unsaturated fluorocarbons, since the possibility remains from earlier work on the unsaturated fluorocarbons that the radicals may be produced due to simple splitting-off of hydrogen atoms at the tip and rupture of the carbon bonds. Moreover it is desirable to specify the conditions necessary for observation of "molecular pictures".

## EXPERIMENTAL

The work was done with the normal electron-emitter setup. $C_2F_4$ and $C_3F_6$* were studied. The method for admitting the gases was changed. The gas to be studied was first admitted at p = 0.1 mm Hg pressure into an ampoule which had been carefully outgassed by prior heating in vacuo ($\approx 10^{-6}$ mm Hg) in the presence of active charcoal. Before the gas entered the emitter, the extension containing the ampoule was chilled in liquid

---

*We take this opportunity to express our thanks to Academician I. L. Knunyants for a gift of these gases.

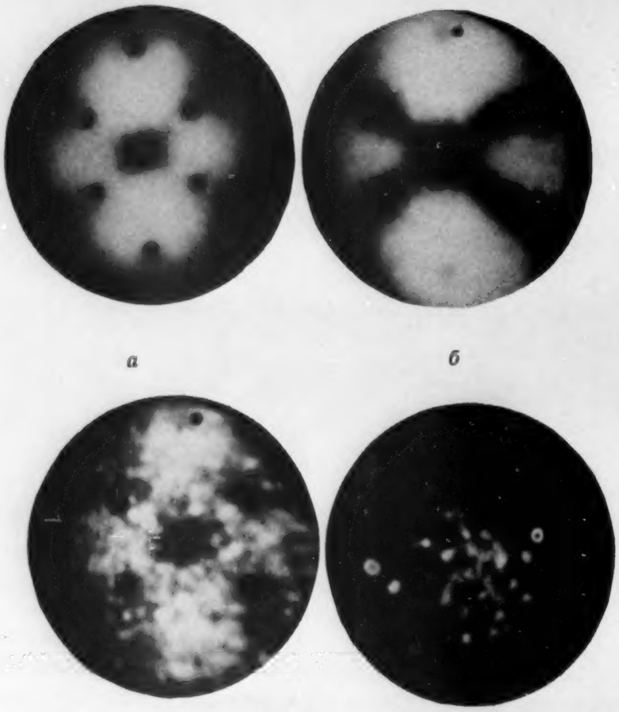

Fig. 1. Absorption of $C_3F_6$ on tungsten ($1\cdot10^{-8}$ – $6\cdot10^{-6}$ mm) $\tau$ = 1/10 sec. a) clean tungsten base at p < $1.10^{-9}$ mm. 2 (g) $C_3F_6$ at P = $1\cdot10^{-6}$ mm, a, b, c) U = 3.3 kv; d) U= 3.5 kv

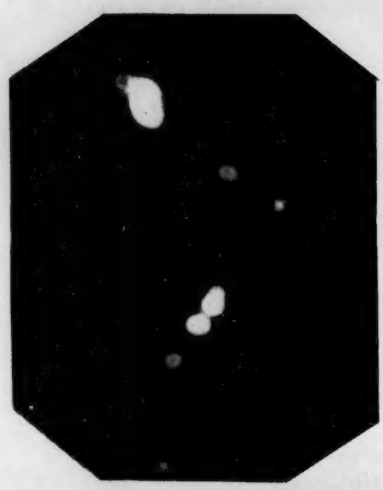

Fig. 2. Doublets of $C_2F_4$ on a reconstructed α W-tip U = 16.4 kv, $\tau$ = 1/10 sec.

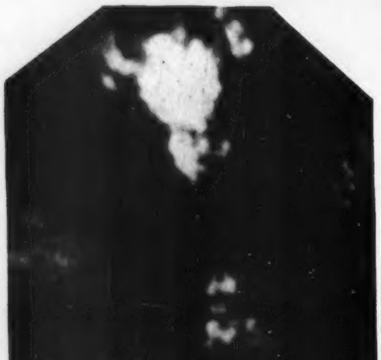

Fig. 3. W - tip in an atmosphere of $C_3F_5$ at p ≅ $5\cdot10^{-6}$ mm.

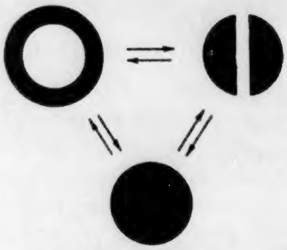

Fig. 4. Observed mutual transmutation of "molecular pictures" for $C_3F_6$.

air, after which the thin end of the ampoule was broken. On changing the temperature of the ampoule containing the carbon, the pressure in the system can be reversibly changed over the limits $10^{-2}$ —$1 \cdot 10^{-7}$mm. After lowering the pressure to $1 \cdot 10^{-9}$mm and taking a picture of the original clean tungsten, the experiment was started. In Fig. 1 is shown the stages of adsorption of $C_3F_6$ at pressures from $1 \cdot 10^{-8}$ to $1 \cdot 10^{-6}$mm. The first stage of the adsorption suggests adsorption of the simple gases ($O_2$,$N_2$,$H_2$). The energy of escape increases with the filling up of the surface. The first part of the gas gives a slightly granular picture; at a pressure of $5 \cdot 10^{-7}$mm Hg separate, bright spots appear which are fixed in position. At a pressure of $1 \cdot 10^{-6}$mm brilliant spots begin to appear, lasting for a limited time, only circular at first but then shaped like a "ring", or cantilever. From the moment when mobile spots appear ("molecular pictures"), the emission current drops 13 times ($O_2$ lowers it at $1 \cdot 10^{-7}$mm ~$10^6$times). After this the emission current increases slightly. The total number of "molecular pictures" and the proportion of complex forms increase with pressure (Fig. 3). Lowering of the pressure always leads to a diminution in their number. The whole picture seems three-dimensional, strongly emitting faces appear multilayered and are projected forward. Exposure in a field at a current of 20-25$\mu$ a (p = $10^{-6}$mm) leads to an almost complete loss of the described contrast. If the tip is maintained at $1 \cdot 10^{-5}$ mm pressure, and then afterwards lowered to $1 \cdot 10^{-7}$mm, the number of spots gradually diminishes. This indicates that the "molecular pictures"are dependent on the molecules which are weakly attached to the substrate. The filling up of this layer depends on $\underline{p}$. The heat of absorption is evaluated by measuring the duration of the existence of these "pictures" at 100 and 300°K; it is about 700 cal/mol.

The relationships which hold for absorption of $C_3F_6$ are true for the absorption of $C_2F_4$ , with the exception that the latter gas does not give circular rings. In order to explain the need for using tips of small radii (because of the increase) and the role of the microtip in the appearance of "molecular pictures", an investigation was made with blunted tips (0.1-2.5$\mu$) similar to that using thin ones. Even with an extremely blunt contact, changed as the result of many hours tempering to a rounded, spherical shape, barely discernible doublets of $C_2F_4$ could be observed. However, to accomplish this it was necessary to increase the pressure in the flask until there was a discharge. The reconstruction of this tip in the field led to an increase (~5 times) in the size of the spots (Fig. 2). Adsorption on microtips formed and made visible due to bombardments leads to the appearance of spots of almost the same form as does adsorption on plane areas. The difference lies in the high luminosity of the spots on projection and in their lesser definition. Sometimes in the dark regions of the picture there appear clear "molecular pictures."

It is probable that for the gases under discussion at least,the filling in of the surface plays as large a part as the possible formation of submicrotips. Microtips, which bring a marked localized increase in emission, do not play an essential part in this process. The admission of $O_2$ at p = $1 \cdot 10^{-7}$mm to the tip covered by $C_2F_4$ led to a gradual fall in emission and to a change in distribution of the bright and dark areas towards the characteristic oxygen picture. Doublets were also observed in the areas, surrounding the direction (100). This indicates a displacement of $C_2F_4$ by oxygen from the layers immediately linked to tungsten. Thereupon, the form and behavior of the "molecular pictures" remain unchanged.

The life time of the"molecular pictures" in the case of both the unsaturated fluorocarbons which were studied was of the order of fractions of a second (rarely seconds). On heating the tip, the frequency of scintillation increased, though, finally, at dull red heat, the adsorbed layer begins to come off quickly in the case of showing very bright and coarse spots well spread out. Desorption in high vacuum does not lead to production of a carbon layer, but heating to a high temperature ( ~2000°C) in an atmosphere of $C_3F_6$ at P = $1 \cdot 10^{-6}$ mm leads to an appreciable layer of deposited carbon. On cooling the tip and the surrounding supports with liquid nitrogen, the emission pattern becomes quiescent and the lifetime of the spots increases to a few seconds. Mutually transmutable forms become distinguishable (Fig. 4). Round spots which change to doublets increase in dimension; with a still bigger increase, they undergo transformation to a ring structure. An increase in the anode voltage shortens their lifetime.

## DISCUSSION OF RESULTS

1. The connection of the appearance of doublets and rings in the presence of a double bond has been confirmed on a new type of compound and the possibility is shown of multiple repetition of the observation without the introduction of fresh quantities of gas.

2. The necessary participation of microtips in the formation of "molecular pictures" was not confirmed.

3. Rings were detected even for the **less-symmetrical** molecules such as $C_3F_8$.

4. The definition of "molecular pictures" and their lifetime increased with reduction in temperature; this permits the clear observation of the change of molecular pictures from one form to another.

5. The data obtained do not contradict the hypothesis expressed earlier on the role of the radicalization of $\pi$-bonds. Thus, the formation of such radicals immediately adjacent to the tip, before adsorption, and, owing to the broken $\pi$-bonds of molecules earlier adsorbed, the possibility, according to Becker, of their migration from lower to upper layers, are both admissible.

6. An explanation of the form of the observed pictures and the interconversion forms is difficult on the basis of those used from simple geometrical considerations by a number of authors [1,2]. The fact that molecules which differ greatly in structure can give a picture of one and the same type with good reproducibility, suggests that there is a very deep underlying relationship between the form of the spots and the electronic structure of the molecules. In particular, it might be considered that the molecular spots transmit the probable distribution of electron clouds, the orbits of which take part in the formation of $\pi$-bonds: the weak chemisorptive nature of these molecular bonds indicates that broken bonds do not become saturated at a surface, but locally in the molecules themselves. Such a variation on the hypothesis is easily combined with the earlier hypothesis, put forward in experimental data, on the role of $\pi$-electron bonds.

The authors wish to thank I. A. Bespalovoi for his assistance with this work.

## LITERATURE CITED

[1] E. W. Müller, Ergebn. exakt. Naturwiss., 27, 290 (1953).

[2] J. Becker, Adsorption on Metallic Surfaces, Collection, Catalysis, Electron Phenomena [Russian translation] (Foreign Lit. Press 1958).

[3] I. I. Tret'yakov, Collection Conference on Catalysis, Moscow 1958.

[4] S. Z. Roginskii, Zh. Fiz. Khim. No.9, 1959.

[5] R. Gomer and D. A. Speer, J. Chem. Phys., 21, 73 (1953).

[6] I. I. Tret'yakov and S. Z. Roginskii, Doklady Akad. Nauk SSSR, 107 857 (1956).*

---

*Original Russian pagination. See C. B. translation.

# THERMODYNAMIC STUDY OF THE REACTION $UO_2(s)+\frac{1}{2}C(graph.)+Cl_2(g)=UOCl_2(s)+\frac{1}{2}CO_2(g)$ BY MEASURING ELECTROMOTIVE FORCES

M. V. Smirnov, I. F. Nichkov, S. P. Raspopin,
and M. V. Perfil'ev

Electrochemical Institute, Ural Branch Academy of Sciences SSSR

(Presented by Academician V. I. Spitsyn, September 19, 1959)

(Translation of: Doklady Akademii Nauk SSSR, Vol. 130,No.3,
1960, pp. 581-584)

Original article submitted September 18, 1959.

In previous investigations [1-3] it was ascertained that oxide-carbon electrodes pressed from intimate mixtures of metal oxides and carbon are reversible in molten chlorides, with respect to the corresponding cations. Therefore, these electrodes may be used in a thermodynamic investigation of some reactions by measuring e.m.f. [4-6]. This applies in particular to two types of chlorinations:

$$1)\quad Me_2O_n(s) + \frac{n}{2}C(s) + nCl_2 = 2MeCl_n(\text{ melt }) + \frac{n}{2}CO_2(g).$$

where the oxide does not react to a measurable extent with the molten chloride, as for instance, is the case with beryllium , calcium and thorium oxide-carbon electrodes, and

$$Me_2O_n(s) + \frac{n-2}{2}C(s) + (n-2)Cl_2(g) = 2MeOCl_{(n-2)}(s) + \frac{n-2}{2}CO_2(g).$$

where the oxide reacts with the molten chloride and forms an insoluble oxychloride.

By using an oxide-carbon electrode containing uranium dioxide in our experiments we verified the usefulness of this method for an investigation of the reaction thermodynamics for a chlorination of the second type. It is known [7] that at and above 600° the dioxide reacts with the molten tetrachloride and forms the oxychloride $UOCl_2$. In the literature there are no data on the solubility of this compound in molten chlorides. In one [8] of our investigations, however, it was found that thorium oxychloride, $ThOCl_2$, is practically insoluble in molten chlorides and in molten mixtures of fluorides and chlorides. One may expect that the oxychloride of tetravalent uranium will have analogous properties.

If this is the case, the uranium oxide-carbon electrode containing dioxide must absorb uranium tetrachloride from the melt until its concentration attains a value corresponding to the equilibrium:

$$UO_2(s) + UCl_4(\text{ melt }) \rightleftarrows 2UOCl_2(s).$$

Obviously, the equilibrium potential which is attained after some time is determined mainly by this concentration and will not depend on the initial tetrachloride concentration in the melt nor on the ratio of oxide and carbon in the electrode. However, one should keep in mind as well that, as a result of the difference in specific weight between the dioxide and the oxychloride, the electrode may disintegrate and, the greater the amount of absorbed tetrachloride, the more disintegration occurs. Such a disintegration caused by the formation of oxychloride was observed by us [1] with thorium when the melt contained more than 25 weight % $ThCl_4$.

Thus, by using the uranium oxide-carbon electrode ($UO_2$+C) in combination with a chlorine electrode in molten alkali chlorides containing uranium tetrachloride and measuring the e.m.f. $\epsilon$ as a function of temperature in cells of the type:

$$UO_2 + C + UOCl_2 | \quad \text{melt} \quad NaCl + KCl + UCl_4 | Cl_2, C,$$

one may find the free energy change, ΔZ, of the reaction:

$$UO_2\,(s) + \frac{1}{2}C\,(gr) + Cl_2\,(g) = UOCl_2\,(s) = \frac{1}{2}CO_2\,(g)$$

$\Delta Z = -46124 \cdot \epsilon$ cal/mole $UOCl_2$

The oxide-carbon electrodes were prepared from uranosic oxide obtained by heating the peroxide in air at 600°. The fine powder obtained in this way was mixed in the required proportion with sugar syrup and the water was evaporated until a powdery substance formed, from which cylinders with a diameter of 10 mm and a length of 5-15 mm were pressed under a pressure of 4000 kg/cm$^2$. These were fired without admission of air under a layer of carbon by gradually raising the temperature to 800°. During this treatment the uranosic oxide was reduced by the carbon. An analysis of the fired electrodes showed that they contained dioxide with a composition varying from $UO_{2.02}$ to $UO_{2.06}$, and sufficient free carbon to convert all oxygen into $CO_2$. In separate experiments the molar ratio of dioxide and carbon was specially varied in broad ranges between 1:1.6 and 1:200. The electrodes were attached to spectroscopically pure carbon leads.

A solution of uranium tetrachloride was used as electrolyte either in a molten eutectic mixture of lithium and potassium chlorides ($t_m$ = 352°), or in a molten equimolar mixture of sodium and potassium chlorides ($t_m$=662°). The uranium tetrachloride was prepared by the chlorination of dioxide with carbon tetrachloride at 500° in a pure argon stream. The sublimated tetrachloride was purified by a second sublimation in vacuum at 700°. The construction of the cell in which the measurements were carried out is shown diagrammatically in Fig. 1. A lead electrode was employed as reference electrode; it was placed in a separate tube filled with a molten eutectic of LiCl and KCl to which 8 weight % $PbCl_2$ had been added. In separately executed experiments the temperature dependence of the e.m.f. between the lead and the chlorine electrode was found. After subtraction of the thermo-e.m.f. between the carbon cylinder of the chlorine electrode and the molybdenum current lead of the lead electrode the following empirical equation is satisfied:

$$\epsilon = (1.639 - 3.04 \cdot 10^{-4}\,T)\text{v}.$$

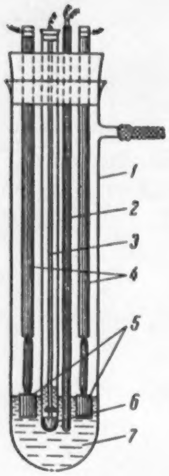

Fig. 1. The cell. 1) Quartz tube; 2) thermocouple; 3) molybdenum current lead to the lead electrode; 4) carbon leads; 5) oxide-carbon electrodes; 6) molten lead; 7) electrolyte.

Before the experiments dry hydrogen chloride was bubbled through the molten salts in the cell to free them of possible hydrolysis products, and after this the melt was kept in vacuum to remove the dissolved gasses. The space above the electrolyte was filled with an equilibrium mixture of $CO_2$ + CO obtained by passing carbon dioxide through a tube filled with broken carbon which was heated to the temperature of the experiment ($C + CO_2 \rightleftharpoons 2CO$). The cell was placed in a massive metal block heated in an automatically regulated electric resistance oven by which it was possible to keep the temperature constant within ± 2°. The e.m.f. of the oxide-carbon electrode and the lead electrode was measured during a long time until it attained a constant value (did not change more than ± 3 mv during an hour).

The equilibrium e.m.f. attained did not depend on the initial concentration of uranium tetrachloride in the melt nor on the ratio of uranium dioxide and carbon in the electrodes, but was determined solely by temperature. These factors, however, had a considerable influence on the way in which the equilibrium e.m.f. of the cell was attained with time. The smaller the amount of uranium tetrachloride and the higher the temperature, the more rapidly the equilibrium values were attained. When the other factors were kept constant, then the electrodes with a higher carbon content (which were more porous) attained the equilibrium potential more rapidly. This may be illustrated by the results of the experiments which are shown graphically in Fig. 2.

When the uranium tetrachloride concentration in the melt was high, such disintegration of the oxide-carbon electrodes was observed that they were entirely used up before the equilibrium potential had been attained. At relatively low $UCl_4$ concentrations in the electrolyte the electrodes did not disintegrate noticeably. They attained the equilibrium potential and, furthermore, did not undergo any perceptible change, just as is the case with electrodes placed in a melt of alkali chlorides to which no uranium tetrachloride has been added. The establishment of the equilibrium e.m.f. corresponds to the attainment of the equilibrium: $UO_2$ (s) + $UCl_4$ (melt) $\rightleftharpoons 2UOCl_2$ (s). An analysis of the solidified electrolyte showed that the equilibrium concentration of uranium tetrachloride amounts to some thousandths of a percent in the temperature range 600-900° investigated by us. The temperature dependence of the equilibrium e.m.f. has been measured in electrolytes containing no more than 6 weight % $UCl_4$. It must be noticed that, after the equilibrium concentration of uranium tetrachloride had been established in the electrolyte, the e.m.f. kept up far more rapidly with the temperature changes. The results of the measurements relative to the chlorine electrode are shown graphically in Fig. 3.

The experimental points lie on the straight line which corresponds to the equation : $\epsilon = (0.713 + 4.8 \cdot 10^{-4} T)$v.

As has already been mentioned before, this quantity is a direct measure of the free-energy change for the chlorination which interests us:

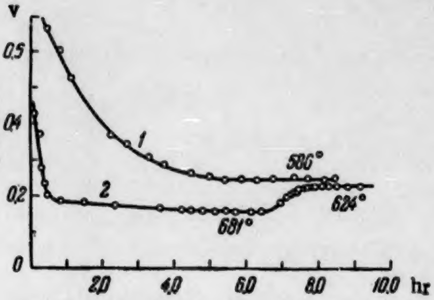

Fig. 2. The change of the cell e.m.f. with time 1) In a melt of LiCl + KCl containing 0.93 weight % $UCl_4$; molar ratio $UO_2$ : C = 1:1.6. 2) Measured in a melt of LiCl + KCl containing 2.0 weight % $UCl_4$; molar ratio $UO_2$ : C = 1: 200.

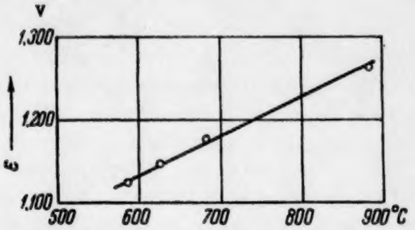

Fig. 3. The dependence of equilibrium e.m.f. on the temperature in the cell $UO_2 + C + UOCl_2$/ LiCl, KCl, $UCl_4$/$Cl_2$ , C.

$$UO_2(s) + \frac{1}{2}C(gr) + Cl_2(g) = UOCl_2(s) + \frac{1}{2}CO_2(g)$$

$$\Delta Z = (-32\,900 - 2{,}2T)\ \text{cal/mole}\ \ UOCl_2.$$

Therefore, the reaction heat $\Delta H = -32.9$ kcal/mole $UOCl_2$ and the reaction entropy $\Delta S = 2.2$ cal/deg · mole $UOCl_2$.

From thermodynamic data in literature [9] and the values of ΔZ found by us, one may calculate the standard formation enthalpy and entropy of uranium oxychloride:

$$\Delta H^0_{UOCl_2} = \Delta H + \Delta H^0_{UO_2} - \frac{1}{2}\Delta H_{CO_2} =$$

$$= 32\,900 - 270\,000 + \frac{1}{2}94\,000 = -255\,900\ \text{cal/mole}$$

$$S^0_{UOCl_2} = \Delta S + S^0_{UO_2(s)} + \frac{1}{2}S^0_{C(gr)} + S^0_{Cl_2(g)} - \frac{1}{2}S^0_{CO_2(g)} =$$

$$= 2{,}2 + 18{,}6 + \frac{1{,}4}{2} + 53{,}3 - \frac{51{,}1}{2} = 49{,}2\ \ \text{cal/deg· mole}$$

For the thermodynamic constants of the oxychloride found are the following values in [7]: $\Delta H_{298} = -261.7$ cal/mole and $S_{298} = 38.1$ eu. Obviously, within the accuracy of the calculations and the errors of the measurements, there is a very satisfactory agreement between the enthalpies of formation but a rather large disagreement between the entropy values. Possibly, this is connected with particularities in the structure of the oxychloride formed under the conditions of our experiments.

This shows that the measuring of electromotive forces is a useful method for a thermodynamic investigation of a chlorination which leads to the formation of oxychlorides.

## LITERATURE CITED

[1] M. V. Smirnov and L. E. Ivanovskii, Doklady Akad. Nauk SSSR 110, 812 (1956).*

[2] M. V. Smirnov and Z. S. Volchenkova, Zhur. Neorg. Khim. 2, 417 (1957).

[3] M. V. Smirnov, S. F. Pal'guev, Yu. N. Krasnov and L. A. Lyapina, Zhur. Prikl. Khim. 31, 66 (1958).*

[4] M. V. Smirnov and L. E. Ivanovskii, Zhur. Neorg. Khim. 2, 238 (1957).

[5] M. V. Smirnov and N. Ya. Chukreev, Zhur. Neorg. Khim. 3, 2445 (1958) .

[6] M. V. Smirnov, S. F. Pal'guev and others, Zhur. Prikl. Khim. 30, 1687 (1957).*

[7] J. J. Katz and E. Rabinowitch, The Chemistry of Uranium, 1 [Russian translation] (IL, 1954).

[8] M. V. Smirnov and L. E. Ivanovskii, Zhur. Neorg. Khim. 1, 1843 (1956).

[9] W. M. Latimer, The Oxidation States of the Elements and Their Potentials in Aqueous Solutions [Russian translation] (IL, 1954).

---

*Original Russian pagination. See C. B. translation.

# THE INFLUENCE OF THE CHROMIUM CONTENT ON THE ELECTROCHEMICAL AND CORROSIONAL BEHAVIOR OF IRON-CHROMIUM ALLOYS

G. M. Florianovich and Ya. M. Kolotyrkin

L. Ya. Karpova Physicochemical Institute Scientific-Research

(Presented by Academician A. N. Frumkin October 1, 1959)

(Translation of: Doklady Akad Nauk SSSR, Vol. 130, No.3, 1960, pp. 585-588)

Original article submitted September 24, 1959.

The opinion that an increase of the chromium content in Fe-Cr alloys enhances their corrosion resistance is widely spread in literature. Besides, it is often pointed out that there exists a definite concentration limit, equal to 13%, above which the corrosion rate of the alloys very sharply decreases.

The existence of such a concentration limit is generally connected with the Tammann rule, according to which there exists a composition limit for alloys, called "resistivity limit" by Tammann; after this limit is reached, the dissolving of alloy in a medium agressive to one of its components practically comes to a stop. However, in this case, one often loses sight of the fact that the "resistivity limit" is not wholly determined by the alloy composition, but depends also upon the composition of the medium, as was already pointed out in the investigations of Tammann himself [1].

The corrosion resistance of an Fe-Cr alloy is highly dependent on the composition of the medium. One may, for instance, point out that for some sulfuric acid concentrations the transition to alloys with a chromium content higher than the aforementioned "limiting" value is accompanied by a sharp decrease in the corrosion rate [2]. An analogous observation has been made for a 65% solution of $HNO_3$, in which the dissolution rate of Fe-Cr alloys also containing some nickel noticeably increases when the chromium content is raised from 9.8 to 19.9% [2]. In other cases, however, the curve describing the dissolution rate of the alloy as a function of its chromium content goes through a minimum, as, for instance, takes place for Fe-Cr-Ni alloys, in a mixture of sulfuric and nitric acid where raising the chromium content of the alloy from 5 to 19% leads to a decrease and raising from 23 to 27% to an increase in corrosion rate [3].

The dependence of the "resistivity limit" value upon the aggressiveness of the medium has been considered in papers of a series of authors [4,5]. However, at present there is no satisfactory explanation of the above-mentioned regularities found from experiment.

In studies executed in our laboratory [6] it was repeatedly shown that the most objective characterization of the corrosional and electrochemical behavior of metals and alloys may be obtained by an investigation by the potentiostatic method. This method, especially in combination with one of the methods suitable for a direct determination of the dissolution rate, makes it possible to evaluate the corrosional characteristics of metals and alloys at various potentials and, therefore, at various states of the metallic surface such as the active or passive state of overpassivation. Since the height of the electrode potential and, therefore, the state of the metallic surface of the alloy depends noticeably upon the alloy composition and on the composition and the concentration of the solution, such a method makes it possible to characterize more completely the corrosional behavior of the metal and the dependence of the parameters of this system.

In this study we used the potentiostatic method combined with a colorimetric determination of the corrosion products in the solution to estimate the influence of the chromium content on the corrosional behavior of iron-chromium alloys. The measurements were executed in 0.1 N sulfuric acid in a nitrogen atmosphere. The fixed potential values were maintained by means of an electronic potentiostat. The curves giving the dependence of the stationary dissolution rate upon the potential have been obtained for pure iron (Armco and Hilger) and also for binary Fe-Cr alloys (prepared from Armco iron and 99.9% chromium) with chromium contents from 0.1 to 35% and for Fe-Cr alloys marked 12Kh6, 1Kh13, Kh17 and Kh28 which contained, besides chromium, up to 0.4% Ni.

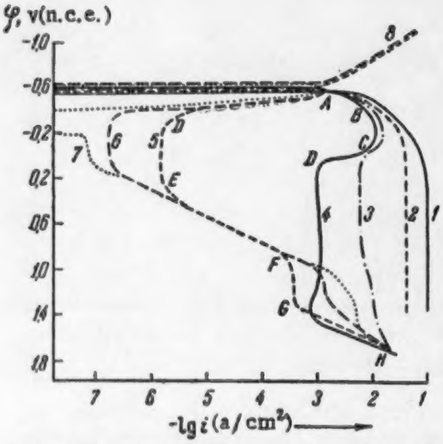

Fig. 1. The dependence upon the potential of the stationary dissolution rate of Fe-Cr alloys with various chromium contents: 1) 0.1%; 2) 4%; 3) 8%; 4) 12%; 5) 20%; 6) 27%; 7) 35%; 8) cathodic curves.

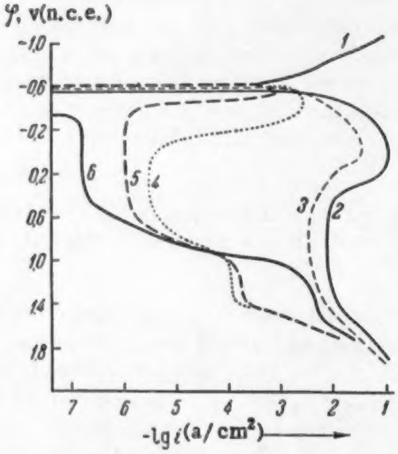

Fig. 2. Cathodic (1) and anodic (2-6) potentiostatic curves measured on Fe (2) and the alloys marked: 3) 12Kh6; 4) 1Kh13; 5) Kh 17; 6) Kh 28.

The curves obtained are shown in Figs. 1 and 2. For some potential values the dissolution rate of the alloys corresponding to various parts of these curves has also been determined directly, i.e., from an analysis of the products dissolved in the solution. In the potential range, more positive than the stationary one and at most + 1.5 v to the normal calomel electrode (n.c.e.), the data obtained in this way coincided with the measured currents.

Just as in our previous investigations of other metals and alloys, the curves obtained in this study for the dependence of the stationary dissolution rate of the alloys upon the potential are characterized by the appearance of some ranges (Fig. 1): active dissolution (AB), the first current limit (BC), passivation (CD), the passive state (DE), overpassivation (EF), the second current limit (FG). The part GH of the curve coming after the range FG corresponds to the rise of the dissolution rate with an increasing positive potential, i.e., constitutes the range of alloy activation. This has been shown, for example, by the alloy Kh17 which the dissolution rate has been measured by an analytical method in the whole range of potentials (Figs. 2, 5).

As is obvious from Fig. 2, the anodic passivation of iron produces a decrease in the dissolution rate to a value scarcely one order of magnitude smaller than the rate in the range of the first current limit. Alloys with a low (up to 4%) chromium content submit still more difficultly to anodic passivation. In the curves for these alloys the passivation range is absent (Fig.1, curves 1,2). A further increase in the chromium content of the alloy has a varying influence on the character of the potentiostatic curves. Alloys containing less than 13% Cr are characterized in the investigated range of potentials by the absence of both overpassivation and the second current limit. In the curves for alloys with a chromium content of 13% and higher the range of the first current limit does not occur. However, the essential difference lies in the sharp decrease (nearly three orders of magnitude) in the dissolution rate of the alloys in the passive state which suddenly appears when one passes from alloys with a Cr content below 13% to alloys with 13% Cr and more.

At the same time it follows from the data obtained that there also exist ranges of the potential in which an increase in the Cr content of the alloy does not produce a decrease but an increase in its dissolution rate.

TABLE 1

| Cr content in the alloy Fe-Cr% | $-\varphi_{\text{stat}}$, mv (n.c.e) | $i_0$, a/cm$^2$ |
|---|---|---|
| 0 | 560 | $9 \cdot 10^{-5}$ |
| 0.1 | 560 | $9 \cdot 10^{-5}$ |
| 4 | 570 | $3 \cdot 10^{-4}$ |
| 8 | 580 | $4 \cdot 10^{-4}$ |
| 12 | 600 | $4 \cdot 10^{-4}$ |
| 20 | 620 | $8 \cdot 10^{-4}$ |
| 27 | 630 | $7 \cdot 10^{-4}$ |
| 35 | 630 | $7 \cdot 10^{-4}$ |

This concerns the range of the second current limit (see Figs. 1 and 2) and also the range of active dissolution, as is obvious from Table 1, in which are given the values of the stationary potential and the corresponding dissolution rates of iron and Fe–Cr alloys.

Thus, an increase in the chromium content of Fe–Cr alloys produces a rise of the dissolution rate in sulfuric acid at potentials near to the stationary one and 1 v positive to the normal calomel electrode, and a decrease at intermediate potentials which is particularly sharp at the transition from alloys with 12% Cr to alloys with 13% Cr.

One may notice that the data obtained by us for Fe and some of its alloys with Cr quantitatively disagree with the data of Franck [7] for Fe and those of Olivier [8] for Fe–Cr* according to which the dissolution rate of Fe in 1 N $H_2SO_4$ and its alloys with 2.8-18% Cr in 10% $H_2SO_4$ in the passive state decreases monotonically with increasing chromium concentrations and has a value below $10^{-5}$ amp/cm$^2$.

Eventual causes of this disagreement have previously been pointed out by us [9]. However, it must be underlined here that, in contradiction to our conclusions, the existence of a composition limit for Fe–Cr alloys characterized by a sharp change of its corrosional stability in any range of potentials does not follow from the data of Olivier. At the same time the existence of such a composition for a series of mediums (characterized by the value of 13% Cr) may be considered a firmly established fact. From the results obtained by us, it follows that the alloy composition cannot serve as an unequivocal characterization of its dissolution rate. For a judgment of the influence exerted by a regular change of the alloy composition upon its corrosional behavior one must inevitably use the potentiostatic curves from which for each potential value one may determine the character of the change in the dissolution rate of the alloy as a function of its composition.

Our conclusions are confirmed by the data of Sugotin and Antonovskaya [10] and those of Pražák [11].

If the dissolution rate of alloys at a given composition is supposed to be unequivocally determined by the potential, then one may use, in accordance with the results of [6], the potentiostatic curves measured in the given medium to deduce the dissolution rate of the alloys in the same medium with any additions. For this it is sufficient to measure the stationary potentials in the corresponding solutions with the additions. At the same time of course, it must be kept in mind that some additions may influence the overvoltage of the anodic reaction or change the current limits. In such cases one must inevitably execute supplementary potentiostatic measurements in solutions with these additions for the involved ranges of potentials.

For Fe–Cr alloys this concerns first of all the range of the second current limit for which at a given potential the composition is extremely important, as follows both from the data in [10] and from data obtained by us (which will be published separately).

From this study it follows that it is impossible to explain the Tammann rule without taking into consideration the potential of the alloy and its potentiostatic curves.

We thank L. A. Banyukova and A. A. Babakov for the supply of the alloys and for the discussion of questions connected with their properties.

## LITERATURE CITED

[1] G. Tammann, Zs. anorg. allg. Chem. 107, 1 (1919).

[2] C. Edeleanu, J. Iron and Steel Inst. 188, 122 (1958).

[3] E. V. Zotova and A. A. Babakov, Zhur. Prikl. Khim. 30, 1795 (1957).**

[4] H. Gerischer, Angew. Chem. 70, 285 (1958).

[5] U. R. Evans, Zs, Elektrochem. 62, 619 (1958).

---

* See also [4] and [7].

** Original Russian pagination. See C. B. translation.

[6] Ya. M. Kolotyrkin, Problems of Physical Chemistry 1, 81 (1958).

[7] U. F. Franck, Werkstoffe u. Korrosion 9, 504 (1958);

[8] R. Olivier, Passiviteit van IJzer and IJzer-Chroom Legeringe, Dissertation, Leyden, 1955.

[9] G. M. Florianovich and Ya. M. Kolotyrkin, Transactions of the Conference on Corrosion and Protection of Metals (Budapest, 1958).

[10] A. M. Sugotin and É. I. Antonovskaya, Zhur. Fiz. Khim. 31, 1521(1957).

[11] M. Pražák, V. Pražák and Vl. Cîhal, Zs. Elektrochem. 62, 739 (1958).

# ADSORPTION OF NITROGEN GAS ON MODIFIED ACTIVATED CARBON

B. P. Bering, Academician M. M. Dubinin,
E. G. Zhukovskaya, and V. V. Serpinskii
Institute of Physical Chemistry Academy of Sciences USSR

(Translation of: Doklady Akademii Nauk SSSR, Vol. 130, No.4, 1960
pp. 793-796)

Original article submitted November 2, 1959.

The introduction to the sorption area of an adsorbent of molecules of substances which are strongly bonded to its surface can change its sorption properties to a considerable extent. Such a "modification" of an adsorbent is obtained either by chemical conversion of its surface (for example by the introduction of chemically combined radicals), or by physical adsorption of "modifiers", i.e., compounds which possess negligibly small vapor pressures on the adsorbent at the temperature of the experiment. In this paper we will speak only of the phenomena which are linked with "physical" modifications. By observing the change in the fundamental characteristics of the adsorption equilibrium of any substance (for example, nitrogen), with the adsorbent and gradually increasing amounts of the modifier, it is possible to discover the variation of the parameters in the adsorption isotherm equation, to follow the gradual change in the curves of pore-volume distribution with the amount, to investigate the character of the variation of the differential heats of adsorption, and to form an idea of some of the properties of the substance in the adsorbed state. It should be seen from this that the sorption of the vapor of any substance on such a modified adsorbent presents a unique and particular case of the sorption of a mixture of two substances, in which the vapor pressure of one of the adsorbate materials on the adsorbent is always practically equal to zero.

The first investigations of the adsorption of nitrogen gas at -195° on activated carbon modified by adsorbed water was carried out by an American worker [1]. The conclusions drawn from this work do not appear to us to be very convincing, since the formal determination of the specific surface of the activated carbon according to the B.E.T. equation in the given case can hardly be justified theoretically [2]. Almost simultaneously with this work [1], an investigation was carried out on the adsorption of water vapor on activated carbon which had been modified with dibutylphthalate [3]; however, this work permitted only qualitative conclusions to be reached. Later Barrer and Rees [4] studied the adsorption at low temperatures of a series of gases on zeolites which were modified by water, ammonia, and methylamine, and showed that by such a method the dimensions of "molecular sieves", which are used for the separation of inert gases, could be varied smoothly. We also noted work by Singleton and Halsey [5] in which the adsorption of argon on adsorbents modified by xenon was studied.

In the present article, we present the reults of our investigation of the adsorption of nitrogen gas at -195° on activated carbons modified with different quantities of water, methyl alcohol, and benzene. We did not use the method of very slow reduction (up to twenty-four hours) of temperature of the adsorbent, which is initially in equilibrium with the vapor of the modifier at a higher temperature. Instead we used a method of rapid temperature reduction of the adsorbent in an atmosphere of helium for the fixation or unique "chilling" condition of the adsorption equilibrium, which was first attained at 20°. In order to carry out the experiments we used an apparatus, described earlier [6], for the measurement of nitrogen gas adsorption by a gravimetric method; with this apparatus we were able to measure small changes. To speed up the cooling process the thickness of the gaseous layer between the adsorbent and the cooled partition of the lower part of the weighing tube was shortened to ~ 3 mm.

The internal diameter of this tube was less than 10 mm and the granules of carbon(usually weighing about 100 mg ) were placed in it vertically suspended on a cylindrical spiral balance of diameter 3 mm, made of nichrome wire 0.1 mm in diameter. To obtain carbon with a specific amount of the adsorbed modifier the adsorbent is first evacuated at 450° and then kept in an atmosphere of the modifier vapor at 20° until the adsorption equilibrium is attained, after which helium is introduced into the weighing vessel at a pressure of ~10 mm Hg. After this the lower end of the tube containing the adsorbent is rapidly immersed in a Dewar flask of liquid nitrogen. Because the thermal conductivity of helium and the rate of diffusion of the modifier vapor through the gas are small, at the temperature of liquid nitrogen, generally no desorption of modifier is observed during cooling. Half an hour after the start of cooling, most of the helium can be recovered in a cylinder by means of a Topler mercury pump, and the weighing vessel is pumped out at a pressure of $\sim 1 \cdot 10^{-6}$ mmHg.

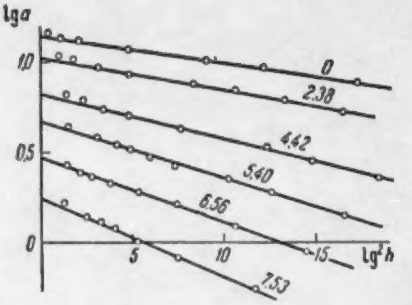

Fig. 1.

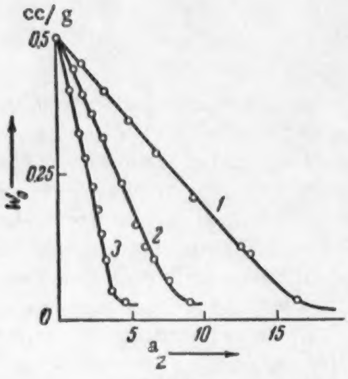

Fig. 2.

A laboratory sample of granulated de-ashed carbon, which had been activated with carbon dioxide at 950° up to 50% charring, was taken for the experiments. From the nitrogen gas adsorption isotherm it was found that for this carbon the micropore volume is equal to 0.480 cc/g, and the volume of the intermediate pores 0.190 cc/g. All measurements were carried out on the same batch of this carbon, successively modified with different quantities of water, methyl alcohol, and benzene. The experimental data obtained were analyzed from the point of view of presenting a possible theory of adsorption developed in our laboratory [7, 8]. For this it was found that in each of three series of experiments the measured adsorption of nitrogen gas over a wide range of relative pressures $\underline{h}$ was represented well by an equation for adsorbents of the first structural type [7]:

$$a = \frac{W_0}{v} e^{-\frac{BT^2}{\beta^2} \lg^2 h}. \qquad (1)$$

where $W_0$ is the limiting volume of the sorption space, V is the molar volume (for liquid nitrogen equal to 34.7 cc/mole) of the adsorbed material, B is a constant which depends both on the dimensions of the micropores, which determine the effect of an increase of adsorption potentials, and on the nature of the adsorbent surface, and B is the affinity coefficient of the characteristic curve.

To illustrate the experimental data, in Fig. 1 the adsorption isotherms of nitrogen gas on carbon modified by methyl alcohol are shown; the coordinates used for the plot correspond to a linear form of Eq. (1). The numbers placed near the isotherms indicate the degree of adsorption of methyl alcohol in mmoles/g. Analogous sets of linear isotherms for adsorption of nitrogen were obtained by us for carbon modified with water, and for carbon modified with benzene. From the values of the intercepts on the ordinate axes and from the slope of the linear isotherm, the parameters $W_0$ and B can be calculated for the series of adsorption isotherms corresponding to each modifier, and the values obtained for these parameters may be represented as functions of the amount of modifier adsorbed $a_2$.

The dependence of the determined micropore volume $W_0$ on $a_2$ for water (curve 1), methyl alcohol (curve 2), and benzene (curve 3), is shown in Fig. 2. In all three cases $W_0$ decreases linearly with increasing $a_2$, and only after a 70-80% saturation of the volume $W_0$ is a divergence from the linear relation observed. The gradient of the linear portion of each curve of Fig. 2 is obviously equal to the molar volume of the modifier, and the reciprocal value to the effective density of the material in the adsorbed state. We call this the effective density, with the aim of emphasizing the distinction between it and the normal density in the bulk phase. In the given case we are speaking of the density of the solid material as it is found in an exceptionally highly dispersed state (in micropores with dimensions of the order of 10 A), and therefore there is no reason to expect that this value will be equal to the normal density in the bulk of the solid phase. In Table 1 the values for the effective density $d_e$ for water, methyl alcohol, and benzene in the micropores of activated carbon at -195° are shown. Also shown are the values for the normal densities $d_n$ of these substances in the bulk phase at -195° as measured by our method of hydrostatic suspension in liquid nitrogen. From a comparison of these values it can be seen that for all three materials the density $d_e$ is 30-40% less than the normal density. We are inclined to think that the abnormally low values obtained for the densities of the solid adsorbed phases in the micropores of carbon characterize the actual properties of these phases. The lower values of the densities are dependent on the extremely high degree of dispersion of the solid modifier, as a result of which a very considerable increase appears in the lengths of the molecules found on the surfaces of submicrocrystals or some quasicrystalline formations in the micropores. It is also possible that in such highly dispersed solid phases, such as are found in the carbon micropores, the normal crystal lattice is distorted by the adsorption fields of the adsorbent itself.

TABLE 1

| Material | $d_e$, g/cc | $d_n$, g/cc |
|---|---|---|
| $H_2O$ | 0.62 | 0.89 |
| $CH_3OH$ | 0.55 | 0.95 |
| $C_6H_6$ | 0.67 | 1.14 |

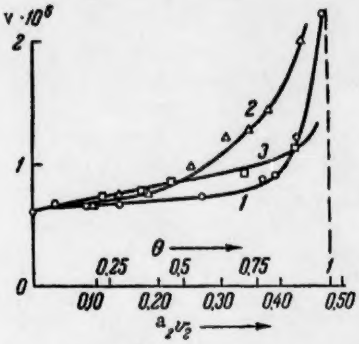

Fig. 3.

In Fig. 3, the dependence is shown for water (curve 1), methyl alcohol (curve 2), and benzene (curve 3), of the parameter B on the value for the saturation by the modifier of the volume $a_2v_2$ in cc/g, and on the value for the degree of filling $\theta = a_2v_2/W_0$. In the construction of this graph the values for the molar volume of the modifier $v_2$ were calculated from the density $d_e$. For all three materials the parameter B at first increases very slowly and nearly linearly, and starts to rise rapidly only at high values of θ. It should be noted that the increase in B and the linear decrease in $W_0$ with the increase in $a_2$ was observed earlier in our laboratory during the analysis of results on the measurement of adsorption of mixtures of water and ethyl chloride on activated carbon [9, 10]. The increase of B can be thought of as a consequence of at least three factors: the change in the distribution function of pore dimensions, which depends on the gradual closing of the finer pores by the adsorption of increasing amounts of modifier; the variation in the dimensions of the pores accessible to nitrogen by adsorption of the modifier on their walls; and finally the variation in the nature of the adsorbent surface brought about by the adsorbed modifier.

The authors wish to thank V. N. Pechenova for help with the construction of the apparatus.

## LITERATURE CITED

[1] P. H. Emmett, Chem. Rev. 43, 69 (1948).

[2] M. M. Dubinin, E. D. Zaverina, et al., Izv. Akad. Nauk SSR, Otdel. Khim. Nauk (in print).*

[3] M. M. Dubinin and E. D. Zaverina. Zhur. Fiz. Khim. 23, 57 (1949).

[4] R. M. Barrer and L. V. Rees, Trans. Faraday, Soc. 50, 852 (1954).

[5] J. H. Singleton and G. D. Halsey, Jr., J. Phys. Chem. 58, 330 (1954).

[6] B. P. Bering, M. M. Dubinin et al. Zhur. Fiz. Khim. 31, 712 (1957).

[7]* M. M. Dubinin, E. D. Zaverina and L. V. Radushkevich. Zhur. Fiz. Khim. 21, 1351 (1957).

[8] K. M. Nikolaev and M. M. Dubinin. Izv. Akad. Nauk SSR Otdel. Khim. Nauk 1165 (1958).*

[9] B. P. Bering and V. V. Serpinskii. Izv. Akad. Nauk SSR Otdel. Khim. Nauk 7, 1186 (1959).*

[10] B. P. Bering. Thesis (Moscow, 1957) [In Russian].

---

* Original Russian pagination. See C. B. translation.

# THE REDUCTION OF INDIUM ON THE DROPPING-MERCURY ELECTRODE IN THE PRESENCE OF CERTAIN ORGANIC AND INORGANIC CATIONS

Kh. Z. Brainina

A. M. Gor'kii Ural State University

(Presented by Academician A. N. Frumkin September 30, 1959)

(Translation of: Doklady Akademii Nauk SSSR, Vol. 130, No.4,
1960, pp. 797-800)

Original article submitted September 24, 1959.

A study of the mechanism of the reduction of indium on the dropping-mercury electrode is of interest because the reversibility of this process is dependent on the nature of the background. The reduction of indium from solutions of sulfates or perchlorates is known to proceed at high overvoltage, whereas the process is reversible and occurs at more-positive electrode potential when ions such as $Cl^-$ and $Br^-$ are present. There is, however, a sharply defined minimum on the polarization curve in that region of potential in which a diffusion current should be observed [1,2].

The effect of a number of organic and inorganic cations on the kinetics of the indium reduction at the dropping-mercury electrode has been studied in the present work. Polarization curves obtained under various conditions are represented in Figs. 1-3. The following cases will be considered:

1. The Reduction of Indium in the Presence of Various Cations from Solutions of Fixed Chloride-Ion Concentration. The first current rise on each of the polarization curves is at -0.55 v and is due to the indium reduction. The current falls off in the potential interval from -0.65 to -0.75 v depending on the background composition, the fall-off being the more strongly expressed the higher the valence of the background cation (Fig. 1, 1, 2, 5 and Fig. 2, 1, 2). It is interesting to note that the minimum in the potential region from -0.67 to -1.35 v becomes deeper when the $La^{3+}$ ion concentration of the solution is increased at fixed chloride ion concentration (Fig. 1, 4, 3, 1). The reaction rate increases, on the other hand, in the order $Na^+ < Rb^+ < Cs^+$ over the potential interval from 0.65 to 1.28 v. Hydrogen reduction and miscellaneous electrode processes account for the further increase in the current in solutions which are highly concentrated in regard to the background (0.9 N).

The current rise comes somewhat nearer the minimum on polarograms obtained in 0.5 N chloride solutions (pH 3.0, Fig. 2) than is the case in more concentrated solutions of this same cation, and a sharp inflection point appears on the polarization curve for the indium reduction in 0.5 N NaCl at a potential of -1.4 v (Fig. 2, 2). Less sharply defined inflections are also observed in RbCl and $LaCl_3$ (Fig. 2, 3, 1), these being at 1.48 and 1.5 v, respectively. Comparison of Curves 4 and 5 which were obtained in 0.5 N NaCl and 0.5 N $LaCl_3$ at pH 3.0 without indium, with Curves 2, 3, and 1 makes it clear that the current rise beyond the minimum is due to indium reduction, and that hydrogen-ion reduction, beginning in this same potential interval, accounts for the fact that the polarogram shows a more or less sharply marked inflection instead of an interval of diffusion currents.

Curves 2, 7, and 8 show the surface tension of mercury at the potentials covered by the negative branch of the electrocapillary curve to be lower in RbCl solutions than in NaCl solutions, this being in agreement with measurements of the differential capacity of the electrical double layer on mercury which have been made in these solutions [3].

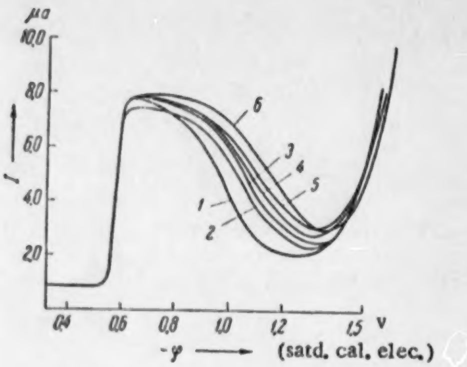

Fig. 1. Polarization curves for the reduction of 0.001 M $InCl_3$ from solutions of: 1) 0.9 N $LaCl_3$; 2) 0.9 N $SrCl_2$; 3) 0.2 N $LaCl_3$ + 0.7NKCl; 4) 0.05N $LaCl_3$ + + 0.85N KCl; 5) 0.9 N KCl (a = 0.56); b) $LaCl_3$ (a = 0.56, pH 3.0).

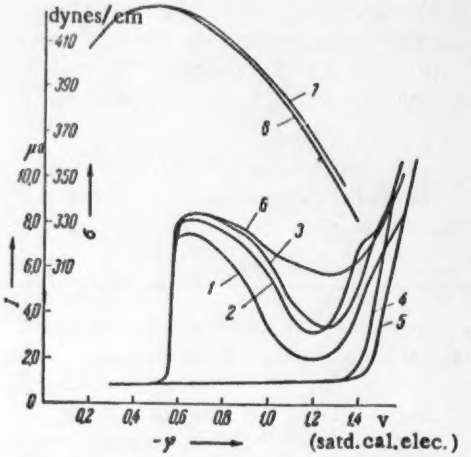

Fig. 2. Polarization curves for the reduction of 0.001 M $InCl_3$ from solutions of: 1) 0.5 N $LaCl_3$; 2) 0.5 N NaCl; 3) 0.5 N RbCl; 4,5) 0.5 N NaCl; and $LaCl_3$, respectively, without indium, 6) 0.5 N CsCl; 7, 8) electrocapillary curves for mercury in 0.5 N NaCl and RbCl, pH 3.0.

2. The Reduction of Indium in the Presence of Various Cations from Solutions with Fixed Chloride-Ion Activity. A comparison of Curves 5 and 6 of Fig. 1 brings out the fact that the retardation of the electrode process in the potential interval from 0.65 to 1.23 v is not so marked in the presence of a trivalent cation ($La^{3+}$). Curve 6 was obtained in the reduction of indium from a potassium chloride solution and lies above Curve 5.

3. The Reduction of Indium in the Presence of Tetraalkyl Ammonium Salts. Figure 3 gives polarograms for the reduction of indium on a background composed of 0.9 N KCl and tetra-salts. A comparison of Curves 1-3 with polarization curve 4 shows that tetrabutyl ammonium chloride at $5 \cdot 10^{-5}$ M concentration markedly diminishes the indium saturation current. The wave is almost completely suppressed when the concentration of this salt is increased to $1.5 \cdot 10^{-4}$M. Tetramethyl ammonium chloride is much weaker in its action.

Indium complexes are known to exist in chloride solutions [1,2]. We have determined the compositions of these complexes from the data of DeFord and Hume [4] the relation between the indium half-wave potential and the chloride-ion activity of the solution:

| | | | | | | | |
|---|---|---|---|---|---|---|---|
| $a_{Cl^-}$ | 0,08 | 0,23 | 0,33 | 0,53 | 0,69 | 1,14 | 1,74 |
| $-\varphi_{1/2}$ v | 0,560 | 0,574 | 0,580 | 0,590 | 0,595 | 0,610 | 0,622 |

The half-wave potential for the reversible reduction of indium in the absence of chloride ions was required for these calculations and its value was obtained by extrapolating the Cozzi and Vivarelli [1] equation relating half-wave potential and chloride-ion concentration at fixed ionic strength to $C_{Cl} = 0$. DeFord and Hume claim that the relation between the $Cl^-$ ion activity and the F-function for the last of the complexes existing under these conditions is linear and yields a straight line parallel to the axis of abscissas, while the corresponding relation for the preceding complex is covered by a straight line of positive slope. The relation is curvilinear in every other case. It can be concluded from Fig. 4 that the complexes $InCl^{2+}$, $InCl_2^+$, and $InCl_3^0$ exist in 0.1-3.0 N KCl solutions.

In chloride solutions, the reduction of indium at the dropping-mercury electrode begins at potentials which are close to the null-charge potential for mercury. It is possible that the indium complexes are then oriented with their negative ends toward the electrode to form a special type of those "anionic ridges" which have been shown by A. N. Frumkin [6] to facilitate the transfer of electrons from an electrode surface to a reducing particle. This kind of orientation can occur only within a rather narrow potential interval near the half-wave potential of indium since anion adsorption becomes impossible when the cathodic polarization is increased and the negative surface charge of the mercury rises. It is clear that the orientation of the complex particles in the electrical double layer will alter in passing from the more-positive electrode potentials to the more-negative and that the conditions will then become unfavorable for the electrode reaction.

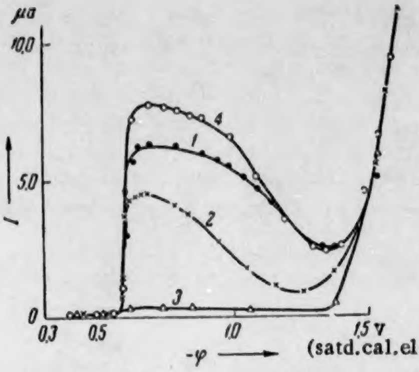

Fig. 3. Polarization curves for the reduction of indium from solutions containing $10^{-3}$ M $InCl_3$ + + 0.9 N KCl + $nR_4NCl$ (R is an organic radical), pH 2.5: 1) 0.02 M $(CH_3)_4NCl$, 2) $5 \cdot 10^{-5}$ M $(C_4H_9)_4NCl$, 3) $1.5 \cdot 10^{-4}$ M $(C_4H_9)_4NCl$, 4) without addition.

It is natural to anticipate that any factor favoring such an orientation of the indium complexes in the electrical double layer as would direct their anionic ends toward the electrode surface would also favor the electrode process.

A. N. Frumkin and his collaborators have shown in a series of papers [7] that the introduction of certain cations into solution will increase the adsorption of anions even in that region of potentials where their adsorption is not otherwise observed. Thus it can be expected that the introduction of $Rb^+$, $Cs^+$, $Sr^{2+}$, $La^{3+}$, or $R_4N^+$ into solution would lead to a partial removal of those kinetic hindrances which are observed in the reduction of indium in KCl and NaCl solutions.

Account should, however, be taken of the fact that the indium complexes as a whole can be either neutral or cathodic, so that foreign ions will exert a twofold effect which will depend on their nature: 1) facilitating the dragging of the indium complexes into the electric double layer by their anionic ends, and 2) completely displacing the positively charged particles from the space adjoining the electrode, thus diminishing the reaction rate by altering the $\psi_1$-potential in the positive direction [7]. It is clear that this effect must increase with the cation charge.

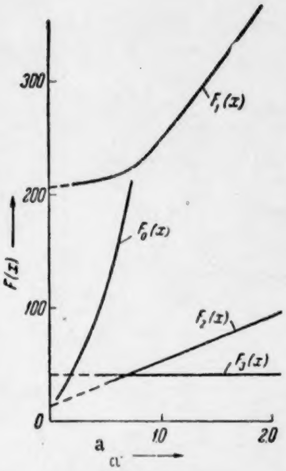

Fig. 4. The relation between the F(X) function and the chloride-ion activity.

The experimental data show that there is a pronounced increase in the reaction rate in the case of the univalent cations, the order of increase being $Na^+ < K^+ < Rb^+ < Cs^+$.

The decrease in the diffusion current of indium in the presence of organic cations could be the result of a retarded penetration of the reducing particles to the electrode surface. Tetramethyl ammonium chloride does not decrease the indium saturation current in the kinetic region.

The second effect prevails in the presence of multivalent cations and is clearly increased by the reduction in $Cl^-$ ion activity arising through replacement of $K^+$ by $Sr^{2+}$ and $La^{3+}$. An insignificant acceleration of the process is observed when $La^{3+}$ is present in electrolytic solutions of sufficiently high activity, but this effect is much weaker than that which is observed with Cs.

The increase in the rate of the cathodic process when the cathodic polarization is high (Fig. 2) and the reducing particle can only so orient that its positive end is toward the electrode surface is obviously due to direct transfer of the electron from the electrode to the indium ion. Foreign cations should exert the same effect on this process as on the hydrogen-ion discharge, if the situation is actually so [5]. It is to be seen from Fig. 2 that the indium overvoltage actually increases in the order $Na^+ < Rb^+ < La^{3+}$.

Thus the mechanism for the reduction of indium ions from chloride solutions proves to be different at different potentials, this being the result of alteration in the conditions for adsorption of the reducing particles. The electronic process is facilitated at potentials in the neighborhood of the half-wave potential by the formation of "anionic bridges", while a direct transfer of electrons from the electrode surface to the indium ion is observed at more negative potentials.

In concluding, I wish to express my sincere thanks to Academician A. N. Frumkin, to N. V. Nikolaeva-Fedorovich, and to V. A. Kuznetsov for their valued remarks in the course of a discussion of these results.

## LITERATURE CITED

[1] J. M. Kolthoff and J. J. Lingane, Polarography (New York, 1952) p. 519; L. I. Busev, The Analytical Chemistry of Indium [in Russian] (Moscow, 1958); D. Cozzi and S. Vivarelli, Z. f. Electrochem. 57, 408 (1953); M.Bulovova, Coll. Czech. Chem. Com. 19, 1123 (1954).

[2] Kh. Z. Brainina and S. K. Chirkov, Abstracts of Reports, Conference of Workers of Universities and Plant Laboratories in Southeastern USSR (Rostov-on-Don, October, 1958).

[3] D. Grahame, J. Electrochem. Soc. 98, 9, 343 (1951).

[4] D. D. De Ford and D. N. Hume, J. Am. Chem. Soc. 73, 11, 5321 (1951).

[5] A. N. Frumkin, V. S. Bagotskii, Z. A. Iofa, and B. N. Kabanov, The Kinetics of Electrode Processes [in Russian] (Moscow, 1952).

[6] A. N. Frumkin, Izvest. Akad. Nauk SSSR, Otdel Khim Nauk 12, 1429 (1957);* A. N. Frumkin, Transactions, Fourth Conference on Electrochemistry, October 6, 1956, (Izd. AN SSSR, 1959).

[7] A. N. Frumkin and N. V. Nikolaeva-Fedorovich, Vestn. MGU, ser. matem., mekh., astr., fiz., khim., 4, 1957; A. N. Frumkin, B. B. Damaskin, and N. V. Nikolaeva-Fedorovich, Doklady Akad. Nauk SSSR, 115, 4, 751 (1957).*

---

*Original Russian pagination. See C. B. translation.

# THE CHEMISORPTION OF OXYGEN ON GERMANIUM

R. Kh. Burshtein, L. A. Larin, and G. F. Voronina

Institute of Electrochemistry, Academy of Sciences, USSR

(Presented by Academician A. N. Frumkin October 7, 1959)

(Translation of: Doklady Akademii Nauk SSSR, Vol. 130, No.4, 1960, pp. 801-803)

Original article submitted September 28, 1959.

It is well known that the surface state of a semiconductor exerts a marked influence on its electrophysical properties. Considerable interest thus attaches to a study of adsorption processes on germanium and the properties of its adsorbed films. The kinetics of the adsorption of oxygen on germanium has been studied here with the aim of elucidating the mechanism of chemisorption on this metal.

A germanium surface is always covered with an oxide film and it is therefore necessary to develop a method for cleaning the surface if gas adsorption is to be studied. Attention has recently been given to this problem in a number of papers [1]. Ionic bombardment in argon with subsequent high temperature degasification in ultrahigh vacuum has been used by Farnsworth and his co-workers for cleaning germanium surfaces [2]. Schlier and Farnsworth [3], and Handler [4] have pointed to the difficulties which arise in cleaning germanium surfaces through ionic bombardment. Low and Garrett [5] consider that a germanium surface which has been subjected to ionic bombardment is not free of chemisorbed oxygen. There is also indication that ionic bombardment increases the number of surface defects in germanium [6].

The possibility of obtaining clean germanium surfaces by vaporizing films has also been considered doubtful since the gases evolved during heating can be taken up by the film in the course of vaporization.

A clean germanium surface can be obtained for adsorption measurements by breaking up monocrystals in an ultrahigh vacuum [7]. It is desirable, however, that the method employed for freeing the surface of oxide films in adsorption measurements be one that could be used in a study of electrophysical properties, as well.

In the present work, the germanium surface was freed of its oxide film by repeated reduction in hydrogen. Reduction of the germanium for one to two hours at 400-450° was followed by an extended degassing in a $10^{-7}$ mm vacuum at this same temperature. The reduction and degassing of the germanium was repeated five or six times. This reduction was followed by a degassing at 400-450° in a vacuum of $10^{-9}$ mm in order to complete the cleaning. Complete desorption of hydrogen adsorbed on germanium at 278° has been observed by Tamaru and Boudart [8]. The data of these authors indicate that the desorption rate increases rapidly with the temperature. Our own experiments also show that it is easy to free a germanium surface of adsorbed hydrogen by degassing it at 400°.

Our studies on the adsorption of oxygen were carried out with a germanium powder which had been obtained by crushing monocrystals. The surface area of this germanium powder was determined by the BET method and proved to be equal to 620 $cm^2/g$. The adsorption experiments were carried out with 60.4 g of germanium. The large surface area permitted a more detailed investigation of the mechanism of oxide film formation. The study of the adsorption of oxygen on germanium was made by the same method which we used earlier in investigating the adsorption of oxygen on iron [9]. This method has also been applied by Rideal and Trappnel [10] to a study of the adsorption of oxygen on tungsten.

Our germanium powder was reduced, degassed, and cooled to room temperature; small portions of oxygen were then adsorbed and study made of the rate of uptake of each of these. The initial pressure of each portion was approximately 0.07 mm. The results obtained in this study of the adsorption of oxygen on germanium are presented in Fig. 1. These data indicate that there are two stages in the adsorption, a rapid and a slow. The rate of adsorption in the rapid stage is practically independent of the degree of coverage of the surface. The amount of rapidly adsorbed oxygen corresponds to the formation of a monoatomic layer when it is assumed that one germanium atom on the surface adsorbs a single oxygen atom. The number of atoms per 1 $cm^2$ surface of ther germanium powder was taken as $7.7 \cdot 10^{-14}$ on the basis of the data of Green, Kafalas and Robinson [7].

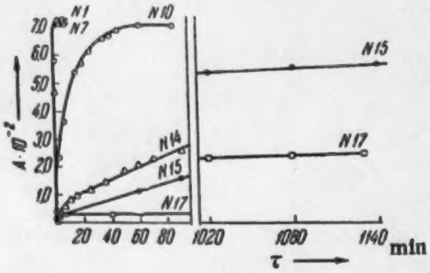

Fig. 1. The kinetics of the adsorption of separate portions of oxygen on germanium (the curve numbers correspond to order of introducing the portions of oxygen).

Figure 2 shows the relation between the amount of oxygen taken up and $1/\tau$, $\tau$ being the time of half-adsorption of the individual portion. This figure shows that the amount of rapidly adsorbed oxygen is equal to the amount of slowly adsorbed oxygen: In distinction to the data of Green, Kafalas, and Robinson [7], our own experiments indicate that a relation of the form $N \approx \approx \log t$ ($N$ is the number of molecules adsorbed and $t$ is the time which has elapsed from the beginning of the experiment) is valid only for the slow stage of the adsorption. The total amount of oxygen chemisorbed on germanium powder which had been cleaned by reduction in hydrogen is equivalent to two monoatomic layers and the same is true of germanium powders obtained by crushing monocrystals in ultrahigh vacuum [7]. This agreement represents the only proof that a clean germanium surface can be obtained by a reduction in hydrogen with subsequent degassing.

The question as to whether a germanium surface could be freed of oxide films by vacuum heating was subjected to experimental test. This was done by taking a germanium powder on which rapid and slow adsorption had taken place at room temperature and heating it in vacuum for two hours at 400°. Oxygen desorption could not be observed during this heating. The germanium was cooled after being heated in vacuum and its adsorptive capacity for oxygen determined again at room temperature. A slow adsorption once more took place on the germanium powder.

It is to be presumed that there is an alteration in the bonding of oxygen with the germanium surface when germanium on which chemisorption of oxygen has occurred is heated, since desorption does not take place during degassing and separation of oxygen from the surface in the form of GeO is not observed[11].

The rapid stage in the oxygen adsorption can be utilized in determining the surface area of germanium. The value of 630 $cm^2$ per gram of germanium powder which was obtained in this way is in good agreement with the surface determined by the BET method. A protective oxide film fails to form on the germanium surface at 400° and oxidation by oxygen proceeds to a considerable depth, this being in distinction to the case at room temperature where the adsorption ceases completely once a definite degree of surface coverage has been reached.

If it is supposed that the rapid stage of the chemisorption corresponds to the reaction

$$2Ge + O_2 \rightarrow 2GeO, \qquad (1)$$

the slow stage would then be clearly associated with the formation of a $GeO_2$ film on the germanium surface through the reaction

$$2GeO + O_2 \rightarrow 2GeO_2. \qquad (2)$$

This hypothesis is supported by the adsorption measurements which have been presented here and by other data on the effect of adsorbed oxygen on the electrophysical properties of germanium.

We wish to express our thanks to Academician A. N. Frumkin for his interest in this work.

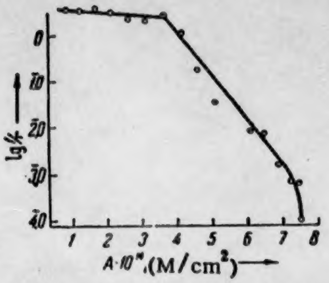

Fig. 2. The relation between log $1/\tau$ ($\tau$ is the time of half-adsorption of an individual portion of oxygen) and the number of adsorbed oxygen molecules per 1 cm² of surface.

## LITERATURE CITED

[1] Semiconductor Surface Physics (1956).

[2] H. E. Farnsworth, R. E. Schlier, T. H. George, and R. M. Burger in: J. Appl. Phys. 26, 252 (1955).

[3] R. E. Schlier and H. E. Farnsworth, in: Semiconductor Surface Physics (1956), p. 3.

[4] P. Handler in: Semiconductor Surface Physics (1956), p. 23.

[5] I. T. Low and C. G. B. Garrett, J. Appl. Phys. 27, 656 (1956); in: Semiconductor Surface Physics (1956); Discussion, p. 40-49.

[6] I. T. Low, J. Phys. Chem. 99, 543 (1955).

[7] M. Green, J. A. Kafalas, and P. H. Robinson, in: Semiconductor Surface Physics, 1956, p. 349.

[8] K. Tamaru and M. Boudart, Adv. in Catalysis 9, 699 (1957).

[9] R. Kh. Burshtein, N. A. Shumilova, and K. A. Gol'berg, Zhur. Fiz. Khim. 20, 789 (1946).

[10] E. K. Rideal and B. M. W. Trappnel, Proc. Roy. Soc. 205A, 409 (1951).

[11] S. P. Wolsky, J. Appl. Phys., 29, 1132 (1951).

# THE MEASUREMENT OF DETONATION-FRONT TEMPERATURES FOR EXPLOSIVES

**I. M. Voskoboinikov and A. Ya. Apin**
Institute of Chemical Physics, Academy of Sciences, USSR

(Presented by Academician V. N. Kondrat'ev September 31, 1959)
(Translation of: Doklady Akademii Nauk SSSR, Vol. 130,
1960, p. 804-806)
Original article submitted September 27, 1959.

A calculation of detonation wave parameters shows the detonation temperature to be most sensitive to the form of the equation of state of the explosion products, and a knowledge of detonation temperatures is thus indispensable to a test of this equation. Nevertheless, very little work on the determination of detonation temperatures has as yet been published. We have attempted to measure detonation-front temperatures in charges of transparent and semitransparent liquid and solid explosives by using an electrooptical method.

## Measurement of Detonation Temperatures in Transparent Liquid Explosives

A FEU-29-M photomultiplier was used to measure the end surface luminosity of the detonation front of a charge of liquid explosive in a plexiglass cell with a transparent bottom, the current being recorded on a single-sweep OK-17 M oscillograph. A study of detonation-front luminosities showed that the spectra of nitromethane and methylnitrate in the 400-600 mμ interval are similar to black-body spectra at 3700° and 4500°K, respectively, and that the two substances have the same emissivity. This justifies the assumption that the detonation front emits as a black or gray body and that its temperature can therefore be measured by a color method in which intensities over two spectral regions are compared; these regions were obtained with SS-5 and ZS-1 filters in our case.

These experiments have involved measurement of the ratio

$$\frac{\Sigma\ \mathrm{SS\text{-}5}}{\Sigma\ \mathrm{ZS\text{-}1}} = \int_{\lambda_1}^{\lambda_2} S_\lambda b_\lambda \cdot \tau_{\mathrm{SS\text{-}5}}\, d\lambda \Big/ \int_{\lambda_1}^{\lambda_2} S_\lambda b_\lambda \cdot \tau_{\mathrm{ZS\text{-}1}}\, d\lambda,$$

($S\lambda$ is the spectral sensitivity of the photomultiplier, $b\lambda$ is the spectral intensity of the source, $\tau_{SS-5}$ and $\tau_{ZS-1}$ are the transmission coefficients of the filters, and $\lambda_1$ and $\lambda_2$ are the limits of the spectral sensitivity of the photomultiplier) from which the temperature was found by using a theoretically developed calibration curve showing the relation between the ratio $\frac{\Sigma_{SS-5}}{\Sigma_{ZS-1}}$ and the reciprocal of the source temperature for an absolute black body. The spectral sensitivity of the photomultiplier and the transmission coefficient of the optical system were measured beforehand with a standard light source.

There was a maximum error of 3% in determining the value of $\frac{\Sigma_{SS-5}}{\Sigma_{ZS-1}}$ at the detonation front of a transparent liquid explosive and a corresponding error or no more than 150°K in the temperature determination. Table 1 contains our values for the color temperatures, T, at the detonation front in various solid and liquid explosives, together with data on the initial density, $\rho_0$, and the detonation rate. The accuracy of the determination of the detonation rate, D, was 100 m/sec in both the electrocontact method and the optical method. The determination of the detonation temperatures of solid explosives was accurate to 300°K.

TABLE 1

| Substance | Density (g/cm$^2$) | Temp. (°K) | D (m/sec) |
|---|---|---|---|
| Nitroglycerine | 1.60 | 4000 | 7650 |
| Nitroglycol | 1.50 | 4400 | 7400 |
| Methylnitrate | 1.21 | 4500 | 6750 |
| Tetranitromethane | 1.14 | 3700 | 6300 |
| Nitromethane | 1.64 | 3100 | 6400 |
| Hexogen | 1.79 | 3700 | 8800 |
| TEN | 1.77 | 4200 | 8500 |
| DINA | 1.70 | 3700 | 8000 |

### Measurement of Detonation Temperatures in Charges of Semitransparent Solid Explosives

Detonation-front temperatures can be measured in charges of semitransparent solid explosives with densities close to that of a monocrystal in the same way as in charges of transparent liquid explosives. The luminosity was registered at the instant when the detonation wave emerged through the end of the charge, just as in the first case, so that there was no necessity for determining the absorption in the charge itself. The exact moment of emergence of the wave from the end could be fixed only with difficulty due to the low transparency of the charge and the high luminosity of the air shock wave arising from dispersion of the products from the end. The luminosity from the air shock wave was cut out by immersing the end of the charge in water. Special care was taken in these experiments to be certain that the charge was free of cracks and that no air adhered to its end surface.

Comparison showed the intensities of the detonation fronts of the investigated explosives over the spectral region from 400 to 600 mμ to stand in the same ratio as for absolute black bodies at the same temperatures (this is equivalent to saying that the emissivity of the detonation front is the same in each case). This makes it possible to check continually the color temperature measurements by comparing the illumination intensity in the detonation of the investigated explosive with the illumination intensity of some other explosive which had been studied earlier and thus have essentially an intensity method for temperature determinations. It can be assumed that the emissivity of the detonation front is close to unity since it remains constant under a temperature alteration from 3500 to 5000°K in passing from one substance to another.

## DISCUSSION OF RESULTS

The paper of Alentsev, Belyaev, et al [1] in which the detonation temperatures of liquid explosives were first measured and the more detailed work of Gibson and his coworkers [2] applying the light pipe, weakly luminous fillers, and the electrooptical method to the measurement of detonation temperatures should be mentioned among the early publications in this field. The temperatures which we have obtained for the detonation of nitromethane and nitroglycerine are in agreement with the results of [2], but the same is not true of our values for hexogen and TEN.

The measured values of the detonation temperatures are so large that they could not arise from the luminosity of a nonreacting shock front traveling ahead of the detonation complex. It can be assumed that these values are quite close to the temperatures in the Chapman-Jouguet plane, since the reaction zone of powerful explosives is a shallow one, the reaction rate increases rapidly within this zone, and the intensity of illumination is strongly dependent on the temperature.

The temperature values obtained here have been combined with the detonation pressures of [3] for TEN ($\rho_0 = 1.77$ g/cm$^3$, $p = 340 \cdot 10^3$ atm), hexogen ($\rho_0 = 1.79$ g/cm$^3$, $p = 390 \cdot 10^3$ atm), nitroglycerine ($\rho_0 = 1.60$ g/cm$^3$, $p = 250 \cdot 10^3$ atm), and nitromethane ($\rho_0 = 1.14$ g/cm$^3$, $p = 133 \cdot 10^3$ atm) to give a test for various types of equation of state for the explosion products. The results which are adduced here do not confirm the calculations of [4-7].

The recent work of Cook [4, 8] has made extensive use of an equation of state of the form $pv = nRT + p \cdot \alpha(v)$, in which n represents the number of moles per gram of products, R is the molar gas constant, and v is the specific volume of the products in the Chapman-Jouguet plane. This type of equation of state plus our own data on pressures and temperatures would suggest an expression for the covolume of the form $\alpha(v) = v\,(1.08 - 0.40\,v)$; this is not consistent, it is true, with the calculated values presented in [8]. The equation of the conservation of energy $E - E_0 = Q + \frac{1}{2}p(v_0 - v)$, is not satisfied by a covolume equation of state when the heat of explosion, Q, is taken from [8]. The internal energy in the latter equation is given by $E \int^{T} c_v dT$, $c_v$ being calculated from the ideal gaseous state of the explosion products since $\left(\frac{\partial c_v}{\partial v}\right)_T = T\left(\frac{\partial^2 p}{\partial T^2}\right)_v = 0$. This indicates that a covolume equation of state, $pv = nRT + p \cdot \alpha(v)$, is not satisfactory for explosion products, especially at high pressures, and that it can be considered as being no more than an approximation suitable for evaluating p, or v, or T, when any two of these quantities are known. It is quite likely that a covolume equation of state of the explosion products resulted from the data on nitromethane, nitroglycerine, hexogen, and TEN simply because these substances have approximately the same value of the detonation temperature.

It is possible to follow Landau and Stanyukovich [9] and introduce terms allowing for mutual repulsion of molecules at high pressures into the equations for the energy and pressure; writing $E = \int^{T} c_v dT + E_{tens}$ and $p = \frac{nRT}{v} + P_{tens}$, gives $E_{tens}$ values for nitromethane, nitroglycerine, and hexogen ($\rho_0 = 1.80$ g/cm$^3$) which are, respectively, 4, 37, and 50% of E, if the latter is considered as equal to the internal energy of the products in the ideal gaseous state. On the other hand, nRT/v alters only slightly, being $23 \cdot 10^3$ atm for nitromethane, to $24 \cdot 10^3$ atm for nitroglycerine, and to $28 \cdot 10^3$ atm for hexogen, or approximately 17.3, 9.2, and 7.2% of the value of the pressure, p. These results point to the importance of experimental temperature determinations in deriving and testing the equation of state of the explosion products and the expression for the internal energy which are required if the parameters of the detonation wave are to be evaluated without great difficulty.

## LITERATURE CITED

[1] M. L. Alentsev, A. F. Belyaev, et al., Zhur. Eks. Teo. Fiz., 16, 990 (1946).

[2] F. C. Gibson, M. Bowser, et al., J. Appl. Phys. 29, 4 (1958).

[3] A. N. Dremin, Doklady Akad. Nauk SSSR, 128, 5 (1959).*

[4] M. A. Cook, J. Chem. Phys., 15, 518 (1947); 16, 1081 (1948).

[5] H. Jones, Third Symposium on Combustion and Flame and Explosion Phenomena (Baltimore, 1949).

[6] S. Paterson, Research 1, 221 (1948).

[7] Cottrell and S. Paterson, Proc. Roy. Soc., A 213, 214 (1952).

[8] M. A. Cook, Science of High Explosives (New York, 1958).

[9] L. D. Landau and K. P. Stanyukovich, Doklady Akad. Nauk SSSR, 46, 339 (1945).

---

*Original Russian pagination. See C. B. translation.

# ALTERATION OF THE WORK FUNCTION OF OXIDE SEMICONDUCTORS BY THE INTRODUCTION OF ADDITIVES

É. Kh. Enikeev, L. Ya. Margolis and S. Z. Roginskii,
Corresponding Member, Acad. Sci., USSR

Institute of Physical Chemistry, Academy of Sciences, USSR

(Translation of: Doklady Akademii Nauk SSSR, Vol. 130,
1960, pp. 807-809)

Original article submitted August 6, 1959.

The study of the mechanism of the action of additives in altering the catalytic properties of semiconductors has directed special attention to a correlation of these properties with the electrical conductivity. A great amount of experimental material [1] on the electrical and chemical properties of semiconductors is available, but the relation between these characteristics is still not understood. It is quite likely that this is due in part to the difficulty of passing from bulk to surface characteristics of semiconductors and to the fact that there can be pronounced differences between body and surface in regard to chemical and phase compositions. To this there are to be added the difficulties associated with comparative measurements of the electrical conductivities of powders and porous bodies. These considerations together with certain theoretical results [2,3] pointing to the great significance of the relative surface charge in fixing surface processes have led us to study the effect of modifying additives on the work function of semiconductors. Many of these experiments were carried out on oxides of divalent metals (NiO, CuO, ZnO) which contained ions of lithium or other alkali metals. These ions exert a very marked effect on the electrical conductivity of the respect oxides, and on their adsorption characteristics and chemical activity as well [4], but insurmountable difficulties attend an attempted interpretation of the observed conductivity–activity relations.

The electronic work function ($\varphi$) was determined from the difference of contact potentials as measured by the vibrating condenser method ($\zeta$). The semiconducting oxide specimens which were to be compared were inserted in various indentations in a metal plate (Fig. 1). These indentations could be brought successively under the vibrating gold electrode 1 by the use of an electromagnet. This procedure minimized effects from variation of the work function of the measuring electrode and, at the same time, assured uniformity in the method of treatment and the conditions of measurement.

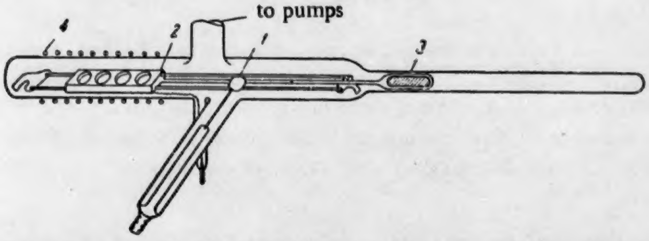

Fig. 1. Apparatus for measuring differences in contact potentials; 1) Measuring electrode; 2) metallic plate with indentations for specimens; 3) iron core; 4) electrical heater.

The experimental results on a single preparation were reproducible to within 0.05 v, the error of measurement of $\varphi$ being no more than 0.01 v. The surface of each specimen was freed of adsorbed oxygen by being aged at 300-400°, either in vacuum or in an atmosphere of CO, with subsequent evacuation to a pressure of $1 \cdot 10^{-6}$mm of Hg. Measurements of the contact differences were carried out at room temperature.

Solid solutions of $Li_2O$ in NiO and CuO were prepared by thermal decomposition of the mixed carbonates in air at 850-900°. The formation of solid solutions in the $Li_2O$ + NiO and $Li_2O$ + CuO systems was confirmed by an x-ray analysis which was made by M. Ya. Kushnerev. Specimens of zinc oxide containing added $Li_2O$ were prepared by decomposing lithium oxalate on zinc oxide at 450, 800, and 1200°.

Figure 2 shows the alteration in the work function, $\Delta\varphi$, which results from introducing lithium into CuO, NiO, and ZnO. The dissolving of lithium into the lattice leads to a diminution of the work function by as much as 0.6-0.8 ev.

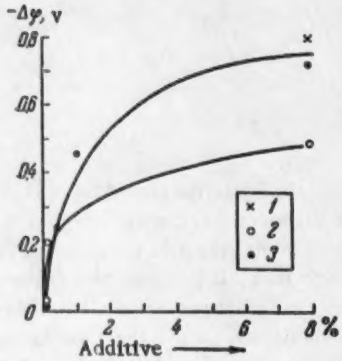

Fig. 2. Alteration of the electronic work function of CuO (1), NiO (2), and ZnO (3) resulting from addition of $Li_2O$ (20°).

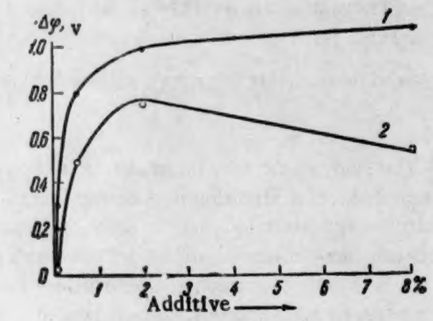

Fig. 3. Alteration of the work function of zinc oxide resulting from introduction of $Na_2O$ (1) and $Cs_2O$ (2) at 20°.

It is to be emphasized that the state of $Li_2O$ in ZnO is not yet as firmly established as that of $Li_2O$ in NiO since the x-ray diagrams do not disclose alterations of more than 0.0002 A in the lattice parameters.

The work function of ZnO falls as the concentration of $Li_2O$ is increased, at first sharply and then more gradually, reaching a value of 0.7 ev at 8% $Li_2O$. It is interesting to note that specimens of ZnO with added $Li_2O$ which had been heated to different temperatures showed almost the same decrease in the work function.

The formation of solid solutions between $Li_2O$ and NiO is accompanied by a marked increase in the electrical conductivity ($\sigma$) and by a decrease in the energy of activation for conduction ($E_\sigma$) [6]. This indicates the Fermi level, $f$, in the body of NiO, a hole semiconductor, to be displaced toward the top of the valence band so that the work function $\Delta\varphi$ should increase. The experimental data show a diminution of $\Delta\varphi$ in this case.

The energy of activation for conduction in ZnO, an electron semiconductor, is increased from 0.2 to 1.6-2.0 ev by the introduction of lithium [7], so that the Fermi level in the body of this crystal is also displaced toward the top of the valence band under the influence of the added $Li_2O$. The work function for $Li_2O$ + ZnO should be increased. Our data show, however, that the work function is altered in the same direction by introducing $Li_2O$ into the electron semiconductor ZnO as by introducing it into the hole semiconductor NiO, $\varphi$ decreasing in both cases.

In the band model, this would be explained by the fact that an additive on the surface affects the $f$ in the opposite manner to an additive in the body so that lithium cations function as electron donors on the surface, and as electron acceptors in the bulk of NiO, CuO, and ZnO semiconductors.

The observed changes in $\Delta\varphi$ are quite consistent with the effect of $Li_2O$ on the adsorption characteristics and catalytic activity of NiO and ZnO.

The alteration in $\varphi$ resulting from introduction of sodium and cesium (Fig. 3) gave confirmation of the conclusion that an additive localized on the surface is a prime factor in fixing $\Delta\varphi$. Preparations were obtained here by decomposing nitrates and oxalates on ZnO at 400-700°. Figure 3 shows that Na and Cs decrease the work function even more sharply, this being obviously due to the fact that these elements are predominantly localized on the ZnO surface. (It is difficult to visualize the formation of solid solutions of ZnO with Na, or especially Cs ions, in view of the great disparity of the ionic radii).

We have studied the effect of iron and chromium oxides in CuO, of magnesium and iron oxides in NiO, and of thorium dioxide in ZnO (Fig.4), among others. Only for MgO was it possible to prove the formation of solid solutions and the absence of mixtures or other phases. The data for the MgO + NiO system indicate that lack of variation in $E_\sigma$ for the solid solutions [8] does not imply that $\Delta\varphi$ is constant for this system.

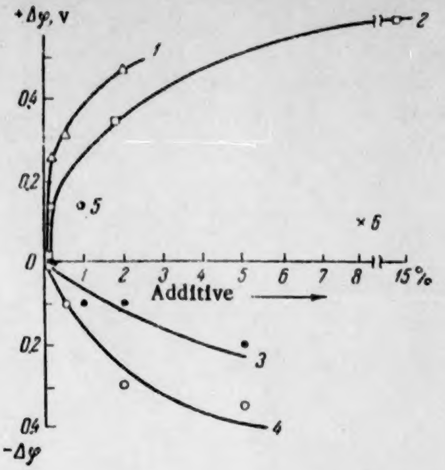

Fig. 4. Alteration of the work function of CuO, NiO, and ZnO resulting from introduction of various additives: 1) $ZnO + ThO_2$; 2) $ZnO + ZnSO_4$; 3) $CuO + Fe_2O_3$; 4) $CuO + Cr_2O_3$; 5) $NiO + FeO_3$; 6) NiO + MgO.

A comparison of the effects of various additives in changing the work function of the semiconducting ZnO show $\varphi$ to be reduced by 0.4 ev in the 2% $Na_2O + ZnO$ system and to be increased by 0.4 ev in the 2% $ThO_2 + ZnO$ system. The introduction of $SO_4^{2-}$ groups into the ZnO surface increases the work function by 0.5 ev. Thus the electronic work function for oxide semiconductors can be altered within wide limits by introducing various additives. The fact that the relation between the bulk and surface electrical properties of the modified semiconductors is a complex one is shown by a comparison of the data of the literature on the alteration of the conductivity of solid solutions with other data on the variation of the work function of these systems.

The authors conclude by expressing their thanks to G. M. Zhabrova for having furnished the preparations of zinc oxide containing the additives and to M. Ya. Kushnerev for x-ray and electron diffraction analyses of the specimens.

## LITERATURE CITED

[1] G. Parravano and M. Boundart, Advances in Catal. 7, 47 (1955).

[2] K. Hauffe, Advances in Catal. 7, 213 (1955); S. Roy Morrison, Advances in Catal. 7, 259 (1955); F.F. Vol'kenshtein, Usp. Khim. 27, 1304 (1958).

[3] S. Z. Roginskii, Doklady Akad. Nauk SSSR 124, 817 (1959).*

[4] G. M. Schwab and J. Block, Zs. Phys. Chem. 1, 42 (1954); N. P. Keier, S. Z. Roginskii, and I. S. Sazonova, Doklady Akad. Nauk SSSR 106, 859 (1956).*

[5] V. F. Bogolyubov, Radiotekhnika i Élektronika 1, 527 (1957).

[6] E. I. W. Verwey, P. W. Haayman and F. C. Romein, Chem. Weekbl. 44, 705 (1948); C. Wagner, J. Chem. Phys. 18, 69, (1950).

[7] N. P. Keier and L. N. Kutseva, Collection: Problems of Kinetics and Catalysis [in Russian], 10 (1959), in press; N. P. Keier, G. I. Chizhikova, Collection: Problems of Kinetics and Catalysis [in Russian], 10 (1959), in press; É. Kh. Enikeev, L. Ya. Margolis, and S. Z.Roginskii, Doklady Akad. Nauk SSSR, 129, 2, (1959).*

[8] I. S. Sazonova, Candidate's Dissertation (Moscow, 1957).

---

*Original Russian pagination. See C. B. translation.

# THE INTERPHASE SURFACE ENERGY OF A METAL AT THE CRYSTAL–MELT INTERFACE

S. N. Zadumkin

Kabardino-Balkarskii State University

(Presented by Academician A. N. Frumkin October 30, 1959)

(Translation of: Doklady Akademii Nauk SSSR, Vol. 130, No.4, 1960, pp. 810-811)

Original article submitted May 7, 1959.

The surface free energy, $\sigma_{12}$, at the solid melt interface in a one-component system is a quantity of importance for processes of melt crystallization. In only one paper [1] has the attempt been made to evaluate $\sigma_{12}$ for metals theoretically. Skapskii [1] used the Dupree* Equation in calculating $\sigma_{12}$, assuming the work of adhesion to be equal to twice the surface tension of the liquid phase at the interface with its own saturated vapors. This value, is however, undoubtedly less than the work required for complete removal of the liquid from the surface of the solid body. Thus the results obtained by Skapskii must be too high.

A simple method for evaluating the interphase surface energy of a metal at a polycrystal–melt interface is given in the present work.

The Gibbs thermodynamic theory of capillarity shows the excess surface free energy of the transition layer separating two phases of volume $v'$ and $v''$ to be given by the expression

$$F_s = F - w' v' - w'' v'', \tag{1}$$

in which $w'$ and $w''$ are the free energies per unit volume of the respective homogeneous phases at points far removed from the interface, and F is the free energy of the entire system.

The excess free energy per unit surface area of the phase interface is designated as the surface free energy

$$\sigma_{12} = F_s/S, \tag{2}$$

S being the area of the surface of separation.

It is known that extended order is lacking in a liquid phase (melt). Thus $\sigma_{12}$ for a crystal face in contact with a melt can be expressed through Eq. [2] as:

$$\sigma_{12} = \sum_{k=0}^{\infty} (F_S^{(k)} - F_v') n_S^{(k)} + \int_{r_0}^{\infty} [w(z) - w''] \, dz, \tag{3}$$

$F_S^{(k)}$ and $n_S^{(k)}$ being, respectively, the total free energy of a single particle within the solid phase and the number of particles per 1 cm$^2$ of surface at a distance $r = kr_0$ from the crystal face which is in contact with the melt ($r_0$ is the interplanar spacing).

Let it be assumed that short-range order is preserved in the melt and that the density of the liquid at the melting point differs from the density of the crystalline phase at the same temperature by p %; then $n_S$ particles on the crystal face which is in contact with the melt will have the same number of neighbors as a particle in the interior of the crystal, while $\Delta n_s = {}^2/_3\ pn_s$ particles each have $\Delta f$ missing neighbors.

---

* Not verified - Publisher's note.

Considering that $w(z) = w''$, and taking the zero-th approximation yields

$$\sigma_{12} = (F_S^{(0)} - F'_v)\, n_S + (F_S - F'_v)\, \Delta n_S. \tag{4}$$

It is clear that

$$F_S^{(0)} - F'_v = \frac{Q}{f_{kv}} \Delta f, \tag{5}$$

since each of the $n_S$ particles at the crystal face–melt interface has $\Delta f$ bonds weakened by an amount $Q/f_{kv}$, where Q is the heat of fusion per particle and $f_{kv}$ is the coordination number in the body.

The second term of (4) will be given by

$$(F_S - F'_v)\, \Delta n_S = {}^2/_3\, p\sigma\,(hkl), \tag{6}$$

according to [3,4], $\sigma$ (hk*l*) being the surface tension of the given metal face at the melting point.

$$\sigma_{12}(hkl) = \frac{\Delta f}{f_{kv}}(hkl)\, n_S(hkl)\, Q + \frac{2}{3} p\sigma\,(hkl). \tag{7}$$

Substitution of (5) and (6) into (4) leads to a final expresion for the interphase surface energy at the (hk*l*) face–melt interface.

A crystal of the cubic system has six (100), twelve (110), and eight (111) faces, and it is thus clear that the following expression should give the surface energy of any polycrystal section at a polycrystal–melt interface.

$$\bar{\sigma}_{12} = \frac{6\sigma_{12}(100) + 12\sigma_{12}(110) + 8\sigma_{12}(111)}{26}. \tag{8}$$

Results on the evaluation of $\bar{\sigma}_{12}$ for certain faced-centered cubic metals and experimental values of the surface tensions of the liquid metals at the melting point are given in Table 1. Experimental values of Q were taken from [5]; values of p came from [1], p being assumed to be 3% when data were lacking.

TABLE 1

Results of Evaluating $\bar{\sigma}_{12}$ from Equation (8)

| Metal | $n_{(100)} \cdot 10^{-14}$ | $Q \cdot 10^{+13}$, ergs/atom | M.p., °K | $P$, % | $\sigma$, ergs/cm$^2$ | $\sigma_{12}$, ergs/cm$^2$ | |
|---|---|---|---|---|---|---|---|
| | | | | | | calc. | exp. |
| Ag | 11,1 | 1,88 | 1234 | 4,5 | 923 | 119 | 126 |
| Au | 11,0 | 2,17 | 1336 | 5,2 | 1120 | 145 | 132 |
| Cu | 14,6 | 2,16 | 1356 | 4,1 | 1154 | 170 | 177 |
| Pb | 7,62 | 0,718 | 600 | 3,4 | 461 | 35,4 | 33 |
| Al | 11,5 | 1,74 | 933 | 3,0 | 860 | 95,0 | 93 |
| Pt | 12,0 | 3,66 | 2047 | 6,9 | 1819 | 288 | 240 |
| β-Ni | 16,2 | 3,00 | 1725 | 3,0 | 1735 | 223 | — |
| β-Co | 16,0 | 2,68 | 1763 | 3,0 | 1936 | 217 | — |

The values of $\bar{\sigma}_{12}$ which have been obtained from Eq. (8) are in satisfactory agreement with the experimental results of [6].

It is to be seen from Table 1 that the interphase tension at the polycrystal–melt interface is approximately 8-15 % of the surface tension of the metal at the melting point.

## LITERATURE CITED

[1] A. S. Skapski, Acta Metallurgica 4, 576 (1956).

[2] S. N. Zadumkin, Izv. Vyssh. Uchebn. Zav. SSSR , Fizika 2, 151 (1958).

[3] S. N. Zadumkin, Doklady Akad. Nauk SSSR 101, 5, 507 (1955).

[4] S. N. Zadumkin, Doklady Akad. Nauk SSSR 112, 3, 453 (1957).*

[5] G. Kaya and T. Laby, Physical Experimenter's Handbook [Russian translation] (1949).

[6] Ya. S. Umanskii, B. N. Finkel'shtein, et al, Physical Metallurgy [in Russian] (1955).

---

* Original Russian pagination. See C. B. translation.

# THE CATALYTIC ACTION OF COPPER IONS IN THE DISSOLUTION OF METALS WITH OXYGEN DEPOLARIZATION

I. A. Kakovskii and N. G. Tyurin

S. M. Kirov Ural Polytechnic Institute

(Presented by Academician P. A. Rebinder October 11, 1959)

(Translation of: Doklady Akad. Nauk SSSR, Vol. 130, No.4,
1960, pp. 812-815)
Original article submitted September 10, 1959.

Many instances of the rate of a redox reaction being increased by an ion of variable valence have been described in the literature [1, 2, 3 -7]. Many authors are inclined to believe that such increase is due to the catalytic action of the ion, but the effect of ions on the rate of dissolution of metals has been studied only incompletely.

Depolarization, i.e., the removal of electrons from the metal surface, is the decisive step in the dissolution of a noble metal [8] since complex formation ( $AgCl + 2CN' = Ag(CN)'_2 + Cl'$ for example) proceeds rather rapidly and without kinetic complications. Reaction with oxygen, and oxidizing agent which takes up electrons in several stages, is usually accompanied by pronounced kinetic complications [1], but depolarization can be facilitated considerably by copper ions which change valence through the loss or gain of a single electron and at the same time aid in the formation of free radicals [2,5]. This effect can have practical significance in attempting to accelerate the dissolution of metals from ores and industrial products. The dissolution of silver in ammonia solutions has been studied here with a view to investigating the catalytic action of copper ions in more detail.

Calculation was made of the thermodynamic probability of the reaction:

$$2Ag + {}^1/_2 O_{2\,(g)} + H_2O + 4NH_{3\,(sol)} = 2Ag(NH_3)_2^+ + 2OH', \qquad (1)$$
$$\Delta G^0 = 2(-4{,}13) + 2(-37{,}60) - (-56{,}70) - 4(-6{,}36) = -1{,}32 \text{ kcal}$$

The free energy change under standard conditions is comparatively small here, but the situation would be more favorable under actual working conditions where the concentrationsfor the silver complex and the hydroxyl ion are each $10^{-3}$ and the ammonia concentration is 2.5 moles/liter:

$$\Delta G = \Delta G^0 + RT \ln \frac{[Ag(NH_3)_2^+ [OH']^2}{[NH_3]^4 P_0^{1/2}} = -1.32 + 1{,}3643 \lg \frac{(10^{-3})^2 (10^{-3})^3}{(2{,}5)^4 1^{1/2}} =$$
$$= -1{,}32 + 1{,}3643 \lg 2{,}5 \cdot 10^{-14} = -1{,}32 - 18{,}54 = -19{,}86 \text{ kcal}$$

This calculation indicates that silver should dissolve readily in ammonia solutions containing oxygen, although the possibility of the reaction rate being reduced by kinetic complications is not to be excluded.

Experiments on the dissolution of silver in pure ammonia solutions and in ammonia solutions containing various additives were set up to elucidate this question. These experiments were carried out by the rotating disc method [10], working in an autoclave with a magnetic stirrer [9] . The concentration of ammonia was the same in all of the experiments and equal to 3.3 mole/liter, the temperature was 67°, the total pressure was 2 atm with a 1.5 atm partial pressure of oxygen, and the silver disc had a surface area of 2 $cm^2$ and was operated at 2800 rpm. Study was made of the effect of added ammonium sulfate, 0.11 g-mole/liter (Experiments 2 and 4), and copper ions,* 0.01 g-ion/liter (Experiments 3 and 4) on the rate of dissolution; Experiment 1 was carried out in pure ammonia. Dissolution rate curves are presented in Fig. 1. The fact that these curves are linear makes it possible to calculate the rate of dissolution (v) of silver in a solution of arbitrary composition. The value of v was $4.3 \cdot 10^{-9}$ g-mole · $cm^{-2}$ · $sec^{-1}$ for solutions containing only ammonia (Experiment 1), 1.7 · · $10^{-8}$ for solutions containing ammonia and ammonium sulfate (Experiment 2), $5.4 \cdot 10^{-8}$ for solutions containing ammonia and the copper-ammonia complex (Experiment 3), and $7.2 \cdot 10^{-8}$ for solutions containing $NH_3$, $(NH_4)_2SO_4$, and the copper complex (Experiment 4).

The relation between the rate of dissolution of silver and the ammonia concentration was studied in experiments in which the temperature was 70°, the oxygen pressure 3 atm, and the copper-ion concentration 0.01 g-ions/liter, the ammonia concentration being varied from 0.09 to 3.3 g-mole/liter. The results of these experiments are presented in Fig. 2. The data indicate that the rise in the rate of dissolution is proportional to the first power of the concentration of ammonia in solution.

A third series of experiments was set up to elucidate the effect of the concentration of the copper-ammonia complex; here the temperature was 70°, the oxygen pressure was 3 atm, the concentration of ammonia was 2.3 g-mole/liter, and the copper concentration was variable. Results from this series of experiments are presented in Fig. 3.

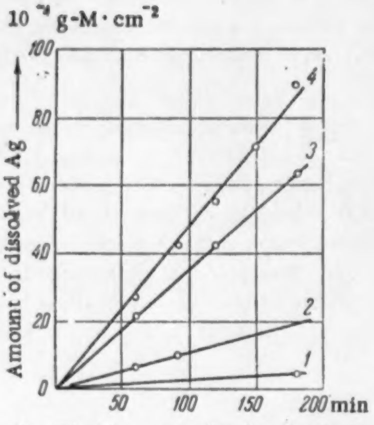

Fig. 1. Kinetic curves for the dissolution of silver in ammonia solutions containing various additives: 1) $NH_3$, 3.36 g-mole/ /liter; 2) the same + $(NH_4)_2SO_4$, 0.11 g-mole/liter; 3) the same + Cu + 0.01 ion/liter; 4) the same + $(NH_4)_2SO_4$ 0.11 g-mole/liter; $Cu^{++}$ 0.01 g-ion/liter.

## DISCUSSION OF RESULTS

The rate of dissolution of the silver in pure ammonia solutions proved to be quite low, just as would be expected since the reaction under study is complicated by the slow depolarization process. The addition of ammonium sulfate accelerates the dissolution considerably, but the effect is weaker than that obtained with the copper-ammonia complex. The addition of ammonium sulfate to a solution containing copper ions and ammonia increases the rate of dissolution of silver by ($7.2 \cdot 10^{-8} – 5.4 \cdot 10^{-8} = 1.8 \cdot 10^{-8}$); this is approximately the same as the increase resulting from a similar addition to an ammonia solution which is free of copper ($1.7 \cdot 10^{-8} – 0.4 \cdot$ $\cdot 10^{-8} = 1.3 \cdot 10^{-8}$). It is clear that the action of the ammonium sulfate is not catalytic (it can be considered as a buffer with respect to the strong alkali, the hydroxyl ion, which retards the oxygen reduction) whereas the copper-ammonia complex can readily take up a single electron and thus facilitate the depolarization of the dissolving noble metal. Copper changes valence more readily in ammoniacal solutions than in sulfate solutions [1] and the resulting $Cu(NH_3)_2^+$ ions are stable and can accumulate in solution at considerable concentration, while the $Cu^+$ ions disproportionate ($2Cu^+ = Cu^{++} + Cu$; $K_0 = 7 \cdot 10^5$). For the reaction*

$$\mathrm{Cu\ (NH_3)_4^{++} + e = Cu\ (NH_3)_2^{+} + 2NH_{3(sol\ )}} \qquad (2)$$

$$\Delta G^0 = -15{,}52 + 2\,(-6{,}36) - (-29{,}11) = +0{,}87\ \text{kcal};\ K_0 = 0{,}23;\ E_0 = +0{,}038\ v.$$

---

*Copper was added to the solution in the form of the hydroxide [11] in order to avoid introducing sulfate ions which will also accelerate the dissolution of silver in ammoniacal solutions to a certain degree.

**The free energies of formation of the substances participating in these reactions have been calculated from the most recent data, since the values listed in handbooks are frequently untrustworthy [12]. Thus Latimer [13] gives an incorrect value, $\Delta G° = -40.8$ kcal, for $Cu(NH_3)_4^{++}$.

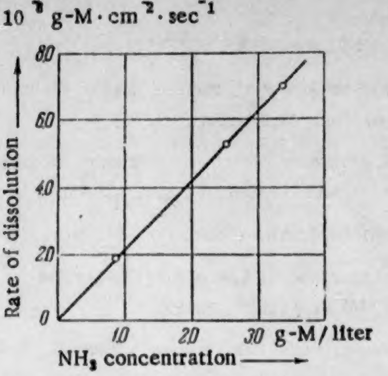

Fig. 2. The relation between the rate of dissolution of silver and the ammonia concentration.

The standard free-energy change of this reaction is close to zero, but the divalent copper complex will readily undergo reduction when the concentration of the univalent copper complex in the solution is low, taking up electrons and then transferring these electrons to the oxygen, a process which is especially favored since each reaction involves a single electron. The thermodynamic probability of this last reaction is illustrated by the following calculation:

$$2Cu(NH_3)_2^+ + {}^1/_2\ O_{2(g)} + H_2O + 4NH_{3(sol)} = \qquad (3)$$
$$= 2Cu(NH_3)_4^{++} + 2OH',$$

$$\Delta G^0 = 2(-29{,}11) + 2(-37{,}60) - 2(-15{,}52) - (-56{,}70) =$$
$$= -20{,}24 \text{ kcal}$$

The calculations which have been made and the experiments which have been carried out all confirm the fact that the ammonia complex of univalent copper is readily oxidized by oxygen which is introduced into solution from the gaseous phase, and this without the kinetic complications which are so often observe in reactions between dissolved substances. The following simple experiment confirms the absence of kinetic complications in the transfer of electrons from metal to oxygen by the copper-ammonia complexes: when metallic copper is added to a solution containing the ammonia complex of divalent copper and the flask closed with a stopper, the solution rapidly decolorizes as the result of reduction of the copper to the univalent form, but it once more becomes blue when the flask is opened and oxidation by atmospheric oxygen is allowed to take place.

Reaction (3) proceeds so intensively that the concentration of the ammonia complex of univalent copper in solution diminishes markedly; the ammonia complex of divalent copper can then function quite readily as a depolarizer, taking electrons from the silver surface and transferring them to the oxygen, thus playing the role of an accelerating catalyst for the dissolving of silver in the ammonia solution. Results from our calculations for the reduction potential for copper in ammoniacal solution (Reaction 2) and for the value of the standard potential of silver in ammoniacal solution (+0.372 v) justify the conclusion that the concentrations of the silver-ammonia complex and the univalent copper-ammonia complex must be low if the transfer of electrons from the silver surface to the $Cu(NH_3)_4^{++}$ ions is to be rapid. The concentration of the $Cu(NH_3)_2^+$ ions will be quite low when oxygen is present and the potential of Reaction (2) will then fall between the potentials of the two reacting substances, silver and oxygen, thus fulfilling one of the conditions which are imposed on a possible catalyst [6].

The simplified picture of the catalytic action of copper ions in ammoniacal solutions is in good agreement with the fact that these ions bring about a considerable increase in the rate of dissolution of silver.

The data which are presented in Fig. 2 indicate that the dissolving of silver in ammoniacal solutions is a reaction of first order with respect to ammonia, the velocity constant for the reaction ($k = Q/sct$) reaching a value of $2.1\text{-}2.4 \cdot 10^{-8}$ liters$^{-1}$ · cm$^{-2}$ · sec$^{-1}$ when catalytic copper ions are present. This is two or three orders less than rate constants for heterogeneous metal dissolution where diffusion is the controlling factor.

Special interest attaches to the experiments whose results are presented in Fig. 3. At fixed experimental conditions of temperature, oxygen pressure, and solution composition there is a certain "maximum" concentration of the copper-ammonia complex above which the rate of dissolution of silver remains practically constant. This maximum concentration is fixed by the rate of diffusion of the components to the silver surface and its existence is characteristic of such multicomponent heterogeneous reactions as the dissolution of noble metals in cyanide solutions in the presence of oxygen. The presence of this maximum concentration of the coppper-ammonia complex is convincing proof that the complex participates in the dissolution of silver in ammoniacal solutions, transferring electrons from the metal to the oxygen, increasing the reaction rate, diminishing the harmful effects of kinetic complications, and functioning, in general, as a catalyst.

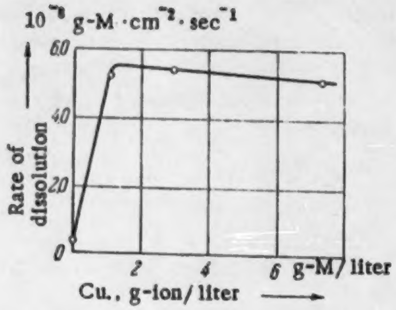

Fig. 3. The relation between the rate of dissolution of silver and the copper concentration.

## LITERATURE CITED

[1] A. N. Frumkin et al, the Kinetics of Electrode Processes [in Russian] (Izd. Mosk. Univ. 1952). .*

[2] N. N. Semenov, Certain Problems of Chemical Kinetics and Reactivity [in Russian] (Izd. AN SSSR, 1958).

[3] J. Klifford, J. Am. Chem. Soc. 80, No.1,245 (1958).

[4] P. I. Levin and E. S. Pronina, Collection: Transactions VNIITsVETMET, 3 (1958), p. 98.

[5] H. Remy, Lehrb. der anorgan. Chem. 1, 9, Aufl. (Leipzig, 1957).

[6] I. M. Kolthoff and V. A. Stenger, Volumetric Analysis 1 [Russian translation] (Moscow, 1950).

[7] A. P. Snurnikov and B. D. Ponomarev, Tsvetnye Metally, 8, 22 (1956).

[8] I. A. Kakovskii, Izvest. Akad. Nauk SSSR, OTN, 7, 29 (1957).

[9] N. G. Tyurin, Yu. B. Kholmanskikh, and I. A. Kakovskii, Izvest. Vyssh. Uchebn. Zavedenii, Tsvetnaya Metallurgiya, 5, 69 (1958).

[10] Ya. V. Durdin and Z. U. Dukhnyakova, Collected Articles on General Chemistry 1, [in Russian] (Izd. AN SSSR) (1953) p. 163.

[11] Yu. V. Karyakin and I. I. Angelov, Pure Chemical Reactants [in Russian] (Moscow, 1955).

[12] I. A. Kakovskii, Zhur. Fiz. Khim. 29, 12, 2268 (1955).

[13] V. M. Latimer, The Oxidation States of the Elements and Their Potentials in Aqueous Solution [Russian translation] (IL, 1954).

# SPECIAL FEATURES OF THE KINETICS OF THE HYDRATIONAL HARDENING OF SULFATES

O. I. Luk'yanova, Academician P. A. Rebinder,
and G. M. Belousova

Department of Colloidal Chemistry, M. V. Lomonosov Moscow State University

(Translation of: Doklady Akademii Nauk SSSR Vol. 130, No.4,
1960, pp. 816-819).

Original article submitted October 31, 1959.

Interest attaches to the study of the hydrational hardening of sulfates containing various cations. The sulfates form the only group of mineral binders with high chemical affinity for water in the Zhuravlev-Moshchanskii classification [1,2] and cyrstallization structures can be formed in them under a wide variety of conditions. These substances differ in regard to hydrate crystal structures, solubilities of hydrates and parent anhydrous salts, and ability to form stable supersaturated solutions in concentrated suspensions.

The work of E. E. Segalova and her collaborators [3-5] has shown that the mechanical strength of the disperse crystallization structure of hardening is determined principally by the kinetics of the formation of the new solid phases, and thus is not a simple single-valued function of the structure and chemical composition of these phases. Here, the most important kinetic characteristics are the length of the induction period for crystallization and the rate of crystallization of the hydrate. We have evaluated these characteristics for concentrated suspensions of nine sulfates by studying the kinetics of the evolution of heat in the course of hydration of partially and completely dehydrated salts, the kinetics of dissolution of these substances, and structure formation in suspensions; we have,at the same time, carried out parallel microscopic observations. The method of study has been described earlier in [6-8].

The investigated salts can be separated into two groups on the basis of the kinetic curves for hydration and hardening, the separation being set up in terms of the length of the induction period for crystallization, $\tau_i$, and its ratio to the time required for full hydration of the salt, $\tau_h$.

The special features of each of these groups can be brought out clearly by studying the effect on the hydration kinetics of such factors as the degree of dispersion of the parent salt and the concentration of the suspension, i.e., the water-solid phase ratio, W/S. Figure 1 illustrates two extreme cases of the effect of the initial degree of dispersion on the kinetics of hydration, the one for $CdSO_4 \cdot H_2O$ and the other for $Na_2SO_4$. There is a clearly expressed induction period for crystallization of the hydrate $CdSO_4 \cdot (8/3) H_2O$ (stable at 20°) which diminishes as the degree of dispersion of the parent salt is increase. Here, $\tau_h$ exceeds $\tau_i$, but only by a factor of 2.5-3 (the corresponding level of evolution of heat is indicated by the simple dotted curve). It is known that calcium sulfate in the form of anhydrous or hemihydrated gypsum shows a kinetic hydration curve of this same type with a similar dependence on the degree of dispersion. Sodium sulfate gives an entirely different type of kinetic curve under these same conditions; $\tau_i \approx 0$ and the retardation of hydration is more marked the lower the degree of dispersion of the parent salt Thus a three-hour interaction with water ($\tau_h$ = 24 hours) is required for 50% hydration of a salt with specific surface area of 3000 $cm^2/g$ (according to Tovarov). Observations with the polarizing microscope, even at magnifications as low as 400 ×, show that this marked retardation of hydration is due to the formation of a densely bound layer of decahydrate crystals on the surface of the parent crystal. Up to

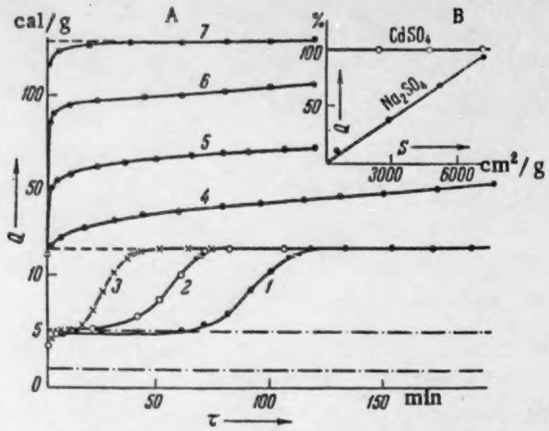

Fig. 1. A) The kinetics of the evolution of heat during hydration of $CdSO_4 \cdot H_2O$, $W/S = 0.21$: 1) A = = 2400, 2) A = 4700, 3) A = 7100 cm²/g and $Na_2SO_4$, $W/S = 1.20$, 4) A = 500, 5) A = 2800, 6) A = 5100, 7) A = 7200 cm²/g. B) The relation between the value of Q at the end of the induction period, expressed as percentage of the heat liberated in complete hydration, and the degree of dispersion, A, of the parent salt.

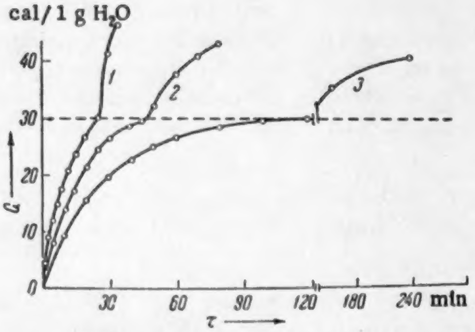

Fig. 2. Kinetics of the evolution of heat in hydration of $NiSO_4 \cdot H_2O$. 1—B/T = 0.65, 2—B/T = 1.00, 3—B/T = 1.40.

the present time, such effects have been observed only in difficultly soluble substances which have low diffusion coefficients. It would be incorrect to acribe this effect, or the related direct proportionality between specific surface area and amount of salt hydrated in the first three-five minutes, to hydration of anhydrous salt which has not undergone preliminary dissolution. Supersaturations corresponding to the tabulated values of the metastable solubility of anhydrous sodium sulfate can be detected at any one temperature by direct measurements of the concentration of the salt in the aqueous phase of an intensely agitated suspension with a sufficiently high W/S ratio. Thus the production of hydrate crystallites, either on the surface of the parent salt or directly before it, is possible because the rate of formation and growth of crystallization nuclei is high in comparison with the rate of diffusion of salt ions into solution.

The sulfates of Mg, Zn, Cu, Co, and $Fe^{II}$ (monohydrates) occupy an intermediate position with respect to their kinetic curves for hydration and hardening, these materials having low $\tau_1$ values ranging from one to three minutes and a weakly expressed tendency toward retarded hydration.

It has seemed desirable to draw on contemporary theories of the structure of electrolytic solutions [9] and information on the crystal structures of the hydrates of the investigated salts in attempting to explain the differences in the hydration kinetics of sulfates containing various cations. The structure of the cation coordination sphere of many hydrating salts is known to be the same in concentrated solutions as in the crystal hydrate. Among the salts which we have studied, the sulfates of Na, Mg, Zn, Co, Ni, and $Fe^{II}$ show this type of similarity between the structures of solutions and crystal hydrates, whereas the stable crystal hydrates of Cd and Ca have lower cation coordination numbers for water (2 for Ca, < 3 for Cd) than those usually met in solutions of these ions (4.6 for Ca, 6 for Cd). The work of formation of crystallization nuclei can be expected to diminish as the similarity between the structures of solution and separating crystal hydrate becomes more marked, and the stability of the supersaturated solution resulting from salt hydration will then fall accordingly. A similar effect is met in melt crystallization of such substances as the esters of salicylic acid for which definite structural differences have been established between melt and solid compound; this condition is indicated by a high value of $\tau_1$. Supersaturated solutions of higher stability are formed with Sr and Ba sulfates. Thus a hundredfold relative supersaturation is obtained with strontium sulfate, $\tau_1$ being equal to several minutes [10]. The alteration in the cation coordination number with respect to water is larger here, the change being from six, or four, to zero.

The fact that the passage of nickel sulfate from the monohydrate to the heptahydrate is associated with a

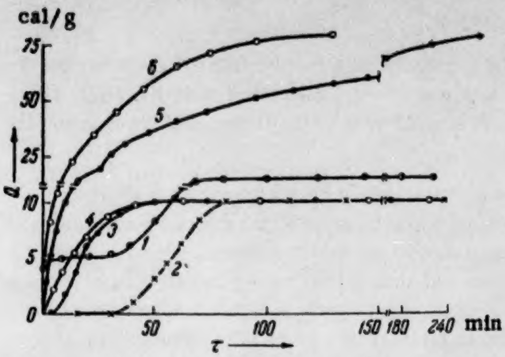

Fig. 3. Kinetics of the evolution of heat in the hydration of $CdSO_4 \cdot H_2O$ (1-4) and $NiSO_4 \cdot H_2O$ (5,6) slaked with water, 1, 5; with a saturated solution of the corresponding salt, 2,6; with a saturated solution containing 20%, 3, and 60%, 4, added stable crystal hydrate, by weight of parent salt.

high value of $\tau_1$ is in apparent contradiction with the ideas expressed here. Concentration measurements during dissolution of this salt and the kinetics of heat liberation in its hydration at various W/S values (Fig. 2) show, however, that the long induction period is the result of retarded dissolution, the liberation of heat being sharply accelerated when the solution concentration reaches a fixed value at a heat of solution of 30 cal per 1 g of $H_2O$. This effect occurs at relative supersaturations of $C/C_0 = 1.09$ and is associated with the beginning of hydrate crystallization, the indication being that these supersaturations are quite unstable. Thus nickel sulfate should be placed in the same kinetic group as the sulfates of Mg, Zn, and Na. It is to be noted that sodium sulfate must occupy a special position in this classification since the structure of the coordination sphere of its cation corresponds, not only to that of the concentrated solutions, but also to the crystal structure of water (coordination number 4); clearly, this accounts for the fact that this compound crystallizes from concentration suspensions without noticeable induction period.

TABLE 1

The Mechanical Strength of Disperse Structures in the Hydrational Hardening of Sulfates

| Salt | A, $cm^2/g$ | W/S | Salt/ /"filler" | $P_m$, $kg/cm^2$ | |
|---|---|---|---|---|---|
| | | | | crys. | coag. |
| $Na_2SO_4$ | 1200 | 1.2 | 1 : 5 | 13.3 | – |
| | 500 | 1.2 | 1 : 5 | 5.7 | 0.3 |
| $ZnSO_4$ | 2400 | 0.7 | 1 : 1 | 140 | 0.8 |
| $NiSO_4$ | 8000 | 1.0 | 1 : 3 | 25.6 | 0.5 |
| $CdSO_4$ | 2400 | 0.2 | 1 : 0 | 166 | 0.8 |
| | 7300 | 0.3 | 1 : 1 | 170 | – |

The lack of uniformity in the induction periods of salts such as nickel and cadmium sulfates which belong to different kinetic groups is reflected in the slaking of their monohydrates by saturated solutions of the respective salts. Figure 3 shows that the slaking of cadmium sulfate by a saturated solution merely diminishes the heat of solution without altering the kinetics of salt hydration essentially. Only by reducing the work of formation of crystallization nuclei through the introduction of crystal seeds is it possible to reduce $\tau_1$ in this case and carry its value practically to zero (Fig. 3, 3, 4). Nickel sulfate does not form stable supersaturations in concentrated suspensions and it will hydrate without an induction period, even when slaked with a saturated solution (Fig. 3, 5, 6).

On hardening, all of the investigated salts interact with water in concentrated suspensions to give stable crystal structures with relatively high W/S values, and this is not only true of the individual salts but also of mixtures containing fillers such as pulverized sand which may be introduced to impede sedimentation at high W/S.

Table 1 shows that sodium sulfate is to be classed among the salts which are capable of hydrational hardening, a fact which was contested earlier. This characteristic appears only on slaking by impregnation with water and without mechanical agitation, and results from the very low $\tau_1$ value.

Table 1 also gives values of the mechanical strength of the coagulation structures which arise after mechanical breakdown of the initial crystallization structure and have strengths one order lower than the latter. This indicates that the mechanical strength of the crystallization structures of most of the investigated salts is not due entirely to the sharp reduction in the W/S ratio in hydration.

The proposed supplement to the classification of binding materials based on the principle of structural similarity between solution and hydration products is only applicable to substances which interact with water to form true crystal hydrates, i.e., to compounds containing water in molecular form. Calcium silicate interacts with water to give materials which are not simple crystal hydrates and thus cannot belong to this class of binders. The inversion in the binding characteristics which is met in passing in the Mendeleev Periodic System from the silicates and their analogs to the sulfates [1] is clearly related to the fact that water in molecular form characteristically enters the cation coordination sphere of the latter compounds. This gives rise to the appearance of binding properties as the cation radius is decreased by moving over a single subgroup of the Periodic System. The hydration of the silicate is expressed in the first instances in an alteration in the anion structure; when the anion increases in dimension, the binding characteristics must rise with the cation radius, just as is actually observed to be the case.

## LITERATURE CITED

[1] V. F. Zhuravlev, The Chemistry of Binding Materials [in Russian] (Moscow, 1951).

[2] N. A. Moshchanskii, Transactions, Conference on the Chemistry of Cement (Moscow, 1956) p.114.

[3] E. E. Segalova, V. N. Izmailova, and P. A. Rebinder, Doklady Akad. Nauk SSSR 114, 594 (1957).*

[4] E. E. Segalova, E. S. Solov'eva, and P. A. Rebinder, Doklady Akad. Nauk SSSR 113, 134 (1957).*

[5] E. S. Solov'eva and E. E. Segalova, Kolloid Zhur. 20, 5, 620 (1958).*

[6] O. I. Luk'yanova, E. E. Segalova, and P. A. Rebinder, Doklady Akad. Nauk SSSR 117, 1034 (1957).*

[7] O. I. Luk'yanova, E. E. Segalova, and P. A. Rebinder, Kolloid Zhur. 19, 1, (1957).*

[8] E. E. Segalova, P. A. Rebinder, and O. I. Luk'yanova, Vestn. MGU 2, 17 (1954).

[9] O. B. Samoilov, The Structures of Aqueous Solutions of Electrolytes and the Hydration of Ions [in Russian] (Izd .AN SSSR, 1957).

[10] N. A. Figurovskii and T. A. Komarova, Zhur. Neorg. Khim. 1, 2820 (1956).

---

*Original Russian pagination. See C. B. translation.

# OXIDATION REACTIONS OF THE OLEFINS

I. I. Moiseev, M. N. Vargaftik, and Ya. K. Syrkin,
Corresponding Member, Acad. Sci., USSR

(Translation of: Doklady Akademii Nauk SSSR, Vol. 130,
1960, pp. 820-823)

Original article submitted November 16, 1959

The following reactions of oxidations of olefins to carbonyl compounds:

$$CH_2=CH_2+H_2O_2=CH_3CHO+H_2O \quad (1)$$

$$CH_2=CH_2+{}^1/{}_2O_2=CH_3CHO \quad (2)$$

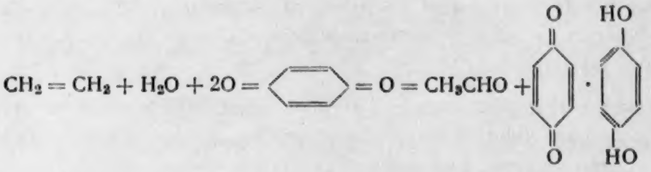

(3)

have been carried out as part of a study of the interaction of the former compounds with palladium chloride. All of these reactions proceed in the presence of divalent palladium salts which function as oxidation catalysts.

This work aimed primarily at investigating the reactions of $Pd^{II}$ salts with olefins, such reactions being instances of processes which involve the formation of intermediate $\pi$-complexes with dative bonds. It is clear that the $\pi$-complexes of the transition elements with olefins or hydrocarbons of the acetylene series are intermediates in many reactions of unsaturated compounds. Thus it is possible that the Kucherov reaction for the addition of water to acetylene proceeds through the formation of a $\pi$-complex between acetylene and divalent mercury ions [1]. There is also reason to believe that $\pi$-complexes are involved in oxy-synthesis reactions, in certain acetylene polymerizations, etc.

Thus, a study of the properties of the $\pi$-complexes of olefins with metals is of great theoretical interest. Zeise's salt, $K[PtCl_3C_2H_4]$,[2] is a representative of this class of compounds. This particular compound is stable, its stability resulting from the fact that there is dative interaction in the complex in addition to the donor-acceptor bond [3, 4] and the effective positive charge on the olefin carbon atoms is reduced accordingly. Anderson has shown [5] that this salt will decompose in boiling aqueous solution with the separation of metallic platinum. Acetaldehyde was found in the reaction products. It can be supposed that the action of the central atom in polarizing the C atoms of the double bond, and the associated polarization of the C—H bond, would be factors of vital importance to this reaction. On the basis, the palladium analog of Zeise's salt should react with water even more rapidly than Zeise's salt itself since the Pd atom has a smaller radius than the Pt atom and it can be presumed that its 4 d electrons would be less inclined to dative interaction than the 5 d electrons of platinum.

Thus, there is reason to believe that the formation of $\pi$-complexes is involved in the reduction of palladium salts by olefins or carbon monoxide in aqueous solution [6]. This reaction has been applied for the detection of olefins and CO in analysis of gaseous hydrocarbons [7], and it has been proposed as a means for separating palladium from aqueous solutions containing other noble metals [8]. The chemistry of the reactions of the olefins with palladium salts has not yet been elucidated; however, Phillips has found [6] that acetaldehyde is formed when palladium salts are reduced by ethylene in aqueous solution. Other authors claim [7] that dichloroethane is produced in the reaction of ethylene with $PdCl_2$. Data on the reaction products from the ethylene homologs were lacking in the literature at the end of 1957, when this work was begun.

A study of reactions involving formation of metallic palladium is rendered difficult by the rarity of the salts of this metal and by the possibility that secondary reactions will occur on the surface of the finely dispersed metallic powders of high catalytic activity. It appeared desirable to use an oxidizing agent which would oxidize the palladium rapidly enough to prevent its deposition from solution and would not, at the same time, interact with either the olefin or its reaction products. The standard oxidation potentials [9] indicate that hydrogen peroxide in acid solution, quinone, oxygen, and certain other substances would function as oxidants of this type.

Our experiments have shown that dilute hydrochloric acid solutions of palladium chloride containing 3-5 % of hydrogen peroxide will slowly take up ethylene and propylene at 40-45° to form acetaldehyde and acetone, respectively. Separation of metallic palladium does not occur here. Thus under these conditions the reduction of palladium salts by olefins is accompanied by an oxidation of the product palladium through hydrogen peroxide.

The over-all reaction is one of oxidizing the olefin by hydrogen peroxide to form a carbonyl compound. This basic reaction is accompanied, however, by breakdown of the hydrogen peroxide in solution to oxygen and water. The rate of this reaction increases more rapidly with rising temperature than does the rate of the basic process. This fact makes for complications in the study of the reactions of palladium salts with olefins under these conditions, just as does the ability of hydrogen peroxide to oxidize carbonyl compounds.

The olefins can be oxidized rather rapidly and smoothly by using n-benzoquinone. The quinhydrone resulting from the reaction in acid solution does not reduce palladium salts. The inherent drawback to the use of this oxidant is that the volatility of quinone and hydroquinone makes for difficulty in separating the oxidation products from the reaction mixture.

Oxygen will oxidize metallic palladium very slowly if other substances are not present. For this reason, the attempt was made to find an oxidizing agent which would be capable of oxidizing metallic palladium, and would itself reduce to a form which could be oxidized by oxygen.

We have been able to show that cuprous salts in halide solutions will function as oxidizing agents of this type. The oxidation of metallic palladium by cuprous salts in nitrate or sulfate solutions is impossible thermodynamically. Acido-complexes such as $PdX_4^{2-}$ are formed in halide solutions. The standard oxidation potential, $E^0_{Pd^{II}/Pd^0}$, is reduced thereby. On the other hand, divalent copper is reduced to monovalent copper salts, $Cu_2X_2$, in the presence of halide ions, and the oxidation potential $E^0_{Cu^{II}/Cu^I}$ rises as the result of stabilization of the reduced form.

A comparison of standard oxidation-reduction potentials [9] shows that the standard free-energy change for the oxidation of metallic palladium by $Cu^{2+}$ ions is 3700 cal/mole in chloride solutions, and 1850 cal/mole in bromide solutions; the corresponding equilibrium constants at 25° are $2.2 \cdot 10^{-3}$ and $2.2 \cdot 10$, respectively.

Thus the thermodynamic factors are such as to favor more extensive oxidation of palladium in bromide solutions than in chloride solutions. The positive sign of $\Delta S$ for this reaction causes the equilibrium constant to rise with temperature in both bromide and chloride solutions. Copper bromide was used as an oxidation catalyst in our experiments.

The experiments on the oxidation of the olefins by oxygen involved the passage of the gaseous mixture through a solution of the palladium salt and copper oxide at 90°. The gas was dispersed by a glass filter. The gas left the reactor to pass through a system of scrubbers in which the reaction products were taken up by water. Thus, propylene yielded acetone, as identified from the melting points of the semicarbazone, the thiosemicarbazone, and 2, 4-dinitrophenylhydrazone, and propyl aldehyde in a small amount which ranged up to 5%, determination being made polarographically. This same method gave acetaldehyde from ethylene and methyethyl ketone from butylene-2. Our data here are in full agreement with those given by Smidt and his co-workers in a paper [10] which appeared when this portion of our own work was being completed. These authors also carried out the oxidation of olefins by oxygen in the presence of copper and palladium salts, but by a somewhat different method.

Thus the following reactions:

$$PdX_4^{2-} + C_2H_4 + H_2O = Pd + CH_3CHO + 2H^+ + 4X^- \qquad (4)$$

$$Pd + 2Cu^{2+} + 6X^- = PdX_4^{2-} + Cu_2X_2 \qquad (5)$$

$$\frac{Cu_2X_2 + {}^1/_2O_2 + 2H^+ + 2X^- + 2CuX_2 + H_2O}{C_2H_4 + {}^1/_2O_2 = CH_3CHO} \qquad (6)$$

take place when a mixture of olefin and oxygen is passed through a solution containing palladium and copper salts.

The rates of Reactions (4), (5), and (6) must be equal if there is to be a possibility of establishing a stationary state. The interaction of the olefin with $Pd^{II}$, (4), proceeds through the formation of a π-complex and it is possibly, for this reason, strongly dependent on the concentrations of those ions which are capable of producing stable acido complexes of the $PdX_4^{2-}$ type. This makes it possible to maintain a stationary state in the reactor by using an excess of halide ions, characteristic of each olefin, and varying the $Cu^{II}$ concentration and the partial pressure of the oxygen.

It should be noted that practical interest also attaches to the oxidation of the lower olefins by oxygen to form carbonyl compounds. Under our experimental conditions, using a catalyst containing 0.02 moles/liter $PdCl_2$, 0.16 moles/liter $CuBr_2$, and 0.04 moles/liter $CuCl_2$, a temperature of 90°, and volume velocity of 100 liters per liter of catalyst per hour, there was a 25% conversion of the ethylene and a yield of acetaldehyde amounting to 95% of the reacted ethylene. Passing a 75% propylene and 25% oxygen mixture through a solution containing 0.02 moles/liter $PdCl_2$, 0.15 moles/liter $CuBr_2$, and 0.15 moles/liter $CuSO_4$ at 90° and a volume velocity of 100-150 liters per liter of catalyst per hour gave a propylene conversion of 15-17%, and a yield of carbonyl compounds amounting to 95-96% of the propylene reacted. There was a 15% olefin conversion on passing a stoichiometric mixture of oxygen and cis and trans butylene-2 through this same catalyst at a velocity of 65 liters per liter of catalyst per hour.

The replacement of a hydrogen atom at a double bond by a methyl group decreases the reaction rate in the order: $CH_2{=}CH_2 > CH_3CH{=}CH_2 >$ cis-and trans $-CH_3CH{=}CHCH_3 > (CH_3)_2C{=}CHCH_3$. The stability of the complexes of divalent platinum with the olefins diminishes in this same order [11]. This justifies the presumption that the retardation of the reaction is related, at least in part, to a decrease in the constant for complex formation, since this quantity enters into the observed rate constant as a multiple.

Thus the over-all reaction in each of the investigated instances of oxidation is such that a π-complex is formed and decomposed in one step and the palladium atoms formed in decomposition are oxidized in another.

The experimental data which are available at the present time are insufficient to justify drawing any conclusions as to the mechanism of this reaction. It seems to us, however, that it would be useful to express certain hypotheses concerning this matter.

It can be presumed that the splitting away of a proton from the strongly polarized carbon atom of the olefin

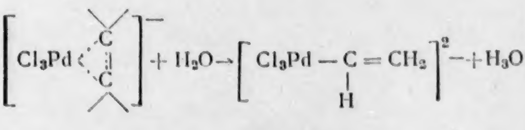

$$\left[Cl_3Pd \langle \begin{matrix} C \\ \| \\ C \end{matrix} \right]^- + H_2O \rightarrow \left[Cl_3Pd - \underset{\displaystyle H}{\underset{|}{C}} = CH_2\right]^{2-} + H_3O^+ \qquad (7)$$

is the first step in the breakdown of the π-complex, the complex being then converted into a metalloorganic compound which reacts with water, possibly through a five-membered complex according to:

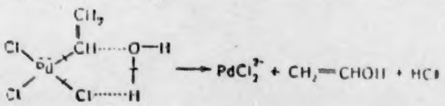

$$PdCl_2^{2-} \rightarrow Pd + 2Cl^-$$

$$CH_2 = CHOH \rightarrow CH_3CHO. \qquad (8)$$

It is to be noted in conclusion that certain olefins interact with palladium salts to give complex compounds whose syntheses and properties have been described earlier [12].

## LITERATURE CITED

[1] I. I. Moiseev, Dissertation, M. V. Lomonosov Institute for Fine Chemical Technology (Moscow, 1958).

[2] W. C. Zeise, Pogg. Ann. 21, 497 (1831).

[3] J. Chatt and L. A. Dunkanson, J. Chem. Soc. 2939 , (1953).

[4] M. E. Dyatkina, Zhur. Neorg. Khim. 3, 2039 (1958).

[5] J. S. Anderson, J. Chem. Soc. 971 (1934).

[6] F. C. Phillips, Z. Anorg. Chem. 6, 213 (1894).

[7] V. A. Sokolov, Analysis of Gases [in Russian] (Moscow-Leningrad, 1950) p. 122.

[8] S. C. Ogburn and W. C. Brastow, J. Am. Chem. Soc. 55, 1308 (1933).

[9] V. M. Latimer, Oxidation States of the Elements and Their Potentials in Aqueous Solutions [Russian translation] (IL, 1954).

[10] J. Smidt, W. Hafner, R. Jira, J. Sedlmeier, R. Sieber, R. Rüttinger and H. Kojer, Angew. Chem. 71, 176 (1959).

[11] A. D. Gel'man, Complex Compounds of Platinum with Unsaturated Molecules [in Russian] (Izd. AN SSSR, 1945), page 84.

[12] I. I. Moiseev, É. A. Fedorovskaya, and Ya. K. Syrkin, Zhur. Neorg. Khim. 4, 11, 2641 (1959).

# A STUDY OF THE RELATION BETWEEN THE DIFFUSION COEFFICIENT AND THE COVERAGE ON SORBENT GRAINS OF ARBITRARY FORM

**D. P. Timofeev**

**Institute of Physical Chemistry, Academy of Sciences, USSR**

**(Presented by Academician M. M. Dubinin October 20, 1959).**

**(Translation of: Doklady Akademii Nauk SSSR, Vol. 130, No.4, 1960, pp. 824-825)**

**Original article submitted October 19, 1959**

The coefficient of diffusion for movement of adsorbing gases in porous bodies varies on passing from one interval of coverage to another [1-3]. The study of this relationship, so vital to an understanding of the mechanism of the transfer of matter, is usually carried out with grains of regular geometrical form and for these, solutions of the differential diffusion equation are available. These grains are prepared either by powder pressing of such materials as lampblack and silica gel, or by breaking down sorbent grains of larger dimensions. The disadvantage of the first method is that pressed grains are not always capable of giving a good reproduction of the structure of a real porous body, and thus represent no more than a model of the latter, whereas there is always the possibility that results obtained by the second method will be distorted to a certain degree by clogging up the coarse pores with small sorbent particles during grain breakdown. Discussion is given below of the possibility of avoiding these indefinite effects from the preparation of experimental materials by studying the relation between the diffusion coefficient and the coverage of real sorbent grains.

Let it be supposed that grains of arbitrary form on which the adsorption corresponds to equilibrium at the concentration $c_1$ are placed in a gaseous medium whose concentration is held constant at $c_2$. Let it be also supposed that the working interval of concentrations is a narrow one within which the diffusion coefficient, D, and the Henry coefficient, $\Gamma = \partial a / \partial c$, are approximately constant (a is the amount of material adsorbed, and c is the concentration).

The equation for a nonstationary diffusion process in a uniform medium will here assume the forms

$$\frac{\partial\gamma}{\partial t} = \frac{D}{1+\Gamma}\Delta\gamma, \tag{1}$$

in which $\gamma = \frac{c - c_2}{c_1 - c_2}$ is the relative concentration, c is the concentration in the grain, a function of the coordinates and the time, and $\Delta$ is an operator whose form depends on the choice of coordinate system.

A supplementary condition for desorption will be that $\gamma = 1$ when $t = 0$.

Most cases will be such that $1 \ll \Gamma$ (an assumption to this effect is not essential to the further development), so that

$$\frac{\partial\gamma}{\partial t} = \frac{D}{\Gamma}\Delta\gamma. \tag{2}$$

The Fourier Method can be used to obtain a particular solution of Eq. (2) in the form of a product of two terms, one, v, depending on time and the other, u, depending on the coordinates, i.e.,

$$\gamma = Avu; \tag{3}$$

A being an arbitrary constant.

The functions v and u are related by an equation of the form

$$\frac{\Gamma}{D}\,\frac{v'}{v} = \frac{\Delta u}{u} = -k^2, \tag{4}$$

k being an arbitrary constant.

It follows from (4) directly that

$$v = e^{-k^2\tau}, \tag{5}$$

$\tau$ being equal to $Dt/\Gamma$. The integration constant has not been written down here since it can be included in the coefficient A.

Substitution of (5) into (3) will give

$$\gamma = Aue^{-k^2\tau} \tag{6}$$

The general solution can be expressed as a sum of particular solutions, i.e.,

$$\gamma = \sum_n A_n u_n e^{-k_n^2\tau}, \tag{7}$$

where the coefficients $A_n$ and $k_n$ are selected so as to satisfy the specified conditions. The form of the function $u_n$ is fixed by (4).

We will be interested subsequently in the amount of material adsorbed and will therefore pass to the mean relative concentration, $\bar{\gamma}$, a quantity which is found by integrating $\gamma$ over the volume of the grain, W:

$$\bar{\gamma} = \frac{1}{W}\int_W \sum_n A_n u_n e^{-k_n^2\tau}\,dW = \sum_n e^{-k_n^2\tau}\,\frac{1}{W}\int_W A_n u_n dW = \sum_n e^{-k_n^2\tau} B_n, \tag{8}$$

the value of $B_n = \frac{1}{W}\int_W A_n u_n dW$ being independent of time.

From the earlier assumption that $a = \Gamma c$, it follows that

$$\bar{\gamma} = \frac{a - a_2}{a_1 - a_2} = \sum_n B_n e^{-k_n^2\tau}, \tag{9}$$

a being the amount of material adsorbed at the time t, and $a_1$ and $a_2$, the equilibrium adsorptions at the respective concentrations $c_1$ and $c_2$.

Equation (9) corresponds to desorption. For adsorption, $a_2 > a_1$, and the equation takes the form

$$\frac{a - a_1}{a_2 - a_1} = 1 - \sum_n B_n e^{-k_n^2\tau}. \tag{10}$$

For a given value of the adsorption (desorption), $a = a_\xi$, and Eqs. (9) and (10) show that

$$\tau_\xi = \frac{Dt_\xi}{\Gamma} = \text{const}, \tag{11}$$

so that the relation

$$\frac{D_2}{D_1} = \frac{\Gamma_2}{\Gamma_1} \frac{t'_\xi}{t''_\xi}. \tag{12}$$

is valid for two different regions on the isotherm.

The quantities with index 1 refer to one of the these concentration intervals and the quantities with index 2, to the other.

Equation (12) makes it possible to find the relation between D and the degree of coverage for sorbent grains of any form. The values of the Henry constant for the various concentration intervals are obtained from the adsorption isotherm , while the time $t_\xi$ is given by direct kinetic measurements.

## LITERATURE CITED

[1] P. C. Carman and F. A. Raal, Proc. Roy. Soc., A 209, 38 (1951).

[2] P. C. Carman, The Flow of Gases through Porous Media (Oxford, 1956).

[3] K. Kammermeyer, Ind. and Eng. Chem. 50 , 697 (1958).

# THE IONIZATION OF TRIPHENYLCARBONYL IN SULFURIC ACID MEDIA CONTAINING ISOPROPYL ALCOHOL.

## MEASUREMENT OF THE DENO ACIDITY FUNCTION

S. G. Éntelis, G. V. Épple, and N. M. Chirkov

Institute of Chemical Physics, Academy of Sciences, USSR

(Presented by Academician N. N. Semenov August 7, 1959)

(Translation of: Doklady Akademii Nauk SSSR, Vol. 130, No. 4
1960, pp. 826-829)

Original article submitted August 4, 1959

The growing interest in the kinetics and mechanism of acid-catalyzed reactions in nonaqueous and mixed solvents has brought out the need for measurements of the acidity function in such systems. Special interest attaches to measurements in alcohol–water media. The very first quantitative work on this problem [1] showed that the relation between the acidity function $H_0$ and the medium composition was a complex one which could not be interpreted in terms of an alteration in the basicity of the medium, as was possible in other simple cases [2].

Both Bartlett and Tsvetkova have shown that the addition of isopropyl alcohol to $H_2SO_4 - H_2O$ [3,4] or $H_3PO_4 - H_2O$ [4] systems results in a much larger molar decrease in the acidity function $H_0$ than that which is obtained from the addition of water. The relation between the acidity function and the medium composition can be expected to be even more complex in the case of indicators such as triphenylcarbonyl [5] which ionize with the liberation of a molecule of water:

$$\mathrm{Ph_3COH} + \mathrm{H^+} \overset{K_{\mathrm{ArOH}}}{\rightleftarrows} \mathrm{Ph_3C^+} + \mathrm{H_2O}, \qquad K_{\mathrm{ArOH}} = \frac{a_{\mathrm{H^+}} a_{\mathrm{Ph_3COH}}}{a_{\mathrm{H_2O}} a_{\mathrm{Ph_3C^+}}} . \tag{1}$$

There is no data in the literature on the value of the acidity function $C_0$ for mixed solvents. Values of the $J_0$ function have been obtained for the $H_2SO_4 - H_2O - CH_3COOH$ system by Gold and Hawes [5].

Measurements have been made in the present work on the relation between the Deno acidity function, $C_0$, of sulfuric acid (43 -60% $H_2SO_4$) and the concentration of added isopropyl alcohol, working over the interval from 0.2 to 1.5 moles/liter at 40, 54, and 60°. Triphenylcarbonyl was used as an indicator in these measurements, the substance ionizing in acid medium according to Eq. (1) [5]. Values of the acidity function for solutions containing alcohol at various concentrations were calculated from the equation

$$C_{0_i} = \mathrm{p}K_{\mathrm{ArOH}} + \lg I_i, \tag{2}$$

$K_{\mathrm{ArOH}}$ being the equilibrium constant for the reaction in the $N_2SO_4 - H_2O$ system, and $I_i = \frac{[\mathrm{Ph_3COH}]_i}{[\mathrm{Ph_3C^+}]_i}$ the indicator ratio at the i-th alcohol concentration (the square brackets are used to designate concentrations). The indicator ratio $I_i$ was determined spectrometrically at $\lambda_{max}$ = 432 mμ, working in the region where adsorption is due to the ionized form alone; the Lambert-Beer Law shows that the measured value of the optical density, D, is equal to $\epsilon l[Ph_3C^+]$. The concentration of $Ph_3COH$ was evaluated from the material balance equation. The measurements were carried out with a SF-2M recording double-ray spectrophotometer, using a thermostatted cell 5 cm in length. Direct measurement of the equilibrium optical density, $D_i$, of the $H_2SO_4$—$H_2O$—i-$C_3H_7OH$ system proved to be a matter of difficulty since a pseudo first-order reaction takes place when isopropyl alcohol is added to a sulfuric acid solution of triphenylcarbonyl and the optical density diminishes with time. For this reason, the optical density $D_i$ was evaluated by extrapolating a straight line in a log D, t graph to zero time (t = 0) (see Fig. 1).

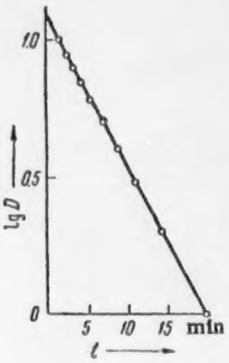

Fig. 1. Graph for determining the initial optical density at t = 40°; 50.96% $H_2SO_4$ and $C_{alc}$ = 0.5 moles/liter.

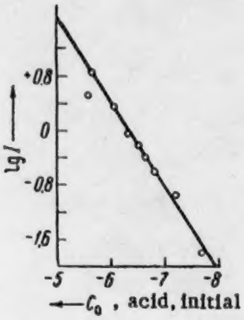

Fig. 2. Graph for determining pK for triphenylcarbonyl at t = 40°.

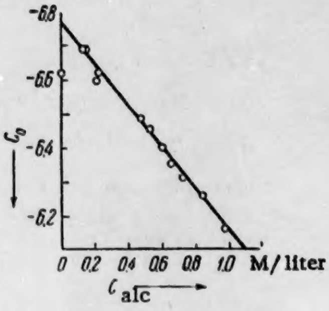

Fig. 3. Relation between the acidity function $C_0$ and the concentration of added alcohol at t = 40°; 50.46% $H_2SO_4$.

TABLE 1

The Relation between the Indicator Ratio and the $H_2SO_4$ Concentration

| t = 30° | | | t = 40° | | | t = 50° | | | t = 60° | | |
|---|---|---|---|---|---|---|---|---|---|---|---|
| $H_2SO_4$, % | $C_0$ | lg I | $H_2SO_4$, % | $C_0$ | lg I | $H_2SO_4$, % | $C_0$ | lg I | $H_2SO_4$, % | $C_0$ | lg I |
| 43,22 | —5,37 | +1,416 | 44,35 | —5,55 | +0,524 | 46,78 | —5,96 | +0,482 | 43,19 | —5,24 | +0,776 |
| 45,05 | —5,65 | +0,78 | 44,90 | —5,64 | +0,845 | 47,80 | —6,13 | +0,086 | 43,29 | —5,27 | +0,627 |
| 46,95 | —6,00 | +0,495 | 47,28 | —6,05 | +0,356 | 48,72 | —6,29 | —0,104 | 45,10 | —5,67 | +0,491 |
| 48,22 | —6,21 | +0,182 | 48,66 | —6,29 | —0,04 | 50,43 | —6,59 | —0,414 | 47,33 | —6,04 | +0,160 |
| 49,17 | —6,38 | +0,083 | 49,90 | —6,51 | —0,213 | 52,01 | —6,89 | —0,746 | 49,42 | —6,40 | —0,20 |
| 50,66 | —6,65 | —0,286 | 50,48 | —6,62 | —0,396 | 53,47 | —7,17 | —1,062 | 51,44 | —6,77 | —0,60 |
| 52,06 | —6,92 | —0,782 | 51,46 | —6,81 | —0,599 | 54,50 | —7,38 | —1,242 | 52,14 | —6,90 | —0,744 |
| 53,89 | —7,31 | —1,194 | 53,42 | —7,19 | —0,942 | 55,60 | —7,61 | —1,638 | 53,28 | —7,11 | —0,895 |
| 55,62 | —7,67 | —1,95 | 55,70 | —7,67 | —1,773 | | | | 54,19 | —7,27 | —0,985 |
| 56,72 | —7,95 | | | | | | | | 55,02 | —7,47 | —1,477 |
| 57,59 | —8,16 | | | | | | | | 56,10 | —7,70 | —1,645 |
| | | | | | | | | | 57,34 | —7,97 | |
| pK = — 6,38 | | | pK = — 6,31 | | | pK = — 6,21 | | | pK = — 6,17 | | |

An evaluation of $I_i$ for a system containing alcohol must take account of the alteration in the specific gravity of the sulfuric acid which results from addition of the alcohol. Here, we have made use of the equation proposed in the paper of V. I. Tsvetkova [4]:

$$d_i = d_0(1 - 0{,}054\,C_{alc}),$$

in which $d_0$ is the initial specific gravity of the sulfuric acid, $d_1$ is the specific gravity of the acid containing isopropyl alcohol, and $C_{alc}$ is the alcohol concentration in gram-moles per 1000 g of the initial acid. We have used values obtained in the $H_2SO_4$–$H_2O$ system without added i-$C_3H_7OH$ in calculating $C_0$ from Eq. (2), considering $pK_{ArOH}$ to be practically constant over the investigated interval of isopropyl alcohol concentrations ranging from 0.2 to 1.5 moles/liter. Some values of $pK_{ArOH}$ at elevated temperatures could not be found in the literature and these were determined in a special series of experiments at 30, 40, 50, and 60°. The values of $pK_{ArOH}$ were obtained graphically from the log I, $C_0$ relation at log I = 0, using Eq. (2). Table 1 shows the dependence of log I on $C_0$, and values of $pK_{ArOH}$ at 30, 40, 50, and 60°. Figure 2 gives a graph of this relation at 40°. The slope of the straight line is close to unity.

TABLE 2

Temperature Dependence of the Acidity Function, $C_0$, of the Medium and Its Variation with the Alcohol Concentration

| $C_{alc}$, M/liter | $C_0$ | $C_{alc}$, M/liter | $C_0$ | $C_{alc}$, M/liter | $C_0$ | $C_{alc}$, M/liter | $C_0$ |
|---|---|---|---|---|---|---|---|
| $t = 40°$ | | | | | | | |
| $C_{H_2SO_4}$ = 48,18% | | $C_{H_2SO_4}$ = 50,46% | | $C_{H_2SO_4}$ = 51,46% | | $C_{H_2SO_4}$ = 53,42% | |
| 0 | −6,21 | 0 | −6,62 | 0 | −6,81 | 0 | −7,19 |
| 0,16 | −6,01 | 0,13 | −6,69 | 0,07 | −6,83 | 0,10 | −7,16 |
| 0,32 | −6,01 | 0,16 | −6,69 | 0,096 | −6,84 | 0,14 | −7,18 |
| 0,43 | −5,84 | 0,21 | −6,60 | 0,19 | −6,79 | 0,144 | −7,19 |
| 0,59 | −5,81 | 0,22 | −6,62 | 0,195 | −6,81 | 0,19 | −7,09 |
| 0,69 | −5,79 | 0,48 | −6,49 | 0,21 | −6,69 | 0,45 | −7,02 |
| 0,71 | −5,61 | 0,53 | −6,46 | 0,250 | −6,77 | 0,47 | −6,96 |
| $C_{H_2SO_4}$ = 49,30% | | 0,60 | −6,40 | 0,28 | −6,77 | 0,48 | −7,02 |
| 0 | −6,41 | 0,65 | −6,35 | 0,31 | −6,71 | 0,83 | −6,87 |
| 0,31 | −6,01 | 0,715 | −6,31 | 0,44 | −6,73 | $C_{H_2SO_4}$ = 58,60% | |
| 0,33 | −6,10 | 0,84 | −6,26 | 0,75 | −6,38 | 0 | −8,39 |
| 0,36 | −6,13 | 0,97 | −6,16 | 0,76 | −6,45 | 0,19 | −8,09 |
| 0,46 | −6,14 | 1,99 | −5,93 | 1,38 | −6,09 | 0,80 | −7,94 |
| 0,68 | −6,01 | | | | | | |
| $t = 54°$ | | | | $t = 60°$ | | | |
| $C_{H_2SO_4}$ = 46,76% | | $C_{H_2SO_4}$ = 51,57% | | $C_{H_2SO_4}$ = 44,24% | | $C_{H_2SO_4}$ = 49,37% | |
| 0 | −5,94 | 0 | −6,79 | 0 | −5,46 | 0 | −6,40 |
| 0,30 | −5,78 | 0,305 | −6,45 | 0,25 | −5,24 | 0,23 | −6,25 |
| 0,40 | −5,66 | 0,49 | −6,44 | 0,36 | −5,34 | 0,35 | −6,19 |
| 0,51 | −5,66 | 0,60 | −6,31 | 0,37 | −5,27 | 0,37 | −6,195 |
| 0,66 | −5,50 | $C_{H_2SO_4}$ = 52,34% | | 0,40 | −5,28 | 0,44 | −6,12 |
| $C_{H_2SO_4}$ = 49,55% | | 0 | −6,95 | 0,48 | −5,26 | 0,46 | −6,14 |
| 0 | −6,42 | 0,39 | −6,78 | 0,49 | −5,25 | 0,47 | −6,13 |
| 0,29 | −6,21 | 0,53 | −6,39 | $C_{H_2SO_4}$ = 46,55% | | 0,48 | −6,13 |
| 0,46 | −6,13 | 0,49 | −6,66 | 0 | −5,91 | $C_{H_2SO_4}$ = 51,26% | |
| 0,46 | −6,15 | 0,55 | −6,51 | 0,18 | −5,78 | 0 | −6,74 |
| 0,60 | −5,99 | 0,70 | −6,57 | 0,29 | −5,81 | 0,28 | −6,62 |
| 0,63 | 6,00 | $C_{H_2SO_4}$ = 54,14% | | 0,40 | −5,73 | 5,38 | −6,50 |
| $C_{H_2SO_4}$ = 50,70% | | 0 | −7,30 | 0,53 | −5,63 | 0,51 | −6,55 |
| 0 | −6,65 | 0,29 | −7,18 | 0,54 | −5,66 | | |
| 0,31 | −6,42 | 0,51 | −7,16 | $C_{H_2SO_4}$ = 46,88% | | | |
| 0,52 | −6,35 | 0,68 | −7,24 | 0 | −5,97 | | |
| 0,64 | −6,31 | | | 0,49 | −5,78 | | |
| 0,77 | −6,23 | | | 0,51 | −5,76 | | |
| | | | | 0,53 | −5,76 | | |

The values of the acidity function, $C_0$, at 30, 40, 50, and 60° which are needed for an evaluation of $pK_{ArOH}$ are lacking in the literature. These evaluations have been carried out through the well-known equation [3]:

$$C_0 = H_0 + \lg a_{H_2O} + \lg \frac{f_{ArC^+}}{f_{ArOH_2^+}}, \qquad (3)$$

in which $a_{H_2O}$ is the thermodynamic activity of the $f_{ArC^+}/f_{ArOH_2^+}$ is the ratio of the activities of the carbonyl ion and the protonized carbonyl. Values of $H_0$ at various temperatures are needed for calculations based on Eq. (3) and these were taken from [6]. Values of $a_{H_2O}$ for the $H_2SO_4$–$H_2O$ system were calculated from tables of data on the vapor pressure of water above sulfuric acid (p) and pure water ($p_S$) [9]. The last member of Eq. (3) was assumed to be independent of temperature. Values of this term at 25° and various $H_2SO_4$ concentrations were taken from the paper of Deno [7].

The data of Table 1 were used to evaluate the heat of protonization of triphenylcarbonyl in the $H_2SO_4$–$H_2O$ system and the entropy change accompanying the process, the respective values being $\Delta H = 3280 \pm 100$ kcal/mole and $\Delta S = -18.4 \pm 0.10$ cal/mole · deg; from these it follows that

$$2{,}3\,R\,\mathrm{p}K_{\mathrm{ArOH}} = -\frac{3280}{T} - 18{,}4.$$

Values of the acidity function $C_0$ of sulfuric acid solutions of various concentrations with added isopropyl alcohol are shown in Table 2, these having been calculated from Eq. (2).

The accuracy of these results does not exceed 20% and the error is 100% in the region of 60% $H_2SO_4$ where the value of $C_{Ph_3COH}$ is quite low, but the following regularities stand out quite clearly nevertheless.

The acidity function $C_0$ resembles $H_0$ in that it diminishes according to a linear law as the concentration of alcohol in the system is increased (Fig. 3)

$$\Delta C_0 = C_{0i} - C_0 = nC_{alc}. \tag{4}$$

This relation is more clear-cut than that for $H_0$. The value of n diminishes with a rise in the initial concentration of the acid and with an increase in the temperature, Fig. 4 showing a relation of the form

$$n = a(C_0 + A), \tag{5}$$

($C_0$ refers to the initial concentration of the $H_2SO_4$) to be valid at any one temperature.

Thus a = 0.304 at 40° and A = 8.69, a = 0.281 at 54° and A = 7.93, and a = 0.228 at 60° and A = 7.60. The dependence of n on $C_0$ at these three temperatures is shown in Table 3, while the relation for t = 40° is given in Fig. 4.

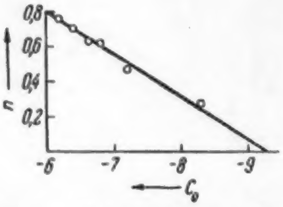

Fig. 4. Relation between the parameter n and the acidity function $C_0$ of the initial acid at t = 40°.

TABLE 3

The Relation between the Parameter n and the Acidity $C_0$ of the Initial Acid

| $t = 40°$ | | $t = 54°$ | | $t = 60°$ | |
|---|---|---|---|---|---|
| $C_0$ | $n$ | $C_0$ | $n$ | $C_0$ | $n$ |
| −6,21 | 0,755 | −5,94 | 0,565 | −5,46 | 0,496 |
| −6,41 | 0,700 | −6,42 | 0,455 | −5,91 | 0,380 |
| −6,62 | 0,626 | −6,65 | 0,334 | −5,97 | 0,320 |
| −6,81 | 0,610 | −6,79 | 0,310 | −6,40 | 0,53 |
| −7,19 | 0,456 | −6,95 | 0,285 | −6,74 | 0,21 |
| −8,39 | 0,247 | | | | |

The alteration which has been observed in the relation between $C_{0i}$ and $C_{alc}$ over the working interval of temperatures and $H_2SO_4$ concentrations is consistent with the hypothesis that the principal effect of the added alcohol on the acidity of the acid-water system comes from a breakdown in the hydrogen bonding in the water molecules with a resultant increase in their basicity [1, 8, 10]. In such a case, an elevation of temperature should act in the same manner as an increase in the acid concentration, decreasing the degree of association of the water molecules and thereby serving to diminish the effect of the alcohol in altering the solvent structure and its basicity. This theoretical prediction finds its full support in the data which have been obtained here, n diminishing with an increase in the $H_2SO_4$ concentration and the parameters a and A decreasing with the temperature. The effect of the alcohol on the thermodynamic activity of the un-ionized water accounts for the different behavior of $C_0$ and $H_0$ when alcohol is added to an acid [3,4]; the alcohol which is added to the $H_2SO_4$–$H_2O$ system binds a portion of the acid, thereby liberating water and increasing the value of $a_{H_2O}$. The rise in $a_{H_2O}$ leads to a diminution in $C_0$.

## LITERATURE CITED

[1] E. A. Braude, J. Chem. Soc. 1971 (1948).

[2] S. G. Entelis and N. M. Chirkov, Zhur. Fiz. Khim. 31, 1311 (1957).

[3] P. D. Bartlett and I. D. McCollum, J. Am. Chem. Soc. 78, 1441 (1956).

[4] V. I. Tsvetkova, Candidate's Dissertation, Institute of Chemical Physics, AN SSSR.

[5] V. Gold and B. W. J. Hawes, J. Chem. Soc. 2102 (1951).

[6] A. I. Gel'bshtein, G. G. Shcheglova, and M. I. Temkin, Zhur. Neorg. Khim. 1, 506 (1956).

[7] N. C. Deno, J. J. Jaruzelskii and A. Schriesheim, J. Am. Chem. Soc. 77, 3044 (1955).

[8] G. Bates and G. Schwarzenbach, Helv. Chim. Acta 38, 699 (1955).

[9] Handbook of Chemistry, 3 [in Russian] (1952) p.234.

[10] A. G. Mitchell and W.F.K. Wynn-Jones, Disc. Farad. Soc. 15, 161 (1953).

# THE LOW-VELOCITY DETONATION OF LIQUID EXPLOSIVES

L. G. Bolkhovitinov

Physicochemical Institute, Academy of Sciences, USSR.

(Presented by Academician V. N. Kondrat'ev, October 9, 1959).

(Translation of: Doklady Akademii Nauk, Vol. 130, No.5,
1960, pp. 1044-1046)

Original article submitted October 5, 1960.

It is known that in some liquid explosives (nitroglycerin, methylnitrate), besides the normal detonation mechanism with a velocity equal to 7-8 km/sec corresponding to their thermodynamic characteristics, there may occur a mechanism to which corresponds an expansion velocity of not more than 1.7-2.2 km/sec [1-4]. The essential difficulty in the explanation of this phenomenon lies in the fact that at a low velocity of the pressure wave, viz. at a velocity near to that of sound (the latter being about 1.5 km/sec), the temperature increase at the compression in the wave is small and cannot initiate the chemical reaction in the substance.

Indeed, an estimate of the temperature increase from the relation

$$\Delta T \cong (D - c)^2 / 2c_v \qquad (1)$$

gives for liquids with $c \cong c_0 = 1.5$ km/sec, $c_V = 0.3$ cal/g-deg, and D=2 km/sec a value $\Delta T \cong 100°$.

Therefore, one generally accepts the assumption of Bowden [5] that the reaction starts at trapped gas bubbles which are heated far more strongly by the compression than the bulk of the explosive. In this it is assumed that the low detonation velocity is connected with the incomplete decomposition of the substance as a result of the dispersion of the reaction products. This assumption, however, does not explain the fact that the low detonation velocity, just like the normal velocity, is practically independent of the diameter of the charge, while the expansion time of the detonation products is connected significantly with the diameter of the charge. Therefore, it also remains difficult to understand that one does not observe detonation mechanisms to which the velocities of 3-7 km/sec would correspond.

We think that this phenomenon may be very simply explained if one uses as starting point the experimentally ascertained fact that the passing of the pressure wave through the substance may be attended by a phase transition [6, 7]. Crystallization is a phase transition which may attend the passing of the pressure wave through liquid explosives. Since the phase transition cannot take place inside the pressure-wave front, whose width is not more than a few intermolecular distances, the change of the liquid into the crystalline state must occur in some zone lying behind the pressure-wave front and having a width determined by the crystallization rate of the explosive.

The possibility of the forming of such a zone depends on the relative location of the phase equilibrium curve and the curve T=f(Δp) which describes the dependence of the temperature increase behind the pressure-wave front on the pressure jump. As an illustration, we give in Fig. 1 the phase equilibrium curves of two liquids (1 and 2) and their joint curve T=f(Δp) (3). It is obvious that a pressure increase to a value $\underline{p}$, $p_a < p < p_b$, must cause the appearance of a crystallization zone in liquid 1, while in liquid 2 a crystallization zone is not produced at any intensity of the pressure wave.

Let us consider the change of the pressure $\underline{p}$, of the specific volume $v \equiv \frac{1}{\rho}$ , and of the flow rate $\underline{w}$ at each side of the crystallization zone. We indicate the values in the unperturbed substance, in the pressure-wave front, and in the plane where the phase transition is completed by the indexes 0, 1, and 2, respectively. The balances give two systems of equations:

$$\rho_0 D = \rho_1 (D - w_1); \tag{2}$$

$$\rho_0 w_1 D = p_1; \tag{3}$$

$$H_1 - H_0 = p_1 \frac{v_1 + v_0}{2} \tag{4}$$

and, correspondingly,

$$\rho_0 D = \rho_2 (D - w_2); \tag{5}$$

$$\rho_0 w_2 D = p_2; \tag{6}$$

$$H_2 - H_0 = p_2 \frac{v_2 + v_0}{2} \tag{7}$$

(we assume that $p_1 \gg p_0$ ). From (4) and (7) it follows that

$$2 (H_2 - H_1) = v_0 (p_2 - p_1) + p_2 v_2 - p_1 v_1. \tag{8}$$

The value $p_2$-$p_1$ is found from (2), (3), (5), and (6):

$$p_2 - p_1 = \rho_0^2 D^2 (v_2 - v_1). \tag{9}$$

If the change of $\underline{v}$ caused by the pressure decrease from $p_1$ to $p_2$ is neglected in comparison with the change in volume caused by the phase transition, then it may be supposed that $v_2 - v_1 = \Delta v_{ph}$, where $\Delta v_{ph}$ is equal to the jump in volume at the phase transition. Modifying (8) to the form

$$2 (H_2 - H_1) = v_0 (p_2 - p_1) + v_1 (p_2 - p_1) - p_1 (v_2 - v_1)$$

and using (2), (3), and (9) we get

$$(H_2 - H_1) = \frac{\Delta v_{ph} p_1}{v_0^2} D^2.$$

Supposing that the change in enthalpy at the transition from state 1 to state 2 is simply equal to the latent heat of melting $\lambda$, we obtain from the preceding equation

$$D = \left[ \frac{\lambda v_0^2}{\Delta v_{ph} v_1} \right]^{1/2}. \tag{10}$$

If one draws in the p-v plane the Hugoniot adiabat (see Fig. 2) for the original substance, then the state at point A corresponding to compression in the strong wave is realized in a detonation with the normal velocity $D_N$. Point B represents state 2 defined above, so that the slope of line OB is fixed and, therefore, the value of the low velocity $D_M$ is determined by relation(10). If it is assumed that the crystallization zone is followed by a chemical-reaction zone with a normal structure (which is only true in so far as we may neglect the chemical reaction in the first zone), then the pressure in the Chapman-Jouguet plane must be equal to 0.5 $p_2$. To this corresponds in the p-v diagram (curve 1) a tangent point of the straight line OB not with the isentrop of the reaction products 2, but with some curve 3 representing the isentrop of the substance when it has only partially reacted. In other words, the low detonation velocity may only be realized when the expansion time of the reaction products is comparable with the chemical-reaction time.

Since for a stationary propagation of the detonation wave it is necessary to satisfy the well-known condition of Yu. B. Khariton $\tau \leq \theta$, where $\tau$ represents the chemical-reaction time (more exactly, the time needed to release the energy necessary to support a stationary wave) and $\theta$ the expansion time of the reaction products, the appearance of a crystallization zone behind the pressure wave causes the dispersion time to increase sharply and, therefore, the condition of Yu. B. Khariton may be satisfied also for larger $\tau$. This follows from the fact that the sound velocity in a two-phase system decreases in comparison with the sound velocity in the liquid [8]. Thus, it cannot be decided whether the temperature increase to some value T is produced by direct compression in the pressure wave (without appearance of a crystallization zone) or by means of the mechanism proposed by us. In the first case, the expansion of the substance starts at once behind the pressure wave, but, in the second case, it does not start until the difference between the solid and the liquid phase vanishes as a result of the chemical reaction. This, in our opnion, also explains the stability of detonations with low velocity, as contrasted with mechanisms with higher expansion velocities but not attended by crystallization.

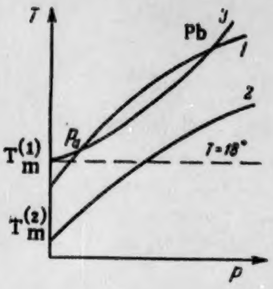

Fig. 1. Possible correlations between the phase-equilibrium curves (1 and 2) and the state of the substance behind the pressure-wave front (3).

As an example we consider a low-velocity detonation in nitroglycerin ($T_m = 13.2°$) for which the heat of fusion and the volume change at freezing are known [9]. Substituting in (10) the values $\lambda = 33.2$ cal/g, $v_0 = 0.62$ cm$^3$/g, and $\Delta v_{ph} = 0.05$ cm$^3$/g, we find that upon changing $v_1$ from $v_0$ to $0.5\ v_0$ the velocity of the stationary pressure wave changes from 1310 to 1830 m/sec. Since we used values of $\lambda$ and $\Delta v_{ph}$ measured at atmospheric pressure and the crystallization takes place at pressures changing from $p_1$ to $p_2$, the velocity value obtained is (up to 30%) too low, because at higher pressures the heat of fusion increases and $\Delta v_{ph}$ decreases [10]. Taking this into account, we may consider the value of D calculated by us to be in good agreement with the experimental results.

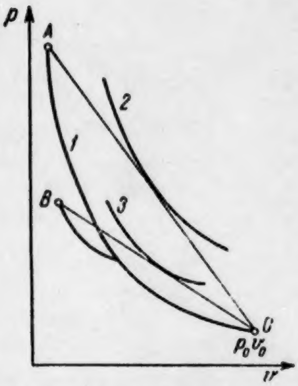

Fig. 2. A p-v diagram for detonations with normal and with low velocity.

If it is assumed that the equation of the isentrops for the products of an incompletely decomposed explosive may be described in the form proposed by L. D. Landau and K.P. Stanyukovich : $pv^n$ = constant, where the value of n may be taken equal to 3, then we deduce from the condition $p_2 = 2\rho_0 D^2/(n+1)$ that at D = 1700 m/sec $p_2$ = 24000 atm and $p_1$ = 19500 atm. At a wave velocity D = 2000 m/sec we deduce correspondingly that $p_2$ = 32000 atm and $p_1$ = 26000 atm. An estimate of the phase-transition temperature at these pressures from the Clausius-Clapeyron equation or from the analogy with Bridgman's experimental data for high-molecular organic compounds gives a value of 450-600° for the temperature in the crystallization zone. In fact, an increase in the temperature of the explosive to the said value may be achieved when the chemical reaction proceeds at the required rate.

## LITERATURE CITED

[1] Yu. B. Khariton and S. B. Ratner, Doklady Akad. Nauk SSSR 41, 293 (1943).

[2] S. B. Ratner, Doklady Akad. Nauk SSSR 42, 265 (1944).

[3] R. Kh. Kurbangalina, Zhur. Fiz. Khim. 22, 49 (1948).

[4] J. Taylor, Detonation in Condensed Explosives, Oxford, 1952.

[5] F. P. Bowden and A. D. Yoffe, Initiation and Growth of Explosion in Liquids and Solids [Russian translation] (IL, 1955).

[6] D. Bancroft et al., J. Appl Phys., 27, 291 (1956).

[7] G. A. Adadurov and A. N. Dremin, Doklady Akad. Nauk SSSR, 128 (1959).*

[8] L. D. Landau and E. M. Lifshits, Mechanics of Compact Mediums, 1953 [In Russian].

[9] F. Naoum, Nitroglycerin [In Russian] (1934).

[10] P. W. Bridgman, Phys. Rev., 3, 126, 153 (1914); 6, 1, 94 (1915).

---

*Original Russian pagination. See C. B. translation.

# KINETIC INVESTIGATION INTO THE ELECTROCHEMICAL REDUCTION OF CHROMIC ACID ON A ROTATING DISC ELECTRODE

E. Budevskii and S. Toshev

Sofia State University, Sofia, Bulgaria

(Presented by Academician A. N. Frumkin, October 7, 1959)

(Translation of: Doklady Akademii Nauk SSSR, Vol. 130, No.5, 1960, pp. 1047-1050).

Original article submitted September 28, 1959.

Polarization curves for the electrochemical reduction of chromic acid show that the reduction proceeds across some phases ,depending upon the electrode potential. In the first phase of the electrochemical reduction— the range with two maximums in the polarization curve — almost 100% of the chromic acid is reduced to trivalent chromium [1]. At a more negative potential there proceed three processes on the cathode: a) reduction to trivalent chromium, b) reduction to metallic chromium, and c) evolution of hydrogen.

Obviously, the mechanism of chromic acid reduction is complicated. The first step in its study has been made, especially in recent times, by numerous investigations of the first phase [2-5]. The result of these investigations may be summed up as follows:

1. Chromic acid is reduced only in the presence of sulfuric or other added acid. In the absence of such an acid only hydrogen is evolved.

2. The current density $i_{max}$ in the first maximum of the polarization curve is proportional to the concentration of sulfuric or other added acid [2,4,5].

3. The mixing conditions apparently exert considerable influence on the value of $i_{max}$. Thus, it was found by Vagramyan that at a vertically stirred electrode the maximum current is proportional to the square root of the number of electrode strokes per minute.

These facts show that the sulfate ions take some part in the process at the electrode during the reduction of chromic acid and that the rate of this process depends upon the diffusion rate of sulfate ions to the electrode. The part played by the sulfate ions is explained in various ways: Müller [6] thought that in the absence of sulfuric or other added acid a thin insulating layer of basic trivalent chromium salts is formed on the electrode. Sulfuric acid dissolves this layer. On the other hand, Vagramyan [2] assumes that chromic acid ions cannot be directly reduced at the electrode. The reduction is only possible in the presence of sulfuric or other added acid with which the chromic acid forms complexes. An intermediate position between these extreme viewpoints is taken by Gerischer [7], and Reinkowsky and Knorr [8], who suggest that the layer which blocks the electrode surface and consists of intermediary products of the chromic acid reduction forms complexes with sulfuric acid which are further reduced to complexes of trivalent chromium.

All three of these assumptions show that the presence of sulfuric acid is necessary to let the current through, but not that the current is limited by the diffusion rate of sulfate ions. To effect such a limiting it is necessary that sulfate ions be consumed in the total electrode process. Such a consumption may be caused by forming complexes of the reduction products with sulfuric acid. This consideration does not require the complex to be very stable. It is sufficient that its mean lifetime is longer than the time it stays in the diffusion layer. Such an assumption is entirely acceptable, since recently there have also been discovered very stable complexes of sulfuric acid with trivalent chromium [3, 9].

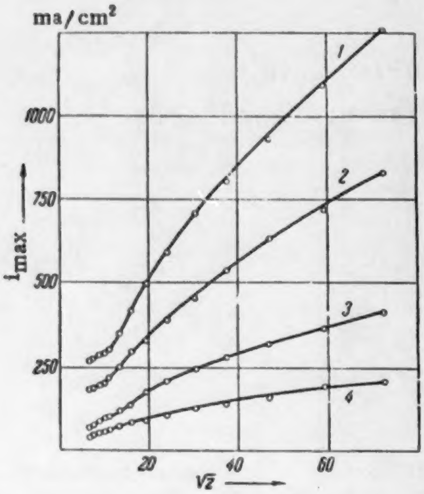

Fig. 1. The dependence of $i_{max}$ (i in ma/cm²) upon $z^{1/2}$ (z in cycles/min) at 200 g/liter $CrO_3$ and 8.0 (1), 4.0 (2), 2.0 (3), 1.0 (4) g/liter $H_2SO_4$. t = 25°C.

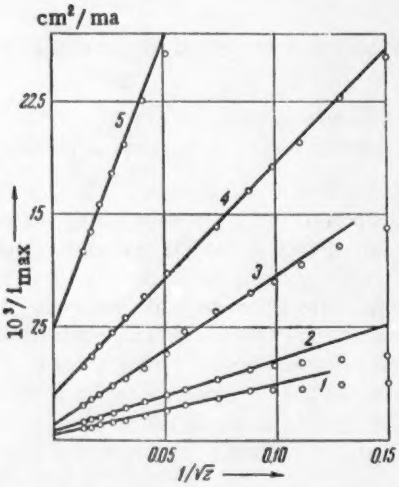

Fig. 2. The dependence of $1/i_{max}$ (i in ma/cm²) upon $z^{-1/2}$ (z in cycles/min) at 200 g/liter $CrO_3$ and 8.0 (1), 4.0 (2), 2.0 (3), 1.0(4), 0.48 (5) g/liter $H_2SO_4$. t = 25%.

In order to elucidate the mechanism and the kinetics of the chromic acid reduction it is necessary to choose diffusion conditions which determine the course of the process as specifically as possible. The rotating disc electrode enables one to do just that. Obviously, the investigations of Matulis and Mitskus [4] uniquely meet these requirements. These authors, however, performed the electrolysis at a fixed current density, which is not the most suitable condition for this kind of experiment. The results of our investigations have been obtained for the reduction of $CrO_3$ at a fixed potential on a rotating disc electrode made of gold. The solution contained 200 g/liter chromic acid and from 0.5 to 8 g/liter sulfuric acid. A thermostat kept the temperature at three levels: 10,25, and 45°.

The dependence of the maximum current density upon the revolution rate z of the electrode is shown in Fig.1. From the graph it is obvious that the dependence of $i_{max}$ upon $z^{1/2}$ is much more complicated than may be expected when the current is limited by diffusion only. At high revolution rates there is observed a current density which is smaller than would correspond to linear dependency, and this may be explained by the occurrence of an additional limiting of the current density. Such a limiting may be caused by some process which precedes the electrode process itself (for instance, the dissolution of the surface layer, the formation of electroactive complexes, etc.). Under conditions where the rate of this process is of the first order with respect to the concentration of the sulfate ions, one may use the following equation for the calculation of the current density

$$\frac{1}{i} = \frac{1}{i_d} + \frac{1}{i_k}, \qquad (1)$$

where $i_d$ represents the value of the current limit determined by the diffusion rate alone and $i_k$ the value determined by the kinetics of the preceding reaction alone [10].

Keeping in mind that the diffusion current $i_d$ is proportional to $z^{1/2}$ according to the equation of Levich [11] and that $i_k$ (the so-called kinetic current) does not depend upon the revolution rate, we find from equation (1) that $1/i$ must be a linear function of $z^{-1/2}$. It is obvious from Fig. 2 that this dependency is neatly satisfied, in any case, at high revolution rates of the electrode. The slope of this line makes it possible to determine $i_d$ at z = 1 and the intercept gives the value of $i_k$.* In Fig. 3 is shown how the kinetic current (calculated in the said way) depends upon the sulfuric acid concentration. In the same graph is also given the dependence of the diffusion current at z = 1 upon the sulfate ion concentration. It is obvious that both the kinetic and the diffusion current are proportional to the concentration of the sulfate ions in the electrolyte. It is interesting to note that, if one uses in the equation of Levich a value of D varying from 1 to $3 \cdot 10^{-5}$ cm²/sec, one obtains for n (the number of electrons exchanged per sulfuric acid molecule) a value varying from 12 to 24. In the reduction, however, only $CrO_3$ participates, so that three electrons are consumed per $CrO_3$ molecule ($Cr^{6+} \rightarrow Cr^{3+}$). Consequently, on the average,8 to 4 chromic acid molecules are reduced in the interaction of one sulfuric acid molecule with the blocking layer.

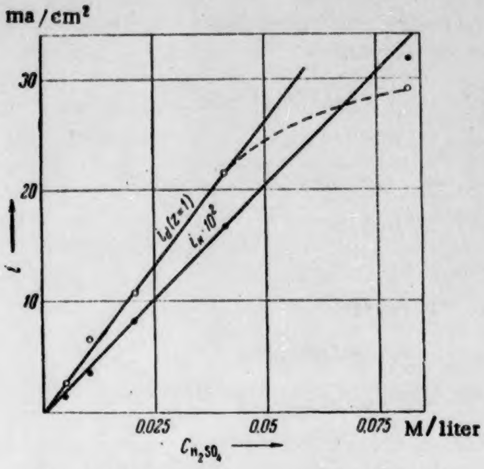

Fig. 3. The dependence of $i_d(z=1)$ and $i_k$ upon the concentration of $H_2SO_4$.

The dependence of the maximum current upon the temperature has also been investigated. The values obtained at 10, 25, and 40° are given in Fig. 4. The coordinates in the graph are: 1/i and $z^{-1/2}$. As has been remarked before, the intercept is equal to the inverse of the kinetic current. It is obvious from the graph that the scattering of the kinetic-current values lies within the accuracy of the measurements and that the kinetic current does not substantially depend upon the temperature. The dependence of the diffusion current upon the temperature, as obtained from the slope of the straight lines in Fig. 4, corresponds to a temperature coefficient $\frac{1}{i}\frac{di}{dt} = 0.019$. This value is in good agreement with the value which may be expected according to the convective diffusion equation of Levich.

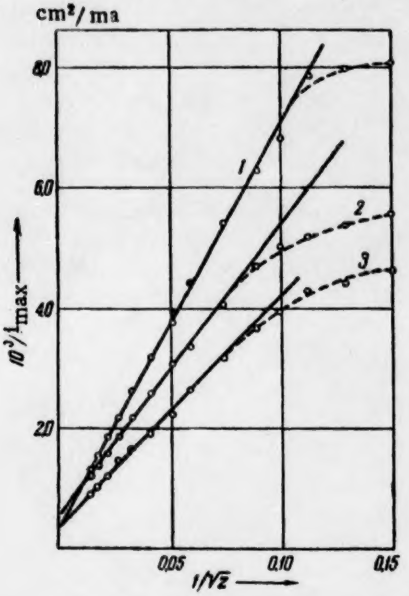

Fig. 4. The dependence of $1/i_{max}$ (i in ma/cm²) upon $z^{-1/2}$ (z in cycles/min) at 200 g/liter $CrO_3$ and 4.0 g/liter $H_2SO_4$. t=10° (1), 25° (2), 40° (3).

The fact that the current density is limited by diffusion shows that sulfate ions are consumed at the surface of the electrode. This may be effected by the formation of complexes from the reaction products and the sulfate ions. These complexes must be sufficiently stable so that they do not decompose during the time they stay in the diffusion layer. In this case the sulfate ions must leave the layer in the form of complexes.

At low revolution rates, however, the diffusion processes are highly retarded and the complexes formed may decompose before they leave the diffusion layer. The sulfate ions thus released, of course, again take part in the diffusion process and the current density will be higher than corresponds to a normal diffusion current. Thus, at low revolution rates, one must observe a catalytic current which in the graph of i versus $z^{1/2}$ gives a curvature analogous to the curvature observed experimentally (Fig. 1).

---

* A similar analysis of the correlation between the current density and the number of revolutions has been given by A. N. Frumkin and co-workers at an investigation of the ionization kinetics of $H_2$ and $C_{12}$ on a platinum electrode [12, 13]

## LITERATURE CITED

[1] A. T. Vagramyan, D. N. Usachev, and G. I. Chervova, Collection: Theory and Practice of Electrolytic Chromium-Plating (Academy of Sciences SSSR Press, 1957) [In Russian].

[2] A. T. Vagramyan and D. N. Usachev, Zhur. Fiz. Khim. 32, 1900 (1958).

[3] M. Frey and C. A. Knorr, Zs. f. Elektrochem., 60, 1093 (1956).

[4] Yu. Yu. Matulis and M. A. Mitskus, Tr. Akad. Nauk Lith. SSR, ser. B, 1, 39 (1958).

[5] H. Feigl, C. A. Knorr, Zs. f. Elektrochem., 63, 239 (1959).

[6] E. Müller, Zs. f. Elektrochem., 45, 243 (1939).

[7] H. Gerischer, M. Käppel, Zs. f. Elektrochem., 61, 463 (1957).

[8] D. Reinkowsky, C. A. Knorr, Zs. f. Elektrochem., 58, 709 (1954).

[9] R. L. Sass, S. L. Eisler, Plating, 41, 497 (1954); Chem. Zbl., 126, 4446 (1955).

[10] E. Budevski, Izvest. Bulg. Akad. Nauk, ser. phys. 5, 89 (1955).

[11] V. G. Levich, Zhur. Fiz. Khim. 18, 355 (1944); 22, 575 (1948).

[12] A. Frumkin and G. Tedoradse, Zs. f. Elektrochem., 62, 251 (1958).

[13] A. N. Frumkin and É. A. Aikazyan, Izvest. Akad. Nauk SSSR, Otdel. Khim. Nauk, No.2, 202 (1959). *

---

*Original Russian pagination. See C. B. translation.

# INVESTIGATION OF THE RADIOLYTIC OXIDATION OF BIVALENT IRON AT HIGH IRRADIATION DOSES

P. Ya. Glazunov and A. K. Pikaev

Physicochemical Institute, Academy of Sciences, USSR

(Presented by Academician V. I. Spitsyn September 28, 1959)

(Translation of: Doklady Akad. Nauk SSSR Vol. 130, No.5,
1960, pp. 1051-1054)

Original article submitted September 25, 1959.

The literature contains scarcely any data on the influence of high doses with a broad range upon radiolytic conversions in aqueous solutions, although this question is of great scientific interest. Even the radiolytic oxidation of bivalent iron in diluted solutions of sulfuric acid in water, which is one of the most widely studied dosimetric systems, has scarcely been investigated in this respect. It is only known [1] that at high doses (commencing with $10^{21}$ ev/ml·sec) the ratio G(Fe$^{3+}$)/G(Ce$^{3+}$) (in diluted aqueous solutions of Fe$^{2+}$ and Ce$^{4+}$ salts) noticeably decreases. Moreover, there is a paper [2] on the determination of the G(Fe$^{3+}$) value at doses of $\sim 5 \cdot 10^{23}$ ev/ml·sec. In that paper it has been found that G(Fe$^{3+}$) at such doses hardly differs from the G(Fe$^{3+}$) value for the doses usually applied in radiation chemistry.

In the cited studies the high doses were effected by electron pulse irradiation. For this purpose linear electron accelerators with a high pulse frequency (50 or more pulses per second were used). In the study [2] the single pulses were applied by means of a mechanical selector which, however, does not eliminate entirely the effects of the background current. In the other study [1] it is not indicated at all which precautions were taken to neutralize the influence of the background current.

Previously [3] we have determined the G(Fe$^{3+}$) value at doses of $10^{21}$ ev/ml · sec. Ferrous sulfate solutions were irradiated by single monoenergetic electron pulses generated in the high-voltage electron tube of a linear accelerator fed by a cascade valve-capacitor voltage multiplier on 1.0-1.2 Mv. By using a special design we managed to diminish the influence of the background current to 3-5% of the total effect of the pulse. The value of G(Fe$^{3+}$) found by us was equal to 15.0-15.1 ion/100 ev. Undoubtedly, it was of interest to determine the value of G(Fe$^{3+}$) at higher doses. Firstly, such an investigation is of the highest importance for the chemical dosimetry of ionizing radiations. Secondly, it gives some insight in the behavior of the radiolysis products of water under conditions where the tracks of the ionizing particles overlap.

For this purpose we perfected the generation of electron pulses in the accelerator tube of a linear accelerator. Thanks to this, we succeeded in investigating the radiolytic oxidation of bivalent iron in aqueous solutions of sulfuric acid at doses up to $10^{23}$ ev/ml · sec. Just as previously [4], the electron pulse radiation was obtained by modulating the rectangular accelerating voltage pulse of the electron gun, which serves as injector tube. In order to diminish the duration of the pulses (down to 1-5 μsec) and to eliminate from the pulse-modulator scheme the raising transformer (an inevitable source of distorted pulse fronts) we used a pulse modulator with two artificial formating lines in a discharge chain and so it was possible to obtain in the output a potential equal to that of the discharge.

In the modulator we used a high-voltage thyratron as discharger. The generator effected the driving of the discharger by means of ignition pulses collected in the circuit of a delayed blocking-generator and the photosensitive apparatus FÉU-19 effected the regulation of the modulator at a distance. With the aid of a time relay the photosensitive device was regulated by a light pulse given by a flash-bulb of the type IS-50. A rectangular negative potential pulse (16 kv) falls on the cathode of the electron gun, which injects an electronic current pulse in the accelerating field of the tube. The emission of the tungsten cathode was increased by an activation with thorium dioxide.

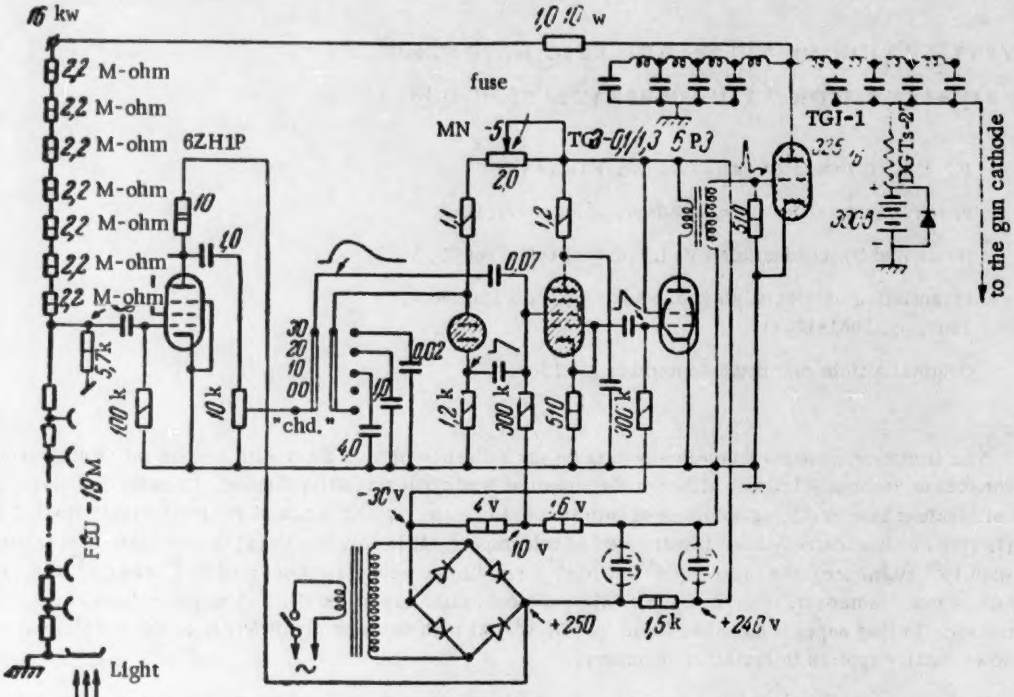

Fig. 1. Pulse-modulator circuit.

However, by raising the pulse dose to $10^{22}$ ev/ml·sec the background current was considerably increased (to 15-25% of the total effect of the pulse) and this, of course, might impair the results of the determination of $G(Fe^{3+})$. Consequently, we used a special circuit, which entirely eliminated the influence of the background current. The scheme of this circuit meant the application of a locking positive potential to the cathode of the gun via the adjusted resistance of the artificial line and it contained an uncoupling element DGTs-27 (see Fig.1).

Previously [3] we used a ballistic galvanometer to measure the energy of the electron pulse radiation absorbed in the irradiated system. When working with a ballistic galvanometer the systematic error is considerable and the calculation of the results takes much time. For this reason we developed an integrator , which records the energy absorbed at each pulse and integrates the result over the whole series of pulses. The amount of electricity in the current pulse is converted by the integrator to a signal whose duration is a function of the current amplitude.

The action of the integrator is based on the following principle. By means of a platinum sonde the pulse of the accelerated electrons absorbed in the reaction vessel is passed to the capacitor C, which is discharged via the reistor R. The discharge signal is amplified and inverted in a phase-inverting amplifier and is applied to the next relay, a Schmitt trigger. The Schmitt trigger gives a rectangular signal whose duration is a function of the pulse amplitude at the discharge of the capacitor C. This signal falls on a gate, which transmits the signals of the fixed-frequency generator during a time interval equal to the duration of the rectangular signal coming from the Schmitt trigger. The pulses of the fixed-frequency generator which pass through the gate circuit are counted by the counting equipment PS-10000. Moreover, the circuit is provided with a counter which counts the number of current pulses arriving at the integrator. The parameters of the pulses are the following: shape rectangular, duration 5$\mu$sec, current pulse 100-120 ma, dose up to $10^{23}$ ev/ml · sec (at an energy of 0.9 Mev). The variation of the pulse radiation doses was achieved by varying the heating of the cathode.

TABLE 1

| Dose, ev/ml · ·sec | $G(Fe^{3+})$, ions/ /100 ev | Dose, ev/ml · · sec | $G(Fe^{3+})$, ions/ /100 ev |
|---|---|---|---|
| $10^{21}$ | 15.0–15.1± ±1.6 * | $4.7 \cdot 10^{22}$ | 10.8± 0.9 |
| | | $7.6 \cdot 10^{22}$ | 10.3± 0.5 |
| $8 \cdot 10^{21}$ | 14.2 ± 1.5 | $1.5 \cdot 10^{23}$ | 10.1± 0.5 |
| $1.1 \cdot 10^{22}$ | 13.4± 0.6 | | |
| $2.7 \cdot 10^{22}$ | 11.7± 1.0 | | |

---

*$G(Fe^{3+})$ at this dose has been determined by us previously [3].

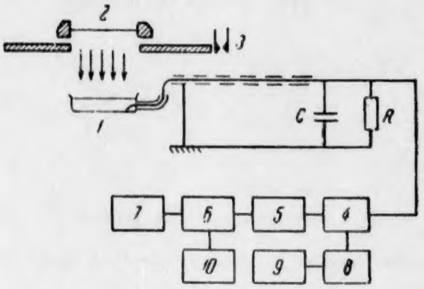

Fig. 2. Scheme of the experimental determination of $G(Fe^{3+})$. 1) glass vessel with a membrane, 2) beryllium entrance window of the accelerating tube, 3) rolling-shutter and connections to the pulse circuit, 4) phase-inverting amplifier, 5) Schmitt trigger, 6) gate circuit, 7) fixed frequency generator, 8) counting circuit, 9) mechanical pulse counter, 10) counting equipment PS-10000.

Twice-distilled water was used for the determination of $G(Fe^{3+})$; the reagents were of high purity. A $3 \cdot 10^{-3}$ M solution of Mohr's salt in 0.8N $H_2SO_4$ without and with an addition of $10^{-3}$ M NaCl was exposed to the radiation. Trivalent iron was determined spectrophotometrically. The molar extinction coefficient of $Fe^{3+}$ in 0.8 N $H_2SO_4$ at 304 mμ was taken equal to 2170 (at 24°) [5]. In the calculations the variation of the extinction coefficient with temperature (0.7% per degree) was taken into account. The solutions were irradiated in a glass vessel provided with a glass membrane (the thickness of the membrane was about 100μ ).

In Fig. 2 is shown the scheme of the experimental determination of $G(Fe^{3+})$ at various doses. The amount of energy absorbed by the ferrosulfate solution was determined by measuring the electron current in the solution by means of the platinum sonde sealed to the vessel and of the integrator and the counting equipment described above. An accurate estimate of the energy lost by the electron ray when passing through the membrane of the vessel was obtained in the way described in [3]. The magnitude and the shape of the pulses were also checked on an oscillograph.

The values of $G(Fe^{3+})$ determined by us at high doses are given in Table 1. Each value of $G(Fe^{3+})$ is an average of 8-20 measurements. The solutions were irradiated by 1-10 electron pulses (with an energy of 0.9 Mev), according to the dose required.

As is shown by the data in Fig. 1, above a dose of $\sim 10^{22}$ ev/ml · sec the value of $G(Fe^{3+})$ decreases considerably when the dose is increased. The value $G(Fe^{3+}) = 14.3$ ions/100 ev at a dose of $\sim 5 \cdot 10^{23}$ ev/ml · sec given in [2] apparently is somewhat too high (as was mentioned above, this may be a consequence of the higher background currents). Therefore, upon executing a chemical dosimetry by means of a dosimetric system with ferrosulfate, one must take into account that the value of $G(Fe^{3+})$ considerably decreases at high doses.

At present it is generally accepted that, in consequence of the extremely low concentration of bivalent iron in the dosimetric system and of the high radiation stability of sulfuric acid, the direct interaction of the irradiation with the dissolved substance is negligibly low and, therefore, the oxidation of $Fe^{2+}$ is brought about by the radiolysis products of water. These products react in the following way with bivalent iron and with the molecular oxygen present in the solution:

$$Fe^{2+} + OH \rightarrow Fe^{3+} + OH^-, \quad (1)$$

$$H + O_2 \rightarrow HO_2, \quad (2)$$

$$H_2O_2 + Fe^{2+} \rightarrow Fe^{3+} + OH + OH^-, \quad (3)$$

$$H^+ + Fe^{2+} + HO_2 \rightarrow Fe^{3+} + H_2O_2. \quad (4)$$

Hence, $G(Fe^{3+}) = 3G_H + G_{OH} + 2G_{H_2O_2}$ where $G_H$, $G_{OH}$ and $G_{H_2O_2}$ are the yields of the corresponding radiolysis products of water.

At higher doses the recombination probability of the H and OH radicals formed at the radiolysis of water increases as a result of the fact that the tracks of the ionizing particles overlap: $H + H \rightarrow H_2$; $H + OH \rightarrow H_2O$; $OH + OH \rightarrow H_2O_2$. This must lead to an increase of $G_{H_2}$ and $G_{H_2O_2}$ and to a decrease of $G_H$ and $G_{OH}$ and, therefore, to a decrease of $G(Fe^{3+})$.

The results of this study show that $G(Fe^{3+})$ begins to decrease at doses above $\sim 10^{22}$ ev/ml · sec. In this connection it may be supposed that in aqueous solutions at such high doses the effects caused by the overlapping of the tracks of the ionizing particles become perceptible.

The possibility that high doses have an influence on reaction (2) is not excluded. However, to solve this problem and also to estimate qualitatively, the decrease of $G_H$ and $G_{OH}$ further investigations are needed.

## LITERATURE CITED

[1] H. C. Sutton and J. Rotblat, Nature, 180, 1332 (1957).

[2] J. P. Keene, Radiation Res., 6, 424 (1957).

[3] A. K. Pikaev and P. Ya. Glazunov, Izvest. Akad. Nauk SSSR, Otdel. Khim. Nauk, in the press. *

[4] P. Ya. Glazunov and M. G. Kuz'min, Collection: All-Union Congress on Radiation Chemistry (Academy of Sciences USSR Press, 1958, p. 324) [In Russian].

[5] R. H. Schuler and A. O. Allen, J. Chem. Phys., 24, 56 (1956).

[6] A. O. Allen, Collection: Contributions of non-Russian Scientists to the Conference in Geneva (Moscow, 1956) [In Russian].

---

* Original Russian pagination. See C. B. translation.

# A NEW CHAIN-INITIATING REACTION IN LIQUID-PHASE OXIDATION

**E. T. Denisov**

Institute of Chemical Physics, Academy of Sciences, USSR

(Presented by Academician V. N. Kondrat'ev, October 9, 1959)

(Translation of: Doklady Akademii Nauk SSSR, Vol. 130, No.5, 1960, pp. 1055-1058)

Original article submitted October 2, 1959.

The rate of oxidation as a chain process depends upon the rate of formation of free radicals. In a reaction which has already been initiated, the formation of free radicals takes place mainly at the expense of intermediate molecular products, in particular, hydrogen peroxide. The chain-initiation rate in the initial instant for an oxidation reaction is tens or even hundreds of times less than in an oxidation reaction in progress, and its order of magnitude is $10^{-9}$-$10^{-8}$ mole/liter · sec. The initial chain-initiation rate determines the duration of the induction period.

At the beginning of the reaction, if no inducing agent is present, chain initiation can take place only at the expense of the initial substance RH and of the dissolved oxygen. Free radicals can, in principle, result from a slow dissociation of the starting substance at the weakest bonds, say, C—C bonds, whose dissociation energy is 60-80 kcal/mole. The free-radical formation rate at the expense of the dissociation of a substance with a substance with a bond energy of 60 kcal/mole is $10^{-18}$ mole/liter · sec ($t = 140°$, [RH] = 10 mole/liter), which is very low . With rare exceptions, the dissociation of the starting substance cannot provide an effective source of free radicals in oxidation reactions.

The bimolecular reaction between RH and $O_2$

$$RH + O_2 \rightarrow R\cdot + HO_2\cdot - q_1 \qquad (1)$$

is generally considered at present as the source of free radicals in the initial stage of a thermal oxidation [1]. If this is actually so, the reaction RH + $O_2$ must ensure such free-radical formation rates as are observed experimentally. The values of $W_0$ determined by the inhibition method [2] are known for a number of substances (Table 1).

Let us evaluate the chain-initiation rate according to reaction (1).and let us compare it with the experimental values. The heat absorbed in reaction (1) is $q_1 = Q_{R-H} - Q_{H-O_2\cdot}$, $Q_{H-O_2\cdot} = 47$ kcal/mole [1] and $q_1 = (Q_{R-H} - 47)$ kcal/mole. The activation energy $E = q_1 + \epsilon \approx q_1$, since $\epsilon$ is apparently not large. The steric factor for bimolecular reactions in the liquid phase is of the order of $10^{-3}$- $10^{-5}$. Let us take in our computations a steric factor of $10^{-3}$. The rate constant of reaction (1) is then equal to $10^{11} \cdot 10^{-3} \exp(-q_1/RT) = 10^8 \exp(-q_1/RT)$ liter/mole · sec, and the radical-formation rate in this reaction will be equal to $W_0 = 2 \cdot 10^8 \exp(-q_1/RT)$ [RH] [$O_2$] mole/liter · sec. In order to calculate the rate, one must know the stability of the bond to be broken $Q_{R-H}$, [$O_2$] and [RH].

In the case of benzaldehyde the energy of the C—H bond in the formyl group represents 78 kcal/mole [7], [RH] = 2 mole/liter, [$O_2$] = $4 \cdot 10^{-3}$ mole/liter, $t = 5°$, $q_1 = 78-47 = 31$ kcal/mole, $W_0 = 2 \cdot 10^8$ exp

$(-31\,000/RT) \cdot 2 \cdot 4 \cdot 10^{-3} = 10^{-8}$ mole/liter · sec. For decyl aldehyde $Q_{R-H}$ can be assumed to be the same as in acetaldehyde, where $Q_{R-H} = 80$ kcal/mole [7], $[RH] = 5$, $[O_2] = 4 \cdot 10^{-3}$, $t = 5°$, $q_1 = 80 - 47 = 33$ kcal//mole, $W_0 = 6 \cdot 10^{-20}$ mole/liter · sec. In cyclohexane the energy of a C−H bond can be taken as 88 kcal/mole, and the steric factor $10^{-2}$, since 12 C−H bonds can participate in the reaction, $[RH] = 10$, $[O_2] = 10^{-1}$, $t = 140°$, $q_1 = 88-47 = 41$ kcal/mole, $W_0 = 5 \cdot 10^{-13}$ mole/liter · sec. In n-decane $Q_{R-H} = 89$ kcal/mole, $[RH] = 5$, $[O_2] = 10^{-2}$, $t = 130°$, $q_1 = 89-47 = 42$ kcal/mole. The steric factor can be taken as equal to $10^{-2}$ as in the case of cyclohexane, $W_0 = 2 \cdot 10^{-15}$ mole/liter · sec. The energy of an $\alpha$ C−H bond in tetralin can be assumed to be the same as in ethylbenzene [8], $Q_{R-H} = 75$ kcal/mole, $[RH] = 7$, $[O_2] = 10^{-2}$, $t = 110°$, $q_1 = 75-47 = 28$ kcal//mole, $W_0 = 2 \cdot 10^{-10}$ mole/liter · sec. In cyclohexanol $Q_{R-H} \approx 85$, $W_0 = 2 \cdot 10^{-11}$ mole/liter · sec.

The above values of $W_0$ must be considered as tentative ones. It must also be noted that the calculations were made purposely with the minimum values of E ($\epsilon = 0$) and reasonable maximum values of the steric factor $f_1$. Therefore reasonable maximum values of $W_0$ have been obtained: these were nonetheless lower by 5-10 orders of magnitude than the experimental values of $W_0$. Such an enormous difference between experiment and calculation cannot be traced back to errors in the evaluation of E and $f_1$: it indicates that in the starting system $RH + O_2$ there is another much more powerful source of free radicals.

TABLE 1

Chain-Initiation Rates in Liquid-Phase Oxidation Reactions

| Substance | Temp. °C | $W_0$, M//liter·sec | $E_0$, kcal/mole | Reference |
|---|---|---|---|---|
| Benzaldehyde | 5 | $3{,}5 \cdot 10^{-8}$ | $11{,}6 \pm 1{,}5$ | (3) |
| Decanal | 5 | $5 \cdot 10^{-9}$ | $15{,}6 \pm 1$ | (4) |
| Cyclohexane | 140 | $4{,}6 \cdot 10^{-8}$ | | (2) |
| n-Decane | 130 | $1{,}3 \cdot 10^{-8}$ | | (5) |
| Tetralin | 110 | $5{,}7 \cdot 10^{-7}$ | | (6) |
| Cyclohexanol | 120 | $2{,}7 \cdot 10^{-8}$ | $33{,}5 \pm 1{,}5$ | |

Such a source of free radicals can be provided by the termolecular reaction between the starting substance and oxygen

$$RH + O_2 + HR \rightarrow R\cdot + H_2O_2 + R\cdot - q_2. \tag{2}$$

$q_2 = 2Q_{R-H} - Q_{H-H} + \Delta H_{H_2O_2}$, $Q_{H-H} = 103$ kcal/mole.

The quantity $\Delta H_{H_2O_2}$ deserves a special discussion. Strictly speaking, one must consider the formation of hydrogen peroxide in the given solvent RH, where the enthalpy of formation of hydrogen peroxide is given by $\Delta H_{H_2O_2\,(gas)} + \Delta H_{sol.}$. Since the heat of solution of hydrogen peroxide in organic solvents is not known, one can consider in first approximation the heat of formation of liquid hydrogen peroxide $-\Delta H_{H_2O_2(liq)} = 45$ kcal//mole, $q_2 = 2(Q_{R-H} - 72)$ kcal/mole. It is not difficult to ascertain that reaction (2) is energetically much more favorable than reaction (1). For instance, for $Q = 90$ kcal/mole, $q_1 = 43$ kcal/mole, and $q_2 = 36$ kcal/mole; for $Q = 80$ kcal/mole, $q_1 = 33$ kcal/mole, $q_2 = 16$ kcal/mole.

Termolecular collisions in the liquid phase are practically as frequent as the bimolecular ones: the ratio of the number of bimolecular collisions to termolecular collisions is $\frac{10^{11} \cdot [RH][O_2]}{10^{10}[RH]^2[O_2]} = \frac{10}{[RH]}$; for $[RH] = 2$ mole/liter it is equal to 5, and it is equal to 1 when $[RH] = 10$ mole/liter. The fact that reaction (2) is energetically favored and the high frequency of termolecular collisions in the liquid phase lead to the conclusion that the rate of reaction (2) should be, as a rule, much higher than that of reaction (1).

Let us compare the rates of the termolecular reaction with the values of $W_0$ obtained from experiment.

TABLE 2

Comparison of Observed and Calculated Values of $W_0$ (mole/liter, sec).

| Substance | $W_0$, observed | $W_0$ according to reaction (1) | $W_0$ according to reaction (2) |
|---|---|---|---|
| Benzaldehyde | $3{,}5 \cdot 10^{-8}$ | $10^{-18}$ | $8 \cdot 10^{-7}$ |
| Decanal | $5 \cdot 10^{-9}$ | $6 \cdot 10^{-20}$ | $4 \cdot 10^{-9}$ |
| Cyclohexane | $4{,}6 \cdot 10^{-8}$ | $5 \cdot 10^{-13}$ | $10^{-9}$ |
| n-Decane | $1{,}3 \cdot 10^{-8}$ | $2 \cdot 10^{-15}$ | $8 \cdot 10^{-13}$ |
| Cyclohexanol | $2{,}7 \cdot 10^{-8}$ | $2 \cdot 10^{-14}$ | $3 \cdot 10^{-10}$ |

Let us compare the rates of the termolecular reaction with the values of $W_0$ obtained from experiment. The activation energy $E = q_2 + \epsilon \approx q_2$. The steric factor for the termolecular reaction will be smaller than for the bimolecular one. As is well known, the steric factor expresses the probability that in energy-rich colliding molecules a part of their energy (larger than E) be localized on the bonds being broken in an elementary collision. A simultaneous localization of the energy of two C–H bonds of two molecules of RH colliding with $O_2$ appears to be a complex event. Its probability will therefore be the product of the probabilities for the localization of energy on each of the reacting C–H bonds. Therefore, in first approximation, one can take $f_2 = f_1 \cdot f_1 = f_1^2$. Since we have chosen $f_1 = 10^{-3}$, $f_2 = 10^{-6}$ (and $10^{-4}$ for decane and cyclohexane). The rate of the termolecular reaction is $W_0 = f_2 \cdot 2 \cdot 10^{10} \exp(-E_2/RT) \cdot [RH]^2[O_2]$. The quantities $Q_{R-H}$, $[O_2]$, [RH] and t are the same as before. The calculated values of $W_0$ are compared in Table 2 with the observed ones and those calculated according to reaction (1).

An examination of Table 2 shows that the values of $W_0$ obtained according to the reaction $2RH + O_2$ do not differ very much from the experimental values (in general by 1-2 orders of magnitude, and only in the case of decane by 5 orders). In addition, it must be noted that the values of $W_0$ calculated for reaction (2) are extremely sensitive to deviations of the values of $Q_{R-H}$ and $f_2$ used by us from the true ones. An error in $Q_{R-H}$ of 2 kcal/mole leads to an error in E of 4 kcal/mole and to an error in $W_0$ of 2 orders of magnitude. The range of $f_2$ lies between $10^{-3}$ and $10^{-12}$. Therefore, the approximate nature of the computations allows us to consider a difference of 1-2 orders of magnitude between observed and calculated values as a good agreement. It is appropriate also to call attention to the fact that the values of $W_0$ calculated according to reaction (2) are in some cases (benzaldehyde) larger, in some cases smaller, than the observed ones. Moreover, reaction (2) gives values of E practically identical to the experimental ones for benzaldehyde and decanal.

The kinetic data indicating a proportionality between the initial reaction rate and $[RH]^2$ [6,9] are in agreement with a termolecular mechanism of chain initiation. The oxidation rate, as is well known, is $V_0 = k \cdot [RH][RO_2\cdot]$; for a quadratic breaking off of the chains $[RO_2.] \sim W_0^{1/2}$ and, according to reaction (2) $W_0 \sim [RH]^2$, consequently $V_0 \sim [RH]^2$. In some cases a dependence $V_0 \sim [RH]^{3/2}$ is observed, which at first sight would support reaction (1). However, just this type of dependence would be observed if the chain were initiated by an impurity of the starting material (say, a peroxide) dissociating into free radicals.

We shall summarize the preceding considerations by noting that the termolecular reaction $2RH + O_2$ suggested in the present paper agrees well with the available experimental data. These are all grounds to conclude that just this reaction, and not the reaction $RH + O_2$ is the main source of free radicals in the initial stage of liquid-phase oxidation. It is very probable that in the case of substances with very weak C–H bonds (aldehydes, 1,4-dienes, 1,3-diphenylalkanes) this reactions remains the main source of free radicals even when oxidation is in progress, successfully competing at not high temperatures with the formation of free radicals at the expense of peroxides.

## LITERATURE CITED

[1] N. N. Semenov, Some Problems in Chemical Kinetics and Reactive Tendencies (Izd. AN SSSR, 1958).

[2] E. T. Denisov, Zhur. Fiz. Khim. 33, 1198 (1959).

[3] T. A. Ingles and H. W. Melville, Proc. Roy. Soc. A218, 175 (1953).

[4] H. R. Cooper and H. W. Melville, J. Chem. Soc. 1984 (1951).

[5] D. G. Knorre, Z. K. Maizus, N. M. Émanuél', Doklady Akad. Nauk SSSR 123, 123 (1958).*

[6] P. George, E. Rideal and A. Robertson, Proc. Roy. Soc. A185, 288 (1946).

[7] P. Gray and A. Williams, Chem. Rev. 59, 239 (1959).

[8] D. G. Knorre, Z. K. Maizus, et al., Usp. Khim. 26, 416 (1957).

[9] J. McNesby and C. Heller, Chem. Rev. 54, 325 (1954).

---

* Original Russian pagination. See C. B. translation.

# ANALYSIS OF THE BOND FORM AND THE STATE OF WATER ABSORBED IN DISPERSED BODIES, BY MEANS OF KINETIC DRYING CURVES

M. F. Kazanskii

Kiev Light Industry Technological Institute

(Presented by Academician P. A. Rebinder, October 8, 1959)

(Translation of: Doklady Akademii Nauk SSSR, Vol. 130, No. 5, 1960, pp.1059-1062)

Original article submitted October 7, 1959.

Drying is a complicated process, not only thermotechnically, but also from a physicochemical standpoint, the regularities of which depend in the first instance on differences in bond form, and in the state of the absorbed water in the material. The influence of the nature of the bonding of the water on the course of drying is most clearly shown in curves showing the kinetics of drying [1-4]-- the so-called drying thermograms, giving the time change of the temperature on drying thin films (1-2 mm) of moist substances; and in drying curves — curves depicting the loss of weight of the same materials.

Figure 1 gives some typical kinetic drying curves for different groups of substances. The thermogram curves were obtained with the automatic recording apparatus [5], and plotted values of the temperature difference, $\Delta \theta$, of the substance being dried, at a constant temperature of the surrounding air, while the drying curves recorded the quantity W of water contained in the material.

Before the experiments, the samples were moistened with water to full saturation point. Under such conditions there was always present under the surface of the samples a thin layer of the free liquid. Therefore the drying of the samples always commenced with the removal by evaporation of this excess of water, so that all the thermograms commenced with an upper horizontal portion, terminating in the singular point 1, which corresponded to complete evaporation of the free liquid.

By projecting the singular points of the thermograms onto the corresponding drying curves, the amount of moisture in the substance being dried at any of the singular points may be determined (see Table 1). In Table 1 are produced comparative values of the moisture content of the same substances obtained by us by other methods as well as the present one, and also borrowed from other published sources [6,7].

The drying thermogram of quartz sand (1a in Fig. 1) is, as to its form and the position on it of the singular points, typical of the drying of coarse-pored bodies, the course of which is due to the evaporation of capillary moisture from pores whose radius exceeds $10^{-5}$ cm. We have shown formerly [2] that the moisture content of coarsely dispersed substances at the first singular point corresponds to its maximum moisture capacity (the saturation moisture content); that at the second point represents the beginning of the evaporation of "junction" water — that is, the water present at the points of contact of the separate grains of the sand, while that at the third point corresponds to the initiation of evaporation of "junction" water when the curvature of the meniscus of the aqueous surface is smaller than $10^{-5}$ cm.

TABLE 1

Differential Water Content from the Weight of the Dry Substance at 20-25°, as Determined by Various Methods (in percentages)

| Body in which water is contained | Content of hygrosc. wtr. | | Maximum quantity of adsorbed water | | | | | Wtr adsorbed in unimolecular layer | |
|---|---|---|---|---|---|---|---|---|---|
| | from adsorption isotherms | from point 3 on thermograms | from adsorption isotherms | from heat of wetting | from indicator method | from hygroscopic method | from point 4 on thermograms | from adsorption isotherms | from point 5 on thermograms |
| **Adsorbents** | | | | | | | | | |
| Silica gel MSM | 32,6 | 31,8 | 13,9 | — | — | — | 14,1 | 7,2 | 8,3 |
| Silica gel KSM | 33,5 | 32,5 | 17,6 | — | — | — | 18,3 | 8,1 | 8,9 |
| Silica gel VKhK.2 | 83,6 | 87,0 | 7,0 | — | — | — | 6,6 | 2,6 | 3,0 |
| Silica gel E | 170,0 | 172,0 | 10,0 | — | — | — | 9,8 | 3,4 | 3,0 |
| Active carbon | 37,8 | 39,6 | 3,6 | — | — | — | 4,5 | — | — |
| **Clays** | | | | | | | | | |
| Zhabin bentonite | 41,1 | 42,5 | — | 22,7 | — | 19,7 | 21,9 | — | 14,9 |
| Pyzhev bentonite | 28,8 | 31,1 | — | 20,1 | 20,7 | 19,2 | 21,4 | — | 14,0 |
| Pobiyankov bentonite | 30,1 | 31,5 | — | 21,0 | — | 18,0 | 21,6 | — | 14,5 |
| Gorb bentonite | — | 23,1 | — | 11,5 | — | 10,0 | 11,4 | — | 7,2 |
| Chasov-yar clay | 16,0 | 14,8 | — | 5,4—7,0 | 7,1 | 6,5 | 6,8 | — | 3,5 |
| Poltav clay | 17,1 | 18,0 | — | 6,0 | 6,8 | 7,0 | 6,0 | — | 3,8 |
| **Soils** | | | | | | | | | |
| Dernov-gley | 13,5 | 13,0 | 7,5 | — | 8,4—10,0 | 9,1 | 8,0 | — | 5,0 |
| Chernozem-gley | 8,9 | 10,7 | 5,0 | — | 7,3—7,5 | 5,4 | 5,8 | — | 3,8 |
| Chernozem thick | 6,8 | 8,7 | 3,4 | — | 5,8—6,1 | 4,5 | 5,2 | — | 2,8 |
| Dernov weak podzolic | 6,0 | 7,0 | 2,6 | — | 3,7—4,7 | 3,5 | 3,3 | — | 1,8 |
| **Polymers** | | | | | | | | | |
| Potato starch (native) | 72,3 | 61,6 | — | 31—35 | 35,0 | — | 33,8 | — | 18,0 |
| Gelatin | 92,4 | 83,0* | — | — | — | — | 34,2 | — | 29,7 |
| Agar | — | 87,1** | — | — | — | — | 39,1 | — | 27,2 |
| Sulphite cellulose | 30,2 | 35,1 | — | 17,5 | — | — | 16,0 | — | 13,1 |

---

* Thermogram at 43.6°.

** Thermogram at 42°.

Thermogram 1b is typical of the drying of fine colloidal, capillary and quasicapillary-pored material, with a well-developed fine-pored structure. In our experiments, materials of this kind included clays of various minerals, soils of different types, starch, flour, egg powder, gelatin, agar agar, hide, cellulose, and others. The drying thermograms of colloidal materials [3,4] consist of a horizontal portion, defined by points 1 to 3, corresponding to the time required for the evaporation of osmotic water, and a lower portion of the curve, S-shaped, corresponding to the removal of hygroscopic water from the materials. The singular points 4 and 5 divide the lower part of the thermogram into three parts, corresponding to the times required for successive stages of drying from the material of water present in three forms: water in a capillary condensed form in micropores of radius less than $10^{-5}$ cm (line bounded by points 3 and 4); water polymolecularly adsorbed (points 4 and 5); and, finally, water more strongly bonded to the surface in a unimolecularly adsorbed condition.

Thermogram 1c is typical of the isothermal drying of polycapillary-pored substances, having a mixed macro- and micro-porous structure. In our experiments we took as examples of such systems thin layers of powdered silica gels and active carbon of various structural types [8], moistened by water or methyl alcohol. The thermogram is divided into two parts by the singular point 3, corresponding to the maximum hygroscopic moisture in the substance: we call these the upper and lower portions. The upper portion of this thermogram, judging by its form and the position of the singular points, is identical with the drying thermogram of coarse-pored

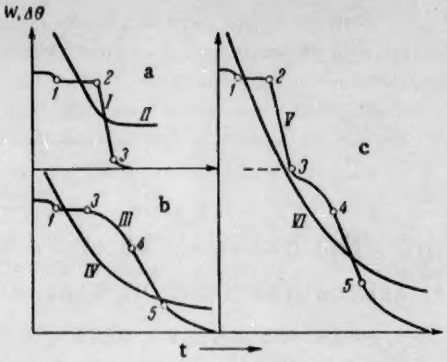

Fig. 1. Curves of the kinetics of drying. Drying thermograms (I, III and V) and drying curves (II, IV and VI), for thin samples moistened with water. 1a) Coarse-pored; 1b) Capillary-pored; 1c) Polycapillary-pored substance. W = moisture content; Δθ = temperature; t = time.

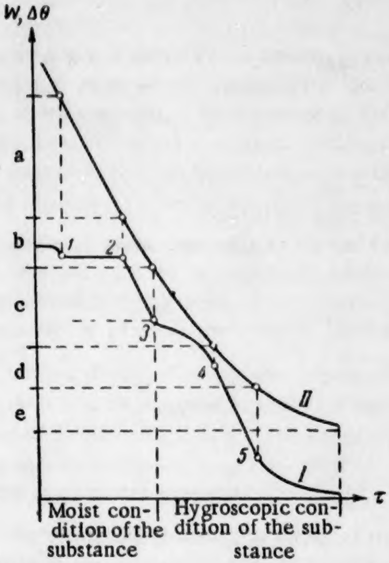

Fig. 2. Diagram of the kinetics of successive evaporation of the moisture on drying thin, capillary-pored materials of various kinds. I) thermogram; II) drying curve. The forms of water bonding are: a) osmotic moisture of colloidal materials, or moisture in a capillary state in the pores; b) "junction" moisture of the pores; c) capillary moisture in the micropores; d) polymolecularly adsorbed moisture; e) unimolecularly adsorbed moisture. For a and b, radius exceeds $10^{-5}$ cm; for c, radius is less than $10^{-5}$ cm.

substances: it has to do with the times of successive drying of capillary moisture, varying according to the state of this moisture in the coarse pores of the intergranular space of the powders. The lower portion of this thermogram also has an S-shaped structure, of the same form as is found in the drying thermograms of fine-pored colloidal substances. With respect to the moisture content of the substance, each portion of this lower part of the thermogram corresponds to the times of the successive evaporation of hygroscopic moisture [2], varying in its form and position with the nature of the binding of moisture with the substance (see Table 1).

Thus, from three drying thermograms, typical of various groups of porous materials, it appears that the thermogram corresponding to polycapillary substances is very common, since here the drying thermograms of coarse-pored and of colloidal substances enter in as constituent parts of a single curve.* It follows therefore that the isothermal drying thermograms of thin specimens of capillary-pored materials of various colloido-physical nature should be regarded as individual cases of the same type of drying thermogram: that for polycapillary-pored substances, from which the separate sections can be identified. Disappearance of one portion or other of this composite curve is therefore to be understood as meaning the absence of the corresponding form of bonding. The general appearance of the isothermal drying thermograms of any substance, and the number of parts making up its structure, depend only on the relative water-absorbing power of the given substance in connection with the various types of moisture bonding.

On the basis of the ideas depicted in Fig. 2, we have devised a scheme of the kinetics of the drying of thin materials, depicting graphically the general laws of the kinetics of the successive removal from materials of moisture of various forms and types of bonding with the substance. By the scheme the possibility is envisaged of the removal from the material of water of two basic forms of bonding: physicochemical and physicomechanical, subdivided by the singular points of the thermogram into six types. To the physicomechanically bound type of moisture there are assigned the three types of capillary moisture, two of which represent capillary water differing in their peculiarities of structure (capillary and "junction") in the coarse pores of the material, and the third represents the capillary moisture of the micropores. But the water with a physicochemical form of bonding may consist of osmotic water and two kinds of adsorbed moisture: the latter including moisture in polymolecular and in unimolecular layers, or loosely and firmly bound moisture.

Since drying is a thermoenergetic process in which the sequence of evaporations of moisture is determined by the degree of intensiveness of its bonding with the substance, then the proposed scheme may also be considered as a scheme for the classification of moisture liberated on drying, according to the different forms and types of bonding which it has with the substance. It must, of course, be borne in mind in this connection that the energetic bonding of water with the substance can be considered to be real only in those cases of water bound by adsorptive forces. The bonding of water of all the remaining kinds, however, can only be thought of as equivalent to a bond energy represented by the energy of isothermal liberation of it on drying [9].

---

*See Fig. 1, c.

The classification of moisture, based on the regularities of the kinetics of drying, is not only not in opposition to the rational scheme of classification of moisture according to form and nature of bonding with the substance which has been proposed by P. A. Rebinder [9], but on the contrary, makes it more precise because of the further detailed subdivision of the different types of bonding.

The scheme in Fig. 2 presents an essentially new thermographic method of quantitative analysis of the moisture in absorbing materials on the basis of its form and nature of its bond with the material. The experimental side of the application of the new method has been carried out by means of simultaneous recording, by means of an automatic recording apparatus providing drying thermograms and drying curves for thin specimens of the substances being investigated. According to the shape of the thermograms obtained it may at one stroke be determined to which of the groups of differential water-absorbing possibilities the given substance must be assigned. For quantitative analysis it is necessary by means of the drying curves to determine the moistness of the material corresponding to each of the singular points of the thermogram, and in harmony with the general scheme shown in Fig. 2 to determine the quantity of moisture of the different forms and types of bonding in the given substance.

As can be seen from Table 1, the results of the analysis of the differential water-absorbing properties of various substances by means of the kinetic curves of drying lie within the limits of magnitude determined by other laboratory methods. The accuracy of the moisture determination in any particular type of bonding by the thermographic method depends on the precision with which the drying curves are recorded. In our experiments the thermograms have been recorded with an accuracy of one hundredth of a degree, and the drying curves with an accuracy of one tenth per cent of the moisture in the substance. Therefore the error in the determination cannot be greater than 1-2%.

The new kinetic method of analysis of the form and nature of the bonding of moisture with the substance is specially distinguished by this: that it leads to the determination of the water-retaining capacity in relationship to all the possible forms and natures of bonding of the water, in one and the same experiment and in the course of a short time (only a few hours).

## LITERATURE CITED

[1] A. V. Lykov, Teoriya Suchka (The Theory of Drying), Moscow 1950 [in Russian].

[2] M. F. Kazanskii, Koll. Zhurn., 19, 6, 633 (1957).*

[3] M. F. Kazanskii, Koll. Zhurn. 21, 6, 620 (1959).*

[4] M. F. Kazanskii, Inzh. fiz. zhurn., 1, 6, 94 (1958).

[5] M. F. Kazanskii, Bentonitovye gliny, Sborn. Akad. Nauk. USSR (Bentonite clays, Collections of the Academy of Sciences of the Ukrainian SSR), 1958. [in Russian].

[6] F. D. Ovcharenko, Gidrofil'nost' glin, Dissertatsiya, Kiev, 1955 (Hydrophilic properties of clays, Dissertation. [in Russian].

[7] E. F. Nekryats, Teploty smachibaniya i gidrofil'nost' bysokopolimerov, Dissertatsiya, Kiev, 1955 (Heat of wetting and hydrophilic properties of high polymers, Dissertation. [in Russian].

[8] A. V. Kiselev, Zhur. fiz. Khim., 23, 4, 452 (1949).

[9] P. A. Rebinder, Dokl. na Vsesoyozn. naucho-tekhnichsoveshch. po intensifikatsii protsessov sushki (Proceedings on the All-Union Scientifico-Technical Council the Intensification of the Drying Process) [in Russian], 1958.

---

*Original Russian pagination. See C. B. translation.

# AN EXAMPLE OF A HOMOGENEOUS EXTENSION TO AN HETEROGENEOUS CATALYTIC REACTION

O. V. Krylov

Physical Chemistry Institute, Academy of Sciences, USSR

(Presented by Academician P. A. Rebinder, October 21, 1959)

(Translation of: Doklady Akademii Nauk SSSR, Vol. 130, No.5, 1960, pp. 1063-1066)

Original article submitted October 8, 1959.

The decomposition of hydrazine is a good example of an exothermic reaction which proceeds readily over a series of catalysts at low temperatures and has a small activation energy. We have already investigated [1] the decomposition of hydrazine over several catalysts: metals (Pt, pure Fe, and Fe activated with a base), semiconductors (Ge, GaAs, $Ga_2Se_3$, $Ga_2Te_3$, GaAs · $Ga_2Se_3$, 3GaAs · $Ga_2Se_3$, and $V_2O_5$), salts (CuBr), acids (aluminosilicate and quartz), and bases (CaO). We suggested a free-radical chain mechanism for the decomposition of hydrazine on metals and semiconductors. On the basis of preliminary thermochemical calculations, similar to those done by N. N. Semenov [2] and V. V. Voevodskii [3], we proposed the hypothesis [1] that the N−N bond in hydrazine is cleaved on the catalyst surface:

$$N_2H_4 + L \rightarrow NH_2 - L + (NH_2\cdot)_{ads}. \qquad (1)$$

Our notation is similar to that of Semenov and Voevodskii: L is a free radical on the catalyst surface; $(A.)_{ads}$ is a radical formed in one of the catalytic reactions steps, such as $(NH_2^\bullet)_{ads}$, and only weakly bound to the surface; A−L, for example $NH_2$−L, are particles which have formed a stable (electron pair) bond with the catalyst. Reaction (1) is followed by the following surface chain reaction:

$$N_2H_4 + (NH_2\cdot)_{ads} \rightarrow NH_3 + (N_2H_3\cdot)_{ads}$$
$$(N_2H_3\cdot)_{ads} + N_2H_4 \rightarrow 2NH_3 + N_2 + (H\cdot)_{ads},$$
$$(H\cdot)_{ads} + N_2H_4 \rightarrow (NH_2\cdot)_{ads} + NH_3.$$

When very little of free surface remains the following free-radical reactions are possible:

$$NH_2 - L + (NH_2\cdot)_{ads} \rightarrow N_2H_4 + L,$$
$$NH_2 - L + (H\cdot)_{ads} \rightarrow NH_3 + L,$$
$$NH_2 - L + (N_2H_3^\bullet)_{ads} \rightarrow NH_3 + N_2 + H_2 + L.$$

On acidic or basic catalysis the reaction proceeds by an ionic or molecular [4] mechanism.

The following facts provide indirect evidences that the decomposition of hydrazine is a chain reaction: a) very large frequency factors in the Arrhenius equation; b) the existence of charged species on the surface, detected by the change in the electron work-function during the reaction (up to 0.2 v); c) an induction period observed in several cases; d) large stoichiometric coefficients when hydrazine is decomposed on semiconductors and metals, indicating a multistage reaction. To obtain a more direct proof for the chain mechanism we could check the possibility of having the reaction escape into the gas phase at temperatures at which the radicals $(NH_2\cdot)$,$(N_2H_3\cdot)$, and$(H\cdot)$ can not be retained on the surface by the adsorption forces. The escape into the gas phase was verified by using the Bogoyavlenskaya –Koval'skii fractional calorimetric method [5]. The reaction was carried out in a molybdenum-glass vessel of the type used by Butyagin and Margolis [6]. A differential thermocouple was introduced into the reactor. One thermocouple junction was inserted into the catalyst, the other into the gas phase. The galvanometer sensitivity was such that a single division corresponded to a 0.05° temperature difference between the two differential thermocouple leads. By means of a Strelkov thermoregulator the temperature was kept constant to ± 0.01°C. Since hydrazine has a low vapor pressure at room temperature the reactions were carried out at low initial $N_2H_4$ pressures (1-8 mm).

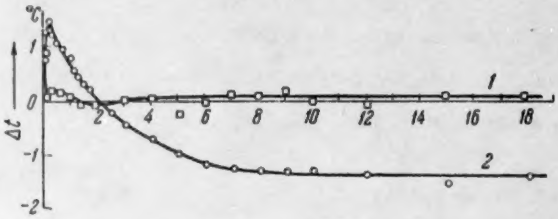

Fig. 1. Changes in the relative temperature of the catalyst during the decomposition of hydrazine on iron: 1) at 120°; 2) at 230°.

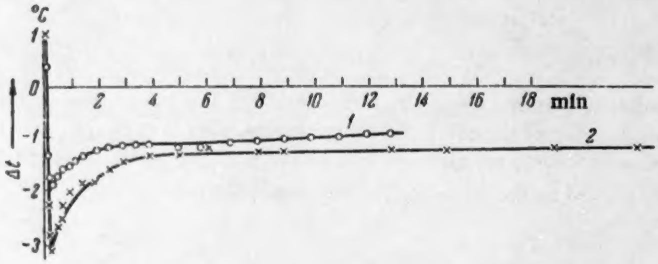

Fig. 2. Changes in the relative temperature of the catalyst during the decomposition of hydrazine on an ammonium catalyst KATZ-55 (2.73 $FeO_3$; 3.94 $Al_2O_3$; 1.82 $K_2O$; red. $H_2$): 1) at 175°; 2) at 250°.

We have presented several typical curves (which were obtained by plotting the galvanometer readings) for some of our catalysts. We studied the following catalysts: iron, ammonium catalyst KATZ-55 (iron activated with a base) ZnO, $3GaAs\cdot Ga_2Se_3$, CaO, and the aluminosilicate catalyst used in cracking. When an inert gas (krypton) was let into the vessel containing the catalyst we observed: a) a short initial cooling of the central thermocouple junction located outside the catalyst, b) a subsequent decrease in the temperature difference Δt caused by the conduction of heat by the gas. When hydrazine vapor was introduced the initial temperature difference became even greater since as the central junction temperature dropped due to the flow of a cool gas the temperature of the junction inside the catalyst was increased by the heat of adsorption or of the ensuing surface reaction. After the initial spurt the subsequent changes in Δt varied from catalyst to catalyst.

In Fig. 1 we have plotted the temperature differences for the decomposition of $N_2H_4$ on pure iron (prepared

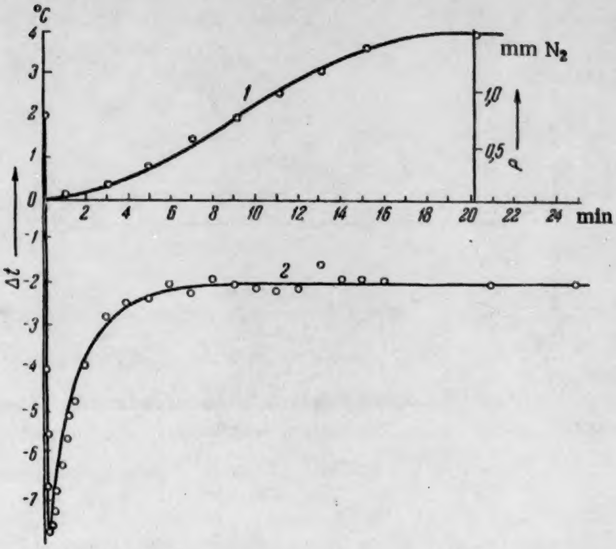

Fig. 3. The decomposition of hydrazine on aluminosilicate at 240°C: 1) kinetic curve; 2) relative temperature curve.

by reducing $Fe_3O_4$ and containing 0.2% $Al_2O_3$) at an initial hydrazine pressure of 7 mm. The initial sharp deflection of the galvanometer needle in the negative direction (cooling of the central junction) occurred within 5-10 sec and therefore it does not show on the scale used in Fig. 1. This was followed by an increase in the relative temperature of the central junction and a gradual leveling of the temperature difference. We can see no other way of explaining the relative temperature rise on the central junction except by assuming that the decomposition of $N_2H_4$ continues in the gas phase, since any other effects, such as cooling on introduction, uneven temperature distribution in the reactor, and catalyst heating caused by the heat of adsorption and the surface reaction, would tend to displace Δt in the opposite direction. The subsequent decrease in Δt results from a decreased reaction rate and an equalization of the catalyst and the gas-phase temperatures. Figure 1 shows that a higher temperatures (230°) the effect is much more pronounced.

No such behavior was observed (see Fig. 2) when the reaction was carried out on an ammonium catalyst KATZ-55 (iron activated with a base). Though the catalyst became initially hot due to the adsorption and surface reaction, from then on the absolute value of $|\Delta t|$ continually declined due to a reduced reaction rate and temperature equalization. Let us recall [1] that the decomposition of hydrazine proceeds in a different manner on the two catalysts: on pure iron the reaction is $3N_2H_4 \rightarrow N_2 + 4NH_3$, while on base-activated iron $2N_2H_4 \rightarrow N_2 + H_2 + 2NH_3$.

On a basic catalyst, CaO, no extention into the gas phase was detected, and the decomposition proceeded according to the reaction: $N_2H_4 \rightarrow N_2 + 2H_2$.

In Fig. 3 we have plotted the kinetic curve and the temperature-difference curve for the decomposition of $N_2H_4$ on an aluminosilicate cracking catalyst (the initial $N_2H_4$ vapor pressure was 5 mm). We observed a very sharp increase in the catalyst temperature (caused by the adsorption of hydrazine) followed by a steady decline of $|\Delta t|$ to a certain constant value.

The experimental results on semiconductors were similar to those obtained on iron. In Fig. 4 we have plotted the Δt-curves for the decomposition of hydrazine on $3GaAs \cdot Ga_2Se_3$ (hydrazine pressure 8 mm, temperature 175°) and on zinc oxide (3 mm and 290°). At lower temperatures(145° on $3GaAs \cdot Ga_2Se_3$ and 240° on ZnO) Δt did not increase after the initial drop. Evidently the gas-phase reaction step is absent at lower temperatures. Figure 4 shows that Δt increases very little on these catalysts after the initial decline, and in the case of zinc oxide the curve does not even intersect the abscissa. After several successive reactions were carried out even the slight increase disappeared entirely and the over-all reaction rate decreased appreciably.

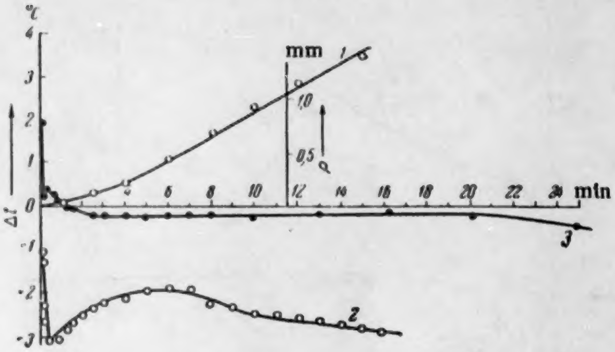

Fig. 4. Decomposition of hydrazine on semiconductors: 1) and 2) on ZnO at 290°, with 1) the kinetic curve and 2) the relative temperature; 3) on $3GaAs \cdot Ga_2Se_3$ at 100° (relative temperature).

Our results provide ample evidence for the previously postulated [1] free-radical chain-reaction mechanism for the decomposition of hydrazine on metallic and semiconducting catalysts. While on the investigated redox-type catalysts, metals and semiconductors (with the exception of base-activated iron), the surface reaction was extended into the gas phase, no such extension was observed on acid-base type catalysts (CaO and aluminosilicate). In the opinion of this author the gas-phase extension to a heterogeneous reaction may be taken as a possible criterion on which the assignment of catalytic reactions to the redox (as opposed to the acid-base) type may be based.

The author wishes to express his gratitude to Corresponding Member Acad. Sci. USSR S. Z. Roginskii for his valuable advice and to M. Ya. Kushnerev for his friendly assistance in the experimental work.

## LITERATURE CITED

[1] O. V. Krylov, V. M. Frolov, E. A. Fokina, and Yu. N. Rufov, The 8th Mendeleev Conference on Pure and Applied Chemistry, Coll. Physical Chemistry (1959) p. 172.

[2] N. N. Semenov, Some Problems in Chemical Kinetics and Reactivity (Izd. AN SSSR, 1954).

[3] V. V. Voevodskii, Problemy Kinetiki i Kataliza 8, 97 (1955).

[4] M. Szwarc, Proc. Roy. Soc. A198, 267 (1949).

[5] M. L. Bogoyavlenskaya and A. A. Koval'skii, Zhur. Fiz. Khim. 20, 1325 (1946).

[6] P. Yu. Butyagin and L. Ya. Margolis, Doklady Akad. Nauk SSSR 66, 405 (1949).

# LIGHT ABSORPTION AND LUMINESCENCE OF COMPLEX MOLECULES

S. I. Kubarev

M. V. Lomonosov Moscow State University

(Presented by Academician V. N. Kondrat'ev, October 10, 1959)

(Translation of: Doklady Akademii Nauk, Vol. 130, No.5
1960, pp. 1067-1070)

Original article submitted October 7, 1959.

There are still several incompletely solved theoretical problems in the field of long-wave electron spectra. Among things still requiring explanation are: the origin of the continuous bond spectra, their unavoidable presence (observed as early as 1922 by S. I. Vavilov [1]), their dependence on themperature and on $\lambda_{\text{excit.}}$ [2], and the mirror-symmetry problem [2, 3].

In the present communication we will show that all these problems can be attacked from a single point if one assumes that the adiabatic approximation is applicable to these systems. Such an approximation can be easily justified in cases where the molecules have discrete infrared spectra and the long-wave band is isolated from the rest of the spectrum [4]. According to Lax [5] the adiabatic approximation will give us the following Fourier representations for the spectral absorption and emission densities:

$$I_{\text{abs}}(t) = \frac{\mathrm{Sp}\left[M^{*}\exp\left(\frac{it}{\hbar}\hat{H}_b\right)M\exp\left(-\frac{it}{\hbar}\hat{H}_a\right)\exp(-\beta\hat{H}_a)\right]}{\mathrm{Sp}\,[\exp(-\beta\hat{H}_a)]}, \tag{1}$$

$$I_{\text{emit}}(t) = \frac{\mathrm{Sp}\left[M\exp\left(-\frac{it}{\hbar}\hat{H}_a\right)M^{*}\exp\left(\frac{it}{h}\hat{H}_b\right)\rho\right]}{\mathrm{Sp}\,(\rho)};$$

where $\rho$ is the distribution function in the excited state.* The general nature of these equations makes them suitable for various approximate calculations, such as the determination of bondshapes and their temperature dependence, and others. To do this it is enough to make just an approximate separation of the operators used in Eq. (1). Together with the criterion of applicability the given expression has a previous quantum mechanical basis.

1. Until very recently (see, for example, [2], p. 173) bands in the electron spectra of various molecules (classified according to the type of mirror symmetry) were considered to have different origins; at the present time this view has been discarded. The difference between the modulation and extinction spectra (as they are now called) is more terminological than actual, since both are covered by the adiabatic approximation. In a strict sence, the actual meaning of extinction spectra involves a consideration of the nonadiabatic nature of the

---

*In examing the luminescence we assume that $\rho$ is real. For solutions with a dense gas phase $\rho = \exp(-\beta\hat{H}_b)$. This explains why the luminescence band is independent of $\lambda_{\text{excit.}}$ Occasionally it is assumed that $\rho = \rho(T^{*})$ [6], where $T^{*}$ is different from the surrounding temperature. One can suppose that the dependence on $\lambda_{\text{excit.}}$ resides entirely in $\rho$.

system since in the adiabatic approximation no relaxation of electronic levels is possible. If the above-mentioned relaxation were pronounced, a low quantum yield of luminescence would be expected, which most experiments have failed to show.

A possible explanation for the origin of continuous bands was previously proposed [11] by us in a rather qualitative way. The applicability criterion of the semiclassical adiabatic approximation requires that the $W_k$ functions of the system be small, and depends on changes in the slow subsystem operators. To get a qualitative idea let us examine a simple case: M is constant and Ha, and Hb are the oscillator Hamiltonians, where $H_b - H_a = h\nu_0 + \Sigma A_i x_i$. The results of Lax [5] indicate that a semiclassical treatment is applicable only to those oscillators for which either

$$C_j^2 \equiv \frac{A_j^2}{2\hbar\,\mu_j\omega_j^3} \gg 1, \tag{2}$$

or,

$$C_j^2 \sim 1, \quad \bar{n} \gg 1. \tag{3}$$

By taking, for example, $\omega \simeq 10^{13}$ sec, $\mu \simeq 10^{-22}$ g, and assuming that the equilibrium distances in the ground and excited electronic states are displaced by about $5 \times 10^{-9}$ cm, we will find that $C^2 \simeq 10$, or in other words, that the semiclassical treatment is quite applicable provided the temperatures are not too low.

A semiclassical analysis of the degrees of freedom satisfying conditions (2) and (3) when the light is absorbed or emitted by a fast subsystem shows that each line in the band will be diffused to the extent given by the sum of the second moments of the semiclassical oscillators;

$$\Lambda^2 = \sum_{i\ (\text{semiclass})} C_j^2\,(2\bar{n}_j + 1)\,(\hbar\omega_j)^2\ . \tag{4}$$

The diffusion may extend over several hundreds of wave numbers. In complex molecules, where the frequencies are rather closely spaced, this will result in a continuous spectrum. If we allow for the fact that M is not constant and that the operators $H_a$ and $H_b$ represent anharmonic oscillators, we will complicate things by introducing additional configuration effects into the semiclassical degrees of freedom.

The proposed explanation for the origin of the band spectrum certainly is not the only possible one. Let us point out another possibility. It is usually assumed (see, for example, [2], chap. 2) that great anharmonicity gives rise to a strong interaction between vibrations. However, if we recall that the optically active electrons are localized on a finite number of bonds, then the effects of "peripheral" molecular sections can be included in the linear approximation to the coordinates of these sections. This observation seems to be very important as a basis for the oscillator approximation to the complex molecules. Since the number of "peripheral" groups in a complex molecule may be very large, then in a good approximation they can be regarded as an energy sink, interactions with which produce the diffused structure. Let us note that a quantitative analysis of the indicated possibility can also be obtained from the general relationships (1).

2. The almost universal occurrence of band spectra and their shape can be explained by means of the point-limit theorem [12]. Here it will involve the fact that the distribution of the normalized function $q = (\nu - \bar{\nu})/\sigma$ approaches the normal function as $n \to \infty$. In this case $\bar{\nu}$ is the location of the maximum, and $\sigma^2$ the second moment. We define $\underline{n}$ in the following manner: if N is the number of molecular degrees of freedom and $N = \sum n_i$, where $n_i$ is the number of oscillators with a frequency $\underline{i}$, then $n = \sum n_i \bar{n}_i$; $\bar{n}_i$, where $\bar{n}_i$ is the Planck mean. In a sufficiently big molecule $\underline{n}$ is large and the distribution can be represented by a converging series. One of such a series (proposed as early as 1955 by Edgewart [12]) has the form (see also [5]):

$$\begin{aligned} I(q) \simeq [\varphi(q)] - \left[\frac{1}{3!}\frac{\mu_3}{\sigma^3}\varphi^{(3)}(q)\right] + \left[\frac{1}{4!}\left(\frac{\mu_4}{\sigma^4} - 3\right)\varphi^{(4)}(q) + \frac{10}{6!}\left(\frac{\mu_3}{\sigma^3}\right)^2\varphi^{(6)}(q)\right] - \\ - \left[\frac{1}{5!}\left(\frac{\mu_5}{\sigma^5} - 10\,\frac{\mu_3}{\sigma^3}\right)\varphi^{(5)}(q) - \frac{35}{7!}\frac{\mu_3}{\sigma^3}\lambda\left(\frac{\mu_4}{\sigma_4} - 3\right)\varphi^{(7)}(q) - \frac{280}{9!}\left(\frac{\mu_3}{\sigma^3}\right)^3\varphi^{(9)}(q)\right] + \ldots \end{aligned} \tag{5}$$

Here $\varphi(q) = (2\pi)^{-1/2} \exp(-q^2/2)$; $\varphi^{(i)}(q)$ is the i-th derivation of $\varphi(q)$; $\mu_i$ moments at the center of mass, and $\mu_2 \equiv \sigma^2$. This series expands $I_{(q)}$ in terms of $1/\sqrt{n}$ with the last retained term being of the same order as the first neglected one [12] (brackets enclose terms of the same order). For the terminal $\underline{n}$ the deviations from a Gaussian distribution may be great especially if $\mu_3$ and $\mu_4$ are large, but for large $\underline{n}$ one will still get a good approximation by limiting the series to terms of the $n^{-1}$ order [i.e. the first three terms in Eq. (5)]. In general we will find that for a large class of complex molecules the radiation densities for both the absorption and emission can be represented by the same expression. Differences between individual molecules reside in the moments $\mu_i$, which can be calculated from Eq. (1).

To explain the temperature dependence of the bands one either has to calculate the traces in Eq. (1) or determine several first moments. Traces of type (1) have been calculated out by several workers for some special cases.

The case where M is constant, $\hat{H}_a$, $\hat{H}_b$ are the oscillator operators, and $\hat{H}_b - \hat{H}_a$ a linear function of the coordinates, was analyzed by Lax [5] (see also [7]). In this approximation

$$I_{\text{abs}}(t) = \exp\Big\{i2\pi\nu_0 t + \sum_j |w_j|^2 \Big[[\exp(-i\omega_j t) - 1] + \frac{\exp(i\omega_j t) + \exp(-i\omega_j t) - 2}{\exp(\beta\hbar\omega_j) - 1}\Big]\Big\}. \tag{6}$$

A more general case where both the equilibrium distances and the oscillator frequencies vary was examined by Kubo and Toyozawa ([13]; [5], p. 45). If M is constant and we assume that the frequencies change insignificantly we will get:

$$I_{\text{abs}}(t) = \exp\Big\{i2\pi\nu_0 t + \sum_j |w_j|^2 \Big[i \sin\omega_j t - \operatorname{cth}\frac{\beta\hbar\omega_j}{2}(1 - \cos\omega_j t)\Big] - \operatorname{cth}\frac{\beta\hbar\omega_j}{2}\frac{it}{2}\Gamma_j\Big\}; \quad \Gamma_j = \omega_j(a) - \omega_j(b). \tag{7}$$

One can readily see that the first moment in Eq. (6) is independent of temperature, i.e., that at this degree of approximation the position of the maximum does not depend as yet on temperature. The moment in Eq. (7) already shows a dependence on temperature.

3. An examination of the mirror symmetry with respect to frequencies using Eq. (1) presents no problem.* The condition for mirror symmetry with respect to $\nu_s$ can be written in the form:

$$I_{\text{abs}}(t) \exp(-i2\pi\nu_s t) \approx I_{\text{emit}}(-t) \exp(i2\pi\nu_s t). \tag{8}$$

with the accuracy as good as the coefficients.

One of the solutions is: $\nu_s = \nu_0$, $\text{Sp}\,e^{-\beta H} = \text{Sp}\,e^{-\beta TH}$, $T^2 = 1$. Where $\nu_0$ is the pure electronic transition frequency, $H_b = h\nu_0 + TH$, $H_a \equiv H$. At the same time M satisfies the condition TM = const · M. The given solution can be regarded as a consequence of the well-known Levshin conditions [14].

In order to be able, at least in principle, to get a qualitative picture for the mirror symmetry with respect to $\lambda$, we will derive in this case an analytical expression for the Fourier representation. Using a well-known property of the delta function,

$$\delta\left(E_{bn} - E_{am} - \frac{hc}{\lambda}\right) = \frac{\delta(\lambda - \lambda_1)}{|hc/\lambda_1^2|}, \quad \lambda_1 = \frac{hc}{E_{bn} - E_{am}}, \tag{9}$$

---

*From now on we will assume that $\rho = \exp(-\beta\hat{H}_b)$.

and then introducing it in an integral form, we get:

$$I_{\text{abs}}(\tau) = A v_m \sum_n \langle am \,|\, M \,|\, bn \rangle \langle bn \,|\, M \,|\, am \rangle \frac{hc}{(E_{bn} - E_{am})^2} \exp\left(-\frac{i\tau hc}{E_{bn} - E_{am}}\right). \tag{10}$$

It is more convenient to carry out the summation using $\frac{1}{y^2}\exp\left[i\tau\left(\lambda_s - \frac{hc}{y}\right)\right]$ ; as a center, where $\lambda_s$ is the line of symmetry. We can show that

$$\frac{1}{y^2}\exp i\tau\left(\lambda_s - \frac{hc}{y}\right) = -\int ikA(k)\, e^{iky} \frac{I_1(2\sqrt{k\tau(\lambda_s y - hc)}}{\sqrt{k\tau(\lambda_s y - hc)}}\, dk; \tag{11}$$

$A(k) = -i/4\pi$ when $k > 0$; $A(k) = 0$ when $k = 0$; $A(k) = i/4\pi$ when $k < 0$. Here $I_1$ is a Bessel function of the imaginary argument $y = E_{bn} - E_{am}$.

Introducing the integral representation of Sonin and Shleffli [15],

$$\frac{2I_1(z)}{z} = \frac{1}{2\pi i}\int_C \exp\left(\zeta + \frac{z^2}{4\zeta}\right)\zeta^{-2}\, d\zeta, \tag{12}$$

we will get:

$$\begin{aligned}\tilde{I}_{\text{abs}}(\tau) = &- A v_m \int ikA(k)\, dk \cdot \frac{1}{2\pi i}\int_C \exp(\zeta)\, \zeta^{-2}\, d\zeta \cdot \exp\left(-\frac{k\tau hc}{\zeta}\right) \times \\ &\times \left\langle am \middle| M \exp\left[\left(ik + \frac{k\tau\lambda_s}{\zeta}\right) H_b\right] M \exp\left[-\left(ik + \frac{k\tau\lambda_s}{\zeta}\right) H_a\right] \middle| am \right\rangle.\end{aligned} \tag{13}$$

A similar expression can be derived for the emission.

The mirror-symmetry condition with respect to $\lambda_s$ is $\tilde{I}_{\text{emit}}(\tau) = \tilde{I}_{\text{abs}}(-\tau)$.

Using Equation (7) to determine whether the necessary conditions for mirror-symmetry are satisfied we get the following formula for $\lambda_s$:

$$\lambda_s = \frac{hc}{h\nu_0 - \frac{\hbar}{2}\sum \Gamma_j \operatorname{cth}\frac{\beta\hbar\omega_j}{2}}. \tag{14}$$

Since $\Gamma_j > 0$, then according to Eq. (14) $\nu_0 > \nu_s$, or in other words the frequency of the pure electronic transition is displaced in this case towards the absorption maximum, which is in accord with the experimental results [16].

In concluding the author would like to thank Prof. N. D. Sokolov for his valuable advice and constant attention during the work.

## LITERATURE CITED

[1] S. I. Vavilov, Coll. Works, [In Russian] 1, (1952) p.8.

[2] B. I. Stepanov, Luminescence of Complex Molecules [In Russian], Izd AN Belorus. SSR (Minsk, 1955).

[3] B. S. Neporent, Zhur. Éksper. Teoret. Fiz. 21, 172 (1951).

[4] M. Born and Kun Huang, Dynamical Theory of Crystal Lattices [Russian Translation] (IL , 1958) Appendix VIII.

[5] M. Lax, J. Chem. Phys., 20, 1752 (1952). [translated in Collection: The Problems of Semiconductor Physics (IL, 1957), p. 42 ].

[6] B. I. Stepanov, Izvest. Akad. Nauk SSSR, Ser. Fiz. 22, 1034 (1958).

[7] O. Rickayzen, Proc. Roy. Soc. A241, 480 (1957).

[8] B. S. Neporent, Tr. GOI, 25, No.5 (1957).

[9] B. S. Neporent, Doklady Akad. Nauk SSSR 92, 927 (1953).

[10] B. S. Neporent and N. A. Borisevich, Optika i Spektroskopiya 1, 2 (1956).

[11] S. I. Kubarev, Doklady Akad. Nauk SSSR 126, 971 (1959).*

[12] H. Kramer , Mathematical Methods in Statistics [Russian translation] (IL, 1948).

[13] R. Kubo and Y. Toyozawa, Progr. Theor. Phys., 13, 160 (1955).

[14] V. L. Levshin, Photoluminescence of Liquids and Solids [In Russian] (1951) p. 96.

[15] M. A. Lavrent'ev and B. V. Shabat, Methods in the Theory of the Function of Complex Variables [In Russian] (1958) p. 592.

[16] N. A. Borisevich, Doklady Akad. Nauk SSSR 99, 695 (1954).

---

* Original Russian pagination. See C. B. translation.

# ISOTOPIC EXCHANGE OF OXYGEN ON OXIDATION CATALYSTS

L. Ya. Margolis and V. A. Kiselev

Physical Chemistry Institute, Academy of Sciences, USSR

(Presented by Academician V. I. Spitsyn, July 9, 1959)

(Translation of: Doklady Akademii Nauk SSSR, Vol.130, No.5, 1960, pp. 1071-1073)

Original article submitted July 6, 1959.

The chemical literature lists several works on the isotopic exchange of oxygen on metal oxides (semiconductors [1]) but hardly any on the exchange of oxygen on metallic oxidation catalysts, such as platinum and silver [2]. No one has studied specifically the effect of impurities on the rate of isotopic oxygen exchange; the only indirect data available are based on the work of G. K. Boreskov and co-workers who noted that traces of potassium sulfate increased the exchange rate on vanadium pentoxide [1]. Introduction of impurities alters the activity and selectivity of oxidation catalysts. The mobility of oxygen adsorbed on the contact surface plays a very important part in determining the course of the catalytic oxidation of various compounds [3]. Isotopic exchange of oxygen presents a means of establishing the actual extent of this mobility. It therefore seemed worthwhile to study the effects of impurities, introduced into the catalyst, on the rate of isotopic oxygen exchange, and this precisely was the purpose of this work.

We selected the following two typical oxidation contacts: silver metal, a catalyst for the oxidation of ethylene to ethylene oxide, containing halide impurities in the form of AgCl and AgI, and copper oxide, a catalyst for the oxidation of propylene into acrolein, containing lithium oxide, chromic oxide, bismuth oxide, and copper sulfate impurities. The halides were introduced into the silver by vigorously agitating powdered silver in a AgCl or AgI solution, and controlling the surface distribution of the halide with the help of $Cl^{36}$ and $I^{131}$ isotopes.

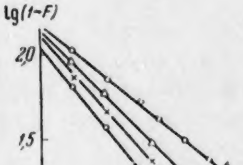

Fig. 1. Kinetic curves for the isotopic exchange of oxygen at 232°C on porous silver containing: 1) 0.0015% AgCl; 2) 0.002% AgCl; 3) 0.004% AgCl; 4) 0.0015% AgCl.

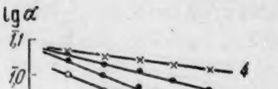

Fig. 2. Kinetic curves for the homolytic exchange of oxygen on porous silver containing: 1) 0.0015% AgCl; 2) 0.002% AgCl; 3) 0.004% AgCl; 4) 0.0015% AgCl.

Various metallic oxides were introduced into copper oxide by mixing or coprecipitating the respective nitrates or carbonates and firing the mixture at 700°. To introduce the $SO_4^{2-}$ ion we mixed ammonium sulfate solutions with copper nitrate solutions, evaporated the mixtures to dryness, and fired the residues at 700°. The experiments were carried out in a static low-pressure system (not over 1 mm of Hg). The $O^{18}$ isotopic content was determined mass-spectrophotometrically from the relative magnitude of the mass-36, 34, and 32 lines. The initial heavy oxygen contained 15-20 mole % of $O^{18}$. From the relative concentration changes of the $O_2^{18}$ (mass 36) and $O^{16}O^{18}$ (mass 34) in the gas phase we determined the rate of the homolytic isotopic exchange of oxygen $O_2^{18} + O_2^{16} \rightleftharpoons 2O^{16}O^{18}$. The isotopic exchange rate was calculated using the equation:

$$(1 - F) = - Kt,$$

where

$$F = \frac{C_0 - C}{C_0 - C_\infty}$$

is the exchange ratio, K the exchange rate constant, $C_\infty$ the concentration of $O^{18}$ at equidistribution, $C_0$ the initial $O^{18}$ concentration, C the concentration of $O^{18}$ at time t.

TABLE 1

| Impurity | Impurity conc., wt. % | $K_{exch.}$, min/m² | $K_{hom.}$, min/m² |
|---|---|---|---|
| Chlorine as silver chloride | 0.0015 | $7.8 \cdot 10^{-4}$ | $3 \cdot 10^{-4}$ |
|  | 0.0020 | $7.5 \cdot 10^{-4}$ | $2.8 \cdot 10^{-4}$ |
|  | 0.0040 | $6.6 \cdot 10^{-4}$ | $2.0 \cdot 10^{-4}$ |
|  | 0.015 | $5.5 \cdot 10^{-4}$ | $1.1 \cdot 10^{-4}$ |

TABLE 2

| Impurity | Conc., mole % | Surface, m²/g | Init. isot. exch. rate per m² |
|---|---|---|---|
| – | 0 | 0.25 | 0.066 |
| $Cr_2O_3$ | 2 | 0.40 | 0.063 |
| $Bi_2O_3$ | 2 | 0.40 | 0.025 |
| $Li_2O$ | 2 | 0.2 | 0.172 |
| $CuSO_4$ | 2 | 1.0 | 0.01 |

In Fig. 1 we have plotted the kinetic curves for the isotopic exchange of oxygen on silver which contained various concentrations of chloride ion. For at least 150 min the reaction was monomolecular. In Fig. 2 we have plotted the kinetic curves for the homomolecular isotopic exchange on these same samples of doped silver ($\alpha$ is the mass ratio, 36/34).

Table 1 lists the rate constants for the isotopic exchange of oxygen at 232° on silver doped with chloride ions.

The exchange rate constant changes monotonically with concentration. When the chloride content of the silver is increased tenfold the exchange rate decreases to two thirds of its former value. The rate constant of the homolytic exchange, which is related to the dissociation of oxygen molecules into atoms, decreases by one third when the chloride concentration is increased by a factor of ten.

The introduction of iodide ion must somehow modify the silver catalyst since it was found that at a certain iodide concentration the yield of ethylene oxide increased [3]. A study of the isotopic catalytic exchange on this particular catalyst revealed that the addition of iodide sharply increases the homolytic oxygen exchange rate but has hardly any effect on the molecular isotopic exchange rate. The addition of halides to silver changes the mobility and the ratio between the molecular and atomic oxygen adsorbed on the catalytic surface. These impurities probably act on the exchange rate by altering the surface charge on the silver metal and, consequently, the heats and activation energies for the adsorption and desorption of oxygen.

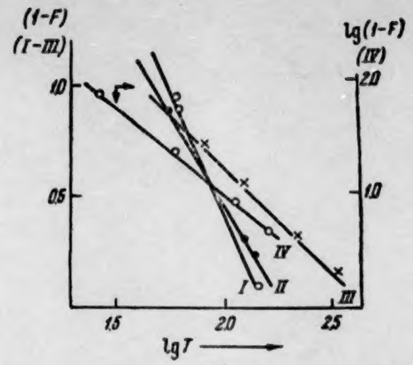

Fig. 3. Kinetic curves for the isotopic exchange of oxygen at 412° on: I) CuO; II) CuO + 2% $Bi_2O_3$; III) CuO + 2% $Cr_2O_3$; IV) CuO + 2% $Li_2O$.

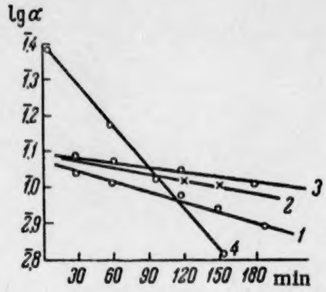

Fig. 4. Kinetic curves for the homolytic isotopic exchange of oxygen at 412° on: 1) CuO; 2) CuO + 2% $Bi_2O_3$; 3) CuO + 2% $Cr_2O_3$; 4) CuO + 2% $Li_2O$).

It also seemed interesting to investigate the effects of impurities in catalysts other than silver, such as metallic oxide semiconductors, on the isotopic oxygen exchange rate. In Fig. 3 we have plotted the kinetic curves for the isotopic exchange of oxygen on copper oxide doped with $Cr_2O_3$, $Bi_2O_3$, and $Li_2O$. The isotopic exchange on these oxides is not a monomolecular process; the experimental results on pure copper oxide, and on CuO doped with $Bi_2O_3$ and $Cr_2O_3$, fit the Roginskii-Zel'dovich equation, $dF/dt =$ $= al^{\alpha F}$ (see Fig. 3 and 4). The deviation of the isotopic exchange rate from first-order kinetics may probably be attributed to a nonhomogenous surface on CuO. Kasatkina and Boreskov observed similar kinetics in the isotopic exchange of oxygen on $MnO_2$ [1].

The isotopic exchange rate on CuO doped with $Li_2O$ obeyed a bilogarithmic law, which also indicates that the CuO surface is not homogeneous; such behavior would indicate a surface, portions of which exhibit an exponential distribution of exchange activation energies.

In Table 2 we have listed the initial isotopic oxygen exchange rates at 412°, reduced to 1 $m^2$ of doped copper oxide surfaces.

Introduction of chromic oxide into CuO has practically no effect on the isotopic oxygen exchange rate. Addition of $Bi_2O_3$ reduces the rate to 1/3, while addition of $Li_2O$ increases the exchange rate by a factor of 3. The presence the $SO_4^{2-}$ ion on the copper oxide surface sharply reduces the isotopic oxygen exchange rate. It is interesting to note that the isotopic exchange rate depends on the surface charge of the semiconducting oxidation catalysts [4].

Thus by introducing impurities into both the metallic (silver) and oxide semiconducting (CuO) oxidation catalysts one can regulate the isotopic exchange rate of oxygen, and consequently its mobility on the catalyst surface.

## LITERATURE CITED

[1] E. R. S. Winter, J. Chem. Soc. 3342 (1954); 2726 (1955); S. M. Karpacheva and A. N. Rozen, Doklady Akad. Nauk 68, 1057 (1949); 75, 239 (1956);*Zhur. Fiz. Khim. 27, 146 (1953); G. Ya. Turovskii and F. M. Vainshtein, Doklady Akad. Nauk 72, 297 (1950); L. Ya. Margolis and G. Plyshevskaya, Izvest. Akad. Nauk SSSR, Otdel Khim. Nauk 415 (1952);*W. C. Cameron, A. Farkes and L. M. Litz, J. Phys. Chem. 57, 229 (1953); L. A. Kasatkina and G. K. Boreskov, Zhur. Fiz. Khim. 29, 453 (1955); L. A. Kasatkina, G. K. Boreskov, Z. L. Krylova, and V. V. Popovskii, Izvest. Vysh. Ucheb. Zaved. 1, 12 (1958).

[2] L. Ya. Margolis, Izvest. Akad. Nauk SSSR, Otdel Khim. Nauk 2, 225 (1959).*

[3] L. Ya. Margolis, Usp. Khim. 28, 5, 615 (1959).

[4] E. Kh. Enikeev, L. Ya. Margolis, and S. Z. Roginskii, Doklady Akad. Nauk 124, 606 (1959).*

---

*Original Russian pagination. See C. B. translation.

# THERMODYNAMIC PROPERTIES OF INDIUM ANTIMONIDE

A. V. Nikol'skaya, V. A. Geiderikh, and Corresponding
Member Acad. Sci. USSR, Ya. I. Gerasimov

M. V. Lomonosov Moscow State Universtiy

(Translation of: Doklady Akademii Nauk SSSR, Vol. 130, No.5,
1959, pp. 1074-1077)

Original article submitted November 5, 1959.

Indium and antimony form a single intermetallic compound InSb with a m.p. of 530 ± 5° [1]. The phase diagram for the In–Sb system is shown in Fig. 1.

Indium antimonide belongs to the $A^{III}B^{V}$ group of semiconductors, all of which have the zinc blende structure; the physical properties of this compound which might have any bearing on its semiconducting nature have been studied quite extensively (see [2] for an extensive bibliography).

The thermodynamic properties of indium antimonide are reported in [3-6]. Its heat of formation was determined by the tin calorimetric method [3,4]. The standard free energies ($\Delta F^0$) and entropies of formation ($\Delta S^0$) have also been calculated [4]. The heat capacity of indium antimonide was determined in the range from 20-500°C together with the heat of fusion [5]. In [6] the heat capacities of several semiconductors, among them indium antimonide, are reported; the latter was studied in the range from 80-300°K.

The purpose of the present work was to calculate some thermodynamic constants of indium antimonide from the e.m.f. determined experimentally in chemical cells. We studied the e.m.f. in concentration cells of the type:

$$\mathrm{In}\,(l)\,|\,(\mathrm{KCl}-\mathrm{LiCl})+\mathrm{InCl}\,|\,(\mathrm{InSb}+\mathrm{Sb})\,(s).$$

by varying the concentration of the electrode material.

The cell reaction:

$$\mathrm{In}\,(l)+\mathrm{Sb}\,(s)=\mathrm{InSb}\,(s)$$

gives rise to an e.m.f., from which the $\Delta F$ can be calculated using the equation:

$$\Delta F=-zFE; \tag{1}$$

where F is Faraday's number, equal to 23,066 cal/g equiv.; E the e.m.f. in volts; and $\underline{z}$ the ionic charge, in this case ($\mathrm{In}^+$), z = 1.

By studying the temperature dependence of e.m.f. we can determine $\Delta F$ as a function of T, and consequently calculate the enthalpy and entropy of formation for InSb by using the equations:

$$\Delta S=-\frac{d\Delta F}{dT}=zF\,\frac{dE}{dT}; \tag{2a}$$

$$\Delta H=\Delta F+T\,\Delta S. \tag{2b}$$

## EXPERIMENTAL

Our study covered the temperature range from 390-490°C. We studied alloys containing 59.9 and 67.2 mole % of Sb, which constituted a heterogeneous mixture of InSb + Sb.

The alloys were prepared by fusing weighed amounts of indium and antimony; the method is very widely used for the preparation of antimonides and arsenides of indium and gallium and has been described in several papers dealing with the electrical properties of these compounds (see, for example, [7]).

In our work the fusion was carried out at 635-650°C in evacuated quartz tubes. The metals used were 99.99% pure. In order to mix metals well, the tubes containing the molten mixture were turned over several times; after being maintained at 635-650° for a while the alloy was cooled to 450° and maintained at that temperature for several hours.

The resulting alloy was thoroughly ground in a jasper mortar and the powder compressed into the alloy electrodes; a 0.5 mm tungsten wire outlet was incorporated into each electrode. The cylindrical electrodes were 6 mm in diameter and 10-15 mm long.

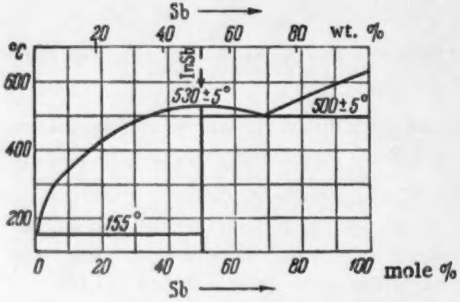

Fig. 1. Phase diagram for the system In–Sb.

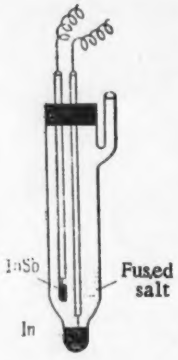

Fig. 2. Exterior view of the cell.

Instead of an electrolyte we used a fused autectic mixture of lithium chloride and potassium chloride with a trace (0.1%) of indium monochloride.

Indium monochloride was prepared according to the instructions given in [8]. First we prepared indium trichloride by burning indium metal in a stream of chlorine, then melted a mixture of indium metal and indium trichloride in an evacuated quartz tube; the fusion was accompanied by the reaction:

$$InCl_3 + 2In = 3InCl.$$

The cell was put together in a specially designed quartz container, shown in Fig. 2. The narrow bottom part was filled with liquid indium, and over it was fastened the alloy electrode. The cell was immersed in a 40 mm wide 450 mm long cylindrical quartz vessel, which was closed with a ground stopper; sealed into the latter were the tungsten leads and a platinum–platinorhodium thermocouple used for measuring the cell temperature. The cylindrical vessel served as a jacket for the cell and made it possible to carry out the experiment in an inert atmosphere (pure argon). The cell was heated electrically in a specially designed cylindrical metal tube. The cell was submerged to the middle of the heater (about 300 mm from the top), where a constant temperature zone 50 mm high was maintained; under these conditions the possibility of a thermal e.m.f. was minimized. The heater was regulated in such a way that the temperature inside the cell could be maintained within ± 1°C. At the beginning of each experiment it took 10-12 hours to establish a reversible e.m.f., but later, in going to other temperatures, equilibrium could be attained in less time. The temperature dependence of the e.m.f. was followed both with increasing and with decreasing temperatures. The results were reproducible to within ± 1.0 mv. Our experimental results are plotted in Fig. 3.

Using the method of leastsquares we derived from our experimental data the equation:

$$E = (0{,}3455 - 0{,}241 \cdot 10^{-3}T)\text{v}$$

from which with the help of Equations (1) and (2) we calculated the change in free energy, enthalpy, and entropy for the formation of 1 mole of InSb from liquid indium and solid antimony:*

$$\Delta F = -FE = -23{,}066\,(0{,}345 - 0{,}241 \cdot 10^{-3}T) = -7{,}97 + 5{,}56 \cdot 10^{-3}T \text{ kcal/mole}$$

And from this we find that within the investigated temperature range

$$\Delta H = -3{,}98 + 0{,}20 \text{ kcal/mole}$$

$$\Delta S = -2{,}78 \pm 0\ 25 \text{ kcal/mole} \cdot \text{deg}$$

The accuracy of the $\Delta F$ depends on the reproducibility of the e.m.f. data, and since the latter was good to within ± 1mv, we get a deviation of ± 0.01 kcal/mole for the free energy.

Using our own experimental values for the specific heats of the pure metals [9] and indium antimonide [5], and for the heat of fusion of indium [9], we calculated the standard values for these thermodynamic functions. The following were obtained:

$$\Delta F_{298} = -3{,}07 \pm 0{,}01 \text{ kcal/mole}$$

$$\Delta H_{298} = -3{,}67 \pm 0{,}20 \text{ kcal/mole}$$

$$\Delta S_{298} = -2{,}01 \pm 0{,}25 \text{ kcal/mole} \cdot \text{deg}$$

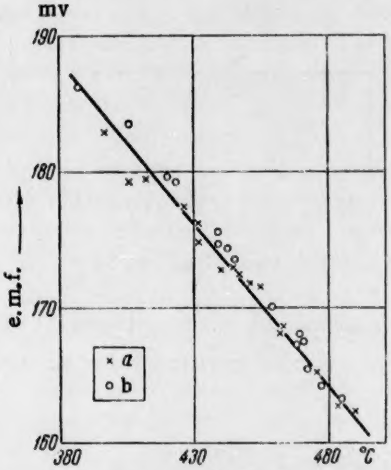

Fig. 3. E.m.f. as a function of temperature at various over-all compositions of the alloy-electrodes. a) Alloy containing 59.9 mole % Sb; b) alloy containing 67.2 mole % Sb.

---

*1 cal = 4.1840 absolute joules.

## A COMPARISON WITH THE LITERATURE DATA

In Table 1 we have compared our results with the literature data on indium antimonide.

The $\Delta H_{723}$ given in the 1st row of Table 1 was obtained by Kleppa, who used the tin calorimetric method, while the $\Delta H_{298}$ we calculated from Kleppa's $\Delta H_{723}$ using the same heat capacity data as that which we used to convert our results to the standard temperature. Rows 2 and 3 contain the standard free energies calculated by two independent routes [4]. The value given in the 2nd row was calculated from the phase diagram of the In–Sb system by using Wagner's method [10] and the liquidus curve, which represents the equilibrium between the alloy and the solid InSb phase; we also determined calorimetrically the heat of fusion of the compound, since both it and the melting point are needed in these calculations. Row 3 contains the values calculated by using the equation $\Delta F = \Delta H - T\Delta S$; we used in these calculations our own experimentally determined heats of formation and the standard entropies of formation calculated from the absolute entropy data taken from the literature. For InSb the latter was determined from tabulated values, $\theta/T$ where $\theta$ is the Debye temperature, taken by us as equal to $200 \pm / 5°$.

Table 1 shows that the differences between our heats of formation and those previously reported [4] for indium antimonide lie entirely within the range of experimental errors. The change in free energy and entropy calculated from the e.m.f. data are also in good agreement with Shottky's and Bever's calculations [4].

TABLE 1

| Nos. | $-\Delta H_{723}$, kcal/M | $-\Delta H_{298}$, kcal/M | $-\Delta H_{273}$, kcal/M | $-\Delta F_{298}$, kcal/M | $-\Delta S_{298}$, kcal/M·deg | Method | Author |
|---|---|---|---|---|---|---|---|
| 1 | 4.30 | 4.00 | | | | calorimetric | [3] |
| 2 | | | | 3.02 | | calculated according to [10] | |
| 3 | | | 3.47 | 2.88 | 1.99 | calculated from calorimetric data | [4] |
| 4 | 3.98 | 3.67 | – | 3.07 | 2.01 | e. m. f. | this paper |

## LITERATURE CITED

[1] M. Hansen and K. Anderko, Constitution of Binary Alloys, (New York-London ,1958) .

[2] New Semiconductors [Russian translation], Coll. of papers translated from English, edited by V. T. Kolomeits (IL, 1958).

[3] O. J. Kleppa, J. Am. Chem. Soc. 77, 897 (1955).

[4] W. Schottky and M. Bever, Acta Metal. 6, 5, 320 (1958).

[5] N. H. Nachtrieb and N. Clement, J. Phys. Chem. 62, 7, 876 (1958).

[6] P. V. Gul'tyaev and A. V. Petrov, Fizika Tverdogo Tela 1, 3, 368 (1959).

[7] R. G. Breckenridge, R. F. Blunt, et al., Phys. Rev. 96 (3), 571 (1954); R. Barrie, F. A. Gunnel et al., Phys. Rev. 20, 1087 (1954).

[8] G. Brauer, ed. A Handbook of Synthetic Inorganic Chemistry [Russian translation] (IL, 1956).

[9] O. Kubaschewski and E. Evans, Metallurgical Thermochemistry [Russian translation] (IL, 1954).

[10] C. Wagner, Acta Metal. 6, 5, 309 (1958).

# THE EFFECT OF ALKALI METAL HALIDES ON THE AMOUNT OF HYDROGEN ADSORBED ON PLATINUM BLACK

Academician Acad. Sci. Kazakh. SSR D. V. Sokol'skii
and G. D. Zakumbaeva

Institute of Chemical Sciences, Academy of Sciences, Kazakh. SSR.

(Translated from Doklady Akademii Nauk SSSR, Vol. 130, No.5
1959, pp. 1078-1080)

Original article submitted October 8, 1959.

It is very important to know the effect of the surrounding medium on the amount of hydrogen adsorbed on platinum black. By studying the reduction of platinum oxide to platinum black [1] it is possible to determine directly the amount of hydrogen adsorbed. In the present work we investigated the reduction rate of reduction oxide to platinum black and determined the amount of hydrogen adsorbed on the latter in the presence of potassium chloride, bromide, and iodide in 50% ethanol solutions. Platinum oxide was reduced in a catalytic duck-shaped vessel. At fixed time intervals we determined by difference the amount of hydrogen consumed and measured the potential of the catalyst electrode (with reference to a 0.1 N calomel electrode).

The curves plotted in Fig. 1 were obtained during the reduction of platinum oxide at 30° in 50% ethanol solutions at various potassium bromide concentrations. Figure 1 shows that the reduction rate of platinum oxide is almost the same in 0.01 N and 0.1 N potassium bromide solution (in 50% $C_2H_5OH$). When the potassium bromide concentration is further increased the rate slightly declines. As the reduction of platinum oxide proceeds the potential of the catalyst electrode increases, approaching its reversible value.

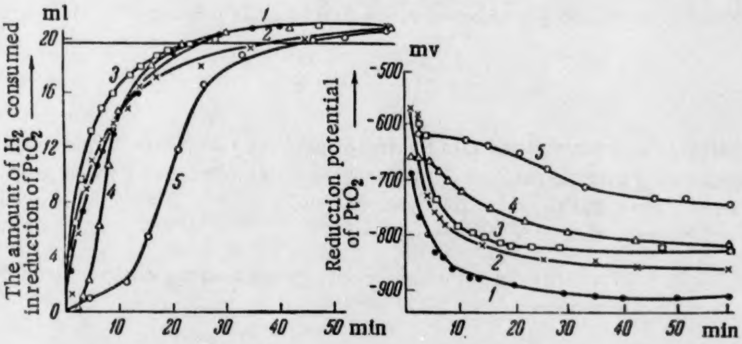

Fig. 1. The effects of potassium bromide on the reduction rate of platinum oxide to platinum black, at 30°. 1) 50% Ethanol; 2) 0.01 N KBr; 3) 0.1 N KBr; 4) 0.5N KB3; 5) 1 N KBr.

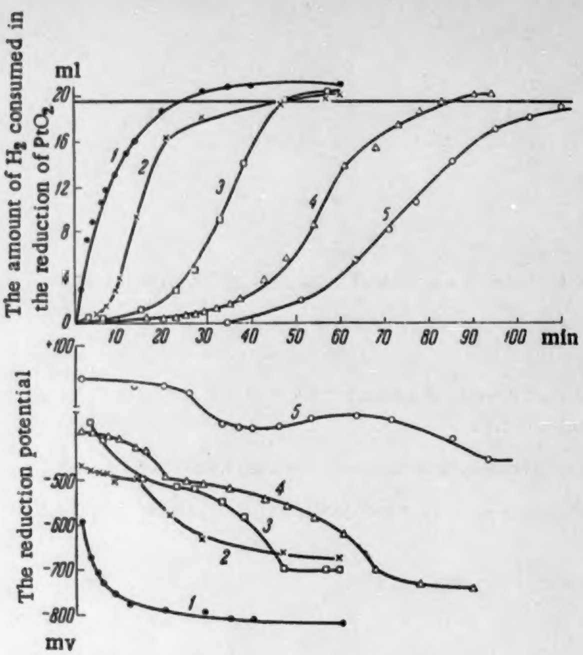

Fig. 2. The effects of potassium iodide on the reduction rate of platinum oxide to platinum black, at 30°. 1) 50% Ethanol; 2) 0.01N KI; 3) 0.1N KI; 4) 0.5N; 5) 1N KI.

In Fig. 2 we have plotted the curves obtained during the reduction of platinum oxide in the presence of potassium iodide at 30°. Figure 2 shows that the reduction rate of platinum oxide in potassium iodide solutions is much slower than the corresponding rate in plain 50% ethanol. This can be noted even in the 0.01 N potassium iodide solution. When the potassium iodide concentration is further increased an induction period appears which attains 6 min in 0.1 N KI and 15 min in 0.5N KI, while in 1N potassium iodide the reduction takes 125-130 minutes. Moreover, during the reduction of platinum oxide in 1 N potassium iodide, free iodine is evolved at the beginning of the experiment, the solution changes first to a red, then a brown color, and the potential drops into the oxide region (+20 mv). The platinum black obtained in 1 N potassium iodide is partially deposited on the electrode and partially on the walls of the duck-shaped vessel, while the portion remaining in solution is highly dispersed. It seems that initially the reduction of platinum oxide proceeds by an electronic mechanism where the iodide ion adsorbed on the Pt-electrode is reduced to elementary iodine:

$$2I^- \xrightarrow{-2e} I_2 \qquad (1)$$

The elementary iodine is soon reconverted into the iodide ion, since after 30-35 minutes the color suddenly disappears. It is interesting that the reaction should occur in a stream of such a strong reducing agent as hydrogen. Figures 1 and 2 show that the reversible potential of the catalyst is more positive in the presence of potassium iodide and bromide than in plain 50% ethanol.

Our results clearly indicate that the nature of the solvent has a strong effect on both the rate and the mechanism of platinum oxide reduction,

$$PtO_2 + 2H_2 \rightarrow Pt + 2H_2O. \qquad (2)$$

Using Eq. (2) we find that 19.7 ml of hydrogen are required to reduce 0.1 g of $PtO_2$. The difference between the amount of hydrogen consumed in the experiment and the calculated stoichiometric amount (19.7 ml) gives the total amount adsorbed on the platinum black. As can be seen in Table 1, the amount of hydrogen adsorbed on a gram of platinum black does depend on the surrounding medium. Thus, for example, in 50%

TABLE 1

**The Effects of Medium of the Adsorption of Hydrogen on Platinum Black**

| Solvent | Electrolyte conc., g-equiv. | Amt of $H_2$ used to reduce and saturate 0.1 g of $PtO_2$, ml | Amt of $H_2$ adsorbed on 1 g of Pt-black, ml |
|---|---|---|---|
| 50% $C_2H_5OH$ | 0 | 20,8 | 12,9 |
| 50% $C_2H_5OH$ + KCl | 0,1 | 20,8 | 12,9 |
|  | 0,5 | 20,6 | 10,5 |
| 50% $C_2H_5OH$ + KBr | 0,01 | 20,7 | 11,64 |
|  | 0,1 | 20,7 | 11,64 |
|  | 0,5 | 20,6 | 10,5 |
|  | 1 | 20,6 | 10,5 |
| 50% $C_2H_5OH$ + KI | 0,01 | 20,6 | 10,5 |
|  | 0,1 | 20,4 | 8,1 |
|  | 0,5 | 20,2 | 5,8 |
|  | 1 | 19,9 | 2,3 |

ethanol 12.9 ml of hydrogen were adsorbed on each gram of platinum black. In potassium chloride and bromide solutions the amount of hydrogen adsorbed is on the average 1.3 ml less than in plain 50% ethanol and is practically independent of concentration. In the presence of potassium iodide the amount of hydrogen adsorbed decreases appreciably with increasing electrolyte concentration. A gram of platinum black adsorbs only 2.3 ml of hydrogen in the presence of 1 N potassium iodide. Thus the adsorption of halides not only decreases the hydrogen to surface bond energy [2], but to a considerable extent changes the amount of hydrogen adsorbed on the catalytic surface.

## LITERATURE CITED

[1] D. V. Sokol'skii and Yu.A. Skopin, Doklady Akad. Nauk 126, No.2, 334 (1959).*

[2] A. N. Frumkin, The Kinetics of Electrode Processes [in Russian] (Moscow, 1952) p. 24.

[3] D. V. Sokol'skii and G. D. Zakumbaeva, Doklady Akad. Nauk 124, 4, 880 (1959).*

---

*Original Russian pagination. See C. B. translation.

# REVERSIBLE CHANGES IN THE GASEOUS PERMEABILITY OF POLYMERS DURING $\gamma$-IRRADIATION

N. S. Tikhomirova, Yu. M. Malinskii, and V. L. Karpov

L. Ya. Karpov Physical Chemistry Institute and the Institute
of Plastic Industry

(Presented by Academician V. A. Kargin, July 30, 1959)

(Translation of: Doklady Akademii Nauk SSSR, Vol. 130, No.5
1950, pp. 1081-1084)

Original article submitted July 14, 1959.

It is a well-known fact that the structural and chemical changes produced in polymers by ionizing radiation are accompanied by a great number of changes in their polymeric properties [1].

Very little work has been done on the diffusion of gases through polymers exposed to radiation, and the little that has been done was mainly concerned with the permanent effects of radiation on the permeability of polyethylene to gases and vapors [2,4]. These studies showed that the gaseous permeability constant depended on the integral radiation dose received by polyethylene. However, the diffusion of gases through polymers while they are exposed to radiation has not been investigated, despite the practical and theoretical importance of the problem.

Mokul'skii and Lazurkin [5] studied the mechanical properties of polymers exposed to the radiation from a nuclear reactor. They detected certain reversible mechanical radiation effects. Some of these changes appeared during irradiation and disappeared when the exposure was discontinued. One would naturally expect a similar reversible radiation effect on the diffusion of gases through polymers. The aim of the present work was to establish the existence of such an effect.

The work was carried out using a manometric technique and $\gamma$-radiation from a $Co^{60}$ source with an activity of 20 kg equiv. of radium [7]; dose intensities up to 700 rad/sec were employed.

The permeability constants were measured on the apparatus represented schematically in Fig. 1.

The apparatus consisted of three principal units: 1) A diffusion cell inside of which the investigated film was fastened between two flanges and sealed tight by means of a lead ring [Fig. 1,1). One side of the film was evacuated while the other contained the gas (under 600-700 mm pressure). The film surface varied from 1.5 to 1.7 $cm^2$, depending on how tightly the film was stretched. Films 90 and 120 $\mu$ thick were studied. 2) A movable vacuum set-up placed on a cart and consisting of a forepump and a mercury diffusion pump (Fig. 1,2). 3) A manometer for the remote determination of pressure (Fig. 1, 3); * the manometer operated on the principle that the inductance of the gauge coil would change when the center core made of a ferro-resonance alloy was displaced. The gauge coil was wrapped around the U-shaped mercury manometer and the reservoir. The core was afloat on the mercury surface. When the pressure inside the system changed, the float was displaced together with the mercury and the accompanying change in the coil inductance was recorded on an ÉPVI-14 instrument (measurements were accurate to ± 0.05 mm of Hg). The permeability constant was measured by recording the pressure increase in the vacuum chamber as a function of time.

---

* The manometer was designed by V. B. Osipov.

The assembled diffusion cell and the chamber filled with the inert gas were tested for leaks. The vacuum set-up and the remote manometer were connected to the cell through ground joints. After the entire system was evacuated the vacuum set-up was disconnected and removed from the irradiated zone.

Before introducing the radiation source we measured the rate of pressure increase in the evacuated portion of the system and plotted the pressure as a function of time, p = f(t). After ascertaining that a steady diffusion rate was achieved and that the function p = f(t) was linear we introduced the radiation source. The pressure in the evacuated chamber began to increase at a higher rate but the function p = f (t) still remained linear. The rate remained constant as long as the integral dose received by the film had not produced any noticeable structural changes in the polymer. After the source was removed the diffusion rate returned to its original value.

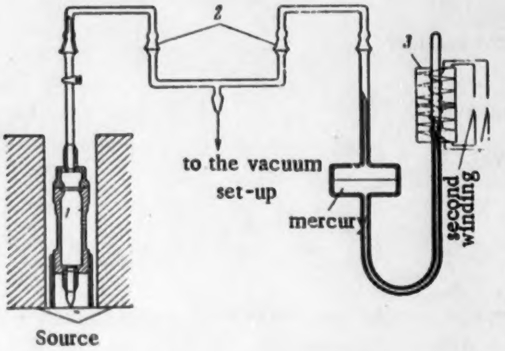

Fig. 1. A schematic representation of the apparatus.

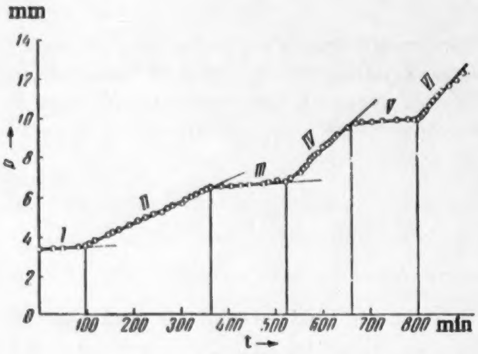

Fig. 2. The increase in helium pressure on the evacuated side of polyethylene at 10° as a function of time. I, III, and V) in the absence of radiation; II, IV, and VI) during irradiation.

Before the experiment a correction was determined for the increase in pressure caused by the evolution of gases from the film and the stopcock grease during irradiation. This was done by evacuating the entire system, placing the diffusion cell right in the middle of the source, and exposing it to uninterrupted radiation for 6 hours. All during this time the pressure remained constant to within ± 0.05 mm of Hg. Therefore the correction for the evolution of gases from the irradiated film and grease could be disregarded.

In Fig. 2 we have plotted the function p = f (t) for helium before and during the irradiation of polyethylene at 10°C; the dose intensity was 720 rad/sec. Figure 2 shows that the pressure increases immediately after the source is introduced and not gradually while the source is brought nearer, as one would have expected. This can be explained by the fact that at lower dose intensities (of the order of 100 rad/sec), as was shown by special experiments, practically no rate increase is observed (at 20-22°). During the experiment water was run through a metallic jacket around the cylindrical source so as to cool the empty space inside and maintain a constant temperature; this was regulated by means of a heating element and a thermal regulator. The experimentally determined permeabilities of polyethylene to helium and xenon at various dose intensities are listed in Table 1. The permeability constants were calculated from Fick's steady-flow equation.

As can be seen in Table 1 the increase in the diffusion rate shows a strong dependence on the dose intensity. The higher the dose intensity the more is the relative diffusion rate increased. Whereas the diffusion rate of helium (t = 17°) increases by a factor of three when the radiation dose intensity is 300 rad/sec, about a tenfold increase is observed at 730 rad/sec (t = 10°).

With xenon the effect is even more pronounced. A dose intensity of 180 rad/sec increased the diffusion

TABLE 1

| Expt. no. | Temp., °C | Polymer | Gas | $p_0$ (from the graph). | Permeability | | $\frac{p_1}{p_0}$ | Dose intensity, rad/sec |
|---|---|---|---|---|---|---|---|---|
| | | | | | in the absence of radia. $p_0 \cdot 10^{10}$ | after radiation $p_1 \cdot 10^{10}$ | | |
| 1 | 17 | polyethylene | helium | 1,8 | — | 4 | 2,22 | 180 |
| | | | | 1,8 | 2,44 | — | 1,65 | 180 |
| 2 | 17 | polyethylene | helium | 1,8 | 1,92 | 6,0 | 3,12 | 300 |
| | | | | 1,8 | 2,68 | 5,6 | 2,08 | 300 |
| | | | | 1,8 | 2,56 | 5,67 | 2,22 | 300 |
| | | | | 1,8 | 2,93 | 5,25 | 1,79 | 300 |
| 3 | 10 | polyethylene | helium | 1,12 | 1,0 | 6,1 | 6,1 | 730 |
| | | | | 1,12 | 1.08 | 12,5 | 11,6 | 730 |
| | | | | 1,12 | 1,15 | 14,8 | 12,9 | 730 |
| 4 | 15 | polyethylene | xenon | 0,24 | — | 2,55 | 10,6 | 730 |
| | | | | 0,24 | — | 3,70 | 15,4 | 730 |
| 5 | 40±2 | polyethylene | xenon | 5,25 | — | 15,6 | 3,1 | 180 |
| | | | | 5,25 | 5,05 | 15,7 | 2,8 | 180 |
| 6 | 15 | polytetrafluoroethylene | helium | — | 8,0 * | 14 | 1,75 | 560 |
| | | | | — | 6,79 | 12,2 | 1,70 | 560 |

---

*Film was tested after exposure to 0.7 Mrad.

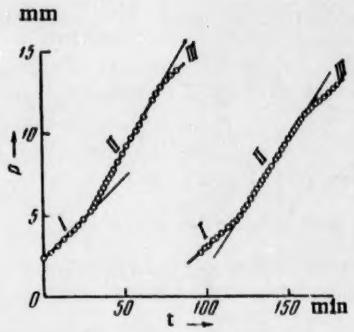

Fig. 3. Increase in the helium pressure on the evacuated side of polytetrafluoroethylene at 15° as a function of time. I and III) in the absence of radiation; II) during irradiation.

rate (at 40°) by a factor of three, while 730 rad/sec increased it by 10-15 times* (at 15°C). At high dose intensities we also noted that each time the source was reintroduced the relative diffusion rate (during irradiation) would increase by a larger factor. When the dose intensities were low and consequently the rate increase rather small ($p/p_0$ 2-3) no increase in the $p/p_0$ ratio was detected after numerous irradiations (experiments 2 and 5, Table 1).

Each time the source is removed the diffusion rate again changes abruptly approaching the initial value but remaining slightly above it. There seems to remain a kind of "aftereffect" which also increases after each irradiation period. Table 1 and Fig. 3 both show that after four exposures to radiation lasting altogether 160 min the permeability constant increased from $1.92 \cdot 10^{10}$ to $2.93 \cdot 10^{10}$ cm$^3$/cm$^2$ sec · cm/atm. However in certain cases this effect is insignificant, see, for example, experiment 3.

---

*Due to the slow diffusion rate through polethylene at 15° and the limited range of pressures that can be measured with the type of manometer used we were unable to determine the permeability constant of xenon at 15°. We therefore used for xenon the values of p from the graph of log p vs. 1/T (Fig. 4); the plotted data were obtained on a polyethylene film at various temperatures using similar apparatus but equipped with a McLeod gauge. The results are presented in Table 1. For comparison we have also listed permeability data for helium and polyethylene.

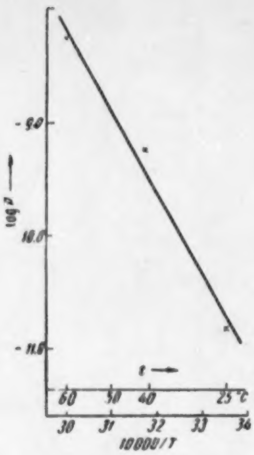

Fig. 4. The permeability of polyethylene to xenon as a function of temperature.

We found that the diffusion rate in the helium–polytetrafluoroethylene system also increased during irradiation (Fig. 3, Table 1). However, since polytetrafluoroethylene is not stable enough to permit long exposure to radiation, the experiments at high dose intensities (500-600 rad/sec) were very short. At the same time we failed to detect any increase in the permeability of polytetrafluoroethylene at lower dose intensities (30, 130, and 200 rad//sec). When the dose intensity was 560 rad/sec the rate of helium diffusion through polytetrafluoroethylene increased much less (only by a factor of 1.5) than in the case of polyethylene and helium at the same temperature. Thus the irradiation of both crystallizing and noncrystallizing polymers is accompanied by an increased diffusion rate. One might have expected that the energy of the incident $\gamma$-radiation would increase the permeability of the polymer to gases by heating the diffusion cell and the film. Measurements showed that the increase in the cell and film temperatures (about 3°) would only raise the diffusion rate by 20% for helium and 50% for xenon, whereas, the corresponding $p/p_0$ ratios were ~ 3-10. Consequently the over-all film heating has no appreciable effect on gaseous diffusion.

It seems that the increased diffusion rate is somehow connected with a localized molecular excitation and increased elasticity resulting from the primary absorption of $\gamma$-ray quanta and a secondary formation of excited molecules. Exposure to radiation may also be accompanied by bond rupture in the principal and side chains, which would alter some mechanical properties, such as the creep. However these ruptures could hardly be responsible for the increased diffusion rate, since the latter is independent of the macromolecular chain length if the molecular weight is fairly large.

## LITERATURE CITED

[1] L. T. Bugaenko, T. S. Nikitina, et al., The Chemical Effects of Ionizing Radiation [in Russian] (Moscow, 1958).

[2] I. Sobolev, J. A. Meyer, V. Stannett, and M. Szwarc, J. Polym. Sci. 17, 85, 417 (1955).

[3] H. A. Bent, J. Polym. Sci., 24, 107 (1957).

[4] C. E. Rogers, A. W. Myers, et. al., Plastics Progress (London-New York, 1957), p. 45.

[5] M.A. Mokul'skii, Yu. S. Lazurkin, et al. Doklady Akad. Nauk USSR 125, No.5, 1007 (1959).*

[6] A. Kh. Breger, V. A. Belynskii, et al., Trans. All-Union Sci. Tech. Confer. on the Application of Radioactive and Stable Isotopes and Measurements to National Economy and Science (Izd AN SSSR, 1958).

[7] T. S. Nikitina, E. V. Zhuravskaya, and A. S. Kuz'minskii, Effects of Ionizing Radiation on Polymers [in Russian] (Moscow, 1959).

# THE LIMITING-DIFFUSION CURRENT ON ROTATING DISC ELECTRODES DURING CATHODIC EVOLUTION OF HYDROGEN

G. P. Dezider'ev and S. I. Berezina

Chemical Institute of the Kazan' Branch of the Academy
of Sciences of the USSR

(Presented by Academician A. N. Frumkin, November 4, 1959)

(Translation of : Doklady Akademii Nauk SSSR, Vol. 130, No.6, 1960,
pp.1270-1272)

Original article submitted October 22, 1959.

As has been shown in an earlier report [1], limiting current densities during the evolution of hydrogen from platinum or nickel cathodes, from sulfuric acid solutions, are characterized by the fact that the discharge reaction of the hydrogen ion: $H^+ + e \rightarrow H$, alternates with the reaction: $H_2O + e \rightarrow OH^- + H$, the process of evolution from the alkaline solution in the layer in immediate contact with the cathode. The alkalization of the electrolyte in this "pre-cathodic" layer takes place as a result of the accumulation of undischarged mixed cations, whose concentration in the original liquid is easily calculated by the application of the A. N. Frumkin equation [2]. If our experimental data are used for the calculation, it appears that the concentration of the mixture of the cations of alkali metals in the solution is around $10^{-8}$ to $10^{-9}$ N, which is in harmony with the approximate spectroscopic determinations made by us.

The reduction of the concentration of the potential-determining ions in the pre-electrode electrolyte film may be diminished by forced circulation of the electrolyte, which leads to a reduction of thickness of the border layer; the relationship between the limiting current and the over-all concentration of the solution may then be found to be simpler than when gas evolution takes place without mixing of the liquid.

According to V. G. Levich [3], the simplest way of producing flow of the liquid around a solid body is by the rotation of discs within it. The thickness of the border layer of liquid is inversely proportional to the square root of the speed of rotation of the disc. The first experimental test of the V. G. Levich theory , carried out by B. N. Kabanov [4], has confirmed that an essentially linear relationship exists between the limiting current and the square root of the speed of disc rotation. The electrode process investigated by B. N. Kabanov (the cathodic reduction of oxygen in acid solution to hydrogen peroxide) is free from complications due to any side phenomena. But in the case of hydrogen evolution on a rotating disc we are concerned with the formation of gas bubbles and their evolution at the electrode surface. This leads to a complication of the hydrodynamic regularity at the electrode surface. Interest centers on the elucidation of the problem as to which of the two factors predominates in this case: the regular movement of the liquid at the surface of the rotating disk, or the stirring effect produced by evolution of gaseous products from its surface.

## EXPERIMENTAL

The potentials have been determined for platinum disc cathodes of diameter 6.00 mm, using velocities of from 1000 to 22,000 revolutions per minute. The compensation circuit was closed for a period of $3 \cdot 10^{-3}$ second [5] after switching off the polarizing current. This made it possible to measure the potential of the electrode nearly at equilibrium: under these conditions the ohmic-resistance potential and the overvoltage disappear [1]. For electrolysis there were used solutions of sulfuric acid of various concentrations (from 0.0005 to 0.05 N); the cathodic and anodic sections of the electrolyzing vessel were connected by a wide siphon. Hydrogen was produced in the cathodic section. The reproducibility of the measurements was verified many times.

In dilute solutions (0.0005-0.004 N), with low rotation speed of the electrode, the size of the limiting current may be obtained directly from the polarization curves: the sharp rise in potential indicates quite clearly to what current density the measurement of the nature of the electrode reaction corresponds. But in solutions of greater acid concentration (up to 0.05 N), with high speeds of disc rotation (10,000 to 20,000 revolutions per minute), it is not possible to determine the position of the potential shift from the polarization curves, for mixing is then caused additionally not only by the evolution of gas, but also by the heating-up of the liquid in the pre-electrode layer owing to the increased resistance. In this case, the limiting-current density $i_d$ may be determined from the equation connecting this quantity with the concentration of the potential-determining ions at the electrode, $C_s$, the over-all concentration, $C_0$, and the current density acually used, $\underline{i}$. Thus:

$$i_d = C_0\, i/(C_0 - C_s).$$

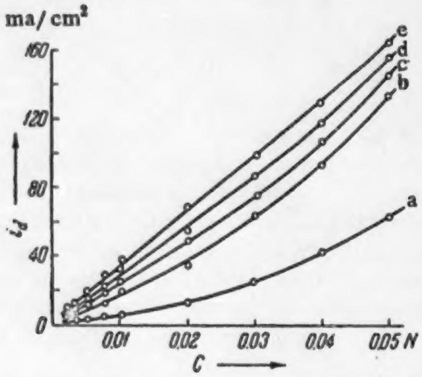

Fig. 1. Relationship between the limiting-diffusion current and concentration of sulfuric acid for various disc rotation speeds. a) 0; b) 3000; c) 8000; d) 15,000; e) 21,000 revolutions per minute.

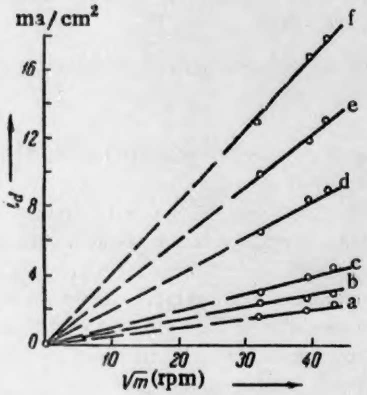

Fig. 2. Relationship between the limiting-diffusion current and disc rotation speed for dilute sulfuric acid solutions. a) 0.0005 N; b) 0.00075 N; c) 0.001 N; d) 0.002 N; e) 0.003 N; f) 0.004 N.

The quantity $C_s$ is determined from the potential of the electrode measured after a period of $3 \cdot 10^{-3}$ seconds after the switching off of the polarization current, since it was established at an early date by various independent methods that the equilibrium of the electrode is established within this period of time.

With a stationary electrode, divergence of the relationship between $i_d$ and C from linearity begins at a sulfuric acid concentration of 0.02-0.03 N. In these and more concentrated solutions, at current densities near to the limiting value, the movement of the pre-electrodic liquid by the hydrogen involved is so strong that $i_d$ is appreciably increased and deviates from the straight line more strongly, the greater the concentration of the solution. If the reaction of the electrode leads to efficient mixing of the solution, the mixing effect of the hydrogen will be less important, so that increased disc rotation speed should be found to lead to a progressive straightening of the curve connecting $i_d$ and C. Figure 1 shows that this in fact occurs. The increase in the speed of rotation of the disc leads to the creation of a more stable hydrodynamic situation.

In those cases where the replacement of one electrochemical reaction by another, in which improvements can be made in the permitted minimum concentration of the potential-determining ions and in which comparatively small gas evolution occurs (for example, in dilute acid solutions with small disc rotation speed), i.e., when the limiting-current density is not very high, we may expect to find that the linear relationship between $i_d$ and the square root of the disc rotation speed is observed. Our experimental material confirms this relationship between the limiting current and the square root of the number of revolutions of the electrode in unit time as a straight line which, when produced, goes through the origin of coordinates (Fig. 2). Increase in the acid concentration and the disc rotation speed gives a pronounced growth in the value of the limiting current. At this point the mixing influence of hydrogen evolution begins to play a large part. It is in this case impossible to create conditions in which the effect of this factor becomes negligible; but as we see in the case of the $i_d$–C relationship, increase in speed of rotation to some extent permits the maintenance of a stable hydrodynamic situation, but all the same the relevant curves are not entirely linear. According to our experimental data, the relationship between the limiting current and the square root of the number of revolutions of the electrode in unit time corresponds to straight lines not passing through the origin of coordinates (Fig. 3); they in fact cut the axis of ordinates at points corresponding to the limiting current at stationary electrodes, or, in the case of the three solutions of highest concentrations even at somewhat higher points (these are, of course, those solutions which most strongly deviate from the linear relationship).

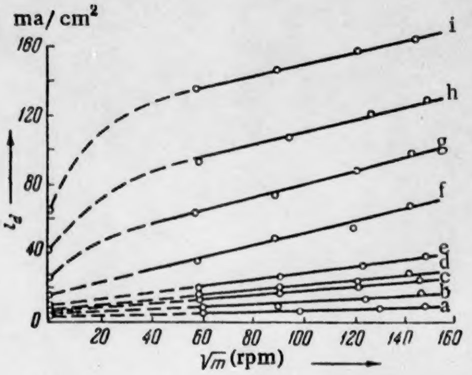

Fig. 3. Relationship between the limiting-diffusion current and the disc rotation speed for wider range of sulfuric acid concentrations. a) 0.002 N; b) 0.003 N; c) 0.005 N; d) 0.0075 N; e) 0.01 N; f) 0.02 N; g) 0.03 N; h) 0.04 N; i) 0.05 N.

Such a result was to be expected, since with reduction of the speed of disc rotation, the thickness of the border layer will be to an increasing degree determined by the mixing effect of the gaseous products from the electrode; and therefore the straight line is deflected from the position corresponding to the limiting current at a stationary electrode. However, as we have seen, conditions are possible in which the mixing of the electrolyte by gas causes very strong upward deviation of the current on rotating electrodes, and the stabilizing effect of the movement of the liquid streaming on the disc is insufficient. In this case the straight line cuts the axis of ordinates at a higher point than that corresponding to the limiting current on stationary electrodes.

According to the results of calculations which have been made, for the polarization curves investigated in the region of current densities not exceeding the saturation value, the equation for concentration polarization takes the form: $\varphi = \varphi_0 + \frac{RT}{nF} \ln C_0 + \frac{RT}{nF} \ln \left(1 - \frac{i}{i_d}\right)$. Deviation of the measured quantities (for potential values) from the values calculated amounted to about 4-6 mv.

## LITERATURE CITED

[1] G. P. Dezider'ev and S. I. Berezina, Izv. Kazansk. fil. Akad. Nauk. SSSR, Chemical Science Series, v. 3, 41 (1957); Thesis for the Proceedings at the 4th Conference on Electrochemistry (Moscow 1956), p. 37 [in Russian] ; S. I. Berezina, G. S. Vozdvizhenskii and G. P. Dezider'ev, Dokl. Akad. Nauk. SSSR, 87, 53 (1951); S. I. Berezina, G. S. Vozdvizhenskii and G. P. Dezider'ev, Zhur. fiz. Khim., 25, 994 (1952).

[2] A. N. Frumkin, Dokl. Akad. Nauk. SSSR, 117, 102 (1957). *

[3] V. G. Levich, Physico-chemical Hydrodynamics (Moscow, 1952), pp. 50, 195 [In Russian]; V. G. Levich, Zhur. fiz. Khim., 18, 335 (1944); 22, 575 (1948).

[4] Yu. G. Siver and B. N. Kabanov, Zhur. fiz. Khim., 22, 53 (1948).

[5] S. I. Berezina, A. Sh. Valeev, et al. , Zhur. Fiz. Khim., 29, 237 (1955).

---

* Original Russian pagination. See C. B. translation.

# THE EFFECT OF THE AGGREGATION OF QUARTZ PARTICLES DURING GRINDING ON THEIR ADSORPTIVE PROPERTIES

V. F. Kiselev, K. G. Krasil'nikov and G. S. Khodakov

M. V. Lomonosov Moscow State University, United Scientific-Research Institute for New Structural Materials.

(Presented by Academician P. A. Rebinder, October 20, 1959)

(Translation of: Doklady Akad. Nauk SSSR, Vol. 130, No.6, 1960, pp. 1273-1276)

Original article submitted October 13, 1959.

It has recently been shown [1] that during the process of grinding quartz in an air-dry state, the size of its specific surface, when determined by the low-temperature adsorption of nitrogen and correlated with increase in time of grinding, ceases to increase and may even fall. This phenomenon has been explained on the basis of aggregation of the quartz particles, in the course of which part of the surface becomes inaccessible to the nitrogen molecules. It is of interest to consider the effect of this aggregation on the adsorptive properties of quartz in relation to other adsorbates, and, especially, to elucidate to what extent the aggregation of the quartz particles can be supposed to affect its adsorptive properties in relation to water vapor, the dimensions of whose molecules and the nature of whose adsorption are significantly different from the dimensions of the molecules and the nature of the adsorption of nitrogen.

The adsorption properties of unit surface of quartz in relation to vapors of water and methanol have frequently been examined [2-8]. There has also been investigated [4, 9-12] the heats of adsorption and of wetting by these liquids. A comparison of the results which have been obtained by the use of the adsorption isotherms of water vapor [8], and by measurements of the heat of wetting by water [12], reveals a profound variation in these adsorption characteristics for various specimens of quartz. In the case of the adsorption isotherms of water vapor, this has been explained [8] by the presence in some natural specimens of quartz of "submicroscopic" cracks, accessible to the water molecules but inaccessible to those of nitrogen, which would give rise to the diminished value of the specific surface determined from the nitrogen adsorption isotherms, and therefore to the increased "absolute" (that is, in relation to unit surface) magnitude of the adsorption of water vapor. This explanation does not seem to us to be at all probable, since during the process of fine grinding the cracking of the quartz particles ought to proceed mainly along the microscopic cracks since these are the weakest places in the lattice, and therefore dispersion ought to promote reduction in the porosity of the powders of different origin, whereas this is not found in practice [8]. No independent experimental data pointing to the presence of ultrapores in specimens under investigation have been carried out [8]. A considerable increase in the specific heat of wetting of quartz by water, with reduction of its dispersion, is noted in paper [12]. A similar relationship, though less marked, was discovered by us at an earlier date for silica gel [13-16]. It was also shown in this case, that the methods of preparing silica gels and quartz powders exert a considerable influence on their adsorption properties. Thus, the reasons for the considerable divergence in the values for the specific adsorption and the energy of adsorption revealed in the literature for different samples of quartz are still not firmly established.

The present work is devoted to our investigations on two samples of highly dispersed quartz. The first sample, Kv-4, was obtained by grinding transparent, crystalline quartz in an excess of water [1], in a steel

TABLE 1

Adsorption Characteristics of Powdered Quartz

| Sample | Specific surface, $m^2/g$ | Structural water content, micromole/$m^2$ | Grinding conditions |
|---|---|---|---|
| Kv-4 | 53.0 | 5.4 | In excess of water |
| Kv-4A | 35.4 | 14.8 | Additional grinding of the dry powdered Kv-4A |

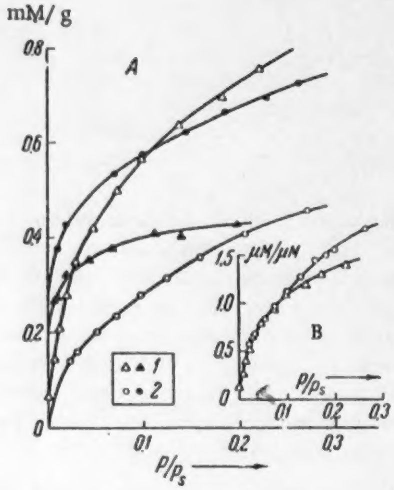

Fig. 1. A) Adsorption isotherms for water vapor (light points) and nitrogen (dark points) on quartz specimens Kv-4A (1), and Kv-4 (2). B) Adsorption isotherms for water vapor on the same specimens, related to the structural water composition in these samples.

vibration mill. The second sample, Kv-4A, was produced by further grinding of the first sample, Kv-4, which had been thoroughly dried, for a period of 16 minutes in air. Both the samples of quartz were purified from iron impurities by treatment with hydrochloric acid, followed by passing the suspension through a chromatographic column filled with a cation exchange resin [18]. The measurement of the adsorption of water vapor and of nitrogen was carried out under volume conditions. The quantity of structural water in the specimens under the same conditions was determined from the volume of water vapor evolved on heating the sample from 300° to 1000°. The specific surface was calculated by the B.E.T. method from the isotherms for the low-temperature adsorption of nitrogen. The results obtained are set out in Table 1.

Fig. 1 shows the reversible adsorption isotherms of water vapor and of nitrogen on samples Kv-4 and Kv-4A, calculated on the basis of 1 gram adsorbent. As can be seen from Fig. 1, the adsorption isotherm for nitrogen vapor on the aggregated specimen Kv-4A lies considerably lower than that for the original specimen. It follows therefore that, in the process of grinding the powder Kv-4 further, its specific surface with respect to nitrogen is reduced by a factor of 1.5 on account of the aggregation of the particles [1] (Table 1). On the other hand the isotherm for water vapor on the aggregated sample Kv-4A behaves in the opposite way, lying above that for the specimen KV-4, which may be accounted for by an increase in the true surface of the specimen as a result of the additional grinding. Thus, these experiments show that, as a result of the aggregation of the particles during the grinding of quartz, the adsorption properties change differently with respect to water vapor and nitrogen. The ultra-porous structure of the aggregated quartz which is formed in this case has evidently nothing to do with the initial quartz specimen, but originates in some other way. The absence in all the investigations [2-12] on quartz of data about the conditions of grinding, and the neglect of the effect of aggregation in production in the value of the specific surface obtained on the basis of the low-temperature adsorption isotherms of nitrogen, does not permit making a comparison amongst themselves of the quantities produced in these projects: that is, the specific adsorption [2-8], the heat of adsorption [4], and the heat of wetting [9,12], in the way this was formerly done [8, 12]. It is possible that this is one of the reasons for the considerable divergences found both with the adsorption and with the energetic characteristics obtained using powdered quartz in the various investigations.

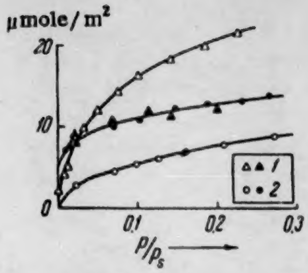

Fig. 2. Specific adsorption isotherms of water (light points) and nitrogen (black points) on samples of quartz Kv-4A (1) and Kv-4 (2).

It can be seen from Fig. 2 that the "absolute" isotherms for the adsorption of water vapor on the two samples of quartz of identical origin and differing only in the conditions of grinding to which they have been submitted are very different. This is associated with the fact that part of the surface of the aggregated sample appears to be inaccessible to the molecules of nitrogen, though it is accessible to those of water. In this case it would be necessary to determine the size of the specific surface of the aggregated sample from the adsorption isotherms of water vapor. This method, however, may lead to considerable inaccuracy, since the deposition area for molecules of water on the surface of silica depends on the degree of hydration of this, which may be quite different for samples of different origin [14-16]. Calculation of the deposition area of the water molecule from the crystallographic section of the quartz [17] is not possible, since as has already been shown [21] there is an amorphous layer on the surface of the crystalline quartz. The facts, however, of the coincidence of the "absolute" isotherms on various specimens of quartz and silica gel [4,8], when specific surfaces are employed which have been calculated from these facts, still gives no information about the identity of the surface of the objects investigated. The "absolute" isotherms agree in this case only because, in the course of calculating the specific surface, the qualitative differences in nature of the different specimens are allowed for in its magnitude [19]. Thus, for example, in the use of such a calculation method, the "absolute" isotherms on ordinary silica gel, and silica gel with a modified surface in which part of the OH-groups have been replaced by $CH_3$-groups, are in agreement: that is, on samples the nature of whose surface is materially different, this agreement is nevertheless found [20].

Since the size of the actual specific surface of the aggregated quartz powder remains unknown, we have inaugurated the method of measuring the adsorption of water vapor directly in terms of the quantity of structural water contained in the specimens under investigation [14]. As is seen from Fig. 1B, in the early part of the $P/P_s$ curve, the isotherms coincide, which is a consequence of the fact that the whole surface of aggregated quartz is accessible to the molecules of water.

At the present time it is not possible to give a comprehensive explanation of the aggregation observed in [1] and in the current work. Apparently, with collision of the particles during the process of crushing, the formation of contacts between them takes place owing to the interaction of active portions of neighboring particles. In particular, such active positions may be the free radicals which arise on the surface of the split. In this way there are formed comparatively compact aggregates, consisting of primary particles which are not disintegrated by the influence of water or heat. But their mechanical strength, is, all the same, appreciably less than that of the initial quartz particles. A short period of grinding of the aggregated quartz with water leads to disaggregation of the particles and a sudden growth in the specific surface. The fact mentioned above concerning the distribution of molecules of water throughout the entire surface of aggregated particles is in harmony with the dispersing (peptizing) properties of water in relation to this system. It should be mentioned further that the phenomenon of the aggregation of particles in the course of grinding is observed not only for crystalline quartz, but also for a number of other solid materials, such as corundum, fused quartz, calcite and others; and also for silica gels, the specific surface of which in dry grinding in a vibrating mill, is in certain cases reduced by a factor of more than 10.

The authors wish to express their thanks to Academician P. A. Rebinder for his interest in this work and its discussion, and also to G. I. Aleksandrova for his assistance with the measurements.

## LITERATURE CITED

[1] G. S. Khodakov and P. A. Rebinder, Dokl. Akad. Nauk. SSSR, 127, 1070 (1959). *

[2] H. K. Livingston, J. Am. Chem. Soc., 66, 569 (1944).

---

*Original Russian pagination. See C. B. translation.

[3] A. N. Sakharov, Izv. Akad. Nauk. SSSR, OKhN, 1956, 150. *

[4] N. N. Avgul' and O. M. Dzhigit,et al., Dokl. Adad. Nauk SSSR, 77, 625 (1951).

[5] W. Stober, Kolloid Z., 145, 17 (1956).

[6] N. Hackerman and A. G. Hall, J. Phys. Chem., 62, 1212 (1958).

[7] S. P. Zhdanov, Dokl. Akad. Nauk. SSSR, 115, 938 (1957).*

[8] S. P. Zhdanov, Dokl. Akad. Nauk. SSSR, 120, 103 (1958).*

[9] G. E. Boyd and W. D. Harkins, J. Am. Chem. Soc., 64, 1190 (1942).

[10] F. L. Howard and J. L. Culbertson, J. Am. Chem. Soc., 72, 1185 (1950).

[11] A. C. Zettlemoyer, G. J. Young et al., J. Phys. Chem., 57, 649 (1953).

[12] A. C. Makrides and N. Hackerman, J. Phys. Chem., 63, 594 (1959).

[13] M. M. Egorov, K. G. Krasil'nikov, and V. F. Kiselev, Zhur. fiz. Khim., 32, 2448 (1958).

[14] M. M. Egorov, T. S. Egorova, K. G. Krasil'nikov and V. F. Kiselev, Zhur. Fiz. Khim., 32, 2624 (1958).

[15] M. M. Egorov, V. F. Kiselev.et al., Zhur. fiz. Khim., 33, 1241 (1959).

[16] M. M. Egorov, V. F. Kiselev and K. G. Krasil'nikov, Zhur. fiz. Khim., 33, 1241 (1959).

[17] S. P. Zhdanov and A. V. Kiselev, Zhur. fiz. Khim., 31, 2213 (1957).

[18] K. V. Chmutov and O. G. Larionov, Koll. zhurn., 19, 396 (1957).*

[19] V. F. Kiselev and K. G. Krasil'nikov, Zhur. fiz. Khim., 33, 2621 (1959).

[20] L. G. Galichenko, M. M. Dubinin et al., Izv., Akad. nauk. SSSR, OKh N, 1960, no. 3. *

[21] P. B. Dempster, P. D. Ritchie, Nature, 169, 538 (1952).

---

* Original Russian pagination. See C. B. translation.

# ELECTRONIC PARAMAGNETIC RESONANCE SPECTRA OF CYANINE DYES

Yu. Sh. Moshkovskii

Institute of Chemical Physics, Academy of Sciences, USSR

(Presented by Academician V. N. Kondrat'ev, September 21, 1959)

(Translation of: Doklady Akad. Nauk SSSR, Vol. 130, No.6, 1960
pp. 1277-1279)

Original article submitted September 18, 1959.

During an investigation into the electronic paramagnetic resonance (EPR) method, for compounds with a conjugated bond system in which it appeared that resonance absorption occurred [1,7], the fact emerged that the molecules possessed noncompensating electronic magnetic moments. Thus, with substances having at the same time the characteristic of fully saturated chemical bonds, there emerge radical structures, the study of which which may, on the one hand, explain some chemical peculiarities of molecules with a large number of conjugated double bonds, and, on the other hand, elucidate what is at present a vaguely understood mechanism of the origin of paramagnetism with such substances.

A convenient object for the investigation of electronic paramagnetic resonance spectra of conjugated systems is found in the cyanine dyes, which are widely employed in practice for the optical sensitization of photographic emulsions. In the present work, the effect on their electronic paramagnetic resonance spectra of the number of conjugated double bonds between the heterocyclic rings, of the structure of the heterocyclic rings themselves, and of the nature of the anion of the dyestuff has been studied. The following symmetrical cyanine dyes were chosen as subjects of the measurements:

1

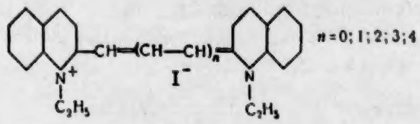

2

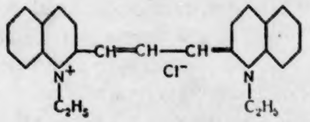

3

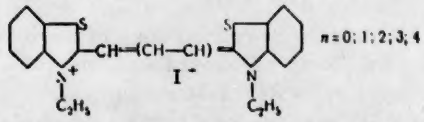

4

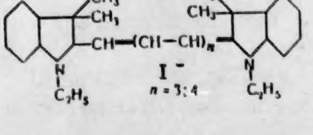

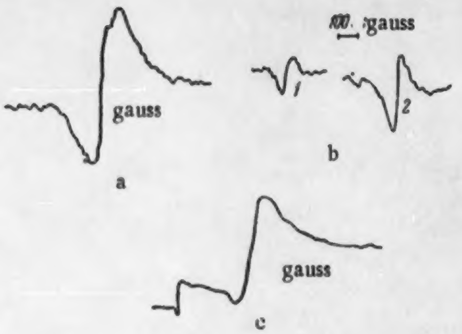

Fig. 1. Electron paramagnetic resonance spectra. a) Dyestuff 1, n = 3; b) dyestuff 3, n = 3: 1) T = 290°K, 2) T = 90°K; c) dyestuff 1) n = 3.

All the dyes were available as pure preparations, with the exception of that corresponding to No.1 with n = 4.

The measurements were carried out on the powdered dyestuff, in quantitites from 20 to 90 mg, in the spectrometer described in [2], using a frequency of $9 \cdot 10^9$ hertz, double-magnetic modulation, synchronous detection, amplification at a frequency of 975 kilohertz, and an arrangement for automatic maintenance of the frequency of the klystron through an operating resonator. The absorption curve was recorded in the form of its first derivative by means of the automatic recorder EPP-09.

The signal of electronic paramagnetic resonance was not obtained with all the dyestuffs investigated. However, when resonance absorption was observed, the line appeared as a symmetrical singlet with a g-factor of 2.003 (Fig. 1a). The breadth of the line varied with the structure of the dyestuff. One of the dyes investigated (No.2, with n = 3) had, in addition to the narrow singlet, a second rather wide singlet with a g-factor of 2.24 (Fig. b). The breadth of lines was determined between the points of maximum slope of the absorption curve, and in the last case was equal to $\Delta H_{MH}$ = 130 gauss.

The concentration of uncoupled electrons was determined against a known standard (diphenylpicrylhydrazil), and corresponded approximately to one free electron per $10^4$ molecules of the dyestuff. Because of the small intensity of the electronic paramagnetic resonance spectrum, and the small quantity of the prepared materials, the determination of the concentration of the uncoupled electrons was only reliable to the limit of one order of magnitude.

The results which have been obtained are shown in Table 1, from which it can be seen that resonance absorption arises for a given homologous series of dyes only with a definite number of conjugated double bonds. With increase in conjugation, the breadth of the electronic paramagnetic spectrum line diminishes. Another factor governing the emergence of radical structure is the nature of the heterocyclic nucleus. In the case of quinoline nuclei, electronic paramagnetic resonance arises with conjugation corresponding to three CH-groups, whereas with benzthiazole, not less than five CH-groups are necessary for the appearance of the signal, and again with indole as many as seven CH-groups are necessary. Apparently the basicity of the heterocyclic ring influences the emergence of radical structure, this being diminished in the same order as the former increases. It is interesting to note that change in the anion (changing from $I^-$ to $Cl^-$) does not have any material effect on the resonance absorption of the dyestuff. The reason for this seems to be that the radical structure arises in the system of double bonds contained in the cation of the dyestuff.

It might be supposed that the electronic paramagnetic resonance spectrum in the dyestuffs investigated is produced by a thermally excited triplet state, the energy of which, with sufficient conjugation is proportional to kT. But this is contrary to experimental evidence at low temperatures. The electronic paramagnetic resonance signal at the temperature of liquid nitrogen does not diminish, but increases approximately by a factor of 2 (Fig. 1b), as is found with paramagnetic substances. Thus the presence of uncompensated electronic magnetic moment in the substances investigated is associated not with the excited but with the ground state of the dyestuff molecule.

As may be seen from Fig. 1b, the reduction of the temperature to 90°K does not diminish the breadth of the electronic paramagnetic resonance lines. It follows that, in this case, the broadening of the electronic paramagnetic resonance lines is not controlled by spin-screening interaction. Apparently the reduction in the breadth of the electronic resonance spectral lines with increase in chain length of the conjugated chains depends on the increase in the delocalization of electrons on many centers [4].

It appears to be very characteristic that the radical state, as has been discovered by us, emerges in those dyes which absorb light in the red and near infrared regions of the spectrum. These dyes are usually very rapidly decolorized in aqueous solutions. On the other hand, when the optical sensitization of photographic emulsions by easily destroyed dyes is carried out, there is often observed an increase in the instability of the photographic

TABLE 1

| Dyestuff number | n | Molec. wt. | Max. absorption | $\Delta H_{MH}$ gauss | g-factor |
|---|---|---|---|---|---|
| 1 | 0 | 454 | 523 | – | – |
| | 1 | 480 | 603 | 8.4 | 2.003 |
| | 2 | 506 | 707 | 4.6 | 2.003 |
| | 3 | 532 | 820 | 4.3 | 2.003 |
| | 4 | 680 | – | 8.0 | 2.003 |
| 2 | 1 | 388 | 605 | 9.5 | 2.003 |
| 3 | 0 | 478 | 424 | – | – |
| | 1 | 504 | 559 | – | – |
| | 2 | 530 | 652 | 15 | 2.003 |
| | 3 | 556 | 762 | 7.3<br>130 | 2.003<br>2.240 |
| | 4 | 582 | 870 | 5.7 | 2.003 |
| 4 | 2 | 630 | 639 | – | – |
| | 3 | 656 | 730 | 15 | 2.003 |

properties. There are indications that oxygen from the air plays a significant part in such processes [4-6]. There has therefore been shown great interest in discovering the effect of atmospheric oxygen on the electronic paramagnetic resonance spectrum. It has been found that evacuation of dyestuff 2 (with $n = 3$) for a period of 4 hours to a vacuum of $2 \cdot 10^{-4}$ mm mercury causes an increase in the signal of 20-30%. After admitting air into the dyestuff ampoule, the resonance signal is correspondingly reduced, which is to be attributed to the interaction of the dyestuff molecule with the oxygen of the air. We regret that we did not succeed in obtaining electronic paramagnetic resonance spectra of solutions of dyestuffs because of the poor solubility. But results indicating the obtaining of very similar resonance signals with solutions of polyphenylvinylene, and also the regular effect on the electronic resonance spectrum of change in the structure of the cyanine dyes, make it possible to maintain with great probability that the radical states are properties of the molecules themselves of the compounds investigated, and not merely of their crystalline structure.

The results considered in this investigation show that the appearance of uncompensated electronic magnetic moments in cyanine dyes is associated, not with thermal excitation, but with the ground state of the molecules of the dyestuff, which in each molecule has an electron-spin density of $10^{-4}$.

In conclusion, the author wishes to express his deep thanks to L. A. Blyumenfel'd and I. I. Levkoev for their help in the work.

## LITERATURE CITED

[1] B. M. Kozyrev, Dokl. Akad. Nauk SSSR, 81, 427 (1951).

[2] A. G. Semenov and N. N. Bubnov, Pribory i tekhnika eksperim., No.1 (1959) (Apparatus and Technique of Experiment) [in Russian].

[3] P. W. Anderson, J. Phys. Soc. Japan, 9, 316 (1954).

[4] T. D. Smith, J. Photogr. Sci., 1, 138 (1953).

[5] S. M. Solov'ev, Zhurn. nauchn. i prikl. fotogr. i kinematogr., 2, 260 (1957).

[6] Yu. Sh. Moshkovskii and A. L. Karpova, Dokl. Akad. Nauk SSSR, 91, 299 (1953).

[7] L. A. Blyumenfel'd, A. A. Berlin et al., Vysokomol. soed., 1, No.9, 1361 (1959).

# A METHOD FOR DETERMINING KINETIC CONSTANTS AND FLOW LIMITS FOR REACTIONS PERFORMED IN FLOW CONDITIONS

G. M. Panchenkov and Yu. M. Zhorov

The I. M. Gubkin Institute of the Petroleum Chemistry and Gas Industries

(Presented by Academician A. V. Topchiev, October 2, 1959)

(Translation of: Doklady Akademii, Nauk SSSR, Vol. 130, No.6, 1960, pp. 1280-1283)

Original article submitted September 20, 1959 .

The widespread employment in laboratory and industry of chemical reactions carried out in the flow state at a constant total pressure, has made it necessary to extend to this field that classical treatment of chemical kinetics which was arrived at for processes carried out at constant volume.

The general equation for the kinetics of flow reactions is given in [1] in the form:

for homogeneous reactions:

$$\frac{n_{0A_i}}{\rho}\frac{dx_{A_i}}{dl} = W; \quad (1)$$

for heterogeneous catalytic reactions:

$$\frac{n_{0A_i}}{s_0}\frac{dx_{A_i}}{dl} = W_s. \quad (2)$$

where $n_{0A_i}$ = rate of supply of the substance $A_i$; $x_{A_i}$ = degree to which the substance $A_i$ undergoes reaction; $\rho$ and $l$ are respectively the cross section and length of the reaction volume; W and $W_s$ are the rates of the homogeneous and heterogeneous reactions respectively, measured in terms of the substance $A_i$; and $S_0$ = surface of catalyst per unit length of the reaction volume.

The most common method of studying the kinetics of flow reactions is the use of the relationship between the degree of conversion, x, and the rate of supply of the reagent, $n_0$. It is not, however, possible to work out the relationship between x and $n_0$ from the formulas (1) and (2), since the variables in these are x and $l$ . In order, therefore, to obtain integrated kinetic relationships it is necessary to arrive at a form of kinetic equation such as $W = \Phi(x)$, after which the integration of equations (1) and (2) becomes possible. If the experimental data then conform to the relationship so obtained, it can be judged that correct assumptions have been made about the kinetics of the process.

Such a method has shown itself to be very productive, and has opened up the possibility of determining the kinetics of a number of reactions [2]. In many cases, however, it is difficult to make assumptions about the form which the kinetic equation should take. In addition to this, in the case of heterogeneous catalytic reactions, the occurrence of diffusion inhibition causes distortion of the kinetics to be observed: thus the necessity arises of carrying out measurements in the kinetic region.

For this purpose, so as to make it possible to determine the kinetic constants without regard to the mechanism of the process, and also so as to determine the flow region, we have worked out a graphical method of studying the kinetics, making use of the experimental curves relating $x$ and $n_0$. The use of these curves makes it possible to measure directly the rate of the reaction to which the values of $x$ and $n_0$ refer. With this object we proceed to substitute the variables in equations (1) and (2) in the following manner.

By integrating equation (2) with respect to $l$, from 0 to $l$, and with respect to $x$ from 0 to $x$, we obtain the relationship:

$$\frac{s_0 l}{n_0} = \int_0^x \frac{dx}{W_s}. \tag{3}$$

Differentiating this equation (3) with respect to $n_0$, we find:

$$-\frac{s_0 l}{n_0^2} = \frac{d\left[\int_0^x \frac{dx}{W_s}\right]}{dx} \frac{dx}{dn_0}, \tag{4}$$

and therefore,

$$W_s = -\frac{n_0^2}{s_0 l} \frac{dx}{dn_0}. \tag{5}$$

Similarly, for homogeneous reactions, we find:

$$W = -\frac{n_0^2}{pl} \frac{dx}{dn_0}. \tag{6}$$

By the use of equations (5) and (6) it is possible to find the rate of reaction from the curves of the relationship between $x$ and $n_0$, since $dx/dn_0$ is the tangent of the angle of slope of the curve against the rate of flow axis. It therefore becomes possible to study the kinetics of the reaction on the basis of the experimental data, regardless of prior assumptions about the mechanism of the reaction.

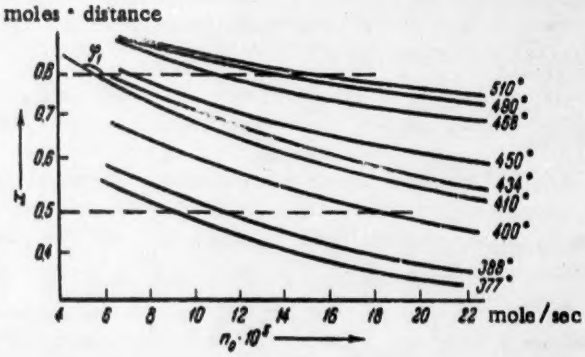

Fig. 1. Experimental curves of the relationship between $x$ and $n_0$ for the cracking of cumene (isopropylbenzene) at atmospheric pressure on an aluminosilicate catalyst at various temperatures. $dx/dn_0 = -\tan(180° - \varphi_1)\,\alpha_1$, where $\alpha_1$ = coefficient depending on the scale chosen.

We will consider, for example, the method of determining the activation energy. In the general case, for irreversible reactions, we may put:

$$W_s = k(T)\, f(C) = Pe^{-E/RT}\psi(C_0,\ x), \tag{7}$$

where k(T) = rate constant of the reaction, P = pre-exponential factor; E = activation energy; R = gas constant; T = temperature of the experiment; C = instantaneous concentration of reagent; and $C_0$ = initial concentration of reagent.

Comparing the right-hand sides of equations (5) and (7), and taking logarithms of the equations obtained, we have:

$$\ln\left(-n_0^2\frac{dx}{dn_0}\right) = -\frac{E}{R}\frac{1}{T} + \ln P\psi(C_0,\ x)\, s_0 l \ ^* \tag{8}$$

or,

$$\ln\left(-n_0^2\frac{dx}{dn_0}\right)_{x=x_1} = -\frac{E}{R}\frac{1}{T} + \mathrm{const}_{x=x_1}. \tag{9}$$

It follows that the dependence of $\ln(-n_0^2 \cdot dx/dn_0)$ on $1/T$ is linear for constant initial concentrations and degrees of conversion, and therefore that the value of the activation energy can be obtained from the angle of slope of the straight line. With constant total pressure $C_0$ will vary with temperature, but the temperature change of $C_0$ may be neglected in comparison with the change in k. In the case of the cracking of hydrocarbons, $W = \Phi(x)$ [3], and the relationship (5) is exact.

Transition to the diffusion region leads to a reduction in the activation energy, and this leads to curvature of the line: $\ln(-n_0^2 \cdot dx/dn_0) = F(1/T)$. This makes it possible to measure the activation energy in the diffusion region itself, using flow reactions. We may note also that in moving over to the diffusion region, a change takes place in the form of $\psi(C_0, x)$, but this will be small compared with the change in the activation energy.

We have carried out a study of the kinetics of the cracking of cumene over a wide range of temperature and a large range of volume velocities, using an industrial aluminosilicate catalyst with a globule size of 0.42 cm. This reaction is taken as a model for the properties of aluminosilicate catalysts, and therefore gives a substantially correct picture of the conditions under which the true kinetics of the reactions are found without distortion.

The experiments were carried out with cumene purified from peroxides, which act as cracking inhibitors, in the standard flow reactor MINKh and GP (for a description of this reactor see [4]). From the results of experiments carried out at a series of temperatures, curves for the relationship between x and $n_0$ are arrived at, and are shown in Fig. 1, using the same methods of experiment and analysis as has been described in earlier works [5].

The method described above was used for the determination of the activation energy of the cracking of cumene in the diffusion and kinetic regions. For this purpose there were derived from Fig. 1 the rate of flow and the slope of the curves, at points corresponding to x = 0.8 and x = 0.5. These values were put into Eq. 9; the results are given in Table 1.

On the basis of the data in Table 1, curves are constructed for the relationship of ln const $(-n_0^2 \cdot dx/dn_0)$ to $1/T$ (Fig. 2). It can be seen from Fig. 2 that at low temperatures (kinetic region) a linear relationship exists, whereas at high temperatures (diffusion region) the points lie on a curve. From Fig. 2 all the regions of the cracking reaction of cumene on the catalyst used may be found, according to the change of the magnitude of the activation energy with temperature.

1. The inner kinetic region is found up to a temperature of 410°. In this region the size of the activation energy is at its greatest, and has the value of 26.0 kcal/mole.

---

*As can be seen by a comparison of (7) with (6), the equation remains the same for homogeneous reactions, except that $S_0$ is replaced by $\rho$.

## TABLE 1

Results Derived from the Experimental Curves for the Relationship between x and $n_0$ by Means of Formula (9)

| $t$, °C | $x$, molec. length | 180° − $\varphi_1$ | $n_0 \cdot 10^4$, mole/sec | $n_0^2 \cdot 10^{10} \times$ × tg (180° − $\varphi_1$) | ln [$n_0^2 \cdot 10^{10} \times$ × tg (180° − $\varphi_1$)] |
|---|---|---|---|---|---|
| 400* | 0,8 | 43,5 | 3,8 | 13,5 | 2,6 |
| 412* | | 32 | 5,6 | 19,7 | 2,98 |
| 434 | | 30 | 6,8 | 26,6 | 3,28 |
| 450 | | 28,5 | 7,5 | 30,6 | 3,42 |
| 468 | | 17 | 10,9 | 35,7 | 3,57 |
| 490 | | 12,5 | 13,4 | 39,8 | 3,68 |
| 510 | | 11 | 14,8 | 42,6 | 3,75 |
| 377 | 0,5 | 22 | 9 | 32,4 | 3,47 |
| 386 | | 19,5 | 11 | 43,3 | 3,76 |
| 400 | | 11,5 | 18 | 65 | 4,16 |

---

* extrapolated.

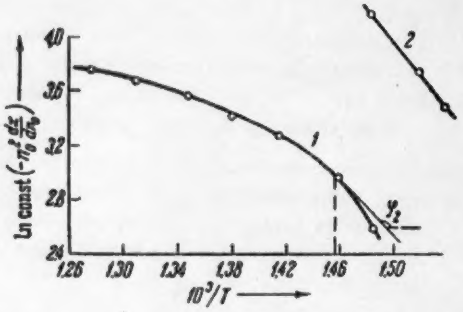

Fig. 2. Relationship of ln const($-n_0{}^2 \cdot dx/dn_0$) to 1/T obtained from the curve of Fig. 1 by the use of formula (9). 1) x = 0.8; 2) x = 0.5; tan $\varphi_2$ = = $-E\alpha_2/R$, where $\alpha_2$ is a coefficient depending on the choice of scale.

2. The inner diffusion region is found between 430° and 460°, and here the activation energy is around 12 kcal/mole, or about half the activation energy in the kinetic region.

3. The outer diffusion region begins at temperatures higher than 490°. Here the activation energy is reduced to its minimum value of 3.3 kcals/mole.

4. Between 410° and 430° the activation energy changes from 26.0 to 12.0 kcals/mole, and therefore the reaction is occurring in an inner transition region.

5. Between 460° and 490° the reaction occurs in an outer transition region, in which the activation energy diminishes from 12.0 to 3.3 kcals/mole.

Of course the limits of all the regions are somewhat provisional, but this demarcation of regions is generally accepted because of its convenience in analysis. We may remark that the starting points of the inner and outer inhibitions are confirmed by experiments using broken-up and ignited catalysts.

It can be said in conclusion that the graphical method of analysis of the experimental curves makes it possible for us to determine the region of flow, and the observed activation energy, without making any analytical assumptions. The same method may also be used for determining other kinetic constants, and also for the quantitative comparison of the activities of various catalysts.

## LITERATURE CITED

[1] G. M. Panchenkov, Zhur. fiz. Khim., 22, 209 (1948); 26, 454 (1952); Vestn. Mosk. gosud. univ., No.6, 105 (1948).

[2] G. M. Panchenkov, Uch. zap. Mosk. gosud. univ., Neorg. i fiz. Khimiya (Inorganic and Physical Chemistry), v. 174, 53 (1955); G. M. Panchenkov and A. S. Kazanskaya, Zhur. fiz. Khim., 32, 1779 (1958); I. M. Kolesnikov, Izv. Vysch. uchebn. zaved. Neft'igaz (Proceedings; of the Board of Higher Education(Petroleum and Gas), No. 11, 77 (1958).

[3] K. V. Topcheva, Sh. Battalova and G. M. Panchenkov, Dokl. Akad. Nauk. SSSR, 78, No. 3, 501 (1951); G. M. Panchenkov and E. P. Kuznetsova, Dokl. Akad. Nauk SSSR, 87, No. 1, 65 (1952).

[4] G. M. Panchenkov and V. Ya. Baranov, Izv. Vyssh. uchebn. zaved., Neft' i gaz. (Proceedings of the Board of Higher Education: Petroleum and Gas), No.6, 77 (1958).

[5] K. V. Topchieva and G. M. Panchenkov, Dokl. Akad. Nauk. SSSR, 74, No.6, 1109 (1950).

# THE PARAMAGNETIC RESONANCE OF CERTAIN INNER COMPLEXES OF COPPER

A. K. Piskunov, D. N. Shigorin, V. I. Smirnova
and B. I. Stepanov.

L. Ya. Karpov Physicochemical Scientific Research Institute
and D. I. Mendeleev Moscow Institute of Chemical Technology

(Presented by Academician V. A. Kargin, August 18, 1959)

(Translation of: Doklady Akademii Nauk SSSR, Vol. 130, No. 6, 1960,
pp. 1284-1287)

Original article submitted August 15, 1959

We examined in this work the paramagnetic resonance spectra (p.m.r.) of inner complexes of copper; complexes with various aceto derivatives [1] as well as with the enol forms of acetylacetone and acetoacetic ester [2] were studied.

The determined magnetic moments of these compounds indicate that copper contributes two valence electrons to the bond formation. If the initial state of a copper atom is $d^9sp$, then there should remain an unpaired electron on the complexed copper. It is known that the metal ion in an inner complex forms more stable bonds than the number of valence electrons it contributes. Thus, for example, a copper atom contributes two valence electrons but forms four equivalent bonds with acetylacetonate. This can only be explained by assuming that the metal atom in inner complexes interacts directly with the $\pi$-electrons of the system. This interaction may occur in various ways. One may assume that one of the electrons on the metal atom interacts with the $\pi$-electrons of neighboring atoms by utilizing its own p-orbital and that the interaction is extended to include all the $\pi$-electrons in the system. Or else a free p-orbital on the metal atom may interact directly with the $\pi$-electrons of neighboring atoms. The "behavior" of the unpaired electron of the metal (as in the case of copper acetylacetonate) presents a serious theoretical problem. It is particularly important to find out whether the unpaired electron is localized on the copper atom or delocalized (distributed) in the molecule. In case there is some delocalization of the electron it is important to determine the effects of structural changes in the molecule on the delocalization. Problems of this type can be partially solved through the study of p.m.r. absorption spectra. In case there should be some hyperfine structure (h.f.s.) it is possible to make certain deductions with regards to the behavior of the unpaired electron from the number and intensities of the h.f.s. lines. However, due to an extensive exchange interaction one can seldom observe the h.f.s. in paramagnetic solids. By using dilute solutions it is frequently possible to eliminate exchange interaction and thus obtain the desired information. For many compounds it is very difficult to find solvents which would effectively eliminate exchange interaction. Moreover, even under conditions where the h.f.s. is resolved the spectra of certain molecules may be practically unanalyzable. One can cite as an example of such a case the spectrum of 0.001 M triphenylmethyl in benzene (observed by Jarrett and Sloan [3]) which contains 72 components.

We believe that in certain cases, particularly in the case of inner complexes of copper, the effects of the nature and structure of the groups surrounding the copper atom can be partially elucidated by comparing the p.m.r. spectra of solid systems, since the delocalization of the unpaired electron greatly depends on the nature of the surrounding atoms and on the number of $\pi$-electrons in the system and should therefore influence the exchange interaction and consequently the absorption band width.

In Table 1 we have listed the inner complexes of copper investigated by us, their band widths ΔH (between points of maximum slope) at the 9370 Mc frequency, their g-factors and magnetic moments. Whereas copper acetylacetonate (I) has a ΔH 158 ± 10 gauss, when a $O=C-OR$ (II) or a (Cl) group (III) is introduced

TABLE 1

| Nos. | Compounds | Band-width, gauss | g-Factors | Magnetic moment, Bohr magnetons |
|---|---|---|---|---|
| I | 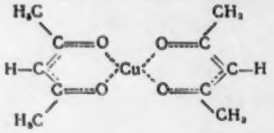 | 158±10 | 2,105±0,01 | 1,75±0,05 |
| II | 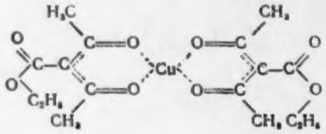 | 75±5 | 2,079±0,01 | 1,87±0,05 |
| III | 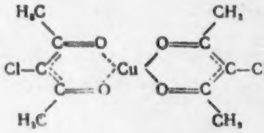 | 56±3 | 2,072±0,01 | 1,83±0,05 |
| IV | 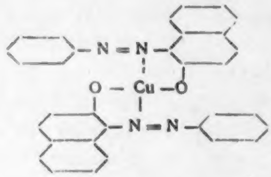 | 117±6 | 2,087±0,01 | — |
| V | 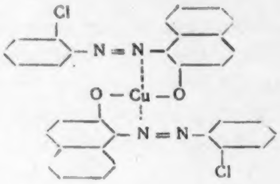 | 48±3 | 2,051±0,01 | — |
| VI | 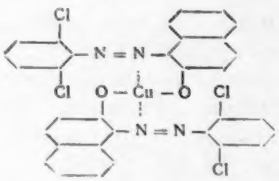 | 38±3 | 2,055±0,01 | — |
| VII | 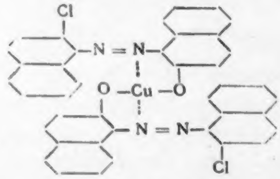 | 29±2 | 2,051±0,01 | — |

TABLE I (continued)

| Nos. | Compounds | Band-width, gauss | g-Factors | Magnetic moment,Bohr magnetons |
|---|---|---|---|---|
| VIII | 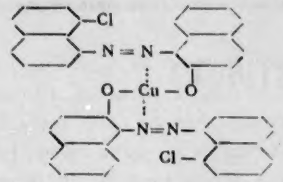 | 79±5 | 2,080±0,01 | 1,80±0,05 |
| IX | 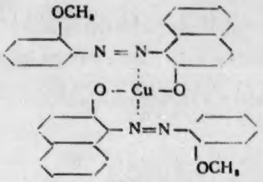 | 85±5 | 2,075±0,01 | 2,06±0,05 |

into the molecule the absorption bands become much narrower (75 ± 5 and 56 ± 3 gauss respectively). A $O=C-OR$ group should interact much more strongly with the π-electrons than does a hydrogen. The π-bond interaction should be even more pronounced in the case of chlorine due to the nonbonded electron pairs. It seems that the interaction enhances the delocalization of the unpaired electron, which substantially affects the exchange interaction and results in a narrowing of the absorption band.

The p.m.r. spectra of copper complexes containing azo groups ($-N=N-$) and other groups rich in π-electrons have an even narrower ΔH[4]. Thus compound IV has a ΔH narrower by 40 gauss than that of copper acetylacetonate. When a chlorine is introduced into the azo compound, particularly in a position ortho to the azo group, the p.m.r. becomes even narrower, just as was observed in the case of copper acetylacetonate. Table 1 shows that the band of compound IV is 2.5 times broader than that of compound I. The presence of two chlorines in the azo compound VI makes the band still narrower (narrower by 38 gauss than that of compound V). If the chlorine is not ortho to the azo group but further removed (as for example compound VIII) the band becomes broader (79 gauss in VIII versus 29 gauss in VII).

When the number of π-electrons in a molecule is increased the absorption band becomes narrower. This is clearly illustrated in the case of compounds V and VII. It should be noted that a chlorine in the ortho position has a greater effect on the band width than does an OR-group (IX).

The above-examined facts indicate that the unpaired electron on the copper interacts with the π-electrons of the azo group and through them with the π-electrons of the entire system. This interaction seems to have a significant effect on the exchange interaction between the copper electrons, which accounts for the band narrowing. The introduction of substituents into the molecule will alter the crystal lattice; this should influence not only the exchange interaction but also the internal crystal field, which determines the shape and width of the band (due to the anisotropy of the g-factor. Let us note that all the bands were highly asymmetric in the direction of weaker fields. Our observations, however, cannot be explained entirely by the changes in the exchange interaction resulting from the indicated causes. Thus, when one proceeds from acetylacetonate to its derivatives II and III, the intermolecular distance increases, and consequently the Cu−Cu exchange interaction should decrease. Nevertheless a sharp band narrowing is observed.

As can be seen in Table 1, in the case of copper acetylacetonate and its derivatives in going from one compound to another band broadening is accompanied by appreciable changes in the g-factor. Yet anisotropic broadening can not account for the observed facts either. A detailed analysis of the spectra obtained with azo compounds provides no basis for attributing the changes in band width entirely to the anisotropic broadening.

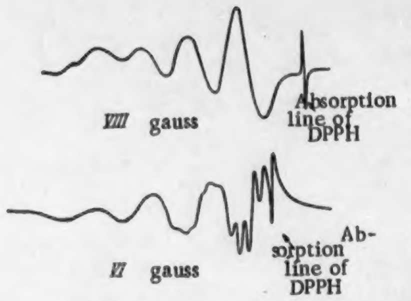

Fig. 1. Derivatives of p.m.r. absorption bands at a 9370 Mc frequency; 0.01 M benzene solutions of compounds VIII and VI.

By studying these compounds in solution it is possible to get more definite results.

We recorded the spectra of several compounds in benzene, chloroform, dioxane, and other solvents. Solutions of copper acetylacetonate (spins $S_{O^{16}} = 0$, $S_{Cu} = {}^{3}/_{2}$) gave spectra similar to those obtained by McGarvey [5]; however, several azo compounds had more complex spectra (see, for example, Fig. 1). The formation of additional hyperfine splitting (of the most intense line), consisting of five components, results from the interaction between the unpaired copper electron and the nuclei of the azo nitrogen ($S_{N^{14}} = 1$).

The formation and nature of additional splitting depend on the state (equivalence and coplanarity) of the azo nitrogens in the compound.

Thus our experimental data clearly demonstrate that the unpaired electrons of copper in inner complexes interact directly with the $\pi$-electrons of the system and that this interaction depends on the nature and structure of the surrounding groups.

## LITERATURE CITED

[1] D. N. Shigorin, Zhur. Fiz. Khim. 554 (1953); Probl. Fiz. Khim. 1, 173 (1958).

[2] D. N. Shigorin, Spectrochim. Acta 14, 198 (1959).

[3] H. S. Jarrett and G. J. Sloan, J. Chem. Phys. 22, 1783 (1954).

[4] B. I. Stepanov, M. A. Salivan, et al., Zhur. Obshchei Khim. 28, (1958);* M. A. Andreeva and B. I. Stepanov, Zhur. Obshchei Khim. 28, 2966 (1958)*, B. I. Stepanov, V. A. Savel'eva, Zhur. Obshchei Khim 28, 2968 (1958)*; B. I. Stepanov and M. A. Andreeva, Nauchn. Dokl. Vyssh. Shk., Khimia, 141 (1959).

[5] B. P. McGarvey, J. Phys. Chem. 60, 71 (1956).

---

*Original Russian pagination. See C. B. translation.

# INTERMOLECULAR INTERACTIONS REVEALED THROUGH FLUORESCENCE SPECTRA OF ACETYLANTHRACENES DISSOLVED IN MIXED SOLVENTS

A. S. Cherkasov

(Presented by Academician A. N. Terenin October 19, 1959)

(Translation of: Doklady Akademii Nauk SSSR, Vol. 130, No. 6, 1960 pp. 1288-1290)

Original article submitted September 24, 1959.

It is well known that the position of the fluorescence spectra of many organic compounds depends to a large degree on the solvent [1-5].

While studying the spectral properties of anthracene derivatives we found that the fluorescence spectra of 1- and 2- acetylanthracenes also depend on the solvent used.* When one changes from a nonpolar solvent (n-hexane) to water, which induces one of the largest spectral shifts, the fluorescence maximum of 1-acetylanthracene is displaced from 22450 $cm^{-1}$ to 17500 $cm^{-1}$, while that of 2-acetylanthracene from 23450 $cm^{-1}$ to 18500 $cm^{-1}$. The spectrum is continuous in polar solvents while in nonpolar n-hexane vibrational structure appears and is particularly well pronounced in the caseof 2-acetylanthracene. At the same time the shift in the absorption spectrum is very negligible and only a diffusion of the vibrational structure is observed in polar solvents.**

It should be noted that solvents containing hydroxyl groups, such as water, glycerin, ethylene glycol, and monofunctional alcohols, produce exceptionally large spectral shifts. One could try to relate this phenomena to the high dielectric constant ($\epsilon$) of these compounds [3] but for the fact that several other solvents with even greater values of $\epsilon$ have very little effect on the spectra. Thus, for example, the fluorescence maxima of 2-acetylanthracene in methanol ($\epsilon$ = 33), benzyl alcohol ($\epsilon$ = 13), and n-octyl alcohol ($\epsilon$ = 10) are shifted towards longer wave lengths by 3650, 3750, and 2740 $cm^{-1}$, respectively, from the fluorescence maximum in n-hexane, whereas the corresponding displacement in acetone ($\epsilon$ = 21.5) and pyridine (12.5) are only 1200 and 1400 $cm^{-1}$, respectively. Evidently the strong effects of solvents containing hydroxyl groups on the fluorescence spectra cannot in this case be solely attributed to the dielectric properties, but it seems that the effects are mainly connected with a specific interaction between the hydroxyl group and the excited acetylanthracene molecules (most probably with their carbonyl groups).

---

*9-Acetylanthracene exhibits no fluorescence at room temperature in the solvents studied by us. The acetylanthracenes were prepared by acetylating anthracene with acetyl chloride (in benzene) in the presence of aluminum chloride and separating the isomers by fractional crystallization [6]. Recrystallization and chromatographic purification on alumina yielded 1-acetylanthracene, m.p. = 107.5-109°, and 2-acetylanthracene m.p. = 187.5-188.5° C.

**Solvent effects on the position and shape of the absorption and fluorescence spectra of acetylanthracenes will be examined in more detail somewhere else.

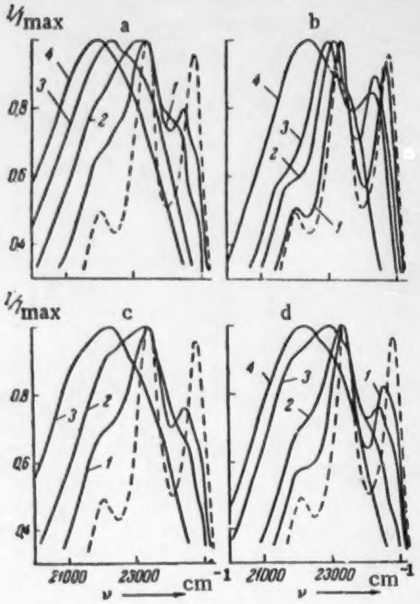

Fig. 1. The fluorescence spectra of 2-acetylanthracene in hexane (dashed curve) and in mixed solvents: a) Hexane and methyl alcohol. Alcohol concentrations: 1) 0.12; 2) 0.25; 3) 0.5; 4) 1. b) Hexane and pyridine. Pyridine concentration: 1) 1; 2) 5; 3) 10; 4) 50. c) Hexane and benzyl alcohol. Alcohol concentration: 1) 0.2; 2) 0.4; 3) 1. d) hexane and octylalcohol. Alcohol concentration: 1) 0.3; 2) 0.6; 3) 1.7; 4) 3.4.(The concentrations are in percent by volume).

Results obtained with the fluorescence spectra of acetylanthracenes dissolved in mixed solvents also indicate that the hydroxyl groups have a specific effect (Fig. 1).* In nonpolar hexane the fluorescence spectra have the shortest wave length and give the best-resolved vibrational structure. In mixtures of hexane and pyridine (Fig. 1b) the vitrational structure becomes gradually more diffused and the spectra shift towards higher frequencies as the pyridine concentration is increased**; yet, if only 1% of pyridine is added to the hexane the spectrum remains almost unchanged. Things are quite different when alcohols are added to hexane.The addition of even insignificant amounts of alcohol (0.1-0.2%) has a very pronounced effect on the form of the fluorescence spectrum. The vibrational structure becomes diffused, and its shape suggests that there are at least two distinct spectra superimposed on each other.

A possible explanation for the strong effects of small alcohol concentrations on the spectra may be provided by assuming that the alcohol molecules become concentrated around the excited acetylanthracene with their hydroxyl groups oriented towards the carbonyl oxygen. Such a mechanism was proposed, for example, to explain a similar effect of small amounts of alcohols on the fluorescence spectra of acridone [5]. However, it seems more probable to us that the observed changes produced in the acetylanthracene spectra by the addition of a little alcohol to neutral solutions essentially indicate the formation of hydrogen bonds between the hydroxyl group on the alcohol and the carbonyl group on the excited acetylanthracene. Moreover, one should keep in mind the fact that as the concentration of alcohol in hexane increases not only should the concentration of 1 : 1 complexes between acetylanthracene and alcohol increase but complexes should also arise with groups of associated alcohol molecules.***

It is a well-known fact that in certain solvents the alcohols become completely dissociated due to hydrogen bonding between the alcohol and the solvent; ethers and amines are particularly effective in this respect [7]. It is quite obvious that if the above-presented reasons for the effect of alcohols on the spectra represent the reality one would expect these effects to be somewhat reduced if the solution also contained some compounds capable of interacting with the alcohols.

The fluorescence spectra of acetylanthracene studied in mixed solvents, of which one was methyl alcohol, fully confirmed this hypothesis. Thus, for example, while it takes only 2% of methanol to shift the fluorescence maximum of 2-acetylanthracene by half the total displacement produced in going from pure hexane to pure methanol, to produce a similar shift in mixtures containing acetone, dioxane, and pyridine one has to increase the alcohol concentration to 20, 20, and 40% respectively.

The interaction between alcohols and other solvents becomes particularly evident in the fluorescence spectra of acetylanthracenes dissolved in mixtures of three solvents. In Fig. 2 we have shown the effects of diethyl

---

[*] The results obtained with 1-acetylanthracene are similar to those shown for 2-acetylanthracene in Fig. 1 and 2.

[**] Similar results were obtained in mixtures of hexane and acetone.

[***] As is well known [7],even at moderate concentrations alcohol molecules in nonpolar solvents will be associated into aggregates containing several molecules.

ether, pyridine, acetone, and anisol on the spectrum of 2-acetylanthracene dissolved in n-hexane to which 0.5% of methyl alcohol was added. Figure 2 clearly shows that by increasing the amount of the third solvent we gradually displace the spectra towards higher frequencies (except in the case of anisole) and restore the vibrational structure, or in other words, that the effect of alcohol is neutralized. If these solvents had not interacted with the alcohol we would have only expected a reverse process—displacement of the spectrum towards lower frequencies (as was observed in the case of anisol), since when these solvents are introduced individually into an n-hexane solution of acetylanthracene the spectrum is displaced towards longer wave lengths (see, for example, Fig. 1b).

From their effects on the fluorescence spectra one can qualitatively arrange these solvents in order of their reactivities towards alcohols. Thus Fig. 2 shows that though 1% of acetone has practically no effect on the spectrum, the same amount of ether produces a slight shift, while corresponding quantities of pyridine and dioxane produce a displacement of ~600 $\text{cm}^{-1}$.

The above-presented results clearly indicate that the fluorescence spectra of acetylanthracene in mixed solvents can be utilized to detect intermolecular interactions between the solution components. One should think that other compounds could also be used for this purpose if their fluorescence spectra are greatly influenced by solvents.

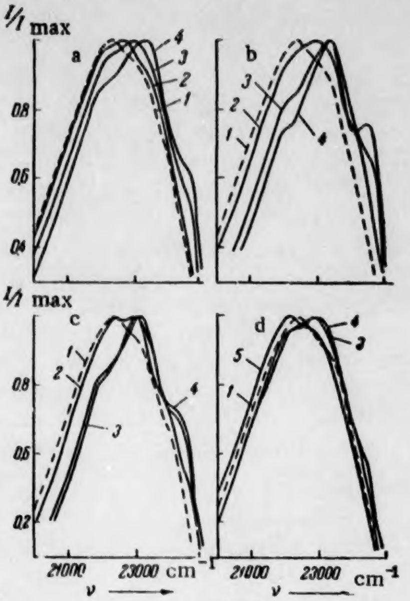

Fig. 2. The fluorescence spectra of 2-acetylanthracene in a mixture of hexane + + 0.5% methyl alcohol + a third solvent. Concentrations of the third solvent (in percent by volume): 1) 0; 2) 1; 3) 5; 4) 10. The third solvent is: a) ethyl ether; b) dioxane; c) pyridine; d) acetone; d5) anisole (5%).

## LITERATURE CITED

[1] V. V. Zelinskii, V. P. Kolobkov, and I. I. Reznikova, Trans. of the 1958 Conference on the Thermodynamics and Structure of Solutions [in Russian] (Moscow, 1959, p. 262); V. V. Zelinskii, V. P. Kolobkov, and L. G. Pikulik, Optika i Spektroskopiya, 2, 402 (1957).

[2] V. P. Klochkov, Optika i Spectroskopiya 1, 546 (1956); V. P. Klochkov, Zhur. Fiz. Khim. 29, 1432 (1955).

[3] N. G. Bakhshiev, Optika i Spektroskopiya, 7, 52 (1959); N. G. Bakshiev, Izv. Akad. Nauk SSSR, Ser. Fiz. 22, 1387 (1958).

[4] E. Lippert and F. Moll. Zs. Electrochem. 58, 718 (1954); E. Lippert, J. phys. et radium 15, 627 (1954).

[5] H. Kokubun, Zs. phys. Chem. 17, 281 (1958); H. Kokubun, Zs. Electrochem. 62, 599 (1958).

[6] P. H. Core, J. Org. Chem. 22, 135 (1957).

[7] W. Hückel, Theoretical Foundations of Organic Chemistry 2 [Russian translation] (IL, 1958).

# THE P.M.R. SPECTRA AND THE ACCUMULATION KINETICS OF FREE RADICALS PRODUCED IN THE RADIOLYSIS OF CERTAIN AROMATIC COMPOUNDS

I. I. Chkheidze, Yu. N. Molin, N. Ya. Buben,
and Corresponding Member Acad. Sci. USSR V.V.Voevodskii

Chemical Physics Institute, Academy of Sciences USSR and the
Chemical Kinetics and Combustion Institute, Siberian Division
of the Academy of Sciences USSR

(Translation of: Doklady Akademii Nauk, SSSR, Vol.130, No.6, 1960,
pp. 1291-1293)

Original article submitted November 13, 1959.

This work was undertaken for the purpose of characterizing the radicals formed during the radiolysis of aromatic compounds and to study the effects of molecular structure on the yield of these radicals. With this in mind we recorded the paramagnetic resonance spectra (p.m.r.) of the radicals formed under the impact of fast electrons (1.6 Mev) and followed the accumulation kinetics. In Table 1 we have listed the compounds investigated. The technique used to detect these radicals during irradiation was carried out at current densities from 1.5 to 4.0 amp/cm$^2$ and temperatures of -124 and + 33°C. The benzene was chemically pure. The remaining compounds were obtained from the laboratory of K. P. Lavrovskii at the Institute of Petrochemical Syntheses. The compounds were purified by sublimation in high vacuum.

In Fig. 1 we have plotted the p.m.r. spectra of benzene, biphenyl, p-terphenyl, and p-ditolyl obtained at −124°C. The spectra of m-terphenyl and o-ditolyl were similar to those of the p-isomers. Para and m-terphenyl had the same p.m.r. spectra at + 33°C as at −124°. The p.m.r. spectrum of benzene consists of a well-defined triplet with the central component much more intense than one would expect from the binomial distribution of intensities, 1 : 2 : 1. A single line superimposed over the central component could give rise to such a spectrum. The triplet in the benzene spectrum can apparently be only attributed to a $C_6H_5$ radical formed by the detachment of an H-atom from benzene:

$$C_6H_6 \rightarrow C_6H_5^{\bullet} + H. \tag{1}$$

The interaction between the unpaired electron and the two adjacent H-atoms gives rise to the three observed lines. It should be noted that the triplet splitting of a phenyl radical $\Delta H$ 45.0 ± 1.5 oerst, exceeds considerably the splitting by $\beta$-hydrogens of alkyl radicals (for example, in the $-CH_2-CH_2^{\bullet}-CH_2$ radical $\Delta H = 30$ oerst [3]). The large $\Delta H$ of benzene can be explained by the fact that the C−C distance in benzene is shorter than in alkyl hydrocarbons and that in the phenyl radical the unpaired electron orbital is coplanar with the C−H bonds.

Figure 1 (a,b,c) shows that each component of the triplet is further split into 4 lines with a $\Delta H = 10.2 \pm \pm 0.5$ oerst. This additional splitting can only be attributed to an interaction between the unpaired electron and the remaining three H-atoms. Interpreting the spectra in this manner we can conclude that these three hydrogens are equivalent.

From the low yield of molecular hydrogen ($G_{H_2} = 0.036$ mole/100 ev [4]) as compared to the yield of

TABLE 1

| Sample | Temp. -124°C. | Temp. + 33°C. |
|---|---|---|
| Benzene | 0.16 | |
| Biphenyl | 0.045 | |
| p-Ditolyl | 0.08 | |
| o-Ditolyl | 0.11 | |
| m-Terphenyl | 0.034 | 0.014 |
| p-Terphenyl | 0.046 | 0.015 |

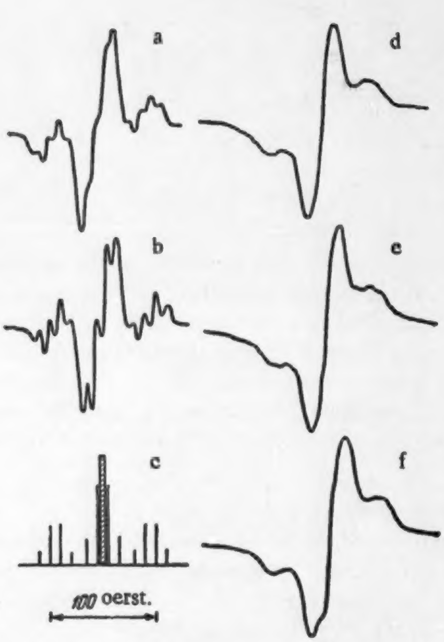

Fig. 1. P.m.r. spectra of irradiated: a) benzene at −132°; b) benzene at −52; c) a schematic representation of the benzene spectrum; d) biphenyl at −124°; e) p-terphenyl at −124°; f) p-ditolyl at −124°C.

polymers ($G_{poly}$=0.75 mole / 100 ev[5]) and the yield of radicals observed by us (see Table 1), one may conclude that not all of the hydrogen produced in reaction (1) is liberated as $H_2$. On the basis of these observations, and certain literature data which show that a $C_6H_7$ radical can be formed from benzene and atomic hydrogen at liquid-air temperatures [6], we may conclude that a large number of the H-atoms formed in reaction (1) interact with benzene to form $C_6H_7$ radicals. The unpaired electron in the $C_6H_7$ radical becomes delocalized throughout the $\pi$ - system and interacts with many hydrogen atoms. In analogy with aromatic ion-radicals [7] one can assume that the total magnitude of hyperfine splitting in a $C_6H_7$ radical would be small (~20 oerst). Since the lines in a solid-state spectrum are fairly broad, the hyperfine splitting in the p.m.r. spectrum of this radical would hardly be resolvable. Therefore a spectrum of the $C_6H_7$ radical should contain a single line 10-20 oerst. wide. A superposition of this line on the central component of the phenyl radical triplet would fully explain all the features in the spectrum of irradiated benzene.

As can be seen in Fig. 1 a, b the hyperfine splitting in the p.m.r. spectrum of benzene is resolved much better at higher temperatures. One can show that this fact could be attributed to the freeing of a hindered molecular rotation around the 6th-order axis of benzene; such rotation was demonstrated in nuclear magnetic resonance experiments [8].

Though biphenyl, terphenyl, and ditolyl give rise to triplet spectra similar to that of benzene, the individual components are poorly resolved and show no additional splitting. A characteristic property of these spectra is their great similarity to each other. All these spectral properties can be explained satisfactorily by assuming that the polyphenyls lose a H-atom or a $CH_3$ group para to the phenyl substituent. As a result, radicals of the type 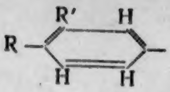 , where R' = $CH_3$ in the case of o-ditolyl and R' = H in all the remaining cases.

A free H-atom or $CH_3$ radical will become attached to a benzene ring producing a radical similar to the $C_6H_7$ radical. The resulting spectrum will obviously be very similar to that observed in the radiolysis of benzene. The poorer resolution in the spectral structure of polyphenyls is probably due to a delocalization of the unpaired electron over the entire system of conjugated bonds, and its consequent interaction with a large number of hydrogen atoms. Moreover, the line narrowing connected with rotation should be absent in polyphenyls.

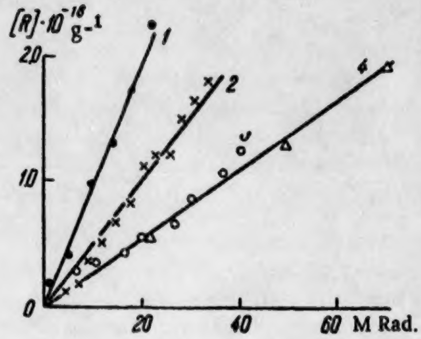

Fig. 2. Radical accumulation kinetics at -124°; 1) benzene; 2) p-ditolyl; 3) biphenyl; 4) p-terphenyl.

The poor resolution in the p.m.r. spectra of polyphenyls could be attributed to the fact that a variety of radicals may be formed by breaking different CH or C—C bonds. However, such an assumption would fail to explain why various polyphenyls yield identical spectra.

In Table 1 we have listed the radiation yields of radicals, determined from the linear portions of the accumulation curves (Fig. 2). The relative error in the determination of $G_R$ was ± 20%.

The decreasing radiation yield of radicals in going from benzene to biphenyl to terphenyls is in full accord with the literature data indicating that polyphenyls are more resistant to radiation than benzene [9]. Ditolyls yield comparatively more radicals than do biphenyls, indicating apparently that side groups reduce the resistance to radiation, which also agrees with the literature data [10]. It is intersting to compare the radical yields from isomeric molecules. According to some workers [11, 12] at large radiation dosages isomeric terphenyls differ considerably in their resistance to radiation, while according to others [13] who detemined the yields of radiolysis end products the differences are small.

Table 1 shows that the differences between the $G_R$ values of various isomers seem to lie within the range of experimental errors.

The authors wish to express their gratitude to A. M. Brodskii and V. B. Titov for providing the polyphenyls and discussing the results, and to V. N. Shamshev for participating in the experimental work.

## LITERATURE CITED

[1] Yu. N. Molin, A. T. Koritskii, et al., Doklady Akad. Nauk 123, 882 (1958).*

[2] A. T. Koritskii, Yu. N. Molin, et al., Vysokomolek. soed. 1, 1182 (1959).

[3] Yu. D. Tsvetkov, N. N. Bubnov, et al., Doklady Akad. Nauk 122, 1033 (1958).*

[4] J. P. Manion and M. Burton, J. Phys. Chem. 56, 560 (1952).

[5] W. N. Patrick and M. Burton, J. Am. Chem. Soc. 76, 2626 (1954).

[6] K. H. Geib and P. Harteck, Ber. 66, 1815 (1933).

[7] D. J. E. Ingram, Free Radicals as Studied by Electron Spin Resonance (London, 1958) p. 142.

[8] E. R. Andrew and R. G. Eades, Proc. Roy. Soc., 218A, 537 (1953).

[9] B. Tolbert and R. M. Lemmon, Radiation Res. 3, 1, 52 (1955).

[10] M. Burton, S. Gordon and R. R. Hentz, J. Chim. Phys., 48, 190 (1951).

---

*Original Russian pagination. See C. B. translation.

[11] E. L. Colichman and R. H. J. Gereke, Nucleonics 14, 7, 50 (1956).

[12] E. L. Colichman and R. F. Fish, Nucleonics 15, 2, 72 (1957).

[13] W. G. Burns, W. Wild, and T. F. Williams, Trans. International Confer. on Peaceful Uses of Atomic Energy, Geneva, 1958, 5 [in Russian] (Moscow, 1959) p. 661.

# ERRATUM

## Vol. 128, September-October, 1959

In the article by E. M. Shustorovich and M. E. Dyatkina, pp. 885-888, there is an error in the values of the dipole moments. All the values given, both those in the tables and those in the text, should be multiplied by 4.8.

# SIGNIFICANCE OF ABBREVIATIONS MOST FREQUENTLY ENCOUNTERED IN SOVIET PERIODICALS

| | |
|---|---|
| FIAN | Phys. Inst. Acad. Sci. USSR. |
| GDI | Water Power Inst. |
| GITI | State Sci.-Tech. Press |
| GITTL | State Tech. and Theor. Lit. Press |
| GONTI | State United Sci.-Tech. Press |
| Gosenergoizdat | State Power Press |
| Goskhimizdat | State Chem. Press |
| GOST | All-Union State Standard |
| GTTI | State Tech. and Theor. Lit. Press |
| IL | Foreign Lit. Press |
| ISN (Izd. Sov. Nauk) | Soviet Science Press |
| Izd. AN SSSR | Acad. Sci. USSR Press |
| Izd. MGU | Moscow State Univ. Press |
| LEIIZhT | Leningrad Power Inst. of Railroad Engineering |
| LET | Leningrad Elec. Engr. School |
| LETI | Leningrad Electrotechnical Inst. |
| LETIIZhT | Leningrad Electrical Engineering Research Inst. of Railroad Engr. |
| Mashgiz | State Sci.-Tech. Press for Machine Construction Lit. |
| MEP | Ministry of Electrical Industry |
| MES | Ministry of Electrical Power Plants |
| MESEP | Ministry of Electrical Power Plants and the Electrical Industry |
| MGU | Moscow State Univ. |
| MKhTI | Moscow Inst. Chem. Tech. |
| MOPI | Moscow Regional Pedagogical Inst. |
| MSP | Ministry of Industrial Construction |
| NII ZVUKSZAPIOI | Scientific Research Inst. of Sound Recording |
| NIKFI | Sci. Inst. of Modern Motion Picture Photography |
| ONTI | United Sci.-Tech. Press |
| OTI | Division of Technical Information |
| OTN | Div. Tech. Sci. |
| Stroiizdat | Construction Press |
| TOE | Association of Power Engineers |
| TsKTI | Central Research Inst. for Boilers and Turbines |
| TsNIEL | Central Scientific Research Elec. Engr. Lab. |
| TsNIEL-MES | Central Scientific Research Elec. Engr. Lab.—Ministry of Electric Power Plants |
| TsVTI | Central Office of Economic Information |
| UF | Ural Branch |
| VIESKh | All-Union Inst. of Rural Elec. Power Stations |
| VNIIM | All-Union Scientific Research Inst. of Meteorology |
| VNIIZhDT | All-Union Scientific Research Inst. of Railroad Engineering |
| VTI | All-Union Thermotech. Inst. |
| VZEI | All-Union Power Correspondence Inst. |

Note: Abbreviations not on this list and not explained in the translation have been transliterated, no further information about their significance being available to us. — Publisher.